

***In vitro* cell and culture models for osteoblasts
and their progenitors**

By

Ewa Maria Czekańska

Supervised by

Dr. Martin Stoddart

AO Research Institute Davos

Davos, Switzerland

&

Dr. Jessica Hayes

Regenerative Medicine Institute

NUI Galway, Ireland

&

Dr. Jim Ralphs

School of Biosciences

Cardiff University

Wales, UK

A thesis submitted to the Cardiff University
for the degree of Doctor of Philosophy

April 2014

DECLARATION

This work has not previously been accepted in substance for any degree or award at this or any other university or place of learning, nor is being submitted concurrently in candidature for any degree or other award.

This thesis is being submitted in partial fulfilment of the requirements for the degree of Ph.D.

This thesis is the result of my own independent work, except where otherwise stated. Other sources are acknowledged by explicit references. The views expressed are my own.

I hereby give consent for my thesis, if accepted, to be available for photocopying and for inter-library loan, and for the title and summary to be made available to outside organisations.

Candidate: *Eva Czekan'ska*

Date: 31st March 2014

THESIS SUMMARY

This thesis aimed to evaluate the relevancy of different *in vitro* cell and culture models for osteoblastic-lineage cells. Cell lines provide a convenient and accessible alternative to primary human osteoblast cells. However, the direct comparison of these cells demonstrated limited similarity of cell lines to the primary human osteoblasts indicating that their use should be limited to appropriate and specific research questions.

To investigate the paracrine regulation of osteogenic development, the immature human osteoblasts and human bone-derived mesenchymal stem cells (MSCs) were co-cultured in monolayer or high density culture. Results from this part of the study suggested the presence of an active signalling pathway between MSCs and osteoblasts. What is more, the effect of cell-cell crosstalk depended on the type of culture system. Co-culture in a 3D micromass system stimulated the osteogenic differentiation of progenitor cells, while in monolayer this was not seen. While the stimulation of MSCs with inflammatory and chemotactic factors successfully regulated the cell gene expression and secretion profile, no effect of the secretome on the osteogenic differentiation of unstimulated cells in monolayer was demonstrated. Altogether, these results indicated the importance of cell-to-matrix interconnectivity.

Therefore, the last part of this thesis focused on the assessment of osteogenic differentiation in 2D and 3D cell culture models, which are physiologically relevant. The progression in osteogenesis depends on the applied 3D culture model. While in both, micromass and type I collagen-hydroxyapatite gel, the differentiation is enhanced compared to monolayer, the regulation of this process is triggered in a different manner in these 3D culture models.

Together these findings demonstrate how diverse outcomes can be obtained by the application of different models in *in vitro* research. Ultimately, the 3D *in vitro* models provide a better choice for a more *in vivo*-related osteogenic differentiation and its regulation.

ACKNOWLEDGMENTS

I would like to acknowledge everyone who has helped in the completion of this thesis and their great support during my PhD studies.

Firstly, I would like to thank Prof. Geoff Richards and Prof. Mauro Alini for giving me the opportunity to join ARI Davos.

I sincerely would like to thank Dr Jessica Hayes and Dr Martin Stoddart for their great support during my studies. Thanks Jessica for the introduction to the cells and biomaterials world and all your comments. To Martin, a great thank you for your constant encouragement and careful guidance throughout this project. I am very grateful that you always have had time to discuss project matters and that you thought me that all results are good.

I would like to thank Ursula Menzel, Nora Goudsouzian, Sandra Thoeny and Christoph Sprecher for their technical support during this thesis. Many thanks to Claudia Loebel, Judith Staudacher and Marc Anton Fuessinger for the nice time in the lab and questions I have never thought about before.

During my time in ARI Davos I met many great people. Special thanks to Estelle, Sandrine, Maria, Katha, Nadine, Laszlo, Olly, Ed, Alex, Matteo, Viktor for making that time so valuable and all your support. I have had the good fortune to share the office space with great students who were always helpful and cheering during all those less sunny days of my studies.

Finally, I would like to acknowledge my 'old' friends, Ania, Karolina and Wojtek, and my family who have been very patient with me, especially in the last 12 months. Many thanks for your support!!!

PUBLICATIONS AND CONFERENCE PROCEEDINGS FROM THIS THESIS

Publications

E. M. Czekanska, J. R. Ralphs, M. Alini, M. J. Stoddart: Enhancing therapeutical potential of mesenchymal stem cells (MSC) – submitted to *Stem Cells and Development*

C. Loebel, **E. M. Czekanska**, J. Staudacher, G. Salzmann, R. G. Richards, M. Alini, M. J. Stoddart: The osteogenic potential of human MSCs can be enhanced by Interleukin-1 β – submitted to *Tissue Engineering and Regenerative Medicine*

C. Loebel, **E. M. Czekanska**, M. Bruderer, G. Salzmann, M. Alini, M. J. Stoddart: Osteogenic Potential of human MSCs is predicted by Runx2/Sox9 ratio – submitted to *Tissue Engineering*

E. M. Czekanska, M. J. Stoddart, J. R. Ralphs, R. G. Richards, J. S. Hayes: A phenotypic comparison of osteoblast cell lines versus human primary osteoblasts for biomaterials testing *Journal of Biomedical Materials Research: Part A* (2013).

E. M. Czekanska, M. J. Stoddart, R. G. Richards, J. S. Hayes: In search of an osteoblast cell model for *in vitro* research. *European Cell and Materials* 24: 1-17 (2012).

J. S. Hayes, **E. M. Czekanska**, R. G. Richards: The cell-surface interaction *Advances in Biochemical Engineering/Biotechnology* 126: 1-31 (2012).

E. M. Czekanska: Assessment of cell proliferation with resazurin-based fluorescent dye *Methods in Molecular Biology* 740: 27-32 (2011).

Conference Proceedings

E. M. Czekanska, J. R. Ralphs, M. Alini, M. J. Stoddart: Enhancing inflammatory and chemotactic signals to regulate bone regeneration. Orthopaedic Research Society Annual Meeting, New Orleans (US), 15th-18th March 2014.

C. Loebel, **E. M. Czekanska**, J. R. Ralphs, M. Alini, M. J. Stoddart: Early prediction of osteogenic potential of human mesenchymal stem cells by Runx2/Sox9 Ratio. Orthopaedic Research Society Annual Meeting, New Orleans (US), 15th-18th March 2014.

E. M. Czekanska, M. A. Fuessinger, F. Duttenehofer J. R. Ralphs, R. G. Richards, M. Alini, M. J. Stoddart: Enhancing the therapeutical potential of human MSC cells. eCM XIV: Stem & Progenitor Cells for Musculoskeletal Regeneration, Davos (CH), 23rd-25th June 2013.

E. M. Czekanska, J. R. Ralphs, M. Alini, M. J. Stoddart: Benefits of chemotactic and inflammatory modulators in bone regeneration. Tissue Engineering and Regenerative Medicine International Society – EU Meeting, Istanbul (TR), 17th-21st June 2013.

C. Loebel, **E. M. Czekanska**, J. R. Ralphs, M. Alini, M. J. Stoddart: The RunX2 - Sox9 "see-saw": A balance for MSC osteogenesis. Orthopaedic Research Society Annual Meeting, San Antonio (US), 26th-29th January 2013.

E. M. Czekanska, J. R. Ralphs, M. Alini, M. J. Stoddart: Investigating the factors directing the process of *in vitro* mineralisation. Tissue Engineering and Regenerative Medicine International Society – World Meeting, Vienna (AT), 5th-8th September 2012.

E. M. Czekanska, J. R. Ralphs, M. Alini, M. J. Stoddart: Human mesenchymal stem cells stimulate *in vitro* mineralization of MG63 osteoblast precursors. International Society for Stem Cell Research, Yokohama (JP), 13th-16th June 2012.

E. M. Czekanska, J. R. Ralphs, M. Alini, M. J. Stoddart: Interactions of MSC and bone cells during the process of *in vitro* mineralization. Swiss Bone and Mineral Society Meeting, Basel (CH), 25th June 2012.

E. M. Czekanska, M. J. Stoddart, J. S. Hayes, J. R. Ralphs, R. G. Richards: Evaluation of osteoblast cell models used in orthopaedic related research. Orthopaedic Research Society Annual Meeting, Long Beach (US), 4th-7th February 2011.

E. M. Czekanska, J. S. Hayes, J. R. Ralphs, R. G. Richards: Characterisation of common osteoblast models used for orthopedic research. European Orthopedic Research Society, Davos (CH), 30th June-2nd July 2010.

E. M. Czekanska, J. S. Hayes, J. R. Ralphs, R. G. Richards: *In vitro* assessment of osteoblast cell models for bone related research. International Bone and Mineral Society Meeting, Davos (CH) 9th-14th March 2010.

ABBREVIATIONS

1,25(OH) ₂ D ₃	1,25-Dihydroxycholecalciferol
2D	Two-dimensional
3D	Three-dimensional
AA	L-ascorbic acid 2-phosphate sesquimagnesium salt hydrate
ALP	Alkaline phosphatase
ARS	Alizarin Red S staining
bFGF	Basic fibroblast growth factor
BSP	Bone sialoprotein
cDNA	Complementary DNA
CHAP	Type I collagen-hydroxyapatite gel
CO ₂	Carbon dioxide
COL1	Type I collagen
Dex	Dexamethasone
DM	Differentiation medium
DMEM	Dulbecco's Modified Eagle Medium
DMSO	Dimethyl sulfoxide
DNA	Deoxyribonucleic acid
dNTP	Deoxy nucleotide triphosphate
ECM	Extracellular matrix
EDTA	Ethylenediaminetetraacetic acid
ELISA	Enzyme-linked immunosorbent assay
FACS	Fluorescence-activated cell sorting
FBS	Foetal Bovine Serum
FCS	Foetal calf serum

GCSF	Granulocyte colony stimulating factor
GM	Growth medium
HAP	Hydroxyapatite
HEPES	4-(2-hydroxyethyl)-1-piperazineethanesulfonic acid
HO _b	Primary human osteoblast cells
IL1 β	Interleukin 1 β
ITS	Insulin-Transferrin-Selenium
ML	Monolayer
MM	Micromass
mRNA	Messenger ribonucleic acid
MSCs	Bone marrow-derived mesenchymal stromal cells
OBM	Osteoblast basal medium
OC	Osteocalcin
PBS	0.1M phosphate buffered saline
RNA	Ribonucleic acid
RT-PCR	Real-time polymerase chain reaction
Runx2	Runt-related transcription factor 2
SCF	Stem Cell Factor
SDF-1	Stromal cell-derived factor-1 α
α MEM	Alpha Minimum Essential Medium
β GP	Glycerol-2-phosphate

CONTENTS

DECLARATION	I
THESIS SUMMARY	II
ACKNOWLEDGMENTS	III
PUBLICATIONS AND CONFERENCE PROCEEDINGS FROM THIS THESIS	IV
ABBREVIATIONS	VII
CONTENTS	IX
LIST OF FIGURES	XIII
LIST OF TABLES	XVIII
THESIS BACKGROUND	1
CHAPTER 1 INTRODUCTION	4
1.1. BONE BIOLOGY	5
1.1.1. Bone function	5
1.1.2. Bone microstructure	5
1.1.3. Bone matrix	7
1.1.3.1. Inorganic compartment	7
1.1.3.2. Organic compartment	7
1.1.3.2.1. Collagen matrix	7
1.1.3.2.2. Non-collagenous proteins and their role in matrix mineralisation	9
1.2. BIOLOGY OF BONE FORMING CELLS	11
1.2.1. The principles of osteoblastic lineage cell development	11
1.2.2. Osteoclast cells	15
1.3. OSTEOBLAST CELL MODELS IN IN VITRO RESEARCH	16
1.3.1. Human primary osteoblast cells	17
1.3.2. Animal primary osteoblasts	20
1.3.2.1. Rat cells	20
1.3.2.2. Bovine cells	22
1.3.2.3. Ovine cells	23
1.3.2.4. Rabbit cells	24
1.3.3. Cell lines	24
1.3.3.1. Human Cell Lines	25
1.3.3.2. Mouse cell lines	28
1.4. IN VITRO CELL-CELL COMMUNICATION MODELS OF OSTEOBLAST LINEAGE CELLS	30
1.4.1. Direct cell-cell communication	30
1.4.2. Indirect cell-cell communication	31
1.5. BONE REGENERATION	34
1.5.1. Primary fracture healing	34
1.5.2. Secondary fracture healing	35
1.5.2.1. Inflammatory phase	36
1.5.2.2. Soft callus formation	39
1.5.2.3. Hard callus formation	39
1.5.2.4. Remodelling	40
1.5.3. Vascularisation	42
1.6. OBJECTIVES AND HYPOTHESES	43
CHAPTER 2 MATERIALS AND METHODS	45
2.1. MATERIALS	46

2.2. METHODS	49
2.2.1. Culture and propagation of cells	49
2.2.1.1. Human bone marrow derived stromal cells (MSC) isolation and propagation	50
2.2.1.2. Primary Human Osteoblast (HOb) cells	51
2.2.1.3. MC3T3E1 cells	51
2.2.1.4. MG63 cells	52
2.2.1.5. SaOs2 cells	52
2.2.2. Cell passaging	53
2.2.3. Cell freezing	53
2.2.4. Cell reconstitution	54
2.2.5. Generating osteoblast cell line with stable GFP expression	54
2.2.5.1. Propagation of pMX-GFP and pCM-VSV-G retroviral vectors	54
2.2.5.2. Transfection of PlatGP cells with pMX-GFP and pCM-VSV-G vectors	55
2.2.5.3. MG63-GFP cell line	56
2.2.6. Monolayer cell culture of cells from different origins	57
2.2.7. High density culture (micromass) of MSC	57
2.2.8. Cell culture in type I collagen-hydroxyapatite gel	58
2.2.9. Stimulation of MSC cells with different factors	58
2.2.10. Conditioned medium collection	59
2.2.11. Indirect co-culture of cells	60
2.2.11.1. Monolayer co-culture of cells	60
2.2.11.2. Micromass co-culture of cells	60
2.2.11.3. Co-culture with conditioned medium	61
2.2.12. Determination of cell number and proliferation	61
2.2.12.1. Manual cell counting	61
2.2.12.2. Hoechst assay	62
2.2.12.3. Cell Titer-Blue [®] assay	63
2.2.13. Determination of cell viability	64
2.2.14. Alkaline phosphatase activity	64
2.2.14.1. Staining	64
2.2.14.2. Quantification	65
2.2.15. Determination of calcification	66
2.2.15.1. Alizarin Red S	66
2.2.15.1.1. Staining	66
2.2.15.1.2. Quantification	66
2.2.15.2. Radioactive calcium incorporation	67
2.2.16. Molecular biology	67
2.2.16.1. RNA extraction	67
2.2.16.2. DNase digestion and clean-up.	69
2.2.16.3. Reverse transcription	69
2.2.16.4. Real-Time PCR	71
2.2.16.5. Gene expression analysis with RT ² Profiler [™] PCR Array	75
2.2.17. Proteomic analysis	76
2.2.17.1. Determination of protein content	76
2.2.17.2. RayBio [®] human cytokine antibody array G-series	77
2.2.18. Immunohistochemistry	80
2.2.18.1. Fixation and cryo-sectioning	80
2.2.18.2. Detection of alkaline phosphatase and osteocalcin	80
2.2.19. Statistical analyses	82
CHAPTER 3 OSTEOBLAST CELL MODELS	84
3.1. INTRODUCTION	85
3.2. RESULTS	87
3.2.1. A phenotypic comparison of osteoblast cell lines versus human primary osteoblasts	87
3.2.1.1. Proliferation of osteoblast cell models	87

3.2.1.2. Alkaline phosphatase activity	88
3.2.1.3. Mineral deposition within ECM of osteoblast cell models	91
3.2.1.4. Expression of osteoblastic genes by osteoblast cell models	93
3.3. DISCUSSION	97
CHAPTER 4 IN VITRO CO-CULTURE OF PROGENITOR CELLS AND OSTEOBLASTS	102
4.1. INTRODUCTION	103
4.2. RESULTS	106
4.2.1. Indirect co-culture of MSCs and MG63 in monolayer and its effect on the osteogenic phenotype of the cells	106
4.2.1.1. The effect of monolayer co-culture on osteogenic gene expression in MSCs	107
4.2.1.2. The effect of monolayer co-culture on MSC functionality	110
4.2.1.3. The effect of monolayer co-culture on osteogenic gene expression in osteoblast (MG63) cells	112
4.2.1.4. The effect of monolayer co-culture on osteoblast (MG63) functionality	115
4.2.2. Indirect co-culture of MSCs and MG63 in micromass and its effect on the osteogenic phenotype of cells	118
4.2.2.1. The effect of micromass co-culture on osteogenic gene expression in MSCs	119
4.2.2.2. The effect of micromass co-culture on osteogenic gene expression in osteoblast (MG63) cells	124
4.2.2.3. The effect of micromass co-culture on ALP and mineralisation	126
4.2.3. Generation and functionality of MG63 cells expressing GFP	128
4.2.3.1. Transduction efficacy and cell colonies selection	128
4.2.3.2. Phenotypic assessment of MGreen63 cell line	132
4.2.3.2.1. Proliferation of MGreen63 cell line	132
4.2.3.2.2. Analysis of osteoblastic functions (ALP & mineralisation)	133
4.2.3.2.3. Osteogenic genes expression in MGreen63 cell line	135
4.3. DISCUSSION	139
CHAPTER 5 ENHANCING INFLAMMATORY AND CHEMOTACTIC SIGNALS TO REGULATE BONE REGENERATION	145
5.1. INTRODUCTION	146
5.2. RESULTS	149
5.2.1. Direct influence of MSCs stimulation with cytokines on MSCs	149
5.2.1.1. Effects of stimulation with cytokines on gene and protein expression profile of MSCs	149
5.2.1.1.1. MSCs cytokine gene expression after culture in serum containing medium	150
5.2.1.1.2. MSCs cytokine gene expression after culture in serum-free medium	154
5.2.1.1.3. Regulation of osteogenic and Wnt signalling genes in stimulated MSCs	158
5.2.1.1.4. Influence of stimulation on cytokine protein secretion by MSCs in serum-free medium cell culture	162
5.2.2. Indirect effects of MSCs stimulation with cytokines on osteogenic differentiation of MSCs	167
5.2.2.1. Conditioned medium from stimulated cells inhibits the proliferation of MSCs	167
5.2.2.2. Regulation of osteogenic genes in response to co-culture with conditioned media	168
5.2.2.3. Influence of MSCs co-culture with conditioned media on cell functionality (ALP activity and mineral deposition in newly formed ECM)	176
5.3. DISCUSSION	180
CHAPTER 6 THE EFFECT OF DIFFERENT 3D CELL CULTURE SYSTEMS ON MSC CELLS	190
6.1. INTRODUCTION	191
6.2. RESULTS	194
6.2.1. Type I collagen gel-hydroxyapatite gel formulation and optimisation process	194

6.2.2. Comparison of in vitro culture systems	196
6.2.2.1. ALP activity & immunolabelling	196
6.2.2.2. Expression of osteogenic genes in MSCs cultured in 2D and 3D	199
6.3. DISCUSSION	207
CHAPTER 7 GENERAL DISCUSSION	213
7.1. CELL CULTURE MODELS	214
7.2. IN VITRO 2D AND 3D CO-CULTURE MODELS	219
7.3. IN VITRO CULTURE ENVIRONMENT AND OSTEOGENIC DIFFERENTIATION	225
7.4. ENHANCING THE SECRETION PROFILE OF MSCs	228
7.5. INFLUENCE OF THE CULTURE MODEL AND DEXAMETHASONE ON OSTEOCALCIN EXPRESSION	232
7.6. SUMMARY	235
REFERENCES	236
APPENDIX 1: CELL TITER-BLUE® PROTOCOL OPTIMISATION	264
APPENDIX 2: PRIMER EFFICIENCY OPTIMISATION	267
APPENDIX 3: RAYBIO® PROTEIN ARRAY MAP	270
APPENDIX 4: PROTEIN RESULTS	272
APPENDIX 5: GENE EXPRESSION RESULTS	276

LIST OF FIGURES

Figure 1.1.	Schematic diagram of the microstructure of mature bone seen in transverse and longitudinal section.	6
Figure 1.2.	Temporal changes in expression of osteoblast cell genes associated with rat calvarial osteoblast cell phenotype.	12
Figure 1.3.	Schematic and histological representation of secondary fracture healing stages.	41
Figure 1.4.	Schematic model of the three types of osseous callus encountered at bone repair site.	42
Figure 2.1.	Phase-separation of bone marrow using Ficoll (Histo-paque, 1077).	51
Figure 2.2.	Schematic representation of pMX-GFP retroviral vector and pCMV-VSV-G envelope vector.	54
Figure 2.3.	Outline of stimulation experiments and analysis.	59
Figure 2.4.	Schematic principle of RayBio [®] Human Cytokine Antibody Array protocol.	78
Figure 3.1.	Cell number quantification of HOb, SaOs2, MG63 and MC3T3E1 cells.	88
Figure 3.2.	Diagram shows the mean alkaline phosphatase activity in primary human osteoblast cells and osteoblast cell lines: SaOs2, MG63 and MC3T3E1.	89
Figure 3.3.	Representative micrographs of alkaline phosphatase activity at day 1, 7, 14, 21 and 28 in primary human osteoblast cells and osteoblast cell lines.	90
Figure 3.4.	Representative micrographs of mineralisation at day 1, 7, 14, 21 and 28 in primary human osteoblast cells and osteoblast cell lines.	92
Figure 3.5A-B.	Comparative real-time PCR results of Runx2 and type I collagen performed at day 1, 7, 14, 21 and 28 of culture period of primary human osteoblast cells and osteoblast cell lines.	95
Figure 3.5C-D.	Comparative real-time PCR result of ALP, osteocalcin performed at day 1, 7, 14, 21 and 28 of culture period of primary human osteoblast cells and osteoblast cell lines.	96

Figure 4.1.	Comparative real-time PCR results of Runx2, type I collagen, ALP and OC genes expression in MSC at day 21 of indirect co-culture with MG63 in monolayer.	109
Figure 4.2.	Diagram shows the mean of alkaline phosphatase protein activity in 30 minutes relative to the amount of DNA at day 14.	110
Figure 4.3.	Diagram shows the mean of ⁴⁵ Ca incorporation relative to the amount of DNA at day 21.	111
Figure 4.4.	Comparative real-time PCR results of Runx2, type I collagen, ALP and OC genes expression in MG63 at day 21 of co-culture with MSC in monolayer.	114
Figure 4.5.	Diagram shows the mean of alkaline phosphatase protein activity in 30 minutes relative to the amount of DNA at day 14.	116
Figure 4.6.	Diagram shows the mean of ⁴⁵ Ca incorporation relative to the amount of DNA at day 21.	117
Figure 4.7.	Comparative real-time PCR results of Runx2, type I collagen, ALP and OC genes expression in MSC at day 21 of co-culture with MG63.	121
Figure 4.8.	Diagrams show the mean of COL1/Runx2, ALP/Runx2 and OC/Runx2 ratio in gene expression at day 21.	123
Figure 4.9.	Comparative real-time PCR results of Runx2, type I collagen, ALP and OC genes expression in MG63 at day 21 of co-culture with MSC.	123
Figure 4.10.	Diagram shows the mean of alkaline phosphatase activity in 30 minutes relative to the amount of DNA at day 14.	127
Figure 4.11.	Diagram shows the mean of ⁴⁵ Ca incorporation relative to the amount of DNA at day 21.	128
Figure 4.12.	Diagrams show the transduction efficiency of MG63 cells with GFP.	129
Figure 4.13.	Diagrams show the post-sort of cells separated with FACS after the transduction with GFP.	130
Figure 4.14.	Representative microphotographs of MG63 expressing GFP and MG63 cells in culture.	130

Figure 4.15.	Diagrams show the analysis of MG63 cells expressing GFP used for establishing single cell colonies.	131
Figure 4.16.	Diagram shows the overlay of histograms of GFP intensity of 3 selected colonies obtained after seeding single cell colonies.	132
Figure 4.17.	The amount of mean DNA quantified during the culture of MG63 and MGreen63 at day 2, 4, 6, 8 and 10.	133
Figure 4.18.	Diagram shows the mean alkaline phosphatase (ALP) activity with the standard error of the mean in MG-63 and MGreen63.	134
Figure 4.19.	Representative microphotographs of MGreen63 and MG63 cells at day 21.	135
Figure 4.20A-C.	Comparative real-time PCR results of Runx2, type I collagen and ALP performed at day 2, 7, 14 and 21 of culture period of MG63 and MGreen63 cell lines cultured in osteogenic (DM) or growth medium (GM).	137
Figure 4.20D-E.	Comparative real-time PCR results of osteocalcin and E11 performed at day 2, 7, 14 and 21 of culture period of MG63 and MGreen63 cell lines.	138
Figure 5.1.	Diagrams show the mRNA levels of cytokines in MSC cells stimulated by IL1 β , SCF, GCSF and SDF1.	153
Figure 5.2.	Gene expression levels of cytokines in MSC cell stimulated with IL1 β .	156
Figure 5.3.	Gene expression levels of cytokines in MSC cells stimulated with SCF.	157
Figure 5.4.	Diagrams show the fold change gene expression relative to control from each donor 48 hours after the stimulation of MSC with IL1 β or SCF for 2 hours.	159
Figure 5.5.	Diagrams show the mean fold change gene expression relative to control 48 hours after the stimulation of MSC with IL1 β or SCF for 2 hours.	161
Figure 5.6.	Protein levels of cytokines in medium conditioned by MSCs stimulated with IL1 β .	165
Figure 5.7.	Protein levels of cytokines in medium conditioned by MSCs stimulated with SCF.	166

Figure 5.8.	Diagram showing the amount of mean DNA with the standard error of the mean, quantified during the culture of MSC cells in GM medium with the addition of conditioned medium.	168
Figure 5.9A-C.	Diagrams show the mean fold change in expression of Sox9, Runx2 and type I collagen genes at day 7 and 14 in relative to Control CM+GM at day 2.	171
Figure 5.9D-E.	Diagrams show the mean fold change in expression of ALP and OC genes at day 7 and 14 in relative to Control CM+GM at day 2.	172
Figure 5.10A-B.	Diagrams show the gene expression ratio of Runx2/Sox9 and ALP/Runx2 at day 7 and 14.	174
Figure 5.10C-D.	Diagrams show the gene expression ratio of COL1/Runx2 and OC/Runx2 at day 7 and 14.	175
Figure 5.11.	Diagram shows the mean alkaline phosphatase activity in 30 minutes relative to the amount of DNA.	177
Figure 5.12.	Representative images of Alizarin Red S staining of MSC at day 28.	178
Figure 5.13.	Diagram shows the mean amount of bound ARS at day 28.	179
Figure 6.1.	Representative microphotographs showing the viability of MSCs cultured within type I collagen-hydroxyapatite gel at day 2 and day 37.	196
Figure 6.2.	Diagram shows the mean alkaline phosphatase activity in 30 minutes relative to the amount of DNA.	197
Figure 6.3.	Micrographs show immunolabelling of alkaline phosphatase detected within micromass and type I collagen-hydroxyapatite of MSCs at day 14.	198
Figure 6.4.	Micrographs show immunolabelling of osteocalcin detected within micromass and type I collagen-hydroxyapatite of MSCs at day 14.	199
Figure 6.5.	Diagrams show the gene expression of Sox9, Runx2 and Runx2/Sox9 ratio in MSCs.	202
Figure 6.6.A-B.	Diagrams show the gene expression of COL1 and ALP in MSCs.	205
Figure 6.6.C-D.	Diagrams show the gene expression ratio of OC and E11 in MSCs.	206

Figure 6.7. Stages of osteoblast lineage cells differentiation implying the results obtained from MSCs cultured in monolayer, micromass and type I collagen-hydroxyapatite for 14 days.

212

LIST OF TABLES

Table 1.1.	Cell models and their culture conditions required.	29
Table 2.1.	Origin of osteoblast and MSC cells used in this study.	50
Table 2.2.	List of supplements used for osteogenic differentiation of MSC, HOOb, MC3T3E1, MG63 and SaOs2 cells.	52
Table 2.3.	Experimental groups and configuration of cells used in monolayer co-culture study.	60
Table 2.4.	Experimental groups and configuration of cells used in micromass co-culture study.	61
Table 2.5.	Primer sequences used for Real-Time PCR with SybrGreen method.	73
Table 2.6.	Primer and probe sequences used for Real-Time PCR with TaqMan method.	75
Table 2.7.	Functional grouping of genes included in Human Common Cytokines RT ² Profiler™ PCR array plate.	76
Table 2.8.	Specifications of blocking reagent, primary antibodies and secondary anti-body used for immunochemistry.	82
Table 4.1.	Description of groups included in the analysis of indirect co-culture of MSC and MG63 in monolayer.	107
Table 4.2.	Description of the groups included for analysis of indirect co-culture of MSCs and MG63 in micromass.	119
Table 5.1.	Details about MSC donor isolation site and short-term stimulation experiment outline.	150
Table 5.2.	Functional grouping of cytokines regulated by 2 hours stimulation of bone marrow derived MSC cells with 10ng/ml IL1 β or 100ng/ml SCF.	163
Table 6.1.	The description of the type I collagen-hydroxyapatite optimisation process.	195

THESIS BACKGROUND

Within bone cells are embedded in a mineralised organic matrix composed of type I collagen, non-collagenous proteins and hydroxyapatite. In this milieu bone cells interact with ECM and each other through soluble factors or direct interactions which determine cell behaviour and phenotype, including proliferation, motility, metabolism, differentiation and survival. All these are important to maintain the specificity and homeostasis of the bone. Since the first attempt of isolation and *in vitro* culture of osteoblast cells from adult human bone by Bard et al (Bard et al., 1972), a great improvement in the knowledge of the biology of bone and, in particular, osteoblastic cells have been made. Nevertheless, the treatment of acute or chronic pathological conditions of bone is challenging. Within the last two decades, new tissue engineering strategies have been developed hoping for supporting the treatment these conditions and bone regeneration. Yet, the proper evaluation and understanding of the occurring processes in *in vitro* is fundamental when aiming for the best clinical outcome. Hence, it is crucial to apply the appropriate and reliable models for osteogenic differentiation of cells and its regulation in *in vitro* research. The research within this thesis responds for the need of reliable *in vitro* models by defining and evaluating their relevance to the physiological context.

Various cell culture models and cell culture systems have been employed for tracking various aspects of osteoprogenitor and osteoblast cell biology. The use of cell models allows overcoming the concern regarding the limited availability of primary cells. Stabilised osteoblastic cell lines have been developed as models for *in vitro* investigation of the regulation of cell differentiation, cytokine and hormonal regulation, synthesis and secretion of matrix proteins, molecular mechanisms of bone diseases, and drug pharmacokinetics. Nevertheless, in the case of osteoblast cells the existing differences, such as species-related, between primary human cells and various osteoblast cell models complicate the evaluation of results and comparisons with human situation. In chapter 3, this problem has been addressed. We aimed to characterise and compare commonly used osteoblast cell

models derived from different sources in order to determine the relevance of osteoblast cell models for bone-related studies.

Taking into account the various cell types present in the bone and the complex ECM, the net of the interactions that occurs is very intricate which makes their *in vitro* investigations challenging. Nevertheless, direct and indirect *in vitro* co-culture models for the investigations aiming to elucidate the manner and importance of cells crosstalk have been developed. Although, models for both type of co-cultures are mainly based on monolayer *in vitro* culture systems, recently more attention has been directed towards a 3D co-culture, including the spheroids or scaffold systems. Regarding the communication of osteoblast cells and their progenitors, most of the evidences are based on the *in vitro* co-cultures of murine or rat cell models. Hence, in chapter 4, we aimed to elucidate the communication modes between cells derived from human bone. Specifically, the indirect communication between human bone forming cells in a monolayer and 3D co-cultures was investigated. The investigations regarding the paracrine communication were continued further. In chapter 5, the aim was to enhance the paracrine activity of cells and its functional evaluation regarding the stimulation of differentiation into an osteoblastic phenotype of MSCs.

For decades, a monolayer culture system has been considered as a gold standard *in vitro* culture model. This simplified system ensures the controlled culture environment. However, it is clear that this system is not physiologically relevant. Results obtained in chapter 4 indicated the co-culture of MSC and osteoblast cells in a 3D micromass system promoted the osteogenic differentiation of MSCs. Encouraged by these results, we investigated the effect of the *in vitro* cell culture environment on the osteogenic differentiation of MSCs. For this, within chapter 6, two 3D culture models were used, including a standard high density micromass culture and a novel type I collagen-hydroxyapatite hydrogel. By employing the two different systems, the importance of the ECM for the osteogenic differentiation of bone derived MSCs was investigated. Additionally, the behaviour of MSCs in the 3D culture models was compared with the monolayer. Ultimately, we aimed to establish a 3D osteoblast cell model resembling a more natural milieu allowing

for better understanding of the osteoblastic cell development and application for cell-cell communication research.

CHAPTER 1

INTRODUCTION

Sections of this chapter have been previously published:

Czekanska E.M., Stoddart M.J., Richards R.G., Hayes J.S. In search of an osteoblast cell model for *in vitro* research. *Eur Cell Mater* 2012 9;24:1-17.

1.1. Bone biology

1.1.1. Bone function

The skeletal system of the human body is comprised of bones, cartilage, muscles, ligaments and tendons. Bone is a complex and dynamic vascular mineralized connective tissue with various mechanical, synthetic and metabolic functions.

The skeleton acts as a frame for the body giving it support and keeping its shape. In particular, bones provide physical protection and support for internal organs, such as the skull protecting the brain, or ribs protecting the lungs and heart. Bone serves as an attachment site for tendons and muscles which together form a movement apparatus. Moreover, the presence of bone is essential for the sense of hearing. The auditory ossicles (*malleus*-hammer, *incus*-anvil, *stapes*-stirrup) present in the middle ear space transmit sounds waves from the air to the cochlea (Gray, 1973). In addition, within the medullar cavity of long bones and the interstices of cancellous bone marrow is found, which is the source of multipotent cells and the centre of haematopoiesis. Finally, by having a direct effect on energy metabolism, bone acts as an endocrine organ whose action influence the whole body (Schwetz et al., 2012).

1.1.2. Bone microstructure

Regarding their macroscopic appearance, two forms of bone in the skeleton are distinguishable, namely compact (dense) bone and spongy (cancellous) bone (Fig.1.1A). Most bones contain both of these forms.

Compact bone is dense, stiff and always located externally to the spongy bone (Fig.1.1A). It consists of a number of irregular cylindrical units named osteons (Harvesian systems) which are predominantly oriented in longitudinal direction. Each osteon comprises of a Harvesian (central) canal surrounded by concentric lamellae of bony tissue varying from 5 to 7 μ m in thickness. Osteocytes, located in lacunae, make contact with other cells via transverse canaliculi canals. These canals connect with the central (Harvesian) canal (Fig.1.1B&C). The central canal

encloses a neurovascular bundle, which connects through Volkmann's canals located perpendicularly to central canals. Usually the central canal is 50 μ m in diameter and contains one or two capillaries and mainly non-myelinated nerve fibres, together with Schwann cells. The network formed by canaliculi canals and Harvesian canal facilitates the exchange of nutrients and metabolic waste.

Compared to compact bone, cancellous bone has a less dense and more porous matrix which results in a higher surface area to mass ratio and weaker mechanical properties. These properties enable cancellous bone to be suitable for metabolic functions. To fulfil all its metabolic functions, cancellous bone is highly vascularised. Here, the large diameter nutrient vessels and arteries, passing from epiphysis towards subchondral bone, form intraosseous anastomoses. The primary structural and functional unit of spongy bone is a honeycomb like trabecular structure. In long bones, cancellous bone is located proximal to joints, whereas in flat bones it is between cortical bone.

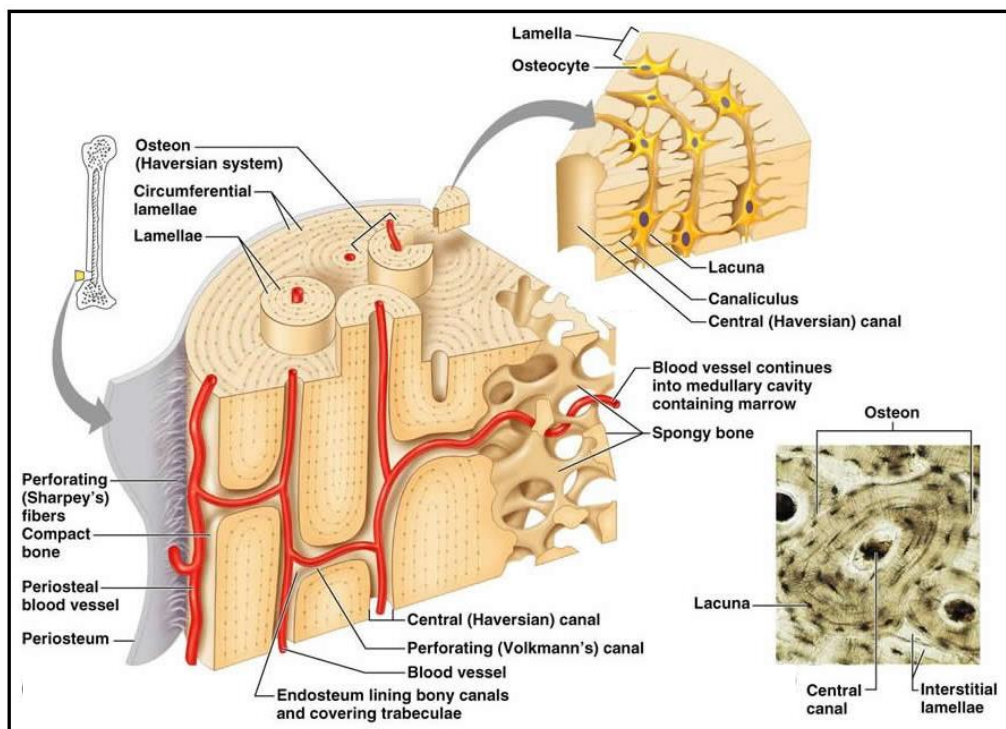


Figure 1.1. Schematic diagram of the microstructure of mature bone seen in transverse and longitudinal section. Taken from: <http://classes.midlandstech.edu>

1.1.3. Bone matrix

1.1.3.1. Inorganic compartment

The main inorganic bone matrix component, which gives bone its hardness and rigidity, is an analogue of naturally occurring hydroxyapatite ($\text{Ca}_{10}(\text{PO}_4)_6(\text{OH})_2$). In hard tissues, such as bone and dentine, the OH group can be substituted with CO_3^{2-} , Mg^{2+} , F^- or H_2PO_4^- (Boskey, 2008). In general, apatite crystals deposited in bone have a needle-shape measuring 20-40nm in length and 3-6nm in breadth (Gray, 1973). The deposition of the apatite crystals is oriented in relation to the collagen fibrils. Specifically, in bone, crystals are located within the individual fibers and along the fibril surfaces in the extrafibrillar space between the fibers (Orgel et al., 2011; Veis and Dorvee, 2013). The process of biomineralisation is initiated and coordinated by the bone-related proteins. Biomineralisation is biphasic, comprising mineral formation within matrix vesicles (MV) and mineral propagation into the extracellular matrix (ECM), which is regulated by enzymes, proteins and phospholipids (Anderson, 2003). The specific role of the main regulators of biomineralisation is discussed in the following paragraphs.

1.1.3.2. Organic compartment

1.1.3.2.1. Collagen matrix

Type I collagen is the most abundant protein in bone comprising about 90% of bone's organic material. It is also abundantly present in the extracellular matrix of tendons, ligaments and skin. In bone it provides tensile strength and torsional stiffness, especially after calcification. Type I collagen belongs to the group of fibrillar collagens, which consist of long triple helical molecules self-assembling into highly organised fibres (Kadler et al., 1996). Each molecule of type I collagen, called tropocollagen, is usually composed of two α_1 and one α_2 chains. In humans, genes coding these chains have distinct locations. Specifically, the gene coding the α_1 chain is located at chromosome 17 (17q21.3-q22), whereas the gene coding the α_2 chain is located at chromosome 7 (7q21.3-q22) (Chu et al., 1984; de Wet et al., 1987; Rosset and de Crombrughe, 2002). Both of these genes are similar in structure, having 52 exons. The difference between the genes for both chains is the location of the coding sequence for the triple helical domain and N-propeptide. The triple

helical domain of the α_1 chain is coded by 3 exons, whereas it is coded by 2 exons for the α_2 chain. Moreover, the N-propeptide is coded by 3 exons for α_1 and 6 for α_2 chain. In both cases, the main triple helix and C-peptide are coded by 41 and 4 exons, respectively. After transcription, the pre-mRNA undergoes exon splicing, capping and addition of poly(A) tail. This mature mRNA is translated in polysomes and the resulting protein is transported to the endoplasmic reticulum where it is subjected to posttranslational modifications. Upon entering the rough endoplasmic reticulum (RER), signal peptides from the N-terminal ends are cleaved, followed by the hydroxylation and glycosylation of both α_1 and α_2 chains at the X and the Y position of the Gly-X-Y triplets. As a result of hydroxylation, approximately 100 proline residues at the Y position, few at the X position and about 10 lysines at Y position undergo hydroxylation by prolyl-4-hydroxylase, prolyl-3-hydroxylase and lysyl-hydroxylase, respectively. Importantly, the hydroxylation process is essential for stable folding into a triple helix at a later time. The hydroxylation process can only progress in the presence of cofactors, such as Fe^{2+} , O_2 , α -ketoglutarate and ascorbic acid. In the next process, glucosyl and galactosyl residues are added to the ϵ -OH group of the hydroxylated-lysines by hydroxylysyl galactosyltransferase and galactosylhydroxyl-glucosyltransferase, respectively. Next, each pro- α chain of C-peptide undergoes the addition of mannose-rich oligosaccharides. Following this process, C-propeptides of both α_1 and α_2 propeptides associate, with the formation of inter and intrachain disulfide bonds. Subsequently, the triple helix is formed progressing from the C-terminal end towards the N-terminal end. The final step in the rough endoplasmic reticulum is directed by HSP47 protein, the collagen specific molecular chaperone, which stabilises the triple helical structure of the procollagen molecule. From the RER, procollagen proceeds into the Golgi complex via ERGICs (Endoplasmic Reticulum to Golgi Intermediate Compartments) or VTCs (Vesicular Tubular Clusters) in a COPII-dependent process (Coat Protein Complex II). Subsequently, it is secreted in the extracellular matrix where specific amino- and carboxypeptidases cleave the N- and C-propeptides, respectively (Rosset and de Crombrughe, 2002). Mature collagen molecules naturally assemble into quarter-staggered/cross-striated fibrils in an entropy-driven process due to the loss of solubility properties resulting from the cleavage of terminal propeptides (Kadler et al., 1996). In the type I collagen

fibril, molecules are parallel to each other. Moreover, they overlap each other by multiples of 67nm (distance D). Each molecule is 4.4D (300nm) long and spaced from another one by 0.6D gap. The final step of collagen biosynthesis is the introduction of covalent cross-links in order to stabilise the supramolecular assembly. In the case of fibrillar collagens, including type I collagen, cross-linking is initiated and driven by lysyl oxidases, which are copper-dependent amine oxidases (Hulmes, 2008; Molnar et al., 2003). These enzymes convert lysine or hydroxylysine in the C- and N-terminal telopeptides to respective peptidyl aldehydes. As a result of this reaction, aldehydes on one molecule condense with aldehydes of other lysines and hydroxylysines on adjacent molecules, forming interchain and intrachain covalent cross-links which significantly increase the tensile strength of the fibrils. The role of collagen synthesis and its proper alignment is essential for osteoblast noncollagenous protein expression, synthesis and differentiation of bone cells. Moreover, in the ECM milieu, collagen, together with the non-collagenous proteins, including bone sialoprotein (BSP), osteonectin, osteopontin and osteocalcin regulate mineral propagation.

1.1.3.2.2. Non-collagenous proteins and their role in matrix mineralisation

The expression and localisation of specified non-collagenous proteins expressed at the mineralisation stage have been studied in detail using human, rat and chicken *in vitro* and *in vivo*.

Alkaline phosphatase (ALP) has an important role in the mineralisation and its expression coincides with the synthesis of the type I collagen (Whyte, 2002). The tissue non-specific isoform of ALP present in bone is bound to the matrix vesicles (MV) within the cell membrane that bud from osteoblasts via phosphatidylinositol-glycan (Moss, 1997; Hoshi et al., 1997). ALP acts locally to increase the phosphate (Pi) concentration *via* hydrolysis of monophosphate esters (inorganic pyrophosphate) at high pH (Harris, 1990), which together with calcium ions form the substrate for hydroxyapatite formation. During the first phase of mineral formation, liberated Pi is transported to the MV via type III Na/Pi co-transporter, whereas calcium accumulation is facilitated by calcium binding

proteins and phospholipids, such as annexin II, annexin V, calbindin D9K and phosphatidyloserine, respectively (Orimo, 2010). The saturation of the microenvironment of MV with calcium and PO_4 ions leads to the precipitation of calcium phosphate that is subsequently released from the MV.

Bone sialoprotein (BSP) and osteonectin belong to the SIBLING (Small Integrin-binding Ligand N-linked Glycoprotein) gene family which contain RGD (Arg-Gly-Asp) motifs in their structure that can bind to various matrix constituents and cell types (Roach, 1994). Studies using a steady-state agarose gel system showed that BSP acts as a nucleation factor for hydroxyapatite formation and deposition (Hunter and Goldberg, 1993), whereas osteonectin is a promoter of hydroxyapatite crystal formation. The detailed analysis of this process revealed that osteonectin acts as a promoter only when connected to the collagen by binding to its discrete fibrillar sites. It reacts with calcium from hydroxyapatite providing the appropriate alignment and organisation of hydroxyapatite with respect to the collagen axis (Lane and Sage, 1994; Termine et al., 1981).

Osteopontin is another glycoprotein with a RGD sequence, that is secreted in mineralising and non-mineralising tissues, and in both normal and pathological states (McKee and Nanci, 1996). Conversely to BSP and osteonectin, osteopontin is believed to act as an inhibitor of mineralisation as it hinders hydroxyapatite nucleation *de novo* in gelatine and agarose gel systems (Hunter et al., 1996), by preventing premature precipitation of calcium phosphate crystals (Roach, 1994). Osteopontin is first expressed in the proliferation phase, where it reaches the level of 25% of maximum that occurs during mineralisation (Sodek *et al.*, 2000). Additionally, owing to a RGD sequence in peptide structure osteopontin serves as a cell-matrix/matrix-mineral mediator (McKee and Nanci, 1996; Hunter et al., 1996).

Another non-collagenous protein, osteocalcin contains three gamma-carboxyglutamic acid residues formed by a posttranslational carboxylation of glutamic acid residues (Romberg et al., 1986). These residues interact with calcium and hydroxyapatite (Poser and Price, 1979) by regulating the process of mineralisation and bone remodelling (Roach, 1994). At the gene expression level,

no osteocalcin mRNA was detected in tissues, such as the liver, heart, lung and skin (Fraser and Price, 1988;Hauschka et al., 1989). Instead, the presence and accumulation of osteocalcin is restricted to the osseous culture systems (Auf'mkolk et al., 1985;Auf'mkolk and Schwartz, 1985;Aarden et al., 1996).

The radioimmunoassay analysis of mineralising tissues from different species timed the accumulation of osteocalcin in extracellular matrix of the bone only after the initiation of the mineral deposition (Price et al., 1981). Thus, the osteocalcin is considered as a marker of late osteoblast differentiation (Owen et al., 1990).

1.2. Biology of bone forming cells

1.2.1. The principles of osteoblastic lineage cell development

Osteoblast lineage cells originate from multipotent mesenchymal stem cells, which can also give rise to bone marrow stromal cells, chondrocytes, muscle cells, and adipocytes (Aubin and Triffit, 2002).

The generally accepted model of osteoblast cell differentiation encompasses the progression from osteoprogenitor cells to preosteoblast, osteoblasts, and then bone lining cells or osteocytes. *In vitro* osteoblast cell differentiation has been studied using various cell models in monolayer culture system. One of the most widely accepted and referenced models of osteoblast differentiation were derived from observations of rat bone-derived cells, which synthesized mineralised matrix (Lian and Stein, 1995).

Based on the results from *in vitro* investigation of progressive establishment of the osteoblast cell phenotype, it is accepted that osteoblast cells differentiate through a characterised temporal sequence of expression osteoblast markers (Lian and Stein, 1992). Specifically, three phases were identified, namely proliferation, matrix synthesis, matrix maturation and mineralisation, with each phase delineated by characteristic changes in protein and gene expression (Fig.1.2).

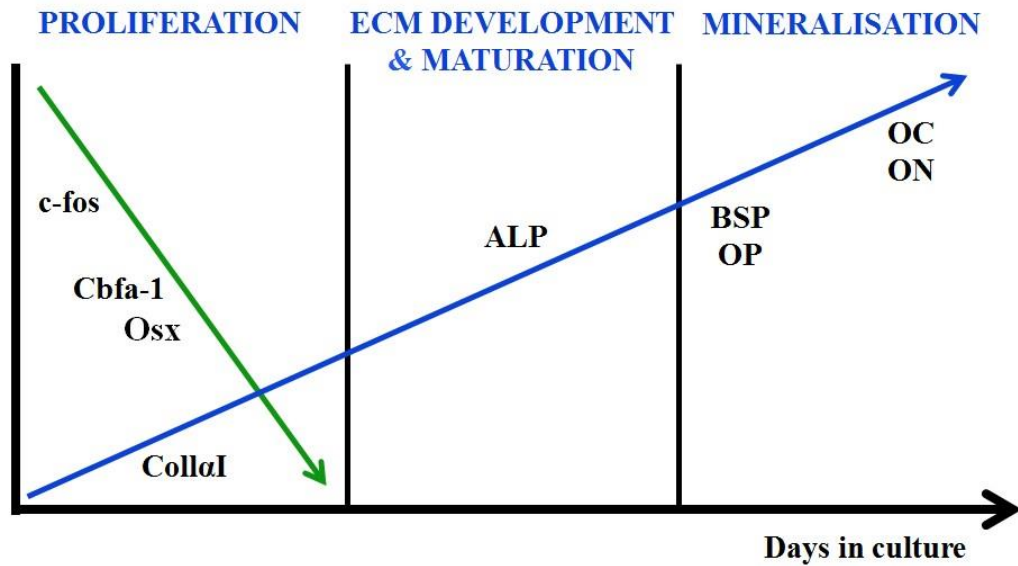


Figure 1.2. Temporal changes in expression of osteoblast cell genes associated with rat calvarial osteoblast cell phenotype. These changes are illustrated as arrows representing changes in cell cycle-regulated genes (green) and genes associated with the osteoblast phenotype differentiation (blue). ALP-alkaline phosphatase, BSP-bone sialoprotein, c-fos-proto-oncogen, Cbfa-1 (Runx2) - core-binding factor $\alpha 1$, Coll $\alpha 1$ -type I collagen, OC-osteocalcin, ON-osteonectin, OP-osteopontin, Osx-Osterix. Adapted from (Lian and Stein, 1992).

The genes associated with the first phase of the cell cycle are histones, cyclines and protooncogenes (c-fos, c-myc, c-jun), which are responsible for modulating cell proliferation. They are up-regulated together with the transcription factors core binding factor alpha 1 (Cbfa1/Runx2) and osterix (Osx/SP7) (Lian and Stein, 1992). Runx2 is a runt-domain gene widely considered as earliest osteoblastic marker. It binds to the osteoblast-specific element (OSE-2), which activates the promoter of the major osteoblast genes expressed, such as osteocalcin, alkaline phosphatase (ALP), bone sialoprotein (BSP), osteopontin and $\alpha 1$ type I collagen genes (Ducy, 2000;Ducy et al., 1997). Gene expression analysis and *in situ* hybridisation have demonstrated Runx2 expression early in lateral plate mesoderm before the existence of actual osteoblast cells (Ducy et al., 1997). Furthermore, studies using Runx2 deficient mice demonstrated a lack of adequate calcification of the skull, humerus and femur resulting in death straight after birth (Komori et al., 1997). Interestingly, maintained expression of Runx2 produces a reduction in cortical bone mass and increased trabecular bone mass mineralisation (Maruyama et al., 2007)

indicating that while this factor is essential for osteoblast lineage specificity, its prolonged expression actually hinders subsequent osteoblast differentiation.

Downstream of Runx2 is the zinc-finger transcription factor Osterix. Similar to Runx2, osterix is essential for osteoblast differentiation and subsequent bone formation. In osterix knockout animals, preosteoblast cells are prevented from differentiating into mature osteoblasts resulting in an inhibition of both intramembranous and endochondral ossification (Komori et al., 1997). Additionally during proliferation, adhesion proteins, type I collagen and growth factors, such as transforming growth factor β (TGF β) and fibroblast growth factor (FGF), are actively synthesized (Aubin and Triffit, 2002).

Other than providing a scaffold for mineral deposition, type I collagen is essential for osteoblast cell functionality based on the fact that dysfunctional fibril formation impair subsequent stages of osteoblast phenotypic development (Wenstrup et al., 1996). Moreover, through interaction with $\alpha_2\beta_1$ integrin, collagen influences activation of the osteocalcin promoter within the nucleus (Xiao et al., 1998). Additionally, the $\alpha_2\beta_1$ integrin-collagen interaction activates mitogen-activated protein kinase (MAPK) signalling pathway, leading to phosphorylation of Runx2 (Wenstrup et al., 1996). In cells expressing truncated pro-collagen $\alpha 1$ and secreting shortened fibrils, cells had higher and longer proliferation and decreased ALP activity. On the other hand, osteocalcin secretion was elevated 5-fold when compared to cells expressing normal collagen (Wenstrup et al., 1996).

Active osteoblasts are cuboidal cells enriched with endoplasmic reticulum as they synthesise large quantities of proteins (Gay et al., 2000). These include proteins, such as osteopontin, osteonectin, osteocalcin, and bone sialoprotein (detailed description in paragraph 1.1.3.2.2), whose expression by osteoblasts reaches maximal levels during mineralisation (Lian and Stein, 1992). Osteoblasts are asymmetric cells meaning that they secrete collagen and non-collagenous proteins in the form of osteoid on one side, whereas their contralateral side is sensitive to regulatory signals (Robey, 2002). Importantly, osteoblast cells also secrete autocrine

and paracrine factors. The latter strongly acts on osteocytes and osteoclast cells regulating their function (Gay et al., 2000).

With the end of the bone formation phase, osteoblast cells can become osteocytes, transform into inactive osteoblasts and become bone lining cells or undergo programmed cell death (apoptosis).

In humans, depending on the bone type and age, between 10-30% of osteoblasts differentiate into osteocyte cells, while the majority of cells undergo apoptosis (Parfitt, 1990; Aubin and Triffit, 2002). When differentiating into osteocytes, osteoblasts become embedded in the osteoid. At this stage, the osteoblast enlarges in size and has a well-developed Golgi apparatus for collagen storage. When fully embedded in the matrix, cells cease their activity and become smaller in size due to reduced Golgi apparatus and endoplasmic reticulum. The bone type, size and the activity of committed osteoblasts influence the shape and the size of newly formed osteocyte. Specifically, in rapidly formed woven bone with randomly oriented collagen fibres, osteocytes are isodiametric. In lamellar bone they are elongated along the longitudinal axis and round or triangular in the transverse plane (Holtrop, 1990).

Currently, five transitional stages from osteoblast to mature osteocyte are distinguished based on the heterogeneity in the cell morphology, molecular and secretory characteristics. These include, osteoblast, osteoblastic-osteocyte (type I osteocyte), osteoid-osteocyte (type II osteocyte), type III osteocyte, young osteocyte, old osteocyte (Palumbo, 1986; Holtrop, 1990; Franz-Odenaal et al., 2006). Importantly, based on research evidence the Bonewald's group suggested that the osteoid-osteocyte regulates and controls the mineralisation process of bone rather than osteoblasts themselves (Dallas and Bonewald, 2010).

As previously stated, gene and protein expression is significantly different between the osteoblast and developing osteocyte cells. In general, osteocytes synthesise a number of proteins important for cytoskeletal function, including CapG, cdc42 and E11/podoplanin (Dallas and Bonewald, 2010). Although, the latter is not

exclusive for bone-lineage cells; it is believed to be the earliest marker for osteocytes. In fact, E11 is highly expressed in osteoid-osteocytes, but not in old osteocytes (Zhang et al., 2006). This protein is associated with the formation and elongation of dendrites, through which osteocytes interact with each other and with cells on the bone surface. The expression of E11 and dendrites is regulated in bone by mechanical load and shear stress (Zhang et al., 2006). In response to the shear stress, osteocytes release nitric oxide (NO), ATP and prostaglandin, all influencing the activity of osteoblasts and osteoclasts, which results in new bone formation (Bonewald, 2010). Instead of E11, more mature osteocytes express high levels of sclerostin, a negative regulator of bone formation that inhibits canonical Wnt/ β -catenin signalling pathway (Dallas and Bonewald, 2010). By the expression of phosphate-regulating neutral endopeptidase X-linked (PHEX), dentin matrix acidic metalloproteinase (DMP-1), matrix extracellular phosphoglycoprotein (MEPE) and fibroblast growth factor 23 (FGF23), osteocytes regulate phosphate and biomineralisation. Upon apoptosis, osteocytes release apoptotic bodies and homing factors for osteoclasts, such as RANKL, responsible for the bone resorption (Bonewald, 2010).

Other osteoblast descendants in the adult bones are the bone-lining cells covering the bone surface. These cells are flat and elongated, without proliferative capacities (Aubin, 1998). Bone-lining cells can be reactivated to active osteoblast cells in response to a specific stimulus, such as parathyroid hormone (PTH) (Dobnig and Turner, 1995). Additionally, they take part in the bone remodelling process by secreting collagenase to remove the unmineralised collagenous layer of matrix, enabling osteoclasts to attach to the mineralised matrix (Manolagas, 2000).

1.2.2. Osteoclast cells

Osteoclast cells differentiate from the granulocyte-macrophage progenitors (myeloid cells) of the hematopoietic origin. Two hematopoietic factors secreted by osteoblasts and stromal cells, RANKL and M-CSF are prerequisite for osteoclastogenesis and the subsequent activation of RANK on the surface of the precursor cells. These factors induce expression of the specific osteoclast lineage genes, such as tartrate-resistant acid phosphatase (TRAP), cathepsin K,

calcitonin receptor and β_3 -integrin (Boyle et al., 2003). Mature osteoclasts are polykaryons arising from multiple (10-20) individual cells with abundant mitochondria and have high number of vesicles and vacuoles. The most characteristic feature of the active osteoclast cell is the ruffled border of their cell membrane which increases surface area interface at the bone resorption site. In the human skeleton, bone remodelling is entirely dependent on the bone resorption conducted by osteoclast cells (Manolagas, 2000). At the resorption site, before formation of ruffled border, osteoclasts attach to the bone through a membrane domain, called the sealing zone. Ruffled border is the resorption area originating from fusion of the cell membrane and intracellular acidic vesicles. On the opposite site of the osteoclast the functional secretory domain is formed (Vaananen et al., 2000). For the dissolution of HAP, osteoclast cells secrete H^+ protons through proton pumps and Cl^- through the chloride channels (Hall and Chambers, 1989). Organic matrix is degraded by proteolytic enzymes belonging to the lysosomal cysteine proteinases and matrix metalloproteinases. Especially, high levels of MMP9, MMP13, cathepsin K and collagenases are secreted into the resorption lacuna (Vaananen et al., 2000). Bone resorption products are eliminated through a transcytosolic vesicular pathway from the ruffled border to the functional secretory domain on the apical side of cells into the extracellular space (Salo et al., 1997; Vaananen et al., 2000). During osteoclastic degradation of the type I collagen network, matrix bound factors, such as IGFs are released and induce new bone formation through the stimulation of osteoblasts in a paracrine manner (Gelse et al., 2003). After fulfilling its resorption task, the osteoclast may repeat it once more or undergo apoptosis (Vaananen and Zhao, 2002).

1.3. Osteoblast cell models in in vitro research

Since the first attempt of isolation and *in vitro* culture of osteoblast cells from the adult human bone (Bard *et al.*, 1972), a great improvement in the knowledge of bone biology and, in particular, osteoblastic cells has been made. Immortalised osteoblastic cell lines have been developed as models for the *in vitro* investigation of the regulation of cell differentiation, cytokine, hormone regulation, synthesis

and secretion of matrix proteins, molecular mechanisms of bone diseases and drug pharmacokinetics. In more recent years, osteoblast cell culture has also evolved to include cytocompatibility and osteogenicity evaluation of the novel biomaterials.

Various cell culture models have been employed for studying osteoblast cell biology, including primary cells from different species, induced osteoblasts from pluripotent stem cells, immortalised and malignant cell lines. The use of these osteoblast models, as well as any *in vitro* cell model, presents advantages and disadvantages which need to be considered before embarking on any notable evaluation (Tab.1.1). In the following paragraphs, factors that influence the phenotype of osteoblast cells derived from different sources are presented and discussed. The advantages and disadvantages of these cell types will also be highlighted.

1.3.1. Human primary osteoblast cells

The main advantage of using primary human primary osteoblast cells (HOb's) is the lack of interspecies differences and they retain their differentiated phenotype *in vitro*. On the other hand, primary human cells represent a heterogeneous population of cells and, therefore, exhibit phenotypic differences relating to the skeletal location from which they were isolated (Kasperk et al., 1995; Martinez et al., 1999).

To date, several primary human osteoblast isolation methods have been developed, including enzymatic digestion and spontaneous outgrowth cultures (Gallagher, 2003; Gotoh et al., 1990). Several studies have identified an effect of the isolation technique on subsequent *in vitro* performance of cells (Voegelé et al., 2000; Jonsson et al., 1999). Specifically, cells obtained through the enzymatic isolation proliferate faster than cells from outgrowth cultures, but alkaline phosphatase (ALP) activity is comparable in cells from both isolation types (Voegelé et al., 2000). Contradictory results in terms of ALP activity were found in another study where the enzyme level was higher in cells obtained from outgrowth culture (Jonsson et al., 1999). This can be further influenced by the donor age. Indeed, cells from donors younger than 65 years-old were shown to have shorter population doubling times, than osteoblast cells from older donors (Voegelé et al., 2000). In agreement with this, a decreased rate of proliferation in trabecular bone cell cultures of donors over 60 years of has

been reported elsewhere (Evans et al., 1990), with the most significant decline being attributed to the first three decades of life (Fedarko et al., 1992; Shigeno and Ashton, 1995). Moreover, in cells isolated *via* outgrowth cultures, mineral deposition was more pronounced 4 weeks after osteogenic induction than in cells obtained from enzymatically digested bone specimens (Jonsson et al., 1997).

In correlation with the proliferation potential of cells, the expression of genes and protein synthesis associated with the osteoblast phenotype is also influenced by the donor age. Synthesis of type I collagen and osteonectin were at the highest level in cells isolated from foetal bones, up to 20 year-old donors. A decrease of approx. 65% in collagen levels were observed in cells obtained from donors above the age of 20 years old (Fedarko et al., 1992). Additionally, after the induction with $1,25(\text{OH})_2\text{D}_3$ the level of osteocalcin secreted by cells isolated from the foetal cortical femoral bone was less than cells from postnatal (age 4-12 years) and adult donors (20-30 years) (Morike et al., 1993; Morike et al., 1995). In cells from donors in the third decade of life, the protein level was 10-fold higher than in the foetal bone cells (Morike et al., 1995). Furthermore, osteocalcin expression became higher in foetal cells after 10 days of culture with osteogenic supplements and $1,25(\text{OH})_2\text{D}_3$ (Montjovent et al., 2004).

Considering the changes in the osteoblast phenotype relating to donor age, it is important to emphasize that bone aging, determined as changes in the degree and distribution of mineralisation occurs differently in cortical and cancellous bone (Bergot et al., 2009; Bonjour et al., 1991). This is reflected in osteoblast physiology with slower proliferation and increased secretion of ALP and OC in cells derived from the femoral head compared to the upper tibia and the lower femur (Martinez et al., 1999). Results from our laboratory also indicate higher proliferation and mineralisation potential of cells derived from knee than from femoral head bone (unpublished observation). Kasperk and colleagues (1995) conducted within-patient comparisons and demonstrated that the mandibular derived osteoblast cells had a higher proliferative rate associated with decreased ALP activity than cells isolated from the iliac crest. Furthermore, decreased expression of the $\text{FGF}\beta$ and IGFII genes was also observed in the mandibular-derived osteoblast cells (Kasperk et al., 1995).

With inclusion of the age defined differences, it was shown that cells from the knee had higher ALP activity in patients over 70 years-old than in those between 50 and 70. The opposite was seen in osteoblasts derived from the femoral head (Martinez et al., 1999). However, as stated above, the major differences in cellular behaviour are the most pronounced at earlier stages of life.

The age changes occurring in the bone composition affect mostly bones in the lumbar and hip regions in postmenopausal women due to the decline of oestrogen (Davis et al., 1994). Indeed, Zhang and colleagues (2004) reported that the expression of ALP, BSP and type I collagen was significantly increased in cells isolated from female patients below 15 years-old, which was observed to subsequently decline with increasing age. Furthermore, a 3.8-fold difference in ALP activity was noted between young and postmenopausal women while the osteocalcin level was shown to be higher in cells from the premenopausal women below 50 years-old (Zhang et al., 2004). In contrast, osteoblasts derived from the male femoral head and long bones did not show the age related differences in terms of ALP and osteocalcin level (Katzburg et al., 1999). Conversely, Battmann and co-workers (1997) reported that osteocalcin production by cells from the femoral head and iliac crest changed markedly with the age of donors, but were not correlated with gender differences (Battmann et al., 1997).

As presented above, many factors influence primary human osteoblast cell behaviour; age, site of isolation and gender differences are the most notable. Thus, the time frames for phenotypic changes *in vitro* differ for cells isolated from different origins. Some studies indicate that nodule formation in the mineralisation of human bone cell cultures may not occur (Siggelkow et al., 1999). Furthermore, the question arises, which factors are of utmost importance and should be included for screening cells (or donors) before applying them for research purposes? The answer is not simple and the selection of cells should be controlled and judged on the perspective of the addressed subject and the aim of study.

1.3.2. Animal primary osteoblasts

Due to limited accessibility of human osteoblast cells and their phenotypic heterogeneity, cells isolated from other species can provide an alternative *in vitro* research model. A distinct advantage is their ease of attainability compared to the human cell sources. For humans, the location of bone specimens for cell isolation are limited mainly to long bones, mandible and the iliac crest, whereas they can be obtained more easily from additional sites from animals, such as the calvaria. The selection of donor animals can be more controlled in relation to age, weight and sex. Unlike human donors, isolation from animals is not restricted to only pathological subjects. On the other hand, the distinct disadvantage of animal cells is the interspecies differences making extrapolation difficult. Furthermore, the biology and structure of bone is different among animals. Here, the sizes of the animal and weight influence bone composition, quality, remodelling method, healing and signalling pathways driving these processes (Pearce et al., 2007).

1.3.2.1. Rat cells

Rat osteoblast cells serve as a model in various *in vivo* and *in vitro* researches. In 1994, the Food and Drug Administration presented guidelines for preclinical and clinical evaluation of agents used in the treatment or prevention of postmenopausal osteoporosis, with the recommendation of using two animal models, rat and sheep, for this evaluation (Thompson et al., 1995). Due to the wide availability of bone samples and known genome, rat osteoblast cells are an attractive model for research focused on hormonal regulation of the cell phenotype (Abe et al., 2000; Aronow et al., 1990), as well as the osteoinductivity and cytotoxicity of polymer or implant biomaterials (Hayes et al., 2010; Liao et al., 2003; Washington et al., 2011; Wirth et al., 2008).

Rat osteoblast cells isolated from foetal, neonatal/adult calvaria or long bones retain their osteoblastic phenotype during *in vitro* culture (Manduca et al., 1997; Yamamoto et al., 2002). Osteoblast isolation from rat tissue is performed mainly through repeated enzymatic digestion and less often through the spontaneous migration from explant specimens. The use of enzymatic treatment has been shown to be an effective isolation method of cells from calvarial bones of foetal or neonatal animals (Declercq

et al., 2004). However, in this case the phenotype of the cells is influenced by many factors. As a result of enzymatic isolation, cells derived from individual fractions of digestion exhibit different osteoblastic differentiation ability and response to hormones (Lian and Stein, 1992). When comparing calvarial cells from five fractions obtained from rat foetuses, the first 3 fractions responded positively to dexamethasone administration with increased ALP activity and calcium deposition, whereas cells from last two fractions did not show this response. Moreover, based on the number of nodules formed and the assumption that nodule formation is correlated to the number of osteoprogenitor cells, fraction three contained the highest number of osteoprogenitor cells (Yamamoto et al., 2002).

Despite the fact that the rat 'donor' selection can be more controlled than for humans, the cell phenotype is similarly affected by age and sex of the animals, as well as the tissue origin. A comparative study by Declercq and colleagues (2004), evaluating osteoblastic cells derived from adult and foetal rat, via explant culture or enzymatic digestion, showed that the osteogenic differentiation was enhanced in cells isolated by proteolytic treatment, as determined by matrix mineralisation and nodule formation. Additionally, for cells originating from explant cultures, both calvarial and long bone (tibia) samples had lower ALP activity and more diffuse mineralisation pattern compared to foetal cells from enzymatically digested tissue. Moreover, the temporal pattern of mineralisation differed between different types of bone (Declercq et al., 2004). Other studies have shown that cells from the mandible of a rat foetus (20 day-old) demonstrated β -glycerophosphate (β GP)-independent matrix mineralisation, whereas β GP was required for nodule formation and mineralisation of calvarial cells obtained from the same animals (Abe et al., 2000; Bellows et al., 1987; Bellows et al., 1992).

Mineralisation was also noted to be influenced by donor age differences. For instance, cells isolated from 7 day-old rat tibia formed mineralised nodules after 41 days in culture compared to positive osteocalcin detection after just 21 days for foetal mandibular cells (Stringa et al., 1995). A more recent study has also revealed gender differences in osteoblast cells isolated from calvaria. Specifically, ALP activity in osteoblasts cells from both genders was positively regulated

by $1,25(\text{OH})_2\text{D}_3$ in similar manner, but cells derived from 6 week-old male rats had higher initial ALP activity compared to aged matched female counterparts. The dose-dependent response to $1,25(\text{OH})_2\text{D}_3$ was evident for cell proliferation and osteocalcin production, with decreased cell number and increased protein synthesis in osteoblast cells isolated from male donors (Olivares-Navarrete et al., 2010).

1.3.2.2. Bovine cells

Bovine and ovine derived osteoblast cells are less often used as osteoblast cell models compared to rodents. This is surprising considering that these animals are frequently used as large animal *in vivo* models, and other skeletal cells from these animals serve as established *in vitro* models. For instance, chondrocytes or intervertebral disc cells from bovine specimens are widely used in tissue engineering research and for investigating basic biological mechanisms (Collin et al., 2011;Peroglio et al., 2011;Sakai et al., 2009;Hoshihara et al., 2011;Dowthwaite et al., 2004). However, studies focused on bovine osteoblast cells are limited. The first attempts to explore *in vitro* bovine osteoblast culture system involved cells isolated from hind-limbs of 3 to 6 month-old foetal calves (Whitson et al., 1992). This resulted in the identification of functional osteoblast cells that secrete ALP, type I collagen, BSP, osteonectin and bone proteoglycans. Moreover, investigations showed 4.5-6 month-old foetus to be optimal for osteoblast cell isolation. The enzymatic extraction of osteoblast cells from foetus at this stage resulted in higher number of viable cells and superior proliferation compared to older foetuses. Additionally, cells from younger foetuses had slower mineralisation potential when compared to 4.5-6 months-old foetuses. In bovine cell cultures after stimulation, ALP activity increased in cultures by day 6, which was followed by an increase in mRNA expression of type I collagen, osteonectin and osteopontin (Whitson et al., 1992). In this system, the deposition of minerals and nodule formation were initiated 6 days after osteogenic induction with β -glycerophosphate and ascorbic acid (Ibaraki et al., 1992). The centres of mineralisation first appeared in the matrix located between the single cell layer adhering to the surface and multi-cellular layer located above (Whitson et al., 1984). Interestingly, these cells also formed independent and interconnected mineralised trabecular structures (Whitson et al., 1992). Interestingly, we have observed that the explant cultured cells isolated

from 6 month-old bovine specimens do not have the ability to form nodules or mineralise matrix. Furthermore, ALP activity remained at basal levels over a 21 day period but then increased rapidly by day 28.

1.3.2.3. Ovine cells

In the majority of orthopaedic research studies, the sheep is considered an established large animal *in vivo* model for the testing of novel implant systems in fracture healing. This is due to the advantage of adult sheep having a similar body weight to humans and the long bone dimensions of long bones being appropriate for the implantation of human implants and prostheses (Newman et al., 1995). Thus, the inclusion of ovine osteoblast cells as an *in vitro* model holds several clear advantages. Unfortunately, there are few *in vitro* studies using ovine osteoblast cells. The main reason for this is the lack of a fully sequenced genome, which limits the application of many molecular biology methods. Currently, institutions such as the International Sheep Genomic Consortium are attempting to address this issue by applying genome mapping research to sheep.

The available literature focusing on osteoblastic activities of ovine cells *in vitro* indicate that these cells are capable of mineralisation (Collignon et al., 1997). Foetal ovine osteoblast cells stimulated post-proliferatively with ascorbic acid, β -glycerophosphate and CaCl_2 exhibited highest ALP activity after 6 days of culturing and formation of the mineralisation centres from day 12. Culture medium analysis demonstrated rapid increase in ALP concomitant with initiation of mineralisation. Furthermore, ovine osteoblast cells produced osteocalcin in a time-dependent manner from day 6 (Collignon et al., 1997). Interestingly, a more recent study has shown that trabecular bone from ovine specimens classed as middle-aged (3-5 year-old) behaved similarly to human cells isolated from the femoral condyle (donor age not known). Ovine cells responded to $1,25(\text{OH})_2\text{D}_3$ stimulation similarly to human osteoblast cells, which resulted in an increase in ALP, osteocalcin and $\text{TGF}\beta 1$ (Torricelli et al., 2003). However, ovine osteoblast cells isolated from trabecular bone from 2 year-old animals, used in our laboratory failed to mineralise. It is not known how common this phenomenon is, since to our knowledge, we are the only group to demonstrate the lack of mineralisation in ovine and bovine cells

of this age under a variety of established culture conditions (unpublished observation).

1.3.2.4. Rabbit cells

Rabbits are a widely used *in vivo* model in various biomedical research applications, such as musculoskeletal research (Neyt et al., 1998), including implant biomaterials testing, infection or gene therapy studies. Differences in bone structure, composition and remodelling between rabbit bone and human bone has been discussed and reviewed recently (Pearce et al., 2007) yet, not much is known about the biology of rabbit osteoblastic cells *in vitro*. Similarly to bovine and ovine osteoblast cells, the available literature is limited and gives poor insight regarding phenotype and behaviour. Early reports established an isolation protocol of enzymatically digesting rabbit bones with 0.1% crude collagenase (Yee, 1983; Shaw et al., 1989). Later, explant cultures from cervical vertebrae were used for isolating cells. The morphological and functional evaluation of cells isolated from the cortical endosteal bone surface of adult rabbits identified that almost all populations of cells had typical osteoblastic polygonal shape, whereas cells migrating out from the cervical bone had more spindle or triangle shape (Cao et al., 2006). The former were positive for ALP activity and were capable of mineralisation. Stimulation with parathyroid hormone (PTH) positively influenced cAMP production (Shaw et al., 1989). Extracellular matrix mineralisation and nodule formation was reported after 3 weeks of culturing rabbit osteoblast cells with ascorbic acid, dexamethasone and BGP (Cao et al., 2006). However, current knowledge regarding rabbit osteoblast cells is lacking and further studies are needed to evaluate rabbit osteoblast physiology and its relation to human osteoblast cells. Recently, it has been shown that the rabbit bone marrow stromal cells can undergo spontaneous immortalisation after prolonged culture and lose their potential to differentiate into chondrocytes and adipocytes (Ahmadbeigi et al., 2011).

1.3.3. Cell lines

The list of advantages of immortalised cell lines is long, including ease of maintenance, unlimited number of cells without the need of isolation and relative

phenotypic stability. On the other hand, some reports present evidence of progressing phenotypic heterogeneity among cell lines, which is correlated with prolonged passaging of cells (Leis et al., 1997; Wang et al., 1999; Grigoriadis et al., 1985). Additionally, both transformed and non-transformed cell lines, as they are stage arrested, do not reflect the whole range of phenotypic features of the normal osteoblast cells. Specifically, in the case of malignant cell lines, proliferation is non-physiological since the mechanism of contact inhibition is disturbed. Despite these disadvantages, the use of osteoblast cell lines is prevalent. The most commonly used cell lines are MC3T3E1 (Quarles et al., 1992), hFOB (Harris et al., 1995), MG63 (Billiau et al., 1977), SaOs2 (Rodan et al., 1987) and U2OS (Ponten and Saksela, 1967). The reader is directed to the excellent review of Kartsogiannis and Ng (2004) which discusses the aforementioned cell lines in addition to many not covered here.

1.3.3.1. Human Cell Lines

Rodan and colleagues (Rodan et al., 1987) characterized the osteoblastic properties of the human osteosarcoma cell line SaOs2, which were isolated from an 11 year-old Caucasian female in 1975. These cells have a mature osteoblast phenotype with high levels of ALP activity. This marker was reported at a much higher level than in other osteosarcoma cell lines, such as MG63 and SaOs1 (Murray et al., 1987). Additionally, when comparing to primary human osteoblast cells, the ALP activity was similar at the early time points, but it increased 120-fold after 14 days of culturing cells under the same conditions (Saldana et al., 2011). In our laboratory, we observed enzyme activity in SaOs2 cells to increase rapidly from day 1 to 7 and subsequently decrease until day 28. Moreover, these cells had twice the activity levels of primary human osteoblast cells at day 7, which even at this early time point, was higher than maximum activity of primary human osteoblast cells at day 21. Even though the differences at different time points occurred, the time sequential pattern of the enzyme activity was similar in both primary and SaOs2 cells (unpublished observations). Interestingly, SaOs2 cells have been reported to form calcified matrix in diffusion chambers akin of woven bone (Rodan et al., 1987). Detailed analysis of the collagen structure synthesised by SaOs2 revealed that it is similar to collagen formed by primary human osteoblast cells but with a higher level of lysyl hydroxylation in SaOs2 cells (Fernandes et al., 2007).

ALP in SaOs-2 cells can be further stimulated by dexamethasone (Rao et al., 1996) and phosphate substrates (Muller et al., 2011). Continuous culturing in medium with dexamethasone has been reported to increase ALP activity and produce a more differentiated phenotype (Rao et al., 1996). Due to the much higher ALP activity level in SaOs2 cells, compared to primary cells in basal conditions, the necessity of the additional administration with dexamethasone should be balanced. Moreover, the supplementation of culture medium with phosphate substrates should be introduced at a much lower level compared to other cell types and specifically at the post-proliferative stage when a layer of matrix is produced to avoid deleterious effects on viability (Figure 3). Finally, cytokine and growth factor expression of SaOs-2 cells have been shown to be similar to primary normal human osteoblast cells (Bilbe et al., 1996). For instance, SaOs2 cells express surface parathyroid hormone (PTH) and $1,25(\text{OH})_2\text{D}_3$ receptors found in osteoblasts *in vitro* and *in vivo*. Dexamethasone administration of SaOs2 cells increases their sensitivity to PTH, $1,25(\text{OH})_2\text{D}_3$ and 17- β estradiol (Rao et al., 1996).

The MG-63 cell line derives from juxtacortical osteosarcoma diagnosed in the distal diaphysis of the left femur of a 14 year-old male (Billiau et al., 1977). These cells display rapid cell growth without exhibiting contact inhibition, resulting in the formation of aggregates (Heremans et al., 1978). This cell type attracted much attention as it produces high yields of interferon (Billiau et al., 1977). Further research identified the responsiveness of MG63 cells to $1,25(\text{OH})_2\text{D}_3$ as affecting cellular morphology and phenotype by increasing ALP activity (Franceschi et al., 1985). MG63 cells represent an immature osteoblast phenotype and undergo temporal development in long term culture. However, inconsistencies exist in the literature regarding the mineralisation capabilities of MG63 cells in monolayer. Kumarasuriyar and colleagues (2009) reported changes in MG63 phenotype that replicate the differentiation model proposed by Lian and Stein (Lian and Stein, 1992). Briefly, ALP activity increased by day 15 and then declined to basal levels, whereas type I collagen expression increased during the second week of the culture. Osteocalcin and osteonectin expression were observed at day 15 and 29, whereas Runx2, BSP and osteopontin were not detected while calcium accumulation was initiated after day 28 (Kumarasuriyar et al., 2009). In our

laboratory, we observed 14-fold lower ALP activity in MG63 cells than in primary human cells and no calcium deposition in the matrix (unpublished observations). Moreover, other reports showed that MG63 cells have low ALP enzyme activity and did not mineralise (Saldana et al., 2011;Pierschbacher et al., 1988). Attempts to successfully select fibronectin positive cells from MG63 cells resulted in the identification of a clone (MG-63.3A) which has been shown to deposit calcium phosphate in culture without the need for phosphate substrate addition to the culture medium (Pierschbacher et al., 1988).

The response of MG63 cells to $1,25(\text{OH})_2\text{D}_3$ administration has been shown to be similar to normal human osteoblast cells (Clover and Gowen, 1994). Additionally, only after $1,25(\text{OH})_2\text{D}_3$ treatment, osteocalcin was detected in the supernatants of the cells, and increased 9- to 20- fold (Clover et al., 1992;Franceschi et al., 1988). The time and dose dependent stimulation of protein secretion by $1,25(\text{OH})_2\text{D}_3$ was reported in both freshly isolated and MG-63 cells. The $1,25(\text{OH})_2\text{D}_3$ stimulates the synthesis of $\alpha_1(\text{I})$ and $\alpha_2(\text{I})$ chains of type I collagen together with type III collagen and fibronectin synthesis (Franceschi et al., 1988). Additionally, both human and MG63 cells produce cAMP in response to PTH treatment (Lajeunesse et al., 1990). Johansen and colleagues (Johansen et al., 1992) showed differences in matrix protein secretion by MG-63 cells and normal human osteoblast cells isolated from foetal and adult femoral head. Osteosarcoma cells secreted gelatinase, YKL-40 protein, tissue inhibitor of metalloproteinase 1 (TIMP-1) and 2 (TIMP-2) and β -microglobulin but no C-terminal propeptides of the α_1 and α_2 chains of type I collagen. Moreover, normal human osteoblasts from the foetal trabecular bone secrete primarily matrix constituent proteins such as C-terminal propeptides of α_1 and α_2 chains of type I collagen together with osteonectin. In addition to this, cells from adult donors secrete gelatinase, TIMP-1 and β -microglobulin (Pierschbacher et al., 1988).

Collectively these results indicate the similarity of MG63 and normal osteoblasts in their response to $1,25(\text{OH})_2\text{D}_3$ and PTH administration which makes them attractive model for hormonal regulation of phenotypic changes investigations. However, the inconsistency in the expression of matrix proteins resulting from their

clonal heterogeneity limits their use as a model for osteoblast phenotype development and matrix mineralisation.

1.3.3.2. Mouse cell lines

MC3T3E1 represents a popular osteoblast cell line representative of a pre-osteoblastic phenotype. Several subclones have been established from this newborn mouse calvaria clonal cell line. Five of them, subclones 4, 8, 11, 14, 26 demonstrate mineralisation with the addition of ascorbic acid and inorganic phosphate (Wang et al., 1999). Mineralising subclones express high levels of mRNA for BSP, OCN, and the PTH/PTHrP receptor. From these clones, only subclone 4 and 14 have been shown to mineralise the collagenous extracellular matrix. Subclone 4 was shown to undergo temporal changes from proliferation to nodule formation and mineralisation in similar manner as in intramembranous osteogenesis *in vivo* (Sudo et al., 1983). Cells proliferated actively *in vitro* and synthesised type I collagen from day 3 in culture. Simultaneously, ALP enzyme activity increased from day 3 to day 21 and the mineral deposition was reported early at day 14 (Quarles et al., 1992).

Ascorbic acid and β GP supplementation is a prerequisite for matrix mineralisation in MC3T3-E1 cells. In the absence of these stimulators, ALP activity remains low and fails to result in mineralisation (Hong et al., 2010). Differentiation of MC3T3E1 cells is also influenced by the type of serum used in culture medium, and serum derived cytokines and growth factors (Yohay et al., 1994). With the addition of complete foetal bovine serum, cells have increased proliferative capabilities during early differentiation. Furthermore, ALP activity, protein and mRNA expression is increased in the post-proliferative stage compared to cells maintained in medium with resin/charcoal-stripped serum (Yohay et al., 1994). Although being a cell line, MC3T3E1 at high passages (above 36) have reportedly decreased proliferation and at very high passages (above 60) exhibit inconsistent cell cycling indicative of replicative senescence (Grigoriadis et al., 1985) similar to human cells, which makes them an attractive tool for *in vitro* investigations relating to bone remodelling and formation.

Cell type	Phenotype	Best isolation method	Culture conditions for matrix mineralisation	References
Primary Human Osteoblast cells	Pre- to mature osteoblast	Outgrowth culture	50 µg/ml a.a., 5-10 mM βGP, 10-100 nM dex	(Gallager, 2003) (Gotoh et al., 1990) (Toesca et al., 2001) (Siggelkow et al., 1999)
Primary Mouse/Rat Osteoblast cells	Pre- to mature osteoblast	Outgrowth (Mouse Ob's); Enzymatic digestion (Rat Ob's)	50 µg/ml a.a., 5-10 mM βGP	(Ecarot-Charrier et al., 1983) (Ecarot-Charrier et al., 1988; Lomri et al., 1988) (Garcia et al., 2002) (Roman-Roman et al., 2003) (Bhargava et al., 1988) (Siggelkow et al., 1999) (Lynch et al., 1995) (Yamamoto et al., 2002) (Bellows et al., 1986)
Primary Bovine/Ovine Osteoblast cells	Immature to mature osteoblast	Enzymatic digestion (foetal tissue); outgrowth culture (adult animal)	50 µg/ml a.a., 10 mM βGP, 0.6 mM Ca, ITS	(Whitson et al., 1992) (Ibaraki et al., 1992) (Whitson et al., 1984) (Collignon et al., 1997)
Primary Rabbit Osteoblast cells	Mature osteoblasts	Enzymatic digestion (0.1% crude collagenase)	Not clearly defined	(Yee, 1983; Yee, 1983) (Shaw et al., 1989) (Cao et al., 2006)
MG63	Immature osteoblast	n.a.	50 µg/ml a.a., 5-10 mM βGP	(Franceschi et al., 1988)
SaOs2	Mature osteoblast	n.a.	50 µg/ml a.a., 0-10 mM βGP (only post-confluent)	(Ahmad et al., 1999) (Saldana et al., 2011) (Hausser and Brenner, 2005) (Rodan et al., 1987) (Rao et al., 1996) (Muller et al., 2011)
MC3T3E1	Mature osteoblast	n.a.	25-50 µg/ml a.a., 5-10 mM βGP	(Hong et al., 2010) (Quarles et al., 1992) (Yohay et al., 1994)

Table 1.1. Cell models and their culture conditions required. The mature phenotype states for the capability of cells to deposit calcium in matrix. Dex – dexamethasone, βGP-glycerol-2-phosphate, Ca- calcium, a.a. – ascorbic acid, ITS - insulin, transferrin, selenium.

1.4. *In vitro* cell-cell communication models of osteoblast lineage cells

Skeletal development, remodelling and repair require a tightly orchestrated interplay among bone cells at all stages of their phenotypic differentiation. Within bone, these cells can communicate through three mechanisms; direct cell-cell contact through cell membrane molecules (tight and adherence junctions), gap junction communication forming cytoplasmic connections between cells and complex paracrine interaction through cell- or matrix-derived secretion factors (Grellier et al., 2009). Taking into account the complex structure of bone, the web of interactions appears highly intricate. Currently, analysis of these interactions *in vitro* is possible to a certain extent, while more complex analysis that includes more variables remains challenging. Nevertheless, established co-culture models enable the investigations of cell-cell communication in both directly and indirectly. Based on the number of scientific reports, there is a high interest in the communication between osteogenic and endothelial lineage cells as a result of the needs of tissue engineering (reviewed by (Grellier et al., 2009)), while less focus is directed towards the interactions among osteoblast cells and their progenitors. The next paragraphs will outline the current knowledge regarding the influence of the *in vitro* communication between osteoblastic lineage cells on their phenotype development.

1.4.1. Direct cell-cell communication

The mode of the crosstalk among cells *in vitro* strictly depends on the type of co-culture. Direct communication can be easily achieved in a 2D or 3D environment, by plating different cell types together. Upon direct cell-cell contact, interactions between cells are mediated by adherence junctions formed by cadherins, and gap junctions formed by connexions (Civitelli, 2008;Stains and Civitelli, 2005). Interestingly, this co-culture model is not very often used for analysis of osteoblast-MSCs interactions. Conversely, to the ease of establishing the direct culture model, the later discrimination between the two cell types and subsequent analysis is difficult. Yet, a number of research groups have employed this co-culture model to evaluate the influence of direct cell-cell communication on osteogenic differentiation (Tsai et al., 2012;Csaki et al., 2009;Wang et al., 2007;Kim et al., 2003). Initial studies suggested limited synergistic interactions between MSCs and

osteoblast cells during *in vitro* osteogenesis when cells were plated at a 1:1 ratio (Kim et al., 2003). Although, there was no influence of co-culture on ALP activity in cells, the calcium deposition was decreased in co-cultured cells compared to single cell type cultures. This, however, could be due to co-culture of cells from two different species, rabbit MSCs with rat osteoblasts, and potential antagonistic influence of factors secreted by these cells (Kim et al., 2003). Additionally, the evidence from further research reports disagrees with those reported by Kim and co-workers. In fact, stimulation of osteogenic differentiation was reported in monolayer and monolayer-3D co-culture of osteoblasts with pluripotent stem cells (Ahn et al., 2006; Tsai et al., 2012). What is more, ALP activity and mineralisation of nodules was higher in co-cultures with increased proportion of osteoblast cells up to 50% in co-cultures compared to single cell type cultures and co-cultures in which lower number of osteoblasts (Tsai et al., 2012; Csaki et al., 2009). On the other hand, it was not evaluated which cell type, MSC or osteoblasts, directs mineralisation of ECM.

The results from Ahn suggest that not only the number of each cell type, but also the phenotypic maturity of the cells influences the differentiation of the other (Ahn et al., 2006). Specifically, the mineralisation of human embryonic stem cells was higher in co-cultures with primary human bone derived cells than with SaOs2 (Ahn et al., 2006). Considering the phenotypic maturity of cells further, Wang and co-workers demonstrated that the direct co-culture of osteoblasts with MSCs had a profound effect on MSCs, but not on osteoblast cells (Wang et al., 2007). This indicated the primary role of the osteoblasts in directing the differentiation of MSCs. Further evidence revealed that proteins involved in the Wnt signalling pathway are implicated in the osteoblast-directed stimulation of MSC osteogenic differentiation (Wang et al., 2007).

1.4.2. Indirect cell-cell communication

Indirect co-culture, based on the action of secreted diffusible factors only, overcomes the limitation of direct co-culture models regarding the separation of two cell populations. Additionally, it allows for the analysis of one-way communication or two-way communication. The former, is achieved when one cell type is cultured

in medium conditioned by other cell type. Two-way communication, in which paracrine factors are secreted by both cell types and affect both cell types, can be investigated using porous membranes separating different populations of cells. Importantly, by applying the indirect co-culture the determination of the importance and necessity of direct cell-cell contact on the secretion of trophic factors and differentiation can be revealed (Grellier et al., 2009). The indirect cell crosstalk between MSCs and osteoblast cells has been extensively studied using human and murine cell models.

Significant influence of one way communication between cells on osteogenic differentiation has been reported. Specifically, ALP activity and ECM calcification were stimulated in MSC cultures in the presence of medium conditioned by human, murine and rat osteoblast cells (Ilmer et al., 2009;Buttery et al., 2001;Ueno et al., 2001;Maxson and Burg, 2008). Importantly, the magnitude of response of co-cultured cells depends on the quality of CM. The CM collected every 3 days up to day 9 after plating of osteoblast cells was the most effective in inducing rat MSC differentiation compared to CM collected from cells at later time in culture (Ueno et al., 2001). Similarly, effects on human MSC differentiation, marked by the up-regulation of ALP, osteocalcin and bone sialoprotein (BSP), was exerted by osteoblast growth medium conditioned by human osteoblast cells for 5 days (Ilmer et al., 2009).

The early osteogenic marker, Runx2, mRNA expression was at similar level in cultures with and without the conditioned medium (Ilmer et al., 2009). Interestingly, serum-free DMEM supplemented with antibiotics conditioned for 48 hours after confluence by less differentiated human MSCs, induced proliferation, Runx2 and osteocalcin gene expression in rat MSCs (Osugi et al., 2012). Moreover, medium collected specifically between day 3 and 6, was the most effective and supported a significant increase of ALP activity, osteocalcin gene expression and mineralisation at specific time points during the culture period (Ueno et al., 2001). The factors secreted by cells after confluence *in vitro*, seem to be the most important for supporting the differentiation of cells in both, paracrine and, potentially, autocrine manner. Indeed, the secretion profile depends on the differentiation state of cells (Hoch et al., 2012;Li and Niyibizi Ch, 2012).

In the indirect co-culture of both cell types, the secretion of paracrine factors from one cell type can be further regulated by the factors released by the other cell type. Most of the reports focused on the analysis of MSCs and only some on osteoblast cells. Results regarding the effect of indirect co-culture demonstrated no effect of co-culture on murine osteoblast cells phenotype (Wang et al., 2007). Conversely, indirect co-culture has a positive effect on osteogenic differentiation of MSCs. In monolayer co-culture with osteoblasts, a 5-fold increase in nodule formation and mineralisation was reported for murine embryonic cells (Buttery et al., 2001). On the gene expression level, the co-culture with osteoblasts significantly stimulated the expression of Runx2, type I collagen, osteopontin and BSP in MSCs when cells were plated in 1:1 ratio (Wang et al., 2007). Similarly for direct co-culture, the osteogenic differentiation of MSCs positively correlated with the number of osteoblast cells. Higher levels of ALP, BSP and OC mRNA expression was reported when MSCs were co-cultured with osteoblasts in 1:2 ratio than in 1:1 ratio (Ilmer et al., 2009). In addition to increasing cell number, MSC differentiation into osteoblasts in co-culture can be stimulated to a greater extent by encapsulating cells in 3D environment. Seto and co-workers demonstrated that MSCs encapsulated in heparin gel and co-cultured with osteoblasts in monolayer had 10-fold higher ALP activity and calcium accumulation than MSCs from single cell type cultures (Seto et al., 2012).

Up to date, only one study has undertaken the interesting aim to compare the osteogenic differentiation of MSCs in direct and indirect co-culture system to evaluate how the contact mode influences the mechanisms directing the differentiation process (Wang, 2007). In both co-culture types, the differentiation of murine MSCs is regulated by Wnt signalling pathways. While upon direct cell-cell contact the cadherin pathway was up-regulated, which resulted in the suppression of Wnt signalling, in indirect co-culture the suppression of cadherin and stimulation of the Wnt pathway was demonstrated. This was further reflected in the higher extent of osteogenic differentiation being reported for cells in indirect co-culture (Wang et al., 2007). Interestingly, in indirect co-culture, the influence on only ALP, but not later osteogenic markers, in human MSCs by osteoblast-induced Wnt pathway was reported (Ilmer et al., 2009).

1.5. Bone regeneration

Upon fracture, the cortical bone and periosteal tissue, together with surrounding soft tissues are ruptured. The process of fracture healing is initiated immediately and is a series of molecular and cellular events leading to the restoration of the tissue. Bone fracture healing is a specific process of wound healing because unlike soft tissue wound healing it does not lead to scar formation. This results in the anatomical realignment and restoration of the physiological function of the bone and complete return to the physiological function. Intensive studies in this area indicate that the bone healing process is regulated by multiple parameters such as pH, oxygen tension, growth factors and cytokines present at the site of the injured tissue, and mechanical stability of the fracture bone fragments (Sfeir et al., 2005). Depending on the nature and the treatment, fracture healing can be divided into primary (direct) and secondary (indirect). Secondary fracture healing differs in the formation of callus compared to the primary healing. Both of these processes are very complex and require stabilization, either absolute or relative. Stabilization can be obtained by external or internal fixation devices.

1.5.1. Primary fracture healing

Primary healing of a fracture involves a direct attempt by the cortex to re-establish itself. To restore mechanical continuity, bone fragments at one side of the cortex must unite with bone in the other side of the cortex. This process occurs when there is anatomical restoration of the fracture fragments, which is achieved by rigid fixation, and when the stability of fracture reduction is ensured by a substantial decrease in interfragmentary strain (McKibbin, 1978; Einhorn, 1998). The process of direct healing is based on the osteonal bone remodelling, which is also observed in normal physiological bone turnover.

As stated above, mechanical stability is crucial in the type of the bone fracture healing observed. The absolute stability of the fracture is at the utmost importance for direct bone healing as it restores and maintains anatomical reduction of fracture fragments by avoiding interfragmentary motion, which results in resorption of the contact surfaces of bone fragments (McKibbin, 1978). Perren proposed the

‘infragmentary strain hypothesis’ to explain the effect of the interfragmentary strain and fracture immobilization on the tissue response in the fracture healing process (Perren, 1979). According to his theory, fracture healing will occur when rigid internal fixation is ensured and when the interfragmentary movement divided by the fracture gap width is lower than 2% (the fracture strain of bone).

Depending on gap width, primary healing can be further divided into gap healing and contact healing. The first occurs when the interfragmentary space is less than 0.1mm and is mediated by marrow derived vessels and vessel-associated osteoprogenitor cells differentiating into osteoblasts (Shapiro, 2008). Primarily, the gap is filled directly by woven bone which is followed by the formation of lamellar bone having perpendicular orientation to the long axis of bone. From the mechanical point of view this union of bone ends is weak and further undergoes secondary osteonal remodelling, restoring stable biomechanical properties of the healed bone. In this process, longitudinal oriented cavities are formed across the fracture plane/line by osteoclasts in cutting cones. This provides pathways for the penetration of blood vessels and capillaries. Later osteoblast cells residing at the end of the cutting cone produce bone which fills the cavity and restores the Harvesian system in the original longitudinal orientation (Sfeir et al., 2005; Shapiro, 2008).

Contact healing occurs only when the gap between the bone ends is less than 0.01mm and its interfragmentary strain is less than 2% (Shapiro, 1988; Marsell and Einhorn, 2011). Under these conditions, the lamellar bone of original axial direction is formed during primary osteonal reconstruction. This process is directed exclusively by the intraosseous Harvesian system osteoblasts and osteoclasts. Initially, the cutting cones are formed at the ends of the osteons closest to the fracture site. These cutting cones generate cavities through the fracture line at a rate 50-100 $\mu\text{m}/\text{day}$ (Griffon, 2007). The developing Harvesian system (osteon) is filled with lamellar bone aligned parallel to the long axis of the bone.

1.5.2. Secondary fracture healing

Secondary (indirect, endochondral) fracture healing occurs under the relative stability. As primary bone repair is akin to bone remodelling, secondary fracture

healing is very similar to the process of embryological development, which includes two distinct and interactive responses, intramembranous and endochondral bone formation. While both these processes result in bone formation, their mechanisms are significantly different. In intramembranous bone formation, bone synthesis is direct and proceeds without cartilage participation. In case of endochondral bone formation, bone synthesis is preceded by cartilage formation that further undergoes mineralization and acts as a scaffold for bone formation. Relative stability allows for motion at the site of injury, which promotes the formation of a cartilaginous fracture callus providing intermediate stabilization of the fracture (Probst and Spiegel, 1997). If the local strain (deformation) is higher than the forming woven bone can tolerate, bone bridging and callus will not occur which will result in a reactive non-union (Kessler et al., 1986). The process of secondary fracture healing is a continuous process that can be divided into consecutive but overlapping stages: inflammation, reparative (including soft and hard callus formation) and remodelling phase (Fig.1.3).

1.5.2.1. Inflammatory phase

Initially, the bone fracture results in the disruption of the blood vessels within the marrow, periosteum, osteons and tissues adjacent to the fracture site (Fig.1.3A). Due to low oxygen and nutrient supply, cells at the margins of the bone fragments undergo necrosis (Sfeir et al., 2005; McKibbin, 1978). Consequently, a hypoxic state forms and initiates inflammatory response (Taguchi et al., 2005). In the rat fracture model, the acute inflammatory response occurs within the first 7 days after the fracture. The immune cells produce a wide spectrum of factors and cytokines within that time, including Interleukin 1 (IL1), IL6, IL8, IL12, platelet-derived growth factor (PDGF), tumour necrosis factor α (TNF α), IL8, vascular endothelial growth factor (VEGF), CXC Receptor 4 (CXCR4) and osteopontin/secreted phosphoprotein 1 (SPP1), which are essential for mobilisation and chemotaxis of other cells, angiogenesis and osteogenesis (Kolar et al., 2011; Park and Barbul, 2004). Moreover, the extravasation forms a hematoma which encloses the fracture area and is a source of signalling molecules to initiate the activation of the complement cascade, platelet aggregation and the release of platelet contents (Bolander, 1992).

Polymorphonuclear neutrophils (PMNs) are the first cells recruited to the fracture site by dead cells, debris and platelet degranulation within 24 hours after fracture. They secrete several chemokines, such as Chemokine CC-motif ligand 2 (CCL2) and IL6, attracting macrophages from the two distinct locations which emerge within 48-96 hours post-fracture and are the principle cell types during inflammatory phase. The first type are macrophages residing on the endosteal and periosteal surface of the bone close to the bone lining cells, which are crucial for intramembranous bone formation during healing. The second type are inflammatory macrophages derived from recruited and divided monocytes from the blood, which affect the endochondral ossification. These cells provide a barrier against bacterial invasion and are essential in wound debridement and at the hypoxic milieu initiate angiogenesis (Leibovich and Ross, 1975). Lastly, lymphocytes are recruited and initiate the adaptive immune response.

Emerging at the fracture site, platelets adhere to the exposed vascular collagens, type IV and V. This interaction initiates the activation and aggregation of the platelets that degranulate releasing their d-granule contents, such as fibronectin, platelet-derived growth factor (PDGF), platelet-activating factor (PAF), thromboxane A₂ (TXA₂) and TGFβ (transforming growth factor β) that are essential for the further stages of blood coagulation process. As a result, a fibrous blood clot is formed around the fracture and the periosteum, providing pathways for the cellular migration of phagocytes, neutrophils and fibroblasts (Fig.1.3A) (Probst and Spiegel, 1997;Shapiro, 2008).

As mentioned above, macrophages are essential for initiating angiogenesis under hypoxic conditions through secretion of factors essential for this process, such as fibroblast growth factor β (βFGF), VEGF and insulin-like growth factor 1 (IGF-1) (Knighton and Fiegel, 1989). These factors induce the formation of capillaries within the clot and the loose aggregate of fibroblasts which forms the granulation tissue. In addition, macrophages produce cytokines and growth factors, such as IL1, IL6, IL8, IL12, platelet-derived growth factor, TNFα, attracting migration of other cells towards the injury site, stimulating proliferation and/or differentiation of these cells and the collagen synthesis (Park and Barbul, 2004).

In endochondral bone healing, the main source of progenitor cells differentiating into osteoblasts is provided by inner osteogenic layer of periosteum and by bone marrow. These cells are recruited to the fracture site by the chemotactic factors. Recently, it has been shown that stromal-derived factor (SDF1) and its receptor, CXCR4, are crucial for recruiting and homing of osteoprogenitor cells to the site of the fracture (Kitaori et al., 2009).

Hematoma, and the inflammatory reaction, initiates the repair of bone by attracting and promoting differentiation of MSCs, initiating angiogenesis and enhancing ECM synthesis. The local increased levels of mRNA expression of IL8, VEGF together with IL6, CXCR4 and SPP1 in fracture hematoma indicate its importance for chemotaxis, angiogenesis and osteogenesis (Kolar et al., 2011). Combating inflammation and removal of the hematoma can negatively affect the bone healing process in various ways. Indeed, the removal of the hematoma, together with the cells contained within, prolonged the time of fracture healing compared to fracture with hematoma (Kolar et al., 2011). One of the reasons is the lack of ability to adapt to the hypoxic conditions, which in physiological scenario is regulated by hypoxia-inducible factor (HIF-1). The expression of HIF-1, which regulates the cellular adaptation to low oxygen by switching the cellular metabolism from oxidative phosphorylation toward glycolysis (Semenza, 1998) and inducing angiogenesis via VEGF and IL8, upregulates in the fracture hematoma.

Furthermore, in the absence of macrophages, the increased levels of tumour necrosis factor-alpha (TNF α) together with reduced levels of transforming growth factor- β_1 (TGF β_1) and vascular endothelial growth factor (VEGF) in the wound, resulted in decreased collagen synthesis and impaired vascularization (Mirza et al., 2009). Furthermore, treatment with non-steroidal anti-inflammatory drugs, such as cyclooxygenase-2 inhibitors (COX-2) can result in prolonged fracture healing. COX-2 is an enzyme implicated in inflammation by converting arachidonic acid to prostaglandin H₂. It is abundant in activated macrophages and, in addition, it promotes differentiation of MSC into osteoblasts and angiogenesis during the fracture healing (Gerstenfeld et al., 2003). Finally, the depletion of all T-lymphocyte cells negatively affects the wound healing (Efron et al., 1990).

1.5.2.2. Soft callus formation

The reparative phase of secondary starts after inflammation and lasts for few weeks. Initially, it begins with soft callus formation (Fig.1.3B). The progenitor cells residing in the cambial layer of periosteum and endosteum differentiate into osteoblast cells, which subsequently deposit woven bone via intramembranous ossification. At the same time, the granulation tissue formed after the fracture is replaced by fibrocartilagenous tissue formed by fibroblasts and chondrocytes. This process is initiated by the growth factors stimulating the cell proliferation and differentiation. In detail, the bone matrix and broken bone cortex are the source of many growth factors, including BMPs (Bostrom et al., 1995). The members of BMP family together with IGF1, platelet-derived growth factor (PDGF), transforming growth factor β (TGF β) and fibroblast growth factor 1 (FGF-1) stimulate fibroblast and chondrocyte proliferation, and chondrocyte differentiation. In addition, the expression of BMP family members was demonstrated in various cells at different stages of the fracture repair, including chondrocytes in soft callus. Moreover, in these cells the distribution of BMPs depended on the cellular differentiation stage and the location within the fracture callus, which may contribute to BMP-mediated response to the injury (Yu et al., 2010).

Initially, the cartilage tissue is formed from the outer sides of the fracture gap and ingress into the centre region where the fibrocartilagenous tissue is formed. This fibrocartilage callus has increased stiffness and, thus, it bridges and stabilizes the fracture sites by resisting the compression and tension (except angular tension). In addition, it acts as a template for the superceding bony callus (Rahn, 2002). Initially, the avascular soft callus is invaded by vascular endothelial cells.

1.5.2.3. Hard callus formation

About one week after the formation of soft callus, the next stage, leading to hard callus formation starts and lasts until the fragments are united by a new bone (3-4 months). With ongoing intramembranous bone formation at the periosteal site of the fracture gap and vascularisation within the soft callus, the chondrocytes from proximal to distal parts of the fracture undergo calcification followed by endochondral ossification forming woven bone (Fig.1.3C) (McKibbin, 1978). The hypertrophic chondrocytes enlarge and vascular buds invade the soft callus.

Then, the osteoprogenitor cells differentiate into osteoblasts which resorb the calcified cartilage and the woven bone replacing them further with mature bone trabeculae (Probst and Spiegel, 1997). The process starts from the fracture periphery towards the fracture gap and results in the final joining of the original cortex (Einhorn, 1998;Ito, 2007).

1.5.2.4. Remodelling

The remodelling phase of fracture healing leads to an optimal stability of the healed bone similar to the bone structure before the fracture occurred. This phase begins with the activation of osteoclasts forming cutting cones in the immature woven bone, where the blood vessels enter bringing osteoblasts that deposit bone matrix, resulting in the formation of the lamellar bone along the longitudinal axis of the bone (Fig.1.3D). This type of bone withstands physiological mechanical load. In addition, the osteoclast activity decreases the size of the callus (Perren, 1979;Probst and Spiegel, 1997). The remodelling process takes from months to years and depends on both the type of bone and fracture. Trabecular bone (cancellous) fractures are more stable and have a better blood supply, therefore, heal faster than cortical bone fractures (Sfeir et al., 2005).

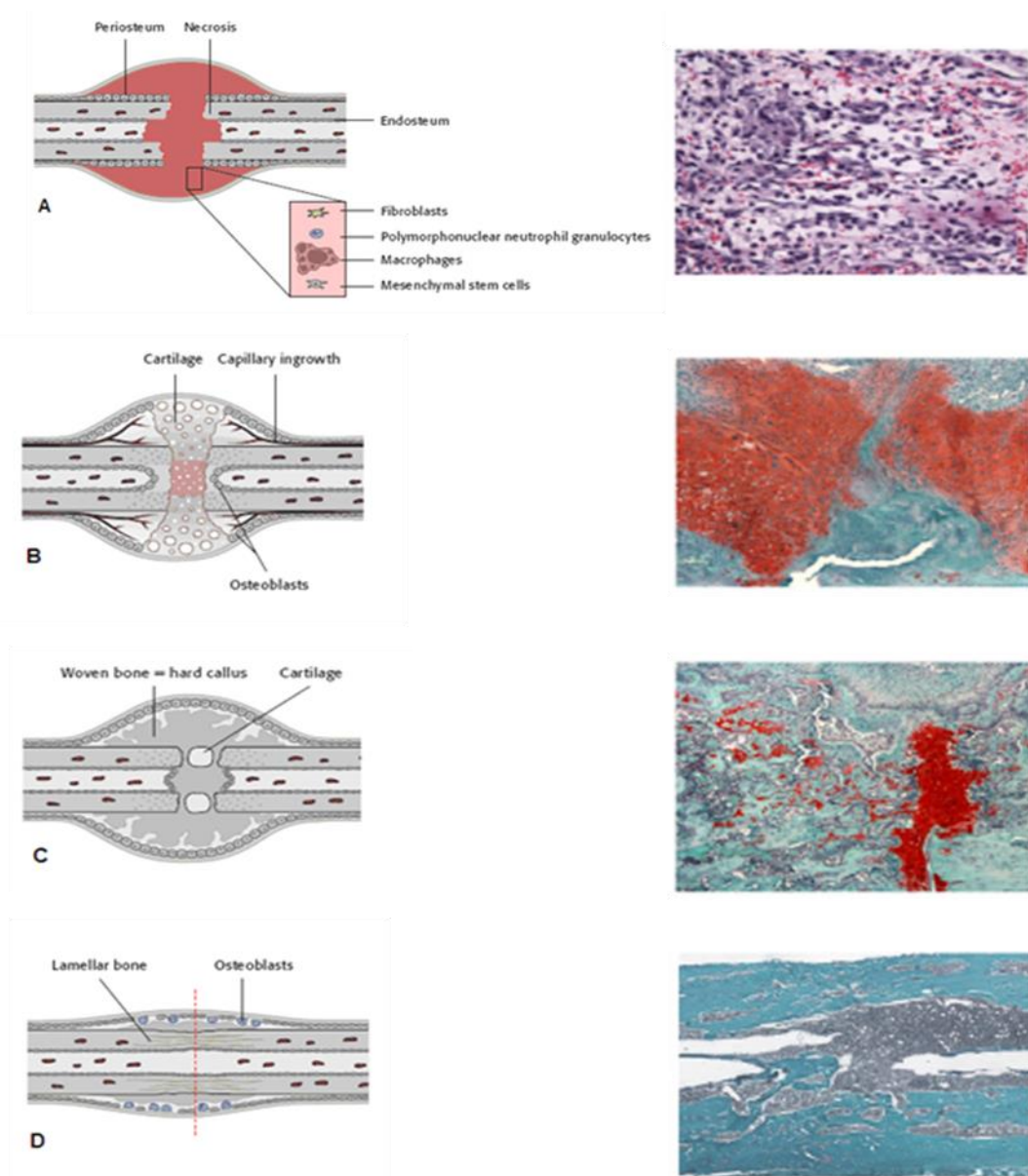


Figure 1.3. Schematic and histological representation of secondary fracture healing stages. A) The inflammatory phase with haematoma formation. Schematic presentation of cells in fibrous clot. B) The soft callus stage. The replacement of granulation tissue by the fibrous tissue and cartilage. Intramembranous ossification starts at the distal parts of fracture fragments followed by capillaries ingrowth into the calcified callus. C) The hard callus stage. At this stage callus is completely calcified. During endochondral ossification the woven bone is formed. D) The remodelling stage. The woven bone is replaced by lamellar bone that withstands physiological mechanical load. Adapted from (Ito, 2007) and Schindeler (2010).

1.5.3. Vascularisation

A bone is a well vascularised tissue and when a bone is fractured, the blood vessel system is severely disrupted. The vascular restoration is extremely important in the bone fracture healing process, as damaged blood circulation leads to hypoxia and acute necrosis of the adjacent bone and marrow (Probst and Spiegel, 1997). After fracture, the disrupted circulation cannot provide the proper and adequate reaction to the injury. Hence, immediately after fracture an additional external blood supply develops from adjacent soft tissues and is referred to as the extraosseous supply. Initially, the extraosseous vascular capillaries supply blood to the soft periosteal callus.

In relation to blood supply in the healing bone, three types of osseous callus are distinguished – periosteal, medullary and intercortical (Fig.1.4). The periosteal callus is situated externally to the bone and during the early stages of healing it is supplied by the extraosseous vasculature. However, with time it receives more blood from the medullary arterial supply which also constitutes vascularisation for the medullary callus confined to medullary cavity. Between the fracture fragments at the opposite sites of cortex the intercortical callus forms and acts as a scaffold for the reconstructing bone. Blood circulation to the intercortical callus is provided by the medulla, when the medullary arterial supply is not damaged. Otherwise, the vascularity comes from extraosseous blood supply, until the medullary blood supply is fully regenerated (Carano and Filvaroff, 2003).



Figure 1.4. Schematic model of the three types of osseous callus encountered at sites of bone repair. Adapted from Sunner-Smith and Fleckerman *Bone in Clinical Orthopedics* 2nd Edition, 2002.

1.6. Objectives and Hypotheses

The ultimate goal of this thesis was to deliver a reliable *in vitro* cell culture model for osteoblast-lineage cells. The specific hypotheses and objectives are outlined below.

Hypothesis I (chapter 3):

Osteoblast cell lines are not relevant models as an alternative to the primary human osteoblasts for investigating osteoblast cell phenotype

Objectives:

- 1) Characterise the phenotype of primary human osteoblast cells and osteoblast cell lines (SaOs2, MG63 and MC3T3E1)
- 2) Compare the osteoblastic phenotype of cell lines with primary human cells

Goal: Determine the relevance of osteoblast cell models for bone-related studies

Hypothesis II (chapter 4):

Paracrine communication regulates the osteogenic phenotype of bone forming cells

Objectives:

- 1) Assess the effect of paracrine communication between osteoblasts and MSC cells in monolayer indirect co-culture
- 2) Assess the effect of paracrine communication between osteoblasts and MSC cells in micromass indirect co-culture
- 3) Establish an osteoblast cell model allowing the analysis of the influence of direct cell-cell communication on osteoblastic phenotype development

Goal: Determine the influence of 2D and 3D environment on paracrine cell crosstalk

Hypothesis III (chapter 5):

Short-term stimulation of human MSCs with inflammatory and chemotactic factors results in functional regulation of the cells paracrine activity

Objectives:

- 1) Assess the direct effects of stimulation on cytokine gene expression profile
- 2) Assess the direct effects of stimulation on cytokine protein secretion profile
- 3) Characterise the secondary effects of stimulation on osteogenic differentiation of unstimulated human MSCs

Goal: Determine the potential influence of the regulation of paracrine activity of MSCs on the processes involved in bone healing processes

Hypothesis IV (chapter 6):

Culturing human bone-derived mesenchymal stem cells (MSCs) in a 3D *in vitro* microenvironment promotes their phenotypic development

Objectives:

- 1) Formulate and establish a physiologically relevant culture system based on type I collagen gel
- 2) Investigate the effect of 2D and 3D cell culture models on osteoblast cell development
- 3) Investigate the importance of the extracellular matrix proteins for osteogenic differentiation

Goal: Develop a 3D osteoblast culture model resembling more natural milieu and allowing the better understanding of osteoblastic cell development

CHAPTER 2

MATERIALS AND METHODS

Sections of this chapter have been previously published:

E. M. Czekanska: Assessment of cell proliferation with resazurin-based fluorescent dye *Methods in Molecular Biology* 740: 27-32 (2011).

2.1. Materials

- 100x Insulin-Transferrin-Selenium+1 (Sigma, I2521)
- 1-Bromo-3-chloropropane for molecular biology (BCP; Sigma B9673)
- 2-Amino-2-methylpropanol (Sigma, A9199)
- 4-(2-hydroxyethyl)-1-piperazineethanesulfonic acid (HEPES; Clonetics, CC-5024)
- 4-(2-hydroxyethyl)-1-piperazineethanesulfonic acid (HEPES; Invitrogen, 15630)
- ⁴⁵Ca, Calcium chloride in aqueous solution (Perkin Elmer, NEZ013)
- 4-nitrophenyl phosphate disodium salt hexahydrate (20 mg tablets; Sigma, N2765)
- Alizarin Red S (Sigma-Aldrich, A5533)
- Alkaline buffer solution (Sigma, A9199)
- Alpha Minimal Essential Medium (α MEM; Gibco, 12000-063)
- Assays on Demand (Applied Biosystems)
- B4-78 antibody (26 μ g/ml, produced on 28.01.2010; DSHB)
- Basic FGF, human recombinant (Fitzgerald, RDZ-118B-218)
- Calcein AM (Fluka, 17783; stock solution: 1mg/ml in DMSO)
- Calf thymus DNA (Invitrogen, 15633-019)
- Cell Titer-Blue® Cell Viability Assay (Promega, G8080)
- Collagen type I from rat tail (Gibco, A10483-01)
- DeoxyNTPs mixture, 0.5 mM each dNTP (Applied Biosystems, N8080260)
- Dexamethasone (water soluble; Sigma, D2915)
- Diethanolamine (Sigma, D0681)
- Dimethyl sulfoxide (DMSO; Fluka, 41640)
- dNTP Mix (Applied Biosystems, 362275)
- Dulbecco's Modified Eagle Medium, high glucose (DMEM, powder; Gibco, 41965-02)
- Dulbecco's Modified Eagle Medium, low glucose (DMEM, powder; Gibco, 31600-083)
- Ethanol (for molecular biology; Fluka, 51976)

- Ethidium homodimer-1 (Fluka, 46043; stock solution: 1 mg/ml in 20% DMSO in H₂O)
- Ethylenediaminetetraacetic acid (EDTA; Sigma, E5134)
- Eukitt® (Fluka, 03989)
- FBS Superior (Biochrom, S0165, lot# 0306A)
- Ficoll (Histopaque, 1077)
- Foetal bovine serum, heat inactivated (Gibco, 10500)
- Formic acid 70% (Fluka, 06460)
- Granulocyte colony stimulating factor, human recombinant (PromoKine, C-60437)
- GenElute HP Plasmid Mini Prep (Sigma, NA0160)
- Glycerol-2-phosphate (Sigma, G62511)
- Hoechst 33258 (Polysciences, Inc., 09460)
- Horse serum (Vector Laboratories, S2000)
- Human basic FGF (PeproTech Inc., AF-100-18B)
- Human Cytokine Antibody Array G-series 2000 (RayBiotech Inc., AAH-CYT-G2000-8)
- Human qualified foetal calf serum (Gibco, 12662)
- Hydrogen peroxide (H₂O₂; Fluka, 95313)
- Hydroxyapatite 'fast flow' (Fluka, 55497)
- Interleukin 1 β , Human recombinant (PromoKine, C-61120)
- ImmPACT DAB (Vector Laboratories, SK-4105)
- L-Ascorbic acid-2-phosphate sesquimagnesium salt hydrate (Sigma, A5533)
- Magnesium chloride hexhydrate (Fluka, 63064)
- Magnesium chloride solution (25mM; Applied Biosystems, N8080010)
- MultiScribe Reverse Transcriptase 50 U/ μ l (Applied Biosystems, 1108105)
- OCT4-30 antibody (Abcam; AB13418)
- OGM Differentiation SingleQuots (Lonza, CC-4194)
- OptiPhase 'Hi Safe' Scintillation Liquid (Perkin Elmer, 1200-437)
- Osteoblast basal medium (Lonza, CC-3208)
- Osteogenesis assay kit (Millipore, ECM815)

- PCR Buffer II 10 x (500 mM KCl, 100 mM Tris/HCL, pH 8.3 ;Applied Biosystems, 4376212)
- PCRArray PAHS-021C-12 (SABiosciences, 330231)
- Penicillin-Streptomycin (10 kIU/ml; Gibco, 15140)
- Phosphatase substrate: 4-Nitrophenyl phosphate disodium salt hexahydrate (20mg tablets; Sigma, N-2765)
- Phosphate buffered saline, tablets (PBS; Sigma, P4417)
- Phosphate-buffered saline (PBS; Sigma, P4417 tablets)
- Platinum Retrovirus Expression System, pantropic (Cell Biolabs, Inc., VPK-302)
- Platinum-GP Retroviral Packaging cell line, pantropic (Cell Biolabs, Inc., RV-103)
- p-Nitrophenol (10umol/mL; Sigma, 104-1)
- p-Nitrophenol solution 10 mM (Sigma, V7660)
- P-Nitrophenyl standard solution 10mM (Sigma, N7660)
- Polyacryl carrier (Molecular Research Center; PC152)
- Polybrene, 10 mg/ml (Millipore, TR-1003-G)
- Potassium chloride (Fluka Chemica, 60130)
- Potassium phosphate monobasic (Fluka Chemica, 60230)
- Power Sybr Green PCR Master Mix (Applied Biosystems, 4367659)
- Proteinase K (Roche, 1000144)
- QuickStart Bovine Serum Albumin, 2mg/ml (Bio-Rad, 500-0206)
- QuickStart Bradtford Dye Reagent 1x (Bio-Rad, 500-0205)
- Random Hexamer 50 μ M (Applied Biosystems, 8080127)
- RNase Inhibitor 20 U/ μ l (Applied Biosystems, N8080119)
- RNaseZap® (Sigma, R2020)
- RNeasy mini kit (Qiagen, 74106)
- RQ1 RNase-Free DNase (Promega, M6101)
- RT² First Strand Kit (Qiagen, 330401)
- RT² SYBR Green ROX qPCR Mastermix (Qiagen, 220522)
- S.O.C medium (Invitrogen, 15544-034)
- Stem Cell Factor, human recombinant (PromoKine, C-63120)

- Stromal cell-derived factor-1 α , human recombinant (PromoKine, C-67220)
- Self-designed primers and probes (Microsynth, CH)
- Sodium bicarbonate (Sigma, 63100)
- Sodium Chloride (Fluka Chemica, 71380)
- Sodium hydroxide (Fluka Chemica, 71690)
- Sodium phosphate dibasic (Fluka Chemica, 71645)
- Superior foetal bovine serum (Biochrom, S0615)
- TaqMan Gene Expression Master Mix (Applied Biosystems, 4370074)
- TNS (Lonza, CC-5012)
- TRI Reagent® (Molecular Research Center, Inc., TR118)
- Tris-EDTA buffer solution (for molecular biology; Sigma, 9285)
- Triton-X-100 SigmaUltra (Sigma, T9284)
- Trypan Blue (Sigma, TB154)
- Trypsin-ethylenediaminetetraacetic acid (10x; 5g/L trypsin, 2g/L EDTA, 8g/L NaCl; Gibco, 15400-054)
- Tween20 (Sigma, P1379)
- Vectastatin ABC Elite kit (Vector Laboratories, PK-6102)

2.2. Methods

2.2.1. Culture and propagation of cells

In this study, 6 types of osteoblast cells from different origins and human bone marrow-derived mesenchymal stem cells (MSCs) were used (Tab.2.1).

The summary list of differentiation medium supplements, used for the induction of mineralisation, is presented in Table 2.2. All cell types were maintained in the same conditions at 37°C with an atmosphere of 5% CO₂ and 95% humidity. Unless otherwise stated, the medium was changed every 2 or 3 days.

Cell name	Type	Animal	Origin	Source
MSC	Primary	Human	Bone Marrow aspirates from iliac crest and vertebral body	Isolated
Human osteoblasts (HOb)	Primary	Human	Human osteoblast cells of a 6-year old female (long bone)	Lonza, USA
MG63	Osteosarcoma	Human	Primary osteosarcoma of a 14-year old Caucasian male	ECACC, UK
SaOs2	Osteosarcoma	Human	Primary osteosarcoma of an 11-year old Caucasian female	DSMZ, DE
MC3T3E1	Cell line	Mouse	Newborn mouse calvariae	DSMZ, DE

Table 2.1. Origin of osteoblast and MSC cells used in this study.

2.2.1.1. Human bone marrow derived stromal cells (MSC) isolation and propagation

Human bone marrow aspirates were obtained with the ethical approval and written consent of donors undergoing total hip replacement, vertebral body isolation or spinal fusion. Bone marrow aspirates were provided by Dr. Lorin Benneker, Dr. Sven Hoppe (Interspital Bern, Bern, Switzerland), Dr. Markus Loibl (Universitätsklinikum Regensburg, Regensburg, Germany) and Dr. Gian Salzmann (Universitätsklinikum Freiburg, Freiburg, Germany). Before proceeding with the isolation protocol, undiluted bone marrow aspirate was pipetted up and down to dislodge any clumps. Next, marrow was mixed with PBS (1:3) and passed through a 70µm cell strainer into a 50ml Falcon tube. One additional volume of PBS was used to rinse the cell strainer. The diluted marrow was transferred into a new tube containing 2.6ml Ficoll per 1ml of undiluted marrow and centrifuged at 800xG for 20 min at room temperature. The mononuclear cells from the interphase were transferred into a new tube and 5ml α MEM with 10% FCS medium was added to each ml of the collected interphase (Fig.2.1). Cells were mixed gently with

medium and centrifuged at 400xG for 15 minutes at room temperature. Supernatant was aspirated and pelleted cells were washed again. After washing, cells were re-suspended in the medium and counted with a Scepter 2.0 Handheld Automated Cell Counter (Millipore, US) using 40µm sensor. Isolated mononuclear cells were plated at a density of 50,000 cells per cm² in αMEM medium with 10% MSC qualified serum, 1% Penicillin-Streptomycin and 5ng/ml basic FGF. Medium was changed 4 days after plating and every 2-3 days thereafter. After reaching 80% confluence, cells were harvested and frozen down to -196°C.

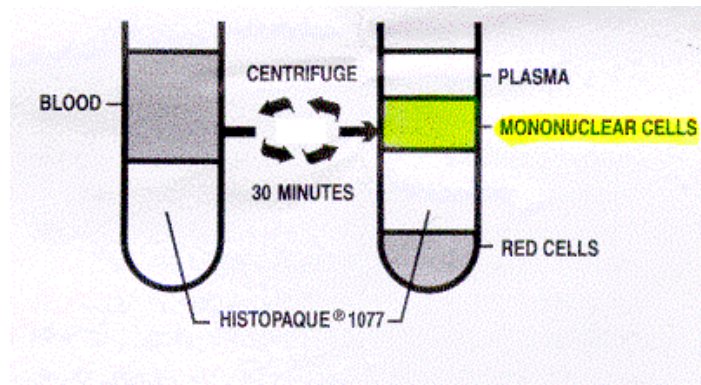


Figure 2.1. Phase-separation of bone marrow using Ficoll (Histopaque, 1077). Adapted from standard operating procedure document PRBT 002-04 (AO Research institute Davos, Davos, CH).

2.2.1.2. Primary Human Osteoblast (HOb) cells

Proliferating cells were maintained in Osteoblast Growth Medium (OGM) composed of Osteoblast Basal Medium supplemented with 10% FBS, 1% Penicillin-Streptomycin and 50µg/ml L-ascorbic acid 2-phosphate sesquimagnesium salt hydrate. For mineralisation experiments OGM was supplemented with 7.5mM β-glycerophosphate and 200nM hydrocortisone.

2.2.1.3. MC3T3E1 cells

Proliferating cells were maintained in standard growth medium composed of high glucose DMEM supplemented with 10% FBS and 1% Penicillin-Streptomycin. Cells from passage 7 were used for the osteogenic assays. Differentiation was induced by addition of 50µg/ml L-ascorbic acid 2-phosphate sesquimagnesium salt hydrate,

10nM final concentration dexamethasone and 5mM final concentration β -glycerol phosphate to standard growth medium.

2.2.1.4. MG63 cells

The MG-63, human cells from an osteosarcoma of 14-year-old male were purchased from ECACC (European Collection of Cultured Cells, UK). Proliferating cells were maintained in DMEM supplemented with 10% FBS and 1% Penicillin-Streptomycin. To induce mineralisation the growth medium was supplemented with 50 μ g/ml L-ascorbic acid 2-phosphate sesquimagnesium salt hydrate, 10nM final concentration of dexamethasone and 5mM final concentration of β -glycerol phosphate. Cells from passage 5-8 were used for experiments.

2.2.1.5. SaOs2 cells

Cells were purchased from DSMZ (Deutsche Sammlung von Mikroorganismen und Zellkulturen GmbH, DE) and received as an active culture in McCoy medium supplemented with 15-20% of FBS. Proliferating cells were maintained in DMEM supplemented with 10% FBS and 1% Penicillin-Streptomycin. Cells from passage 7 were used for osteogenic assays and from passage 8 for cell growth experiment. Proliferating cells were maintained in DMEM supplemented with 10% FBS and 1% Penicillin-Streptomycin. Differentiation was induced by the addition of 50 μ g/ml L-ascorbic acid 2-phosphate sesquimagnesium salt hydrate.

Cell type	Differentiation medium supplements
MSC	50 μ g/ml AA, 10 nM dex, 5 mM β GP
HOb	50 μ g/ml AA, 7.5 mM β GP, 200 nM hydrocortisone
MC3T3E1	50 μ g/ml AA, 10 nM dex, 5 mM β GP
MG63	50 μ g/ml AA, 10 nM dex, 5 mM β GP
SaOs2	50 μ g/ml AA

Table 2.2. List of supplements used for osteogenic differentiation of MSC, HOb, MC3T3E1, MG63 and SaOs2 cells; AA - L-ascorbic acid 2-phosphate sesquimagnesium salt hydrate, β GP - β -glycerol phosphate, dex - dexamethasone.

2.2.2. Cell passaging

Cell subculture was performed using 0.05% Trypsin-EDTA solution in PBS at 70-80% confluence of the monolayer cell cultures. The protease, trypsin, breaks down the proteins responsible for cell-cell and cell-matrix adherence by cleaving peptide bonds at lysine and arginine residues. The presence of divalent cations, such as calcium, which inhibits trypsin properties, is reduced by chelating it with EDTA. Before exposing cells to trypsin-EDTA solution, monolayer was washed twice with sterile PBS to ensure a total removal of medium and cell debris. Small volume of pre-warmed 0.05% Trypsin-EDTA in PBS (0.03ml per cm²) was applied into cell culture flasks containing cells. Depending on the cell type, cells were incubated with trypsin solution for 3-10 minutes at 37°C, followed by assessing of the cell detachment using an Axiovert 25 microscope (Carl Zeiss AG, Oberkochen, Germany) and the trypsin inactivation with growth medium containing 10% FBS. Cell suspension was transferred to the Falcon tube and centrifuged at 250xG for 10 minutes. Then, the supernatant was aspirated and cells were re-suspended in medium prior to manual cell counting of viable cells. After counting the desired concentration of cells per cm² was plated in a flask filled with respective volume of medium.

2.2.3. Cell freezing

For cryopreservation of cells, freezing medium containing 10% DMSO (dimethyl sulphoxide) in FBS was used. DMSO is commonly used cryoprotectant to prevent cells from rupture by the formation of ice crystals. Furthermore, for successful cryopreservation and viability of cells after reconstitution, cells were frozen at a rate 1°C per minute by -80°C using 5100 Cryo 1°C Freezing Container (Nalagene, USA).

After trypsinisation and counting procedure, cells were centrifuged again at 250xG for 10 minutes and re-suspended in freezing medium to obtain 1-2 million cells per ml. Then, 1ml aliquots of cells were distributed into cryotubes (Nunc, Rochester, NY) which were placed in freezing container. For initial freezing cells were placed at -80°C overnight and then cryotubes with frozen cells were stored in liquid nitrogen.

2.2.4. Cell reconstitution

Frozen cells were transferred into the sterile cell culture room on ice and reconstituted by quick thawing in water bath. The cryotube containing cells was cleaned with 70% ethanol before transferring into sterile laminar flow. Reconstituted cells were slowly transferred into 50ml tube containing 10ml pre-warmed growth medium. Cells were centrifuged at 250xG for 10 minutes. After resuspension in fresh growth medium, cells were counted manually and plated into a cell culture flask at the density 3000-6000 cells per cm², depending on cell type.

2.2.5. Generating osteoblast cell line with stable GFP expression

2.2.5.1. Propagation of pMX-GFP and pCMV-VSV-G retroviral vectors

pMX-GFP and pCMV-VSV-G retroviral vectors (Fig.2.2) were propagated in chemical competent TOP10 E. coli bacteria. After thawing on ice, 2µl of both vectors were added to bacteria, mixed gently and incubated on ice for 5 minutes. Next, bacteria underwent heat-shock for 30 seconds in the 42°C water bath. After adding 250µl S.O.C medium, bacteria was incubated for 1 hour in 37° C water bath under agitation (SWB25 Haake, Thermo Fisher Scientific Inc., US). Following this, 50µl bacteria were distributed evenly on pre-warmed ampicillin selective agar plates. Plates were incubated overnight in a 37°C. Next, two colonies were transferred from agar plate to 50ml Falcon tube containing 10ml LB medium supplemented with 100µg/ml ampicillin. Liquid cultures were grown for 16 hours under agitation (260 rpm) in a shaking incubator at 37°C.

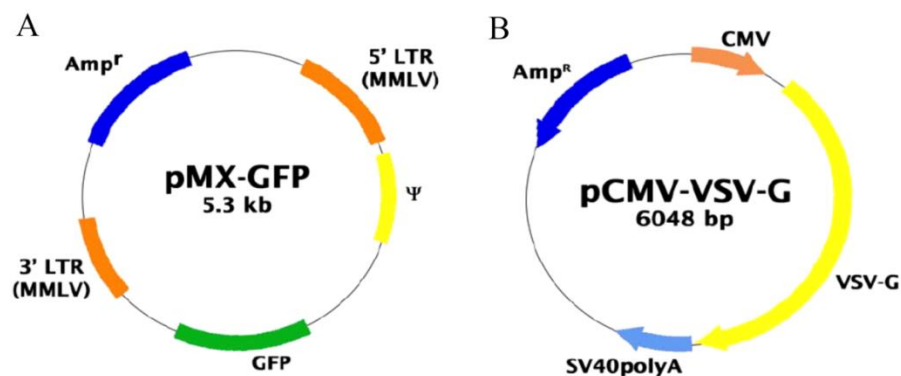


Figure 2.2. Schematic representation of pMX-GFP retroviral vector (A) and pCMV-VSV-G envelope vector (B). Figure adapted from the Product Manual provided by Cell Biolabs, Inc.

Isolation of pMX-GFP and pCM-VSV-G DNA was performed using Gene Elute Plasmid Miniprep Kit (Invitrogen). Briefly, liquid cultures were transferred to 15ml falcon tubes at 5ml per tube and bacteria were pelleted by centrifugation at 3000xG for 10 minutes (5810R, Eppendorf, DE). After removing supernatant, pellet was mixed with 200µl resuspension buffer. Then, 200µl cell-buffer mixture was transferred to the supplied tubes and mixed with 200µl lysis buffer by inverting the tubes gently 8 times. Lysis was stopped after 3.5 minutes by adding 350µl neutralization buffer into the each tube. The neutralization buffer was mixed with the lysate by inverting columns 8 times. Next, tubes were centrifuged at 12000xG for 10 minutes (Micro22, Hettich, DE). In the meantime, 500µl column preparation buffer was added to each column supplied by manufacturer and centrifuged at 12000xG for 1 minute. The flow-through was discarded and approx. 600µl supernatant from the lysed bacteria was added to the column and centrifuged at 12000xG for 1 minute. After discarding flow-through, 500µl of 'first washing buffer' was added and centrifuged as before. When finished, 750µl 'second washing buffer' was added to the columns and again, centrifuged at 12000xG for 1 minute. Additional centrifugation was performed at 12000xG for 4 minutes after discarding flow-through. Any leftovers of the buffers were removed from column using a 10µl pipette. Columns were air dried and transferred into the new collection tubes. Then, 50µl elution buffer was added to the membrane of the columns and incubated for 2 minutes. To ensure better binding of the DNA, elution buffer was pre-warmed before adding to the column. DNA was collected by centrifugation at 12000xG for 1 minute. The purity and amount of the DNA was assessed using 260/280 and 260/230 ratio using the NanoDrop system (Witec GmbH, DE) and associated software. Samples were then stored at -80°C until required.

2.2.5.2. Transfection of PlatGP cells with pMX-GFP and pCM-VSV-G vectors

The packaging PlatGP cell line cells were transfected with pMX-GFP and pCM-VSV-G vector using FuGENE[®] HD Transfection Reagent carrier. This carrier is composed of lipids and other components which form a complex with DNA. It has high transfection efficiency and very low cytotoxicity. Before transfection all reagents and DNA were adjusted to the room temperature. First, 6µg pMX-GFP

DNA and 3µg pCMV-VSV-G was diluted with 300µl high glucose DMEM (without serum, antibiotics and fungicides). The transfection complex was formed by adding 27µl FuGene[®] to the diluted DNA followed by incubation for 15 minutes at room temperature. After that time, PlatGP cells at 80% confluence were transfected. The transfection complex was added to the cell culture medium drop-wise. Flasks were swirled to ensure the even distribution of the transfection complex in the flasks. After 48 hours the supernatant from the flask was collected and centrifuged at 500xG for 10 minutes to eliminate any cell debris. Collected supernatant was snap frozen in liquid nitrogen and stored at -80°C until required.

2.2.5.3. MG63-GFP cell line

For generating an osteoblast cell line with stable expression of green fluorescent protein (GFP), MG63 cells were transduced with retroviral vector containing GFP insert. MG63 cells were thawed, plated in 75cm² flask and cultured in standard conditions for 48 hours before proceeding with retroviral transduction. On the day of transduction, cell morphology and confluence were assessed using an Axiovert 25 microscope. Retroviral vectors and 'Polybrene' were thawed on ice. After aspiration of the cell culture medium, 900µl supernatant was mixed with 7.2µl Polybrene and added to flask with MG63 cells. Transduction was conducted under standard conditions for 2 hours. To ensure even distribution of transduction mix, the flask was gently rocked every 15 minutes. After transduction, 15ml complete medium was added to the flask and changed after 24 hours. In addition, mock-treated control group was included where retroviral supernatant was substituted with 900µl of serum free DMEM. Transduced and non-transduced cells were trypsinised at 70% confluence as described in paragraph 2.2.2. Before counting cells were passed through 40µm cell strainer. Subsequently, cells were sorted with FACS Aria III (BD Biosciences, Franklin Lakes, USA). For acquisition and analysis manufacturer software BD FACSDiva version 6.1.3 was used followed by histogram analysis using non-commercial software Cyflogic version 1.2.1 (CyFlo Ltd., FI). After analysis, single cell cultures from a positive cell population were seeded in 96-well plates to obtain pure MG63 colonies expressing GFP. For proliferation or osteogenic differentiation cells were maintained in the same conditions as MG63 (paragraph 2.2.1.4).

2.2.6. Monolayer cell culture of cells from different origins

For the study comparing the osteoblast cells from different origins, cells from human, bovine and ovine bone, SaOs2, MG63 and MC3T3E1 cells were cultured in 6 or 24 well plates on the Thermanox® discs (Nunc, Rochester, NY). To assess matrix mineralisation, alkaline phosphatase activity and mRNA expression of osteoblast specific genes cells were plated at a density of 5000 cells per cm² in 6-well plates on 25 mm Thermanox discs and cultured in cell differentiation medium specific for the each cell type (Tab.2.2) by 21 days. Samples for analysis were collected at day 1, 7, 14 and 21. Cells for the growth assay ('CellTiter Blue') were seeded at a density of 10000 cells per cm² in 24 well plates on 13mm diameter Thermanox® discs and cultured in growth medium specific for each cell type as described above (Tab.2.2).

In the study comparing cells differentiation in different cell culture models, monolayer cultures of MSC or MG63 cells were made by plating 20000 cells per cm² in 24-well plates. Subsequently, 500µl differentiation or growth medium was added to each well. At day 2, 7, 14 and 21 of cell culture samples were collected for ALP activity, DNA content quantification and mRNA expression analysis of genes specific for differentiation.

2.2.7. High density culture (micromass) of MSC

The high density culture was used for a single cell type culture and co-culture experiments. In single cell type culture, micromass was produced by suspending 200000 cells in 10µl of growth medium consisting of low glucose DMEM, 10% FBS and 1% Penicillin-Streptomycin. This volume was placed in the middle of 24-well plate. Then, approximately 50µl of medium was placed around the well edge and samples were incubated for 3 hours in incubator to let micromass attach. After that time, additional 500µl of differentiation or growth medium was added. At day 14 of the cell culture, samples were collected for ALP activity, DNA content quantification and mRNA expression analysis of genes specific for differentiation.

2.2.8. Cell culture in type I collagen-hydroxyapatite gel

All solutions used for the gel preparation were at 4°C and the preparation was carried out on ice. To prepare 1ml type I collagen gel, 320µl DMEM and 50µl 10xPBS were mixed in 50ml tube. Then, 833µl type I collagen gel was added and mixed with other constituents by slow pipetting. Subsequently, the pH was elevated by adding 30µl 1N NaOH and mixed. The final concentration of prepared gel was 2.5mg type I collagen per ml and pH ~7. In order to stabilise gel when culturing with cells and prevent shrinkage as well as cell dropping through the gel, the hydroxyapatite (HAP) was added before gelation. Several HAP concentrations (0.2-1.25mg HAP per 1 ml type I collagen gel) were tested. As a result, 1mg HAP per 2.5 mg type I collagen (CHAP) per ml was used.

Collagen type I-hydroxyapatite (CHAP) gel was applied for the cell culture. The expanded and harvested cells were centrifuged and counted. Then, the desired amount of cells was re-suspended in small volume of DMEM containing hydroxyapatite particles. Type I collagen gel was prepared as described above. The volume of DMEM used in gel preparation was subtracted by the volume used for the cell re-suspension to ensure that the final concentration of type I collagen gel is 2.5mg/ml. This mixture containing cells was transferred to the tube containing type I collagen and mixed by slow pipetting. After ensuring uniform distribution within the CHAP, 250µl CHAP with cells were transferred into a well of 24-well plate. One million of cells were used per ml of CHAP. Thus, one sample contained 250000 cells in 250µl CHAP. Samples were incubated for an hour at 37°C for gelation to occur, before adding 500µl medium.

2.2.9. Stimulation of MSC cells with different factors

Expanded MSC were harvested, counted and plated at a density of 15000 cells per cm² in cell culture polystyrene flasks and cultured in DMEM supplemented with 10% FCS and 1% Penicillin-Streptomycin overnight at 37°C with an atmosphere of 5% CO₂ and 95% humidity. Two experimental designs for cell stimulation were applied. The schematic presentation is presented on figure 2.3.

On the day of stimulation, medium was aspirated and fresh medium containing 10ng/ml IL1 β , 100ng/ml SCF, 100ng/ml GCSF or 1 μ g/ml SDF1 was added. For negative controls, cells were kept in medium without any factor. After 2 hours, medium was aspirated and cells were washed with PBS to ensure complete removal of the factors. For the following 48 or 72 hours, cells were cultured in fresh DMEM supplemented with 1% pen/strep (Fig.2.3B) and, in part of the experiments, 10% FBS (Fig.2.3A).

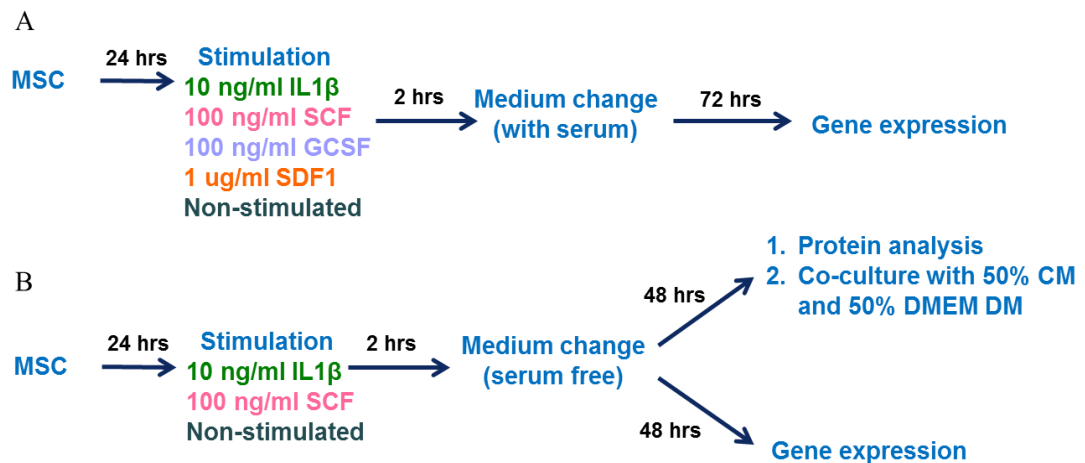


Figure 2.3. Outline of stimulation experiments and analysis. A: 24 hours after plating MSC cells were stimulated with 10 ng/ml IL1 β , 100 ng/ml SCF, 100 ng/ml GCSF or 1 μ g/ml SDF1 for 2 hours. After that time fresh medium with 10% FBS and 1% Penicillin-Streptomycin was added to cells. Gene expression analysis was performed 72 hours later. B: 24 hours after plating MSC cells were stimulated with 10 ng/ml IL1 β or 100 ng/ml SCF. After stimulation, cells were maintained in DMEM with 1% Penicillin-Streptomycin for 48 hours before conditioned medium collection.

2.2.10. Conditioned medium collection

Medium conditioned for 48 hours by stimulated or unstimulated cells was collected and centrifuged at 1000g at 4°C for 20 minutes to remove any cell debris. Subsequently, supernatant was transferred into fresh tubes and stored until required at -20°C.

2.2.11. Indirect co-culture of cells

2.2.11.1. Monolayer co-culture of cells

Indirect co-culture of cells in ML was set up in 24-well plates (BD Falcon, Belgium) and inserts (tissue culture treated polyethylene terephthalate-PET membrane with 0.4µm pore size) and MM in 24-well plates (TPP, Switzerland). The expanded and harvested MSC and MG63 cells were centrifuged and counted. Twenty thousand cells per cm² were seeded onto the insert membrane and companion tissue culture plate according to the design presented in table 2.3. Five hundred microliter of differentiation (DMEM DM) or growth (control; DMEM GM) medium was added to each well, whereas 300µl of media were applied into each insert. Medium was changed every 2-3 days. Samples were harvested at day 14 for ALP activity and DNA quantification assays; and at day 21 for the gene expression analysis.

Group	1	2	3	4	5	6	7	8
Top (insert)	MSC	MG	MG	MSC	MSC	MG	MG	MSC
Bottom (well)	MG	MSC	MG	MSC	MG	MSC	MG	MSC
Medium	DM	DM	DM	DM	GM	GM	GM	GM

Table 2.3. Experimental groups and configuration of cells used in monolayer co-culture study. MSC – bone derived mesenchymal stem cells; MG – MG63 cells; DM – differentiation medium; GM – growth medium.

2.2.11.2. Micromass co-culture of cells

The procedure of micromass cultures preparation was similar as described in paragraph 2.2.7 with the exception of cell number used. Table 2.4 summarises the subdivision of the experimental groups. Cultures were prepared in 24 well plates (TPP, Switzerland). Briefly, micromass' made of 100000 cells of MSC or MG63 cells per 5µl were prepared. To each well 500µl of differentiation (DMEM DM) or growth (control; DMEM GM) medium was added. Medium was changed every 2-3 days. Samples were harvested at day 14 for ALP activity, DNA content assay and at day 21 for gene expression, ⁴⁵Ca incorporation and DNA content analysis.

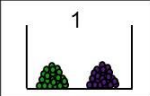
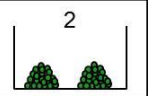

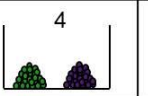
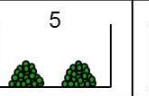
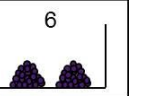
Group						
Cell type	MG+MSC	MG	MSC	MG+MSC	MG	MSC
Medium	DM	DM	DM	GM	GM	GM

Table 2.4. Experimental groups and configuration of cells used in micromass co-culture study. MSC – bone derived mesenchymal stem cells; MG – MG63 cells; MG+MSC – co-culture of MG63 and MSC; DM – differentiation medium; GM – growth medium

2.2.11.3. Co-culture with conditioned medium

Human bone marrow MSC were expanded and plated in monolayer on Thermanox® discs at a density of 20000 cells per cm² for differentiation and 5000 cells per cm² for proliferation analysis. For differentiation, cells were maintained in medium consisting of conditioned medium collected from MSC cells stimulated with IL1 β , SCF or unstimulated cells mixed with control or osteogenic medium in 1:1 ratio. Control medium contained DMEM low-glucose supplemented with 1% FBS and 1% Penicillin-Streptomycin. Osteogenic medium was composed of the control medium supplemented with 100 μ g/ml ascorbic acid salt, 20nM dexamethasone and 10mM glycerol-2-phosphate. Medium was changed twice per week. For the analysis of cell proliferation cell samples were harvested at day 2, 4, 7 and 10. Osteogenic differentiation was assessed at day 7 and 14 by gene expression and ALP activity, and at day 28 by Alizarin Red S staining and quantitation.

2.2.12. Determination of cell number and proliferation

2.2.12.1. Manual cell counting

In order to determine cell number and distinguish between viable and nonviable cells the Trypan Blue exclusion method for cell counting was used. This method is based on the principle that live cells having intact cell membrane exclude this diazo-dye, whereas the dye transverse the membrane of dead cells. As a result, viable cells have clear cytoplasm and nonviable cell is as a distinctive blue colour under a microscope. Manual cell count was performed during passaging of cells, freezing of cells or cell seeding for an experiment. For cell counting, 20 μ l cell suspension was

mixed with 20µl of Trypan Blue before filled into the chamber of a Neubauer haemocytometer. Using a bright field microscope (Carl Zeiss AG, Oberkochen, Germany) cell count was performed. Unstained cells were counted within each of the four corner squares. Cells located on the top and left-hand lines of each square, whereas those on the bottom or right-hand lines were included in the counting. Cell number was calculated using the following formula:

$$\textit{Total cell number} = n * d * v * 10000,$$

where n - average number of cells per square, d – dilution factor, v – total volume of cell suspension.

2.2.12.2. Hoechst assay

The method is based on the enhancement of fluorescence seen when bisbenzimidazole (Hoechst 33258) binds to the minor groove of DNA. Crude homogenates in which chromatin has been dissociated with high salt buffer can be assayed directly in a few minutes. The dissociation of chromatin is critical to accurate determination of DNA in biological materials. The fluorescence of Hoechst 33258 is related to the AT content of a DNA sample, so it is very important to use a standard similar to the sample under investigation. The calf thymus DNA standard is double-stranded, highly polymerized, and it has an approximate content of 60% AT (40% GC).

The DNA was assessed in samples digested in Proteinase K solution, which consists of 0.5mg proteinase K per ml of PBS containing 3.36g/L disodium-EDTA with pH6.5. Before overnight incubation of samples with proteinase K solution, samples were washed with PBS. Plates sealed with parafilm and wrapped in aluminium foil were incubated overnight at 56°C. Then, samples were transferred into a 1.5ml tubes and stored at -20°C until further analysis. The determination of DNA content for all samples from one experiment was performed at the same time.

Calf thymus DNA was used as a standard to determine DNA content in samples. For this, 2-fold dilutions of the DNA ranging from 0.39 to 12.5µg/ml were made in PBS containing 2M NaCl (DPBS). Forty microliters of each sample, standard

and blank were pipetted in duplicates into a white opaque 96 well plate (Falcon® Becton Dickinson Labware, France). Then, 160µl of assay solution containing 0.1µg/ml Hoechst 33258 in DPBS were added into each well. Plate was wrapped in aluminium foil and incubated for exactly 20 minutes at room temperature. The fluorescence values were measured (excitation/emission: 360/465 nm) using a Multilabel Counter Wallac 1420 (Perkin Elmer). The results were calculated by averaging fluorescent values of the samples and subtracting average value of blank. The amount of DNA was calculated from the equation defined by a linear standard curve vs DNA amount (µg/ml).

2.2.12.3. Cell Titer-Blue® assay

The assessment of cell accumulation was performed using the Cell Titer-Blue® Assay. This method is based on the ability of viable cells to metabolically reduce resazurin (indicator dye) into highly fluorescent resorufin (Czekanska, 2011). Cells were seeded at the density 5000 cells per cm² in 24 well plates. Cell number was evaluated every 24 hours up to 10 days. At each time point, the media was aspirated from 4 wells and the samples were subsequently washed with 0.1M phosphate buffered saline (PBS) solution. After rinsing, 350µl of fresh medium containing a 10% solution of Cell Titer-Blue® were added to the wells. Three no cell control wells were included. Culture plates were wrapped in aluminium foil and incubated at 37°C with an atmosphere of 5% CO₂ and 95% humidity. The incubation time was 4 hours for MC3T3E1, bovine and ovine osteoblast cells and 2 hours for HOb cells. For the optimisation of incubation time see Appendix 1.

After incubation, 150µl aliquot of each sample and media with dye alone, were transferred to a white opaque 96 well-plate (Falcon® Becton Dickinson Labware, France) in duplicate. Subsequently, the fluorescence values of samples were measured (excitation/emission: 560/590 nm) using a Multilabel Counter Wallac 1420 (Perkin Elmer, US). The results were calculated by averaging fluorescent values of the samples and subtracting average value of samples without cells. Cell number at each time point was calculated using the equation defined by a standard curve generated from fluorescence values obtained from known number of cells.

2.2.13. Determination of cell viability

Viability of cells cultured in type I collagen-hydroxyapatite gel was assessed with fluorescent dyes, calcein AM and ethidium homodimer-1 which allow to discriminate between live and dead cells. Calcein AM, acetomethoxy derivate of calcein, is an indicator of live cells. After the transport through the cellular membrane into live cells, intracellular esterases remove the acetomethoxy ester group from dye molecule. Liberated calcein gives strong green fluorescence at excitation and emission wavelengths of 495/515nm. Ethidium homodimer is a membrane-impermeable fluorescent dye with excitation/emission maxima at 528/617nm. It has a high nucleic acid binding affinity and upon binding to DNA emits strong red fluorescence.

Before staining with fluorescent dyes, CHAP gels were washed twice with PBS. Second washing was performed for 5 minutes. During that time dyes were mixed with DMEM in light shield tube to obtain working solution containing 10ng/ml calcein and 1ng/ml ethidium homodimer-1. Gel was incubated with working solution for 20 minutes at room temperature followed by 10 minutes incubation at 37°C. For the incubation, plate containing gel was covered with aluminium foil to avoid exposure to light. After incubation, working solution was aspirated and fresh medium was added to the samples. Labelled cells within the gel were visualised with Axiovert 200 M microscope (Carl Zeiss AG, Oberkochen, Germany).

2.2.14. Alkaline phosphatase activity

2.2.14.1. Staining

Qualitative alkaline phosphatase activity measurement was performed using Leukocyte Alkaline Phosphate Kit. It consists of naphthol AS-MX phosphate and fast violet B salt (4-Amino-5-methoxy-2-methylbenzanilide diazotated zinc double salt). By the action of Alkaline Phosphatase (ALP) the phosphate group is hydrolysed and liberated naphthol AS-MX and reacts with a diazonium salt forming an insoluble blue pigment at sites of phosphatase activity. The concentration and intensity of this pigment reflect the activity of the enzyme.

The Fast blue dye solution (dissolved fast blue salt from one tablet in 48ml deionised water and 2 ml Naphthol AS-MX) was prepared according to the manufacturer protocol. Prior to fixation, samples (n=4) were washed three times with 0.1M PBS solution and then fixed in 90% ice cold ethanol for 4 minutes. Then, samples were washed three times with deionised water. Fast Blue dye solution was added subsequently to three dishes. At each time point one sample was included as a negative control that was incubated with the dye and 10mM tetramisole hydrochloride (Sigma, UK). All samples were wrapped in aluminium foil and incubated for 1 hour at room temperature. After incubation, samples were washed three times with deionised water and visualised with Axiovert 200 M microscope (Carl Zeiss AG, Oberkochen, Germany).

2.2.14.2. Quantification

Samples (n=4 per time point) were washed three times with PBS and cell layers were extracted with 0.1% Triton-X in 10mM Tris-HCl pH 7.4 for 1 hour at 4°C on a gyratory shaker. Then samples were transferred into tubes and frozen until required.

Prior to analysis, samples were thawed and stored at 4°C for 30 minutes. Then, 250µl 1.5M alkaline buffer pH 10.3 (2-amino-2-methylpropano), 50µl phosphate substrate solution (4-nitrophenyl phosphate disodium salt hexahydrate) were added into the tube. For part of this study (chapter 3), 100µl deionised water followed by 100µl sample were added into the reaction mixture. Otherwise, 200µl cell lysate were pipetted into each tube. The mixture was mixed and incubated for 30 minutes at 37°C in a heated block. The reaction was stopped by adding 500µl 0.1M NaOH. The standard curve was prepared by using serial dilutions of 1mM p-nitrophenol in 0.1% Triton-X in 10mM Tris-HCl added to the mixture instead of the unknown sample and incubating for 15 minutes at 37°C. The absorbance of 250µl standard and samples were measured at 405nm in duplicates on a Multilabel Counter Wallac 1420 (Perkin Elmer, US). The standard curve was prepared and sample values were calculated as nM p-Np per minute per µg of protein or nM p-Np in 30 minutes per µg DNA.

2.2.15. Determination of calcification

2.2.15.1. Alizarin Red S

2.2.15.1.1. Staining

Qualitative mineralisation was performed using 40mM Alizarin Red S dye at pH4.1-4.3. Prior staining cell cultures were washed twice with PBS followed by fixation with 4% paraformaldehyde for 15 minutes. After that time, samples were washed with deionised water for 5 minutes and this step was repeated two times. Subsequently, 250 μ l per cm² of 40mM Alizarin Red S solution was added into each sample. Samples were covered with aluminium foil and incubated for 1 hour at room temperature on a rotating plate. After incubation, samples were washed five times with deionised water and stored at 4°C for until required for image analysis performed on Axiovert 200 M microscope (Carl Zeiss AG, Oberkochen, Germany).

2.2.15.1.2. Quantification

After staining, calcium-bounded Alizarin Red S dye was quantified. As a standard Alizarin Red S dye in concentration range from 0.47 μ M to 30 μ M. Serial dilutions were prepared from 40 μ M stock solution used for staining of samples. Alizarin Red S was diluted with 'standard solution' composed of 10% ammonium hydroxide and 10% acetic acid (1:4).

For this, stained samples were incubated for 30 minutes at room temperature with 10% acetic acid. Subsequently, the loosely attached monolayer with acetic acid was transferred into 1.5ml Eppendorf tube which was later sealed with parafilm. After incubating at 85°C for 10 minutes, samples were placed on ice for 5 minutes. Next, samples were centrifuged at 20000g for 15 minutes. The supernatant was transferred into a new tube and 120 μ l 'standard solution' was added to each sample to neutralize the acetic pH to 4.1-4.5. One hundred and fifty microliters of 'standard solution' used as blank, standard and samples were transferred into transparent 96-well plate in duplicates. The absorbance was read at 405nm on a Multilabel Counter Wallac 1420 (Perkin Elmer, US). The concentration of bounded-Alizarin Red S in samples was determined using the equation defined by standard curve.

2.2.15.2. Radioactive calcium incorporation

Biosafety procedures level II was followed at all the times during the procedures. Medium from samples was aspirated and samples were washed with PBS. Three hundred microliter medium containing 1.25 μ Ci 45 Ca per ml was pipetted per each sample in 24-well plate. Then, plates were carefully wrapped in aluminium foil and incubated overnight at 37°C in cell culture incubator. The following day, samples were transferred in the radioactivity hood (cabinet) and medium was removed. After rinsing with PBS, 500 μ l 70% formic acid were added into each well. The plate was wrapped in parafilm and aluminium foil and incubated at 65°C for 60 minutes. The plate was then stored at room temperature within the laminar flow. After 2 days of incubation, the whole volume of formic acid from each well was transferred into a scintillation tube and 3.5 ml of scintillation fluid was added. Samples were mixed and placed into the scintillation counter rack. Scintillation was measured with WinSpectral 1414 Liquide Scintillation Counter (Perkin Elmer, US). The amount of incorporated calcium was expressed in counts per minute and made relative to total DNA amount.

2.2.16. Molecular biology

2.2.16.1. RNA extraction

The RNA isolation was performed by combination of the traditional single step method based on TRI reagent and RNeasy Mini-Kit. Since its introduction by Chomczyński and Sacchi the TRI-reagent is the most effective method of extraction a whole spectrum of RNA molecules (Chomczynski and Sacchi, 1987). The TRI reagent solution consists of combination of phenol and guanidine thiocyanate in a mono-phase solution that inhibits RNase activity. Using the spin column with silica-based membrane as an additional step allow to obtain a high quality of RNA (>200 bases).

At specific time points, the RNA isolation started with the removal of the culture medium from the cells. One millilitre of TRI reagent was added to each well to perform lysis of cell monolayer. Samples were incubated with the reagent for 2 minutes at room temperature (20-23°C) and cell lysis was completed

by repetitive pipetting. Then, the cell lysate was transferred to an RNase-free Eppendorf tube containing 5 μ l of Polyacryl Carrier, which consists of acryl polymer facilitating the isolation of small amounts of RNA. The cell lysate was mixed with Polyacryl Carrier by repetitive pipetting and subsequent shaking on Vortex-2 Genie Shaker. Next, the 100 μ l 1-bromo-3-chloro-propane was added to the samples and they were immediately shaken vigorously for approximately 30 seconds and incubated for 15 minutes at room temperature to achieve phase separation. To complete this process the incubation was followed by centrifugation at 12000xG for 15 minutes at 4°C (5417R Eppendorf, DE). In phase separation process the homogenate separates into three phases: aqueous containing RNA, interphase with DNA and organic phase where proteins are present. After centrifugation, the tubes were collected very carefully and about 270 μ l of aqueous phase of each sample were transferred into new 1.5ml RNase-free Eppendorf tube and an equal volume of 75% ethanol was added to the aqueous phase. Then the RNA precipitate was transferred to RNA binding column and centrifuged for 25 seconds at 8000xG.

The collected ethanol was discarded. Subsequently, the Qiagen protocol for RNeasy Mini-Kit was followed. The 700 μ l RW1 buffer contained within the Qiagen kit was applied to the column and it was centrifuged for 25 seconds at 8000g. The flow through was discarded and 500 μ l RPE wash buffer containing ethanol was applied to the column and centrifuged as previously. Once completed, the flow through was discarded and again, 500 μ l RPE wash buffer was added to the column. To ensure complete buffer penetration of the membrane, samples were stored at room temperature for 2 minutes. This was followed by the centrifugation for 2 minutes at 8000xG. Then, to prevent the ethanol carryover, the column was transferred to a new 2 ml collection tube and centrifuged for 1 minute at 12000xG. Finally, the column was transferred to a 1.5ml collection tube and 30 μ l RNA-free water was applied directly to the membrane and column was centrifuged for 1 minute at 8000xG. Upon completion, the eluted RNA was transferred to RNase free 1.5ml tubes. Samples were then stored at -80°C until required.

The purity and amount of the RNA was assessed using 260/280 ratio and 260/230 ratio using the NanoDrop system (Witec GmbH, Germany) and associated software. Samples were then stored at -80°C until required. While the first ratio determines the amount of nucleic acids versus protein in the sample, the second one describes the amount of nucleic acids versus salts in the sample. For pure RNA both ratios are expected to be about 2.0.

2.2.16.2. DNase digestion and clean-up.

Samples designated for analysis with RT² PCRArray were treated with RQ1 (RNA-Qualified) RNase-Free DNase to ensure very high quality of RNA samples. DNase I RQ1 RNase-Free DNase is an endonuclease enzyme that degrades both double-stranded and single-stranded DNA, producing 3'-OH oligonucleotides.

The protocol of DNase digestion reaction for 1µg RNA encompassed 1µl RQ1 RNase-Free DNase 10X Reaction Buffer, 1U/µg RNA RQ1 RNase-Free DNase and 1µg RNA. At the end, the reaction mix was completed with nuclease-free water to a final volume of 10µl. The reaction was performed at 37°C for 30 minutes. After the incubation, the reaction was terminated by adding 1µl RQ1 DNase Stop Solution and subsequent inactivation of DNase at 65°C for 10 minutes. Then, the enzyme and buffer components were removed with on-column RNA Clean-Up protocol. Briefly, samples were diluted with RNase-free water to 100µl and then, 350µl RLT Buffer was added. Diluted samples were mixed with 250µl ethanol (100%). The mixture was transferred to RNA binding column and centrifuged for 30 seconds at 8000xG using 5415R centrifuge (Eppendorf, Germany). The collected flow-through was discarded and 500µl RPE wash buffer containing ethanol was applied to the column and centrifuged. From this point, the protocol described in previous paragraph 2.2.16.1 was followed.

2.2.16.3. Reverse transcription

Two protocols of reverse transcription were applied within this study. The reverse transcription for most of the samples was performed using "Multiscribe™ Reverse transcriptase", which is a recombinant Moloney murine leukemia virus (rMoMuLV)

reverse transcriptase that uses single-stranded RNA as a template in the presence of a primer to synthesize a complementary DNA (cDNA) strand.

For each reaction, between 0.5 and 1µg of isolated RNA was used in 20µl reaction. First, the non-enzymatic components were mixed in RNase free tube. This included 2.0µl 10x TaqMan RT Buffer (PCR Buffer II), 4.4µl 25mM Magnesium chloride, 4.0µl deoxy nucleotide triphosphates mixture (dATP, dCTP, dGTP, dTTP; each 25mM), and 1.0µl Random Hexamers (50µM). The mixture was briefly vortexed before adding 0.4µl RNase inhibitor (20U/µl) and 0.5µl Multiscribe Reverse Transcriptase (50U/µl). The mixture was carefully mixed by inverting the tube. Then, the appropriate volume of total RNA sample was added. Lastly, the reaction mixture was made up to 20µl by adding RNase free water. The reaction was performed in a GeneAmp 5700 SDS instrument (Applied Biosystems, US) at 10 minutes at 25°C for primer incubation, 30 minutes at 48°C for reverse transcription, and 5 minutes at 95°C for reverse transcriptase inactivation. When reaction was completed, 20-60µl Tris-EDTA buffer was added to stabilise the pH of the cDNA in thawed samples. Samples were then stored at -20°C until required.

A different protocol for reverse transcription was used for samples undergoing gene expression analysis with RT² Profiler™ PCR Array. For these samples, cDNA was prepared using RT² First Strand Kit containing genomic DNA elimination and reverse transcription reagents. Before the reactions, RNA concentration and purity was checked using NanoDrop spectrophotometer. To eliminate genomic DNA 0.5µg RNA sample was mixed with GE Buffer and supplemented with RNase-free water up to 10µl. Then the reaction was performed at 42°C for 5 minutes and followed by immediate termination at 4°C for 5 minutes. Samples were then placed on ice for subsequent steps. Ten microliters of the reverse transcription mix used for one reaction contained 4µl 5x buffer BC3, 1µl control P2, 2µl RE3 Reverse transcriptase mix and 3µl RNase-free water. This RT mixture was added to tube containing 10µl genomic DNA elimination – RNA mix. The reverse transcription was performed in a GeneAmp 5700 SDS instrument at 42°C for 15 minutes and then immediately stopped by the incubation at 95°C for 5 minutes. After the competition,

the obtained cDNA was diluted with 91µl RNase-free water and stored at -20°C until required.

2.2.16.4. Real-Time PCR

For the gene expression analysis two systems of cDNA amplification were applied; DNA-binding agent (Sybr Green) and hydrolysis probes (TaqMan© probes).

Sybr Green is a fluorescent intercalating agent which upon binding to double stranded DNA emits a strong fluorescent signal that is proportional to the amount of double stranded DNA present. This method was used in the study comparing different cell models. The primers for alkaline phosphatase (ALP), Osteocalcin (OC), Runx2/Cbfa1, collagen type I (COL1), Sp7 and housekeeping gene 18S rRNA were purchased from Mycosynth (Tab.2.5). The procedure optimising primer concentration was carried out to determine the minimum primer concentrations giving the lowest threshold cycle (C_T ; the cycle in which there is a significant increase in reporter signal above the threshold) and the maximum ΔR_n (the magnitude of the signal generated by the given set of PCR conditions) while minimising nonspecific amplification. For each gene, reactions with different concentrations of forward and reverse primer were performed. Nine conditions were tested with mixed concentration (200, 400 and 800nM) of primers. Based on the results the concentration of 400nM was chosen as optimal for both primers.

In addition, the primer concentration was tested for the amplification efficiency using a diluted template from a positive control of osteoblast cells cultured in differentiation medium. This point is important for the direct comparison of C_T values between the target gene and the reference gene (relative quantification). The amplification efficiency of both, the target and reference gene, should be close to 100% and not different than $\pm 10\%$. The efficiency was calculated from the linear regression curve of concentrations against the logarithm of dilution (Appendix 2).

The Real-Time PCR reactions were performed in AB 7500 thermocycler (Applied Biosystems, US). Duplicate reactions were performed for each sample. The reaction mixture for one 20µl reaction contained 10µl Power SybrGreen PCR Master Mix,

0.4µl forward and reverse primer (final concentration of 400nM), 7.2µl RNasy free water and 2µl cDNA template. Reaction mixture was transferred into flat deck thermo-fast 96 detection plates (Thermo Scientific, UK) and sealed with optical clear adhesive seal sheets (Thermo Scientific, UK). As a negative control one sample with all reagents but without template was included for each primer set. Plate was centrifuged for 2 minutes in a Rotanta 46 plate centrifuge (Hettich, CH) to ensure all reaction mixture was at the bottom of each well. After transferring to an Applied Biosystems 7500 thermocycler the plate was incubated for 10 minutes at 95°C for AmpliTaq Gold polymerase activation and then 40 cycles of PCR reaction were run at 95°C for 15 seconds and 60°C for 1 minute. To confirm the absence of nonspecific amplification a dissociation curve was generated (60-95°C for 20 minutes).

Gene	Accession number	Forward 5'-3'	Reverse 3'-5'	Species
ALP	NM_000478	CCG TGG CAA CTC TAT CTT TGG	GCC ATA CAG GAT GGC AGT GA	Human
Osteocalcin	NM_199173	AAG AGA CCC AGG CGC TAC CT	AAC TCG TCA CAG TCC GGA TTG	Human
Runx2/Cbfa1	NM_004348	AGC AAG GTT CAA CGA TCT GAG AT	TTT GTG AAG ACG GTT ATG GTC AA	Human
Type I collagen	NM_000088	CCC TGG AAA GAA TGG AGA TGA T	ACT GAA ACC TCT GTG TCC CTT CA	Human
Sp7	NM_152860	CCT GCT TGA GGA GGA AGT TCA	GGC TAG AGC CAC CAA ATT TGC	Human
18S rRNA	X03205	GCA ATT ATT CCC CAT GAA CG	GGC CTC ACT AAA CCA TCC AA	Human
ALP	NM_007431	GGA ATA CGA ACT GGA TGA GAA GGC C	CAG TTC AGT GCG GTT CCA GAC ATA G	Mouse
Type I collagen	NM_007742	CTG GCT TTG CCG GCC	ACC TTT AAC ACC AGT ATC ACC AGG T	Mouse
Osteocalcin	NM_007541	GCA ATA AGG TAG TGA ACA GAC TCC	CAT CCA CTT CTG CTT CTT CGT TCT C	Mouse
Cbfa1	NM_001146038	AAA TGC CTC CGC TGT TAT GAA	GCT CCG GCC CAC AAA TCT	Mouse
Sp7	NM_130458	CCC TTC TCA AGC ACC AAT GG	AGG GTG GGT AGT CAT TTG CAT AG	Mouse
18S rRNA	NR_003278	GCA ATTA TTC CCC ATG AAC G	GGC CTC ACTA AAC CAT CCA A	Mouse

Table 2.5. Primer sequences used for real-time PCR with SybrGreen method.

In chapter 4, 5 and 6 gene expression was analysed with TaqMan probes method. In addition to primers, additional oligonucleotide-probe is included in the reaction. This probe contains both a reporter and a quencher dye attached. During real time PCR reaction probe is cleaved by the 5' nuclease activity of the *Taq* DNA polymerase which generates a fluorescent signal that increases with each binds to the amplicon during each annealing step of the PCR.

Primers and probe for Runx2, OC, type I collagen, Sp7 were purchased from Mycosynth, CH (Tab.2.6). Primers and probes for 18S rRNA (4310893E), RPL13a (Hs_01926559_g1), ALP (Hs00758162_m1), Sox9 (Hs00165814_m1), interleukin-6 (IL6; Hs00985639_m1), interleukin-8 (IL8; Hs00174103_m1), interleukin 10 (IL10; Hs00961622_m1), TNF α (Hs01113624_g1), Wnt3a (Hs00263977_m1), Wnt4 (Hs00229142_m1), Wnt5a (Hs00998537_m1), Wnt7b (Hs00536497_m1), β catenin (Hs00170025_m1), Sox9 (Hs00165814_m1) were bought from Applied Biosystems as 'Assay On Demand' (no sequences provided). The optimal concentration for primers and probe (Tab.2.6) and primer efficiency were assessed previously by the other members of AO Research Institute Davos. Plates for the Real-Time PCR were prepared as described above. The 20 μ l reaction mixture included 10 μ l of TaqMan Universal Master Mix, 0.4 μ l forward and reverse primer (final concentration 900nM), 0.4 μ l probe (final concentration 250nM), 6.8 μ l RNasy free water and 2 μ l cDNA template. The PCR was run at standard conditions with 2 minutes at 56°C, 10 minutes at 95°C, followed by 40 cycles of 15 seconds at 95°C and 1 minute at 60°C.

Gene	Forward 5'-3'	Reverse 3'-5'	Probe 5'-3'
Osteocalcin	AAG AGA CCC AGG CGC TAC CT	AAC TCG TCA CAG TCC GGA TTG	ATG GCT GGG AGC CCC AGT CCC
Runx2	AGC AAG GTT CAA CGA TCT GAG AT	TTT GTG AAG ACG GTT ATG GTC AA	TGA AAC TCT TGC CTC GTC CAC TCC G
Type I collagen	CCC TGG AAA GAA TGG AGA TGA T	ACT GAA ACC TCT GTG TCC CTT CA	CGG GCA ATC CTC GAG CAC CCT
E11/podoplanin	GGT ACT CGC CCT AAA GAG CTG AA	GCA CAG AGT CAG AAA CGG TCT TTT	TTA CGC CCT GCT GCC AAC GTG C
Sp7	CCT GCT TGA GGA GGA AGT TCA	GGC TAG AGC CAC CAA ATT TGC	TCC CCT GGC CAT GCT GAC GG
BMP2	ACC ACT GTG CGC AGC TTC	CTC CGG GTT GTT TTC CCA C	CCA TGA AGA ATC TTT GGA AGA ACT ACC AGA ACC

Table 2.6. Primer and probe sequences used for real-time PCR with TaqMan method.

2.2.16.5. Gene expression analysis with RT² Profiler™ PCR Array

RT² Profiler™ PCR Array system was applied to analyse the expression of human cytokine genes. Each 96-well plate contains primer assays for 84 genes of interest (Tab.2.7), 5 housekeeping genes, genomic DNA control, 3 reverse transcription controls and 3 positive PCR controls.

Diluted with RNase-free water cDNA samples (102µl) were thawed and mixed with 1350µl 2xRT² SybrGreen mastermix and 1248µl RNase-free water. Then, 25µl reaction mix was added to each well of RT² Profiler™ PCR plate. Plate was sealed with the Optical Adhesive Film and centrifuged for 1 minute at 1000g to remove any air bubbles. The reaction was performed on StepOne Plus cycler (Applied Biosystems, US). Plate was incubated for 10 minutes at 95°C for HotStart DNA Taq polymerase activation and then 40 cycles of PCR reaction were run at 95°C for 15 seconds and 60°C for 1 minute. To confirm the absence of nonspecific amplification a dissociation curve was generated (60-95°C for 20 minutes). After all reactions, the same threshold was set across all PCR array runs according to the Qiagen's guidelines; i.e. threshold value was set above the background but within the lower one-third to lower one-half of the linear phase of the amplification plot and the C_T was 20±2 for PCR positive controls for all arrays). The C_T values for all genes were exported to a blank Excel spread

sheet and analysed with the SABiosciences PCR Array Analysis Web-based software. Average of two housekeeping genes, β -2-microglobulin and RPL13A, were used for calculating ΔC_T . Gene expression was calculated using $2^{-\Delta\Delta C_T}$ method. All genes which were ± 1.5 -fold different than control were considered as responsive to the treatment.

Functional Gene Grouping	
Interferons	IFNA1, IFNA2, IFNA4, IFNA5, IFNB1, IFNG
Interleukins	IL10, IL11, IL12A, IL12B, IL13, IL15, IL16, IL17A, IL17B, IL17C, IL18, IL19, IL1A, IL1B, IL1RN, IL2, IL20, IL21, IL22, IL23A, IL24, IL25 (IL17E), IL27, IL3, IL4, IL5, IL6, IL7, IL8, IL9, TXLNA (IL14)
Growth Factors	CNTF, CSF1 (MCSF), CSF2 (GM-CSF), CSF3 (GCSF), FIGF (VEGFD), LEFTY2 (EBAF), LIF, NODAL, OSM, PDGFA, TGFA, THPO, VEGFA
TGFbeta family	BMP1, BMP2, BMP3, BMP4, BMP5, BMP6, BMP7, BMP8B, GDF2 (BMP9), GDF5 (CDMP-1), GDF9, INHA, INHBA, MSTN (GDF8), TGFB1, TGFB2, TGFB3
TNF Superfamily	CD40LG (TNFSF5), CD70 (TNFRSF7), FASLG (TNFSF6), LTA (TNFB), LTB, TNF, TNFRSF11B, TNFSF10 (TRAIL), TNFSF11, TNFSF12, TNFSF13, TNFSF13B, TNFSF14, TNFSF4 (OX40L), TNFSF8
Other cytokines	ADIPOQ, FAM3B, SPP1 (Osteopontin)

Table 2.7. Functional grouping of genes included in Human Common Cytokines RT² Profiler™ PCR array plate.

2.2.17. Proteomic analysis

2.2.17.1. Determination of protein content

The protein content was assessed with colorimetric 'Bradford assay' based on the proportional binding Coomassie Brilliant blue G-250 dye to proteins. The dye reacts primarily with arginine residues and less with histidine, lysine, tyrosine, tryptophan, and phenylalanine residues. Coomassie Brilliant blue G-250 dye exists in three different forms: doubly-protonated (red), neutral (green) and unprotonated (blue) which absorbs UV at different wavelengths. Upon binding to protein the dye

is stable in doubly-unprotonated blue form ($A_{\max}=595\text{nm}$). The concentration of solubilised protein in the sample is measured with a spectrophotometry and assessed relatively to the standard curve.

For the assay, 4 μl sample, which was extracted with 0.1% Triton-X in 10mM Tris-HCl pH 7.4 for 1 hour at 4°C on a gyratory shaker, was applied in duplicates into a 96-flat bottom transparent well-plate. Subsequently, 196 μl Bradford reagent was added and the plate with samples and the dye was incubated for 5 minutes at the room temperature. After the incubation time, the absorbance was read at 595nm on a Multilabel Counter Wallac 1420 (Perkin Elmer, US). The protein concentration in samples was determined using the equation defined by standard curve that was prepared with different concentrations of bovine serum albumin in range 0-25 $\mu\text{g/ml}$.

2.2.17.2. RayBio[®] human cytokine antibody array G-series

The analysis of proteomic profile of cytokines secreted by cells was performed using RayBio[®] Human Cytokine Antibody Array G-series 2000, which enables detection and semi quantitative evaluation of multiple cytokines present in the conditioned media. Specifically, 174 antibodies for various cytokines are divided within 3 glass slides: RayBio[®] Human Cytokine Antibody Array G6, G7 and G8. The overview of the antibody array map is presented in Appendix 3. Detection of proteins by RayBio[®] Human Cytokine Antibody Array is semiquantitative and based on indirect Enzyme-linked immunosorbent assay (ELISA; Fig 2.4.).

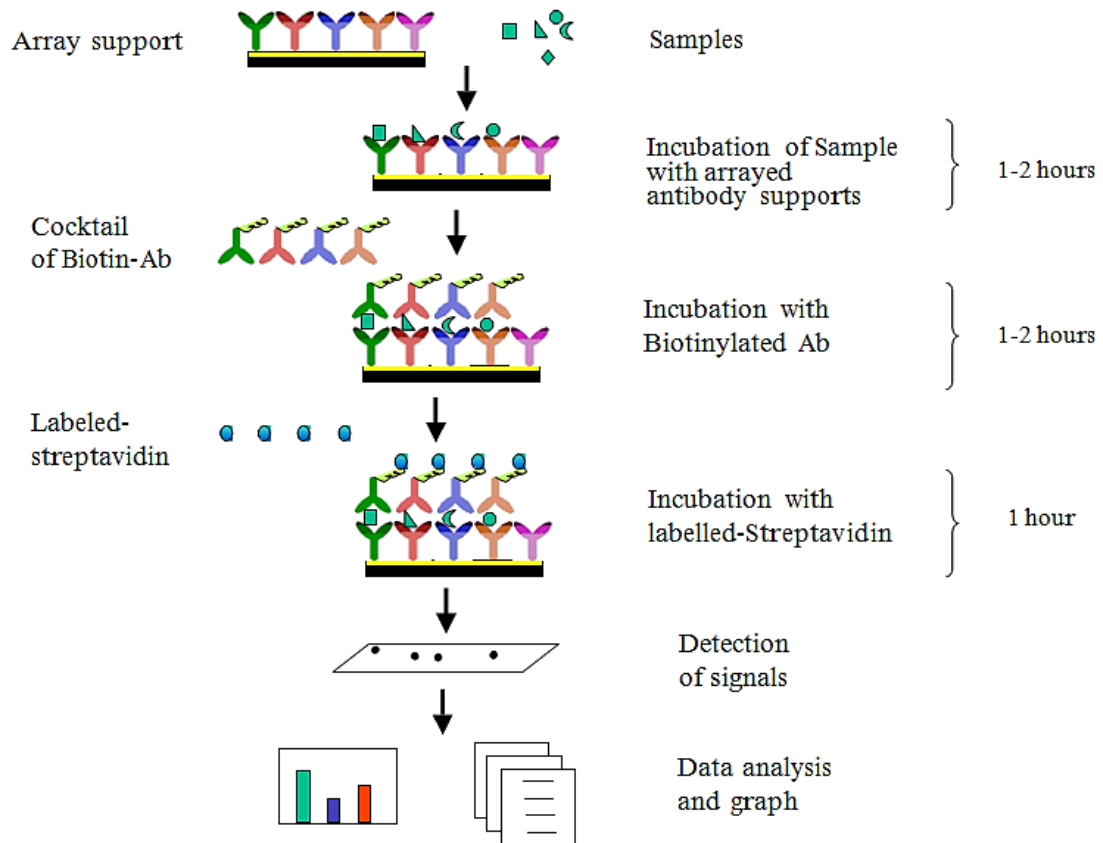


Figure 2.4. Schematic principle of RayBio® Human Cytokine Antibody Array protocol. Glass slide is pre-coated with different primary antibodies against specific cytokines. After adding samples, specific cytokines within samples binds to its antibody. After adding mixture of biotinylated secondary antibodies, they bind specifically to using a different epitope to their respective cytokine. In the following step, added Streptavidin labeled with HiLyte Plus Fluor 532 binds to the biotin on secondary antibody. The signal intensity can be obtained by a laser scanner using the Cy3 channel. Figure adapted from the User Manual (revised July 2, 2012) provided by RayBiotech, Inc.

All reagents were prepared according to the supplied instructions; Wash buffers I and II 20X stocks were diluted with deionised water, Biotin-conjugated anti-cytokines were mixed with 300µl 1X Blocking Buffer and Streptavidin-Fluor reagent was diluted with 1X Blocking Buffer to a final volume of 1500µl. All reagents were prepared prior to use and kept on ice while proceeding with the protocol.

First, glass slides were let to equilibrate to room temperature and subsequently air-dried for 2 hours. Next, 100µl 1X Blocking Buffer was added into each well and incubated at room temperature for 30 minutes to block slides. After decanting the blocking buffer, 100 µl conditioned media samples were added to each sub-array

on all three glass slides. Chambers were covered with adhesive films and arrays were incubated with sample at 4°C overnight with gentle shaking. Then, samples were aspirated from sub-arrays and washed for 2 minutes with 150µl 1X Wash Buffer I at room temperature. This washing procedure was repeated additional two times. Glass slides in the assemblies were placed in a plastic container which was then filled with approx. 50ml Wash Buffer I ensuring that all glass slides with chamber assemblies are submerged. Washing was performed for 10 minutes at room temperature with gentle rocking. After that time, Wash Buffer I was decanted and the washing step was repeated once with Wash Buffer I and 2 times with Wash Buffer II. To ensure the complete removal, all leftovers of the Wash Buffers were carefully aspirated with pipette. Then, 70µl 1X Biotin-conjugated Anti-Cytokines was added to each sub-array. Chambers were covered with adhesive film and incubated for 2 hours at room temperature with gentle rocking. After aspirating Biotin-conjugated Anti-Cytokine reagent, each sub-array was washed 3 times for 2 minutes with Wash Buffer I and then with Wash Buffer II making sure to completely remove buffer between washes and after final wash. Next, 70µl 1X Streptavidin-Fluor was added to each sub-array. Chambers were covered with adhesive film and entire chamber assemblies were covered with aluminium foil to avoid exposure to light during 2 hour incubation at room temperature with gentle rocking. Following careful removal of Streptavidin-Fluor reagent, each sub-array was washed 3 times for 2 minutes with Wash Buffer I and then with Wash Buffer II making sure to completely remove buffer between washes and after final wash. Glass slides were removed from the frame assemblies, placed in provided 30ml centrifuge tubes containing approx. 20ml Wash Buffer I and rocked at room temperature for 10 minutes. Wash buffer was decanted and washing was repeated once more. Then, glass slides were removed from the tube and gently rinsed with deionized water. Glass slides were placed again in the tubes and centrifuged at 1000rpm (Rotanta RP, Hettich, DE) for 3 minutes to remove water droplets. At last, protected from exposure to light glass slides were placed in laminar hood to dry. Glass slides were sent to THP Medical Products Vertriebs GmbH (Vienna, Austria) for laser scanning using GenePix 4000B Microarray Scanner (Axon Instruments; Molecular Devices, CA, US) and raw data processing. Background normalization was performed by subtracting from samples the measured value of the negative

control sample. Negative control spots are printed with a protein containing buffer and detect unspecific binding of Biotin-conjugated anti-cytokines and/or Streptavidin-Fluor. After subtracting background signals, measurement values were normalized to Positive Control which is a controlled amount of biotinylated antibody attracted to the glass slide. The results were expressed as *n*-fold signal intensity compared to positive control samples. For further analysis, these results were normalized to number of cells harvested after the collection of conditioned media from cells stimulated with 10ng/ml IL1 β , 100 μ g/ml SCF or unstimulated cells. In order to estimate differences in protein synthesis between groups, *n*-fold change was calculated between stimulated groups and control.

2.2.18. Immunohistochemistry

2.2.18.1. Fixation and cryo-sectioning

The micromass and type I collagen-hydroxyapatite samples were fixed and kept in 70% methanol until processing. The day before cryo-sectioning, the samples were placed in a 5% sucrose + PBS solution, to replace the methanol. On the following day, samples were transferred to the tissue freezing medium (Jung Tissue Specific Medium) and incubated for 15 minutes at room temperature before placing on the specimen holder and freezing in the 'Cryostat-Microtome HM 560 MV' (Microm, Walldorf, Germany). After freezing, 10-12 μ m sections were cut. The sections were carefully transferred onto 'SuperFrostPlus' slides and stored at -20°C until immunohistochemical analysis.

Sectioning of samples was performed by Sandra Thoeny, AO Research Institute Davos, AO Foundation, Davos.

2.2.18.2. Detection of alkaline phosphatase and osteocalcin

Cryo-sections were used to detect alkaline phosphatase and osteocalcin. Slides were brought to room temperature for 5 minutes and rehydrated for 5-10 minutes in distilled water. Endogenous peroxidase activity within sections was inactivated by 30 minutes incubation in 0.03% hydrogen peroxide in methanol. Slides were removed from solution, dried and then a Dako pen was used to draw a hydrophobic border

around the sections to prevent them from drying during the labelling procedure. Subsequently, samples slides were washed twice in PBS (for 1L: 0.32g $\text{NaH}_2\text{PO}_4 \cdot \text{H}_2\text{O}$, 1.42g $\text{Na}_2\text{HPO}_4 \cdot \text{H}_2\text{O}$, 9g NaCl) containing 0.1% 'Tween20' (PBS-T) for 5 minutes. Sections were then treated for 60 minutes at room temperature with horse serum, which was chosen according to the origin of the secondary antibody (Tab.2.8). Serum used for blocking was diluted 1:20 in PBS-T and used to mask nonspecific binding sites. After removing the blocking solution, the primary antibody was applied. The concentration and incubation times are given in Tab.2.8. For each sample, one slide was used as negative controls and therefore, not exposed to the primary antibody. The slides were washed three times in PBS-T for 5 minutes each, to remove non-specifically bound antibody, before incubating with the secondary antibody (Tab.2.8). Subsequently, 3 washes with PBS-T were repeated as before.

To detect the antibody-antigen reaction the 'Vectastain ABC Elite kit mouse IgG' was used. The 'ABC-complex' was prepared 30 minutes before using by mixing 960 μl PBS-T with 20 μl ABC-A and 20 μl ABC-B solutions and kept at 4°C. Avidin, which binds irreversibly to the biotinylated secondary antibody, is the constituent of solution A, while solution B consists of the biotinylated HRP. Avidin contains four binding sites for biotin and can effectively enhance the signal intensity. After 30 minutes incubation of sections with the 'ABC-complex', the slides were washed three times with PBS-T (5 minutes each). In the following step, sections were incubated with 'ImmPACT™ DAB' reagent for 4 minutes at room temperature in the dark. This reagent is a diaminobenzidine based peroxidase substrate which produces a dark brown reaction product. To stop the reaction, sections were washed with distilled water for 5 minutes. Before cover-slipping, sections were dehydrated in increasing ethanol concentrations of 50%, 70%, 96% 100% and 100% (5 minutes each). Then, sections were transferred to a fume hood and incubated in xylene for 5 minutes. This incubation step was repeated once more, before applying Eukitt[®], a quick-hardening mounting medium. Finally, sections were cover-slipped and the polymerisation of the mounting medium was facilitated by incubation of slides for 1 hour at 37°C on a heated stretching table (Medite Medizintechnik GmbH, Burgdorf, Germany).

Visualisation was performed with Axioplan microscope (Carl Zeiss AG, Oberkochen, Germany).

The immunohistochemistry of samples was performed by Sandra Thoeny and Nora Goudsouzian, AO Research Institute Davos, AO Foundation, Davos. Technical assistance during visualisation was provided by Christoph Sprecher, AO Research Institute Davos, AO Foundation, Davos.

Antigen	Blocking Reagent	Primary Antibody		Secondary Antibody	
		Type	Dilution & Incubation	Type	Dilution & Incubation
Alkaline Phosphatase	1:20 diluted normal horse serum	B4-78, monoclonal IgG1 mouse anti-human; DSHB	5.2 µg/ml; 30 min; RT	Concentrated biotinylated horse anti-mouse IgG (H+L) secondary antibody; Vector Labs	7.5 µg/ml; 30 min; RT
Osteocalcin	1:20 diluted normal horse serum	OC4-30, monoclonal IgG2a mouse anti-human; ABCAM	10 µg/ml; 30 min; RT	Concentrated biotinylated horse anti-mouse IgG (H+L) secondary antibody; Vector Labs	7.5 µg/ml; 30 min; RT

Table 2.8. Specifications of blocking reagent, primary antibodies and secondary antibody used for immunochemistry. min- minutes, RT – room temperature.

2.2.19. Statistical analyses

Statistical analysis was performed with the SPSS version 19.0 and version 21.0 (Chicago, IL, USA) software package. All data was analysed for normal distribution by the use of a histogram and the Shapiro-Wilk test. To assess whether variances between groups are equal Levene's Test. Statistical significance for normally distributed data was analysed with analysis of variance (ANOVA) with Games-Howell post-hoc test and two-way ANOVA with Least Significant Difference (LSD) test.

For not normally distributed data a nonparametric Kruskal–Wallis ANOVA for more than 2 groups was used to define the differences between groups. Subsequent analysis using Mann Whitney test with Bonferroni correction was performed to determine statistically significant group pairs. In the set of experiments where the comparison

was performed for only two groups of not normally distributed data, the statistical analysis was performed with Mann-Whitney U test.

All results which underwent statistical analysis are displayed as means \pm standard error (SE) of at least three independent experiments. Significance was defined as $p \leq 0.05$.

CHAPTER 3

OSTEOBLAST CELL MODELS

Sections of this chapter have been previously published:

Czekanska E.M., Stoddart M.J., Ralphs J.R., Richards R.G., Hayes J.S. A phenotypic comparison of osteoblast cell lines versus human primary osteoblasts for biomaterials testing *Journal of Biomedical Materials Research: Part A* 2013 6th Sept.

3.1. Introduction

Bone is a complex and dynamic vascular mineralized tissue with various functions. It serves as an attachment site for muscles and tendons, protects and supports internal organs and acts as storage of minerals. During foetal development, bone is formed *via* two different mechanisms, intramembraneous and endochondral ossification. Flat bones of the skull, sternum and maxilla are formed by the cells derived from neural crest through the process of intramembraneous ossification. In this process, mesenchymal cells undergo direct transformation to osteoblast cells starting from the ossification centres (Aubin and Triffit, 2002). In contrast, long bones are formed through endochondral ossification. In this case, bone formation is preceded by a cartilaginous template acting as a scaffold. This tissue is then resorbed and replaced by mineralized matrix of bone (Shapiro, 2008; Aubin, 1998). In adulthood, healthy bone is subjected to a constant remodelling directed by various factors, pathways and mechanisms coordinating the action of bone cells.

Since the first attempt of isolation and *in vitro* culture of osteoblast cells from adult human bone by Bard and co-workers (Bard et al., 1972), a great improvement in the knowledge of the biology of bone, and in particular osteoblastic cells, has been made. A plethora of osteoblast cell models have emerged to tackle the surge in research in this area and to compensate to some degree for the ever present problem relating to sustainable supply of primary cells from either healthy or diseased donors. These include cells isolated from different species (Abe et al., 2000; Bellows et al., 1986; Cao et al., 2006; Ecarot-Charrier et al., 1983; Collignon et al., 1997), immortalised cell lines (Wang et al., 1999; Harris et al., 1995) malignant cell lines (Billiau et al., 1977; Rodan et al., 1987; Ponten and Saksela, 1967), and more recently induced pluripotent stem cells (Bilousova et al., 2011; Tashiro et al., 2009). All of these cell models are employed for the investigation of the regulation of cell differentiation, cytokine and hormonal regulation, synthesis and secretion of matrix proteins, molecular mechanisms of bone diseases, and drug pharmacokinetics. Nowadays, in the area of bone tissue engineering, cell culture also serves as an important step in biomaterial testing before *in vivo* evaluation. Cyto-

compatibility and osteogenicity of novel biomaterials are tested using cell culture to determine potential candidates for bone repair.

Immortalised cell lines are mostly used due to their advantages, including availability of unlimited number of cells, ease of culturing and higher phenotypical stability comparing to primary cells (Kartsogiannis and Ng, 2004). Moreover, in the case of human derived cell lines, both normal and malignant, the concern about effects of species differences can be avoided (Czekanska et al., 2012). In contrast, the reported drawbacks of cell line features are many (Leis et al., 1997;Grigoriadis et al., 1985;Wang et al., 1999). One of the main issues regarding cell lines is their stage specific differentiation profile which essentially limits comprehensive study of phenotypic features of associated with primary human osteoblast cells (Kartsogiannis and Ng, 2004;Maes et al., 2007). Thus, their use as pre-screening *in vitro* models is somewhat limited. Furthermore, aberrations in cell mitotic processes limits their use in long term *in vitro* investigations as the lack of growth inhibition have negative influence on later stages of osteoblast cell phenotype development (Read and Strachan, 1999). Despite being characterised as phenotypically stable and homogeneous, previous reports suggest cell proliferation rate and phenotypical changes between cells from early and late passages (Hausser and Brenner, 2005;Leis et al., 1997;Grigoriadis et al., 1985). The potential of isolating clones from cell lines contradicts the opinion of their homogeneous phenotype (Wang et al., 1999;Pierschbacher et al., 1988;Lou et al., 2010).

In the era of advanced research in pharmacokinetics for bone disease and bone tissue engineering there is an increasing need for the reliable and adequate cell culture model which would resemble as close as possible the behaviour of primary osteoblast cells. While it is often stated that cell lines do not fully recapitulate the biology of primary human osteoblasts, few comprehensive comparisons have been performed (Saldana et al., 2011;Pautke et al., 2004). Here, we addressed this problem and compared three osteoblast cell lines widely used in bone biology research, namely MC3T3E1, MG63 and SaOs2 by assessing the phenotypic

similarities and differences among those cells and primary human osteoblast cells during a 4 week culture period.

3.2. Results

3.2.1. A phenotypic comparison of osteoblast cell lines versus human primary osteoblasts

3.2.1.1. Proliferation of osteoblast cell models

No significant differences in growth kinetics were detected between (HOb) and MC3T3E1 cells up to day 10 (Fig.3.1). Both HOb and MC3T3E1 cells presented gradual increases in cell number by day 10. SaOs2 at day 8 and 10 demonstrated a significant 43% ($p=0.017$) and 61% ($p=0.0001$) respective increase in cell number compared to HOb's (Fig.1.). Compared to HOb's, MG63 cells demonstrated a sustained significant increase in cell number from day 2 to day 10 ($p<0.05$). The most significant increase was noted after 6 days when 87% ($p=0.0001$) more MG63 cells compared to HOb's were observed (Fig.3.1). By day 10, there was still a significant 53% increase ($p=0.0001$) in the number of MG63 cells compared to HOb cells.

In addition, the differences in cell proliferation among cell lines were reported. Similarly as compared to HOb's, MG63 cells had a significantly greater increase in growth kinetics from day 2 to day 10 ($p<0.05$). Moreover, SaOs2 cell number was significantly lower than MG63 cells from by day 6 ($p<0.05$). At later time points the number of both cell types equalled. The growth kinetics of SaOs2 and MC3T3E1 cells presented similar trend up to day 8, whereas at day 10 the 41% increase in SaOs2 cell number over MC3T3E1 was found at significant level ($p=0.002$).

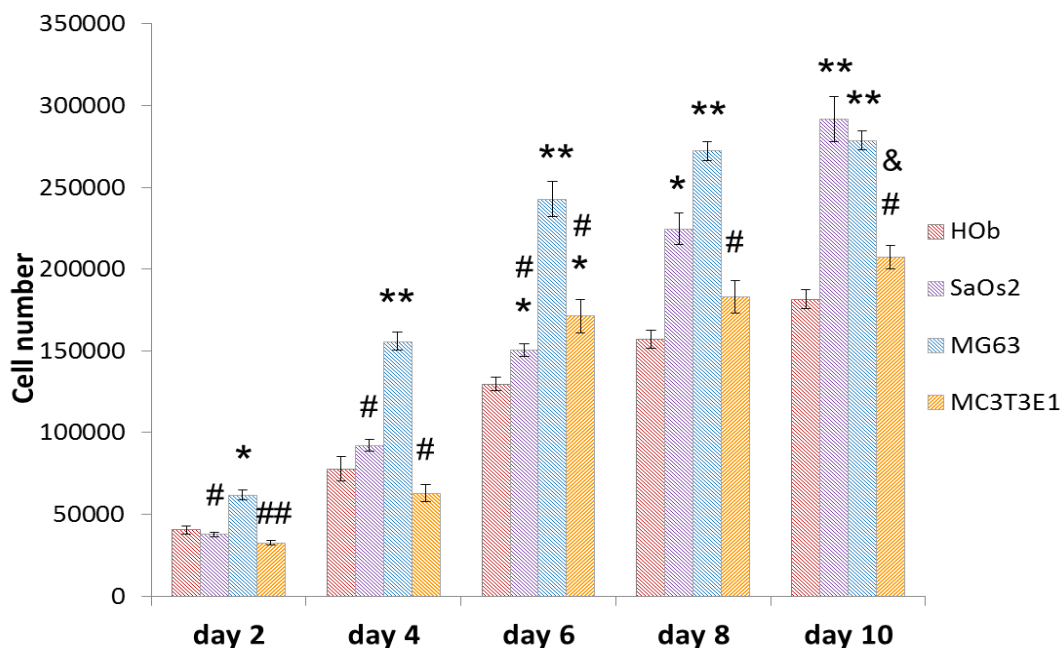


Figure 3.1. Cell number quantification of HOOb, SaOs2, MG63 and MC3T3E1 cells. The diagram represents the mean \pm SE from three independent experiments (n=12) for each cell type. Data were not normally distributed: Kruskal-Wallis ANOVA was used for statistical analysis with statistical significance at $p < 0.05$ (* # &: < 0.05 ; ** ##: < 0.001); *: significantly different compared to HOOb cell culture; #: significantly different compared to SaOs2 cell culture; &: statistically significant compared to MG63 cell culture.

3.2.1.2. Alkaline phosphatase activity

The ALP activity was qualitatively and quantitatively detected in osteoblast cells at day 1, 7, 14, 21 and 28. At each time point one sample was included as a negative control (data not shown). Representative images from three individual experiments performed for each cell type are shown (Fig.3.2).

In vitro ALP activity changed in a time- and cell type dependent manner. HOOb's were positive for ALP from day 1 reaching maximum levels by day 14 (1.0788 ± 0.23), which was confirmed by qualitative results (Fig.3.2&3.3). Compared to HOOb cells, SaOs2 cells produced a significant 2.4 and 1.7-fold higher ALP levels at day 1 ($p < 0.0001$) and day 7 ($p = 0.001$), respectively. After day 7, the enzyme level declined in a time dependent manner, reverting by day 28 to activity levels similar to those observed after 1 day. Interestingly, by day 28 a significant 2-fold decrease ($p = 0.029$) in ALP activity was observed for SaOs2 cells compared to HOOb cells (Fig.3.2). Temporal changes in ALP activity in SaOs2 cells

were confirmed by qualitative results (Fig.3.2). The intensity of the labelling increased by day 7 and was uniform through the cell layer. At later time points, the staining intensity decreased and was localised within the cell layer.

ALP enzyme activity was significantly lower in MG63 and MC3T3E1 cells during the whole culturing time compared to HOb cells ($p < 0.05$) (Fig.3.2). For MG63 cells, ALP activity remained at comparable levels during the 28 day culture period with only small areas within the monolayer becoming positively labelled for ALP. The enzyme activity in MG63 cells reached the maximum levels by day 28, however, this was still noted to be approximately 26-fold lower ($p = 0.00013$) compared to HOb cells at the same time point (Fig.3.2). While a significantly lower ALP activity was observed for MC3T3E1 cells compared to HOb's, similar temporal changes were noted. For both MC3T3E1 and HOB's, the enzyme level increased by day 14 and then reached plateau (Fig.3.2). The staining for ALP corresponded with quantitative results, showing an increase in staining intensity by day 14 followed by decrease at later time points (Fig.3.2).

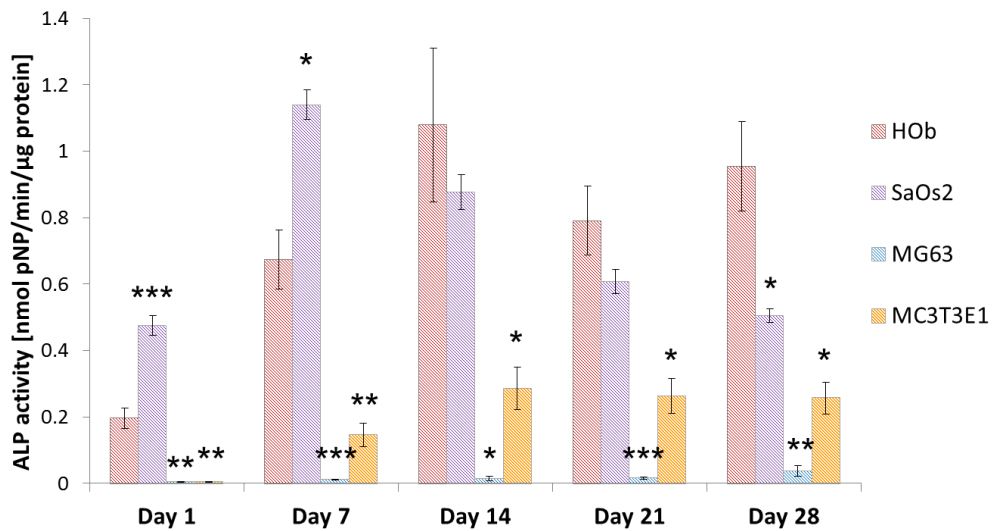


Figure 3.2. Diagram shows the mean alkaline phosphatase (ALP) activity with the standard error of the mean in primary human osteoblast cells (HOb) and osteoblast cell lines: SaOs2, MG63 and MC3T3E1 cultured in osteogenic media. For each cell type ALP activity was assessed as nmol pNP released per minute and normalised to protein content (3 experiments, $n=9$). Data normally distributed: one-way ANOVA with Games-Howell. Statistical significance was determined as $p < 0.05$ (*: < 0.05 ; **: < 0.005 ; ***: < 0.0001).

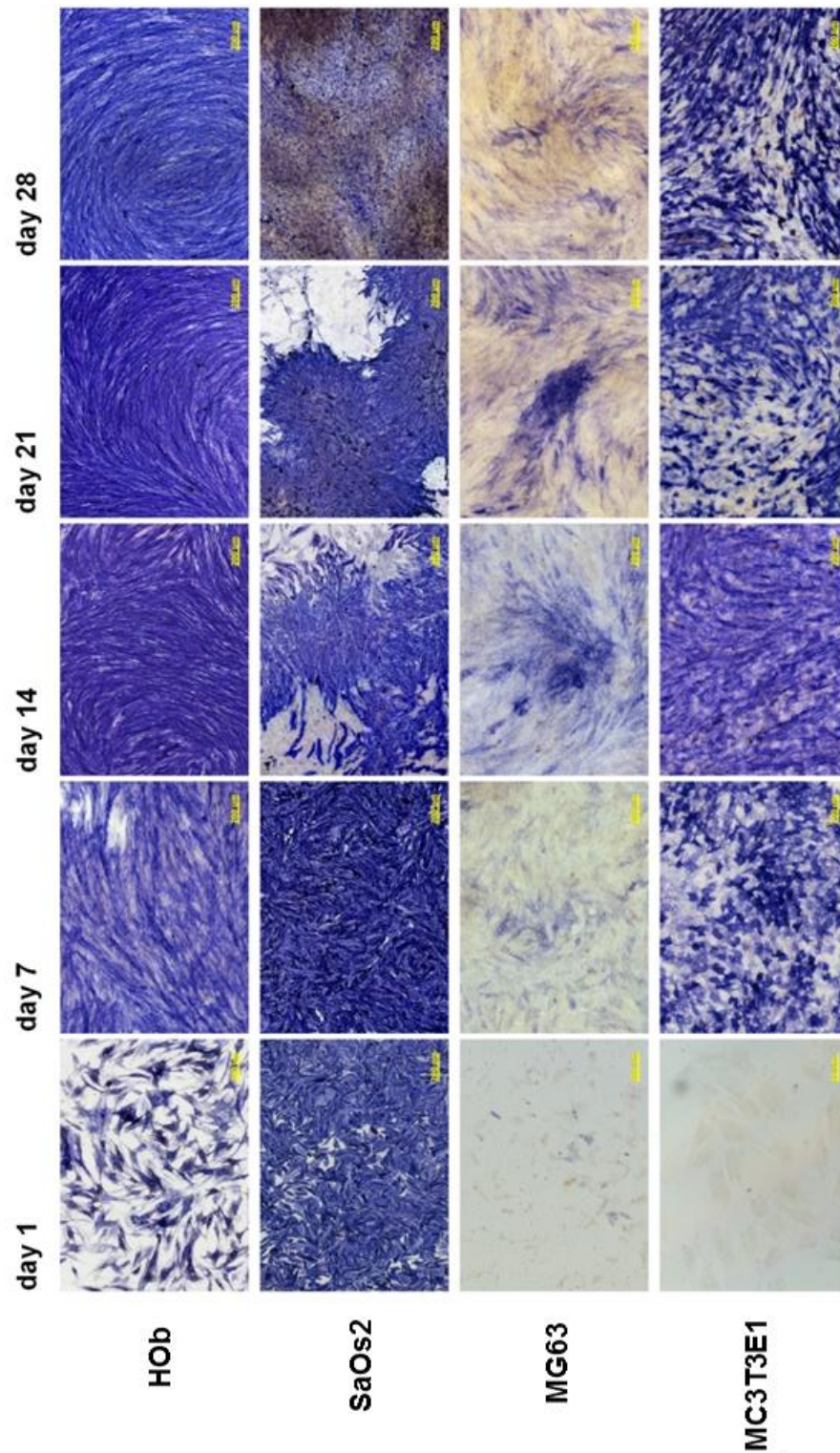


Figure 3.3. Representative micrographs of alkaline phosphatase (ALP) activity at day 1, 7, 14, 21 and 28 in primary human osteoblast cells (HOb) and osteoblast cell lines: SaOs2, MG63 and MC3T3E1 cultured in osteogenic media. Scale bar 200 µm.

3.2.1.3. Mineral deposition within ECM of osteoblast cell models

The visual detection of mineralisation of osteoblast cells was assessed using Alizarin Red S staining at day 1, 14, 21 and 28 of culture. Representative images from three individual experiments performed for each cell type are shown (Fig.3.4).

The mineral deposition was detected in HOb cells from day 21 and by day 28 (Fig.3.4). Similar to HOb, MC3T3E1 cells developed regions rich in calcium and by day 28 calcium deposits were detected throughout the whole cell layer. Mineral deposition was more scattered throughout cell layer in MC3T3E1 cells than in HOb cells (Fig.3.4). SaOs2 cells formed a thick cell multilayer with nodule mineralisation noted from day 14 to day 28. In our culture system, no positive staining for mineralisation was observed in MG63 cell cultures (Fig.3.4). However, similarly to SaOs2 cells, MG63 cells formed a thick cell layer with evident nodules after 14 days of culture, however, no calcium deposition within the extracellular matrix (ECM) was seen (Fig.3.4).

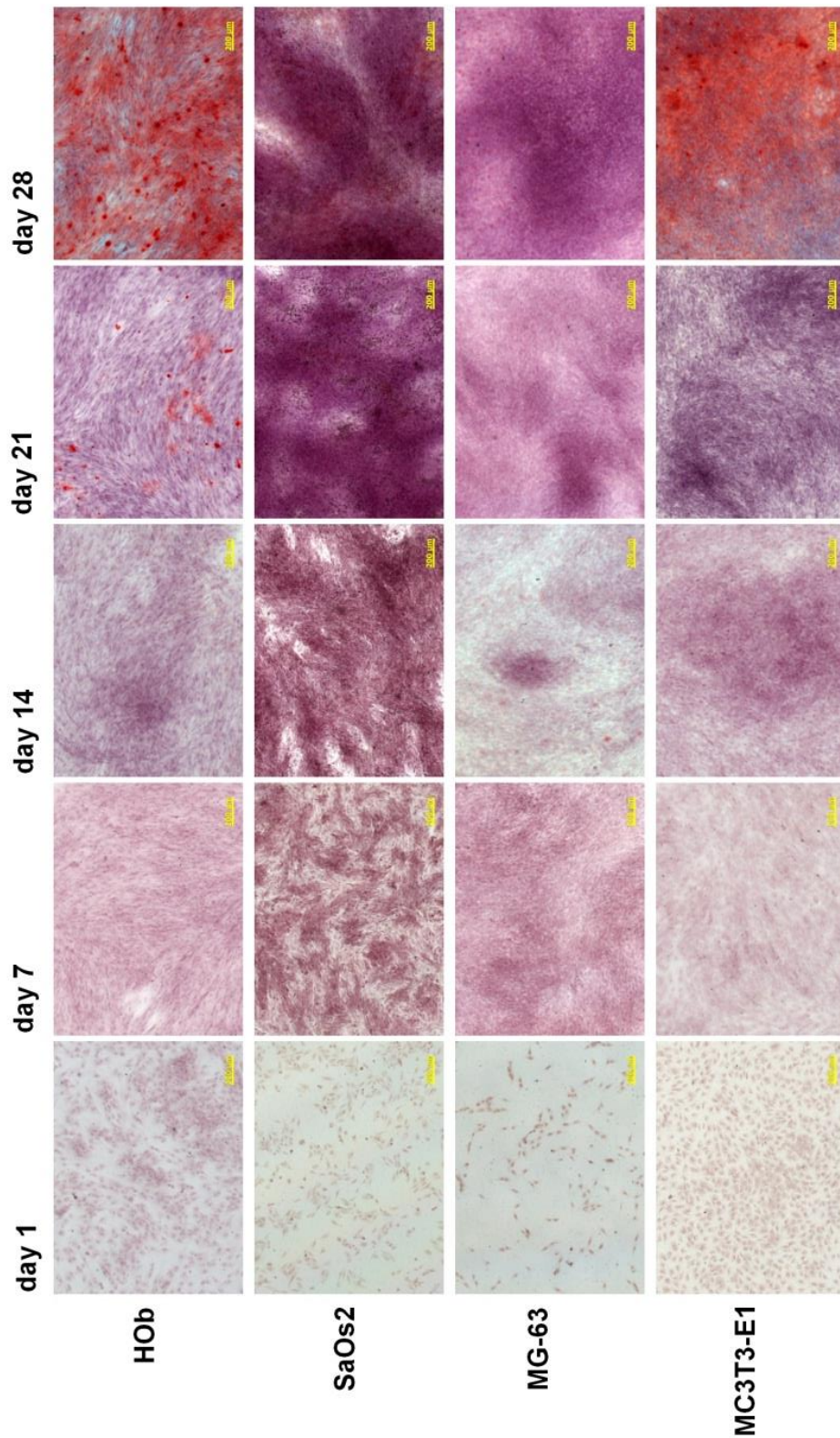


Figure 3.4. Representative micrographs of mineralisation at day 1, 7, 14, 21 and 28 in primary human osteoblast cells (HOb) and osteoblast cell lines: SaOs2, MG63 and MC3T3E1 cultured in osteogenic media. Cultures were stained with Alizarin Red S dye for deposited within extracellular matrix calcium. Scale bar 200 µm.

3.2.1.4. Expression of osteoblastic genes by osteoblast cell models

To obtain a more complete insight into the phenotypic profile of different osteoblast cells during differentiation, the transcriptional changes of osteoblast-specific genes over 28 days were analysed. Gene expression for early, mid-term and late osteoblast specific markers was evaluated and made relative to the expression of these genes in HOB cells at day 1.

The expression of the early osteoblastic transcription factor, Runx2, showed distinct differences in expression among the different cell types (Fig.3.5A). The initial mRNA expression of Runx2 was significantly higher compared to HOB cells at day 1 in MG63 ($p=0.024$) and MC3T3E1 ($p=0.008$) cells with 51- and 73-fold higher expression, respectively. The expression of Runx2 in SaOs2 cells was not significantly different ($p=0.318$) compared to HOB cells at this time point. However, after 21 days, a significant increase ($p=0.041$) in Runx2 was observed for SaOs2 cells compared to HOB (Fig.3.5A). MC3T3E1 cells demonstrated the highest upregulation of Runx2 of all the cell types tested. Specifically, in relation to HOB Runx2 was significantly higher in MC3T3E1 cells day 7 ($p=0.001$), 14 ($p=0.005$) and 28 ($p=0.002$). Interestingly, MG63 cells displayed a distinct temporal expression of Runx2 compared to HOB cells, however, these differences were not observed to be significant after day 7 (Fig.3.5A).

Expression of type I collagen (COL1) is demonstrated in Fig.3.5B. Again, distinct temporal expression was noted between cell types. MC3T3E1 cells were noted to have the highest increase in COL1 expression after 1 and 7 days, however, this was not observed to be significantly higher compared to HOB cells (Fig.3.5B). Comparable levels of COL1 were observed between SaOs2 and HOB cells for day 1-14, however, by day 21 COL1 mRNA levels were observed to significantly decrease by 3.5- and 5.5-fold at day 21 ($p=0.001$) and 28 ($p=0.012$), respectively (Fig.3.5B). With the exception of day 21, COL1 mRNA was noted to be significantly lower in MG63 cells after 1 ($p=0.002$), 7 ($p=0.003$), 14 ($p=0.001$) and 28 days ($p<0.001$) (Fig.3.5B) compared to HOB cells.

SaOs2 cells displayed comparable levels of ALP mRNA levels from day1-28. Nevertheless, SaOs2 ALP expression was significantly higher at day 21 ($p=0.018$) compared to the other cells types studied (Fig.3.5C). MC3T3E1 cells demonstrated significantly lower ALP expression at day 1 compared to HOb cells ($p=0.003$) (Fig.3.5C). MC3T3-E1 ALP expression then underwent a significant 39-fold increase compared to HOb at day 7 This expression was maintained for 14, 21 and 28 days ($p<0.002$). No significant differences were found in ALP gene expression between MG-63 and HOb cells (Fig.3.5C).

Similar to ALP and type I collagen, expression levels of the late osteoblast cell marker, Osteocalcin (OC), remained at the similar levels in HOb cells through the 28 day period (Fig.3.5D). Neither MG63 nor MC3T3E1 cells demonstrated any significant distinctions in OC expression compared to HOb over 28 days, although levels were generally higher in the two cell lines. (Fig.3.5D). While SaOs2 cells displayed a lower OC expression over the 28 days compared to HOb, only OC mRNA levels at 28 days were found to be significantly lower ($p=0.035$) compared to HOb cells (Fig.3.5D).

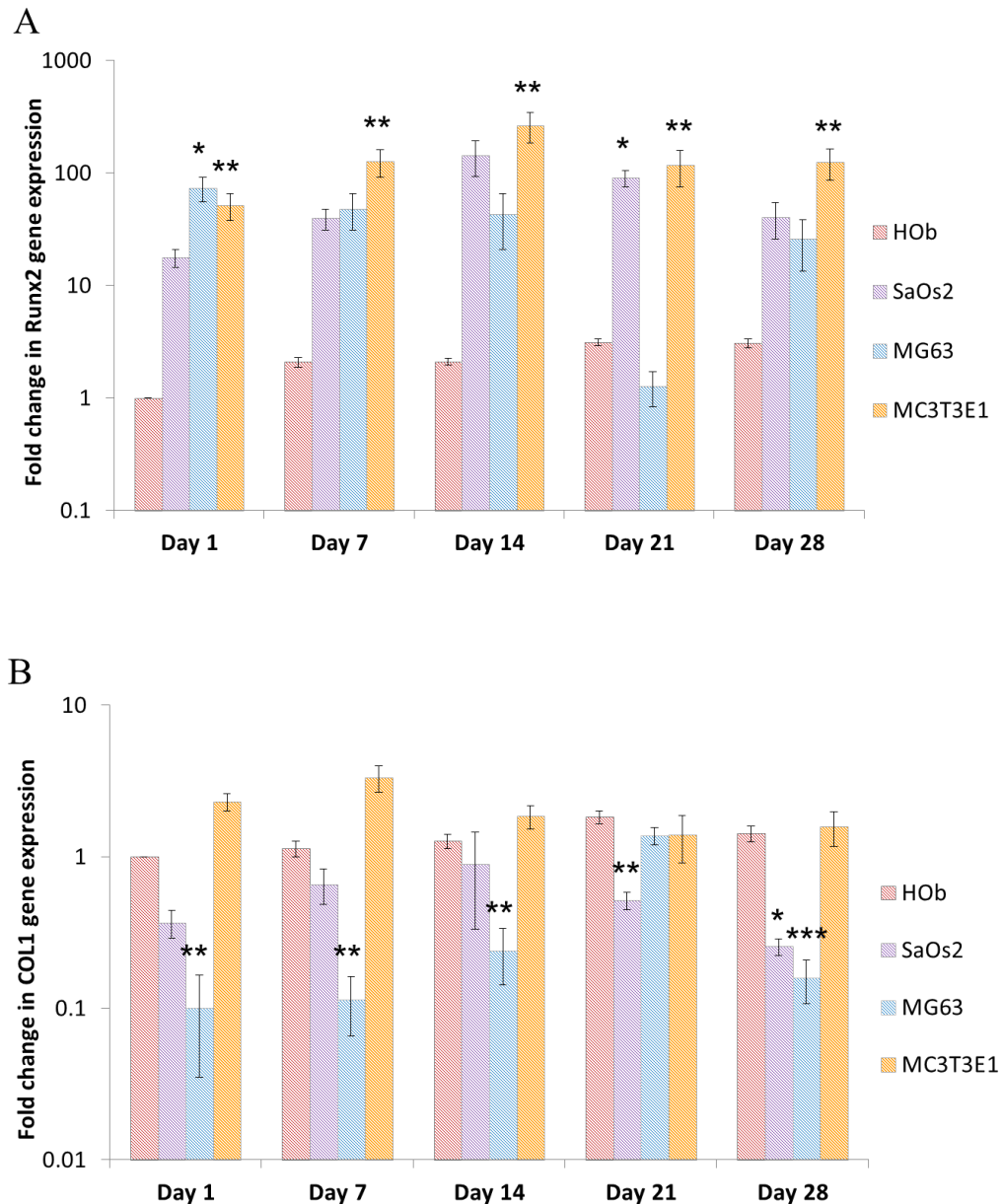


Figure 3.5.A-B. Comparative real-time PCR results of Runx2 (A) and type I collagen (COL1; B) performed at day 1, 7, 14, 21 and 28 of culture period of primary human osteoblast cells (HOOb) and osteoblast cell lines: SaOs2, MG63 and MC3T3E1 cultured in osteogenic media. Diagrams show the mean fold change in relative gene expression with the standard error of the mean (3 experiments, n=9). Gene expression levels were normalised to 18S rRNA and were made relative to expression levels in primary human osteoblast cells at day 1 of culture. Data not normally distributed: Kruskal-Wallis and Mann-Whitney with Bonferroni correction. Statistical significance was determined as $p < 0.05$ (*: < 0.05 ; **: < 0.005 ; ***: < 0.0001).

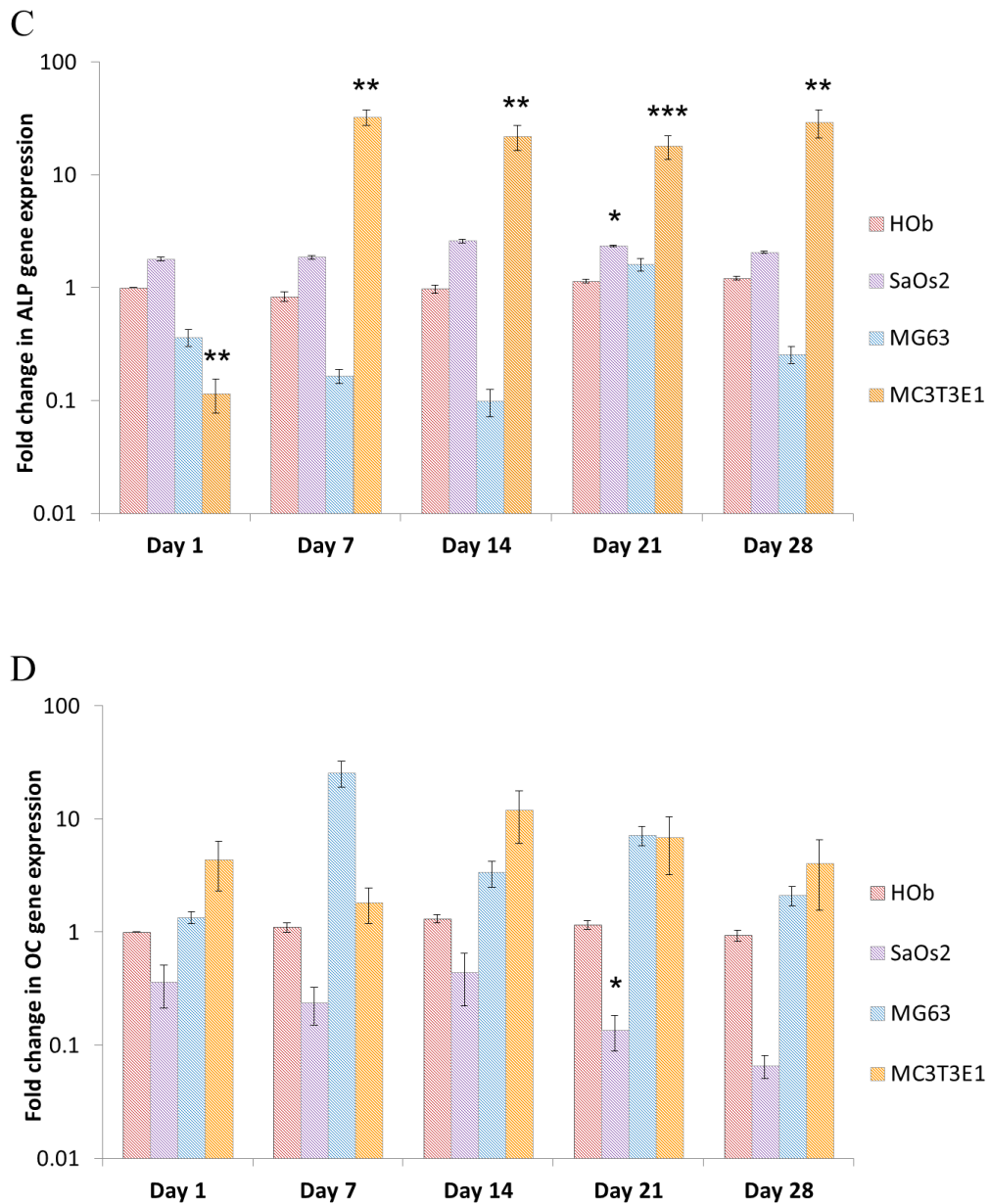


Figure 3.5.C-D. Comparative real-time PCR results of ALP (C), osteocalcin (OC; D) performed at day 1, 7, 14, 21 and 28 of culture period of primary human osteoblast cells (HOb) and osteoblast cell lines: SaOs2, MG63 and MC3T3E1 cultured in osteogenic media. Diagrams show the mean fold change in relative gene expression with the standard error of the mean (3 experiments, n=9). Gene expression levels were normalised to 18S rRNA and were made relative to expression levels in primary human osteoblast cells at day 1 of culture. Data not normally distributed: Kruskal-Wallis and Mann-Whitney with Bonferroni correction. Statistical significance was determined as $p < 0.05$ (*: < 0.05 ; **: < 0.005 ; ***: < 0.0001).

3.3. Discussion

Within last few decades there has been increasing interest in different aspects of bone cells. The development of various techniques allowing for a more in-depth and complex analysis of the osteoblast phenotype and the exceeding need for available osteoblast cells for *in vitro* research has contributed to establishing many osteoblast cell models.

While a number of cell lines have been well characterised, few studies have directly compared their behaviour to primary human osteoblasts in order to determine their suitability for use in a model. Here, we characterised key aspects of phenotype and function of three osteoblast cell lines, SaOs2, MG63 and MC3T3E1, and compared them with the phenotypic traits of cells isolated from human bone. According to the 'gold standard' of osteoblast cell phenotype development established from rat calvarial osteoblastic cells, osteoblasts progress through 3 phases, proliferation, matrix synthesis and maturation and mineralisation (Stein and Lian, 1993). We focused on assessing these stages in two human osteoblast cell lines, SaOs2 and MG63 derived from human osteosarcoma (Billiau et al., 1977; McAllister et al., 1971) and MC3T3E1, a non-transformed cell line derived from mouse calvarial bone (Wang et al., 1999). These cell types represent the most commonly used cell models in *in vitro* studies focused on physiological and pathological aspects of osteoblast cell biology.

Cell proliferation was similar for primary HOb and the MC3T3E1 cell line with the exponential phase being observed between days 2-6, followed by a gradual plateau between days 6-10. Thus, MC3T3E1 cells exhibited contact-dependent inhibition of proliferation similar to human primary cells. This observation for MC3T3E1 proliferation is in line with previous studies examining the proliferation of MC3T3E1 cells from different passages on tissue culture polystyrene (Peterson et al., 2004). Conversely, the osteosarcoma cell lines SaOs2 and MG63 both differed significantly compared to primary human osteoblast cells in terms of proliferative capacity. Specifically, significant increases in cell number were noted at later time points for SaOs2 cells (day 8 and day 10), whereas

for MG63 cells produced significant higher proliferative rates as early as day 2 in culture. Interestingly, the cell growth kinetics of MG63 cells was comparable to HOb cells in that the exponential phase was observed between days 2-6, which was followed by the plateau phase from day 6-10. In contrast, SaOs2 cells appeared to sustain a phase of exponential growth from day 2 onwards, with no obvious plateau phases becoming evident by the end of the experiment at day 10. Indeed, malignant cells, like SaOs2 and MG63, inherently lack control of their cell cycle resulting in infinite proliferation capability in suspension cell cultures *in vitro*, contributing to tumour progression (Read and Strachan, 1999). On the cell culture surface, the saturation density is influenced by the cell size. Morphometric analysis of primary osteoblast cells and osteosarcoma cell lines indicated the significantly lower size and volume mean for tumour cells (Pautke et al., 2004). Hence, the saturation density for non-tumour cells is lower, which was reported here and by others (Pautke et al., 2004).

In terms of osteoblast differentiation, SaOs2 and MC3T3E1 cells are commonly described as displaying a 'mature' differentiated phenotype while MG63 represents an 'immature' osteoblast phenotype. Compared to the *in vitro* osteoblastic functionality we observed for primary human osteoblasts, our results support previous observations regarding the maturity of cell phenotype and their mineralisation potential. *In vitro* ALP is expressed at the early phase in matrix synthesis stage and is required for matrix mineralisation to occur. Although significantly lower during 28 days *in vitro*, MC3T3E1 cells presented a similar profile of ALP enzyme activity to primary osteoblasts. This is reflected in the later onset of mineralisation in mouse cells reported by Alizarin Red S-calcium deposition assay at day 28 for MC3T3E1 and at day 21 for HOb cells. The MC3T3E1 cells, obtained from newborn mouse calvaria, were already characterized as committed immature osteoblast cells sequentially expressing the osteoblastic markers and mineralising when culturing in the presence of ascorbic acid and β GP (Sudo et al., 1983).

SaOs2 cells had significantly higher initial level of the enzyme activity confirming more mature phenotype of cells. The direct comparison of this cell type with HOb

cells in a recent study showed opposite results with initial ALP activity at the same level which, similarly as here, was followed by higher increase in SaOs2 cells by day 7 (Saldana et al., 2011). Nodule formation was observed in SaOs2 cells from day 7 which developed with time and mineralised from day 28. Indeed, the potential of SaOs2 matrix mineralisation and formation of structures resembling woven bone in *in vitro* have been reported previously (Rodan et al., 1987). During the 28 day cell culture we observed a significantly lower ALP activity in MG63 cells than primary cells. The low ALP enzyme level has been reported previously (Scheven et al., 2002; Kumarasuriyar et al., 2009). Conversely, Kumarasuriyar *et al.* presented ALP temporal changes in MG63 cells with an increase by day 15. However, comparing the actual values for ALP activity between the latter study and results obtained here MG63 enzyme activity was similar and hence, much lower in MG63 than HOb cells (Kumarasuriyar et al., 2009).

In order to track the phenotypical changes of osteoblast cell models to compare them with primary cells, we analysed the expression of key osteoblast specific genes during 28 days of culture. This revealed further differences among included in this study osteoblast cells.

We compared the changes in Runx2 gene expression as an early osteoblast marker. Runx2 transcription factor, first identified as activating osteocalcin gene expression, was subsequently shown to regulate gene expression of all important bone matrix proteins, including alkaline phosphatase, osteocalcin, bone sialoprotein and $\alpha 1$ type I collagen (Schinke and Karsenty, 2002;Ducy et al., 1997). Moreover, it is up-regulated at the stage of mesenchymal condensation in cells differentiating into osteoblastic lineage (Ducy et al., 1997). We reported a significantly higher Runx2 mRNA level in MC3T3E1 cells than HOb cells and a trend of higher Runx2 gene expression in SaOs2 during the whole culturing time and MG63, except day 21, compared to HOb cells. Furthermore, the expression of ALP and OC genes (with and without statistical significance, respectively) was higher in MC3T3E1 than HOb cells. This could suggest the positive correlation between the expression of Runx2, ALP and OC. Interestingly, at the same time when ALP gene expression was significantly up-regulated compared to HOb cells, the enzyme activity was

higher in HOB cells. The inversed results regarding gene expression and ALP activity could be attributed to poor post-translational efficiency of ALP cells in MC3T3E1 cells, but not in HOB cells, however this would require further work to confirm. In SaOs2 cells the ALP mRNA expression was low and similar to HOB cells, with the exception of day 21, whereas the protein synthesis and activity suggest high post-translational efficiency in human cells. Moreover, results for MG63 cells may imply that this efficiency can be high only if the threshold level for ALP expression is reached or that due to genetic alterations in tumour cells the post-translational processes are aberrant.

Type I collagen, the most abundant ECM protein in bone, is essential for osteoblast cell functionality since improper fibril formation impair subsequent stages of phenotypic development (Wenstrup et al., 1996). Specifically, type I collagen expression is highly up-regulated in the stage before the matrix mineralisation and its fibril formation is essential for further physiological matrix maturation (Lian and Stein, 1995). We report similar expression of type I collagen in MC3T3E1 cells over 28 days and SaOs2 up to day 21 comparing to HOB cells, whereas lower expression was noted in MG63 cells compared to HOB cells. This low expression and potentially low protein synthesis and fibril assembly together with low ALP activity could suggest the insufficient maturation of collagenous matrix precluding mineral deposition for MG63 cells. In fact, the MG63 cells were shown previously to express more type III than type I collagen (Jukkola et al., 1993). In addition, the synthesis of other ECM constituents by MG63 cells differs comparing to primary human osteoblast (Johansen et al., 1992; Pierschbacher et al., 1988; Pautke et al., 2004).

Further differences were reported for the expression of late osteoblast cell marker, osteocalcin. Although its biological role is not fully understood, its importance has been determined in the differentiation of osteoblast progenitor cells with significant up-regulation at matrix synthesis and mineralisation stage (Ryoo et al., 1997; Kirkham and Cartmell, 2007). The differences in OC mRNA expression in MG-63 and MC3T3E1 compared to HOB cells did not achieve statistical significance. Nevertheless, we observed a trend of higher OC gene expression

in these cells with specific rebound pattern, which was not the case of HOb cells. The expression of OC mRNA is directly linked to the Runx2 expression, the master regulatory transcription factor (Ducy et al., 1997). Hence, results obtained here suggest a direct correlation in the OC and Runx2 expression in HOb, MG63 and MC3T3E1. In the case of SaOs2 cells, the trend of lower OC gene expression and higher Runx2 may suggest involvement of an alternative regulatory mechanism in OC gene expression. This, however, requires additional work to confirm.

Altogether, the results showed many similarities between primary osteoblast cells and MC3T3E1 or SaOs2, but less with MG63 cells. Thus, the use of these osteoblast cells models should be considered with caution and explored in more detail to include comparisons with primary cells. Although MC3T3E1 has a similar cell proliferation rate to HOb and mineralise their matrix in similar manner, the gene expression differed significantly from HOb, which is possibly due to species-specific differences in gene regulation (Thomas et al., 2000). From the three cell types tested here, SaOs2 cells resembled HOb in the best manner regarding mineralisation potential, ALP activity and gene regulation, but not with respect to cell proliferation. MG63 showed the least similarities with primary human mature osteoblasts; however, based on results from previous studies, these cells are reliable in recapitulating OC synthesis and regulation, and integrin subunit expression (Clover et al., 1992). Moreover, due to their immature phenotype, MG63 cells are a suitable cell model to investigate the differentiation process into a mature osteoblast phenotype.

In summary, while cell lines provide a convenient and accessible alternative to HOb, their use should be limited to appropriate and specific research questions with careful extrapolation of results, rather than as widespread use for recapitulating general bone biology and disease as is currently the case.

CHAPTER 4

***IN VITRO* CO-CULTURE OF PROGENITOR CELLS AND OSTEOBLASTS**

4.1. Introduction

The behaviour and phenotype of cells are regulated by the 3D network structure of extracellular matrix, cell shape and complex cell-cell communication (Hammoudi et al., 2012). It is of great interest to define these interactions between various cell types which reside in a close proximity within the bone, including the osteogenic lineage cells, osteoclasts and blood vessels forming cells. A better knowledge of these interactions would be of benefit for the understanding of the bone development processes and is crucial for the improvement of the bone tissue engineering approaches. In fact, based on the evidence from *in vivo* investigations focusing on stem cell therapy, the beneficial effect of implanted cells on tissue regeneration has been shown to occur in various manners. Recently, it became evident that in addition to their direct contribution to tissue regeneration as a consequence of differentiation into specific phenotypes, implanted cells aid regeneration by producing various bioactive molecules, including growth factors, cytokines and extracellular matrix molecules (Hsiao et al., 2012; Tsiridis et al., 2007; Zhukareva et al., 2010). These secreted factors act in an auto- and paracrine manner regulating the cell phenotype. The indirect action of progenitor cells implanted within a bone healing environment is less understood; nevertheless, the importance of various factors secreted by cells present in the fracture milieu is known to have great importance on bone regeneration (Kolar et al., 2011).

The communication among cells *in vivo* is possible through the three mechanisms, including direct cell-cell contact through cell membrane molecules (tight and adherence junctions), gap junction communication and complex paracrine interaction through cell- or matrix-derived secretion factors (Grellier et al., 2009). *In vitro* co-culture models have been used for investigations aiming to elucidate the manner and importance of cells cross-talk. Specifically, direct and indirect *in vitro* co-culture systems have been used. Both types of cultures are mainly based on monolayer culture systems. Nevertheless, recently more interest has been directed towards 3D co-culture, including spheroids or scaffold systems.

Direct models aim to support maximum interaction between different types of cells. On the other hand, in this system, it is not easily possible to discriminate the response of the cell type of interest from response of the other cell population. This can be overcome when applying an indirect co-culture approach where cell cross-talk is based on the action of secreted diffusible factors. This type of communication can be achieved when one cell type is cultured with conditioned medium or ECM from the other cell type. In this case one-way communication is analysed. The two-way cross-talk, in which paracrine factors are secreted by both cell types and they affect both cell types, can be investigated using porous chambers separating different populations of cells. Moreover, the indirect co-culture systems allow the determination of the importance and necessity of direct cell-cell contact on the secretion of trophic factors (Grellier et al., 2009).

Taking into account the various cell types present in the bone and its ECM, the net of the interactions that occurs is very intricate which makes their *in vitro* investigations challenging. Bone cell-cell communication *in vitro* focus mainly on the interactions between endothelial cells and MSCs (Duttenhoefer et al., 2013;Hsiao et al., 2012;Chen et al., 2008;Saleh et al., 2011) or endothelial cells and osteoblasts (Unger et al., 2007;Fuchs et al., 2009;Hofmann et al., 2008;Stahl et al., 2004;Zhang et al., 2010;Hoch et al., 2012). Nevertheless, the communication between MSCs and osteoblasts (Tsai et al., 2012;Wang et al., 2007;Ueno et al., 2001;Buttery et al., 2001;Ilmer et al., 2009) or osteoblasts and osteocytes (Civitelli, 2008;Jaehn K., 2010;Clarke et al., 2013) attracts more and more attention.

Based on the published evidence from both direct and indirect *in vitro* co-culture models, MSCs exert multiple effects on endothelial cells, such as stimulation of migration, proliferation, capillary-like structure formation and ‘sprouting’ and wound healing (Hoch et al., 2012;Hsiao et al., 2012;Chen et al., 2008). Similarly, through the secretion of various factors, endothelial cells stimulate gene expression of osteogenic markers, including alkaline phosphatase (ALP), osteocalcin (OC), osteopontin (OP) and osteonectin (ON), and promote the onset of ECM mineralisation, which emphasise the importance of endothelial cells and MSCs

interaction on osteogenic differentiation of MSCs (Saleh et al., 2011;Kaigler et al., 2005).

The standard protocols for *in vitro* culture of osteoblasts or their progenitors include the requirement of various supplements to induce the mineralisation of the ECM. Interestingly, the direct co-culture of murine MSC with osteoblast cells was able to induce the mineralisation of the ECM in the absence of osteogenic supplements (Tsai et al., 2012). Similarly, evidence from indirect co-cultures of murine cells showed that osteoblasts were able to stimulate differentiation and nodule formation in progenitor cells (embryonic cells) cultured in the absence of any exogenous osteogenic supplement (Buttery et al., 2001). This indicates that osteoblasts secrete factors directing MSC differentiation and ECM mineralisation. Interestingly, the influence of co-culture on MSC differentiation highly depends on the phenotype of osteoblast cells and their ability to mineralise the ECM, suggesting that cell secretome is phenotype dependent (Ueno et al., 2001). More detailed analysis of the mechanisms directing the process of osteogenic differentiation in direct and indirect co-culture with osteoblast cells showed Wnt and cadherin signalling pathways components being implicated in this process (Wang et al., 2007).

However, while the results from studies focusing on osteoblast communication with progenitor cells are valuable; they are mostly based on the research evidence from *in vitro* co-cultures of murine or rat cell models. Therefore, to obtain a better insight into the communication modes between cells in human bone, the communication between human bone forming cells will be investigated in this chapter. For this approach human MSCs will be co-cultured with osteoblast cells. MG63 cells were chosen as osteoblast cell model for these investigations as their immature phenotype allows for investigation of differentiation process, which is not possible when using mature osteoblast cells. Through this, we aim to limit any inconsistency associated with the use of primary cells to only one cell type. Ultimately, the importance of the type of the cell-cell communication between MSC and osteoblast cells will be determined. In addition, a newly developed highly homogeneous GFP expressing osteoblast cell line will be presented.

4.2. Results

4.2.1. Indirect co-culture of MSCs and MG63 in monolayer and its effect on the osteogenic phenotype of the cells

A monolayer co-culture model was used to analyse the indirect effects of cell-cell communication on the osteogenic differentiation of MSCs and osteoblast phenotype maturation. MSCs and MG63 cells were co-cultured for 21 days using BD Falcon™ cell culture inserts and companion plates. This system includes polyethylene terephthalate (PET) insert membrane with the pore size 0.4µm and pore density $2\pm 0.6 \times 10^6$ per cm². For co-culture, MSCs were cultured on top, i.e. in the insert, while MG63 cells were plated in the bottom of the well (bottom). The opposite configuration was included as a control group. As further controls MSCs and MG63 were plated as single cell type cultures in the well (bottom) and in the insert (top). The detailed description of the groups is included in paragraph 2.2.11.1 and table 4.1. During the culture time, cells were maintained in growth medium (GM) as control or differentiation medium (DM). Growth medium consisted of DMEM (1g glucose/L), 10% FBS and 1% Penicillin-Streptomycin. Differentiation medium had the same components as GM and was supplemented with 50µg/ml L-ascorbic acid 2-phosphate sesquimagnesium salt hydrate, 10nM dexamethasone and 5mM β-glycerolphosphate.

The investigation of gene expression, ALP activity, DNA and ⁴⁵Ca incorporation included eight groups in DM and eight groups in GM conditions (Tab.4.1).

<i>Group</i>	<i>Description</i>
MSC CC tp	MSCs located in the insert co-cultured with MG63
MSC CC bt	MSCs located in the well co-cultured with MG63
MSC tp	single cell type culture of MSCs located in the insert
MSC bt	single cell type culture of MSCs located in the well
MG63 CC tp	MG63 located in the insert co-cultured with MSCs
MG63 CC bt	MG63 located in the well co-cultured with MSCs
MG63 tp	single cell type culture of MG63 located in the insert
MG63 bt	single cell type culture of MG63 located in the well

Table 4.1. Description of groups included in the analysis of indirect co-culture of MSCs and MG63 cells in monolayer.

4.2.1.1. The effect of monolayer co-culture on osteogenic gene expression in MSCs

Regarding MSCs, the location of cells in co-culture (inserts or well) had less influence on Runx2, ALP and OC gene expression (Fig.4.1.) than in MG63 cultures (Fig.4.4). There were no significant differences in Runx2 mRNA expression between MSCs from co-culture DM groups and MSCs cultured alone (Fig.4.1A). However, there was a trend of higher Runx2 expression in MSCs on the bottom of the well from the single cell type culture in differentiation medium (MSC bt DM) compared to other DM groups. When cells were cultured in GM, the Runx2 mRNA was lower compared to DM groups. Similarly as for DM groups, the Runx2 gene expression was the highest in MSCs single cell type culture in the wells (MSC bt). This trend reached significance for MSCs in GM cultured in the well compared to MSC from co-culture with MG63 located in the well in GM ($p=0.007$) and MSC GM from co-culture located in the insert ($p=0.023$) (Fig.4.1A).

In differentiation medium, COL1 expression showed a 2.3- and 2-fold higher level in co-cultured MSC and control MSC seeded in the insert compared to co-cultured

MSC and control MSC seeded in the well, respectively (Fig.4.1B). These differences did not reach significance. Additionally, a trend of higher COL1 expression was reported for MSC co-cultured on the top (insert) with MG63 cells in DM and control MSC located in the insert in DM compared to their respective GM controls (Fig.4.14B). The highest COL1 mRNA expression in GM conditions was detected in the control MSCs group in which cells were located in the well compared to co-cultured with MG63 MSCs located in the insert ($p=0.002$) or in the well ($p=0.015$) and single cell type MSCs seeded in the insert ($p=0.032$) (Fig.4.1B).

The expression of ALP was at similar levels in all GM groups, except of MSCs from the co-culture with MG63 maintained in the insert in GM (Fig.4.1C). For this group, the ALP mRNA level was significantly lower than in the single cell type culture of MSCs in the well cultured in GM ($p=0.021$). Although, the ALP expression was higher in control MSCs GM group located in the well compared to other DM groups, no significant differences were determined for ALP expression (Fig.4.1C). For this group a high deviation of the mean ALP expression was detected, which explains the lack of significance between this and other groups (Fig.4.1C).

No significant differences were found for OC gene expression between MSCs co-cultured with MG63 cells or cultured without MG63 cells (Fig.4.1D). In both, DM and GM conditions, there was a trend of higher OC gene expression in MSCs cultured alone compared to MSC co-cultured with MG63 cells (Fig.4.1D).

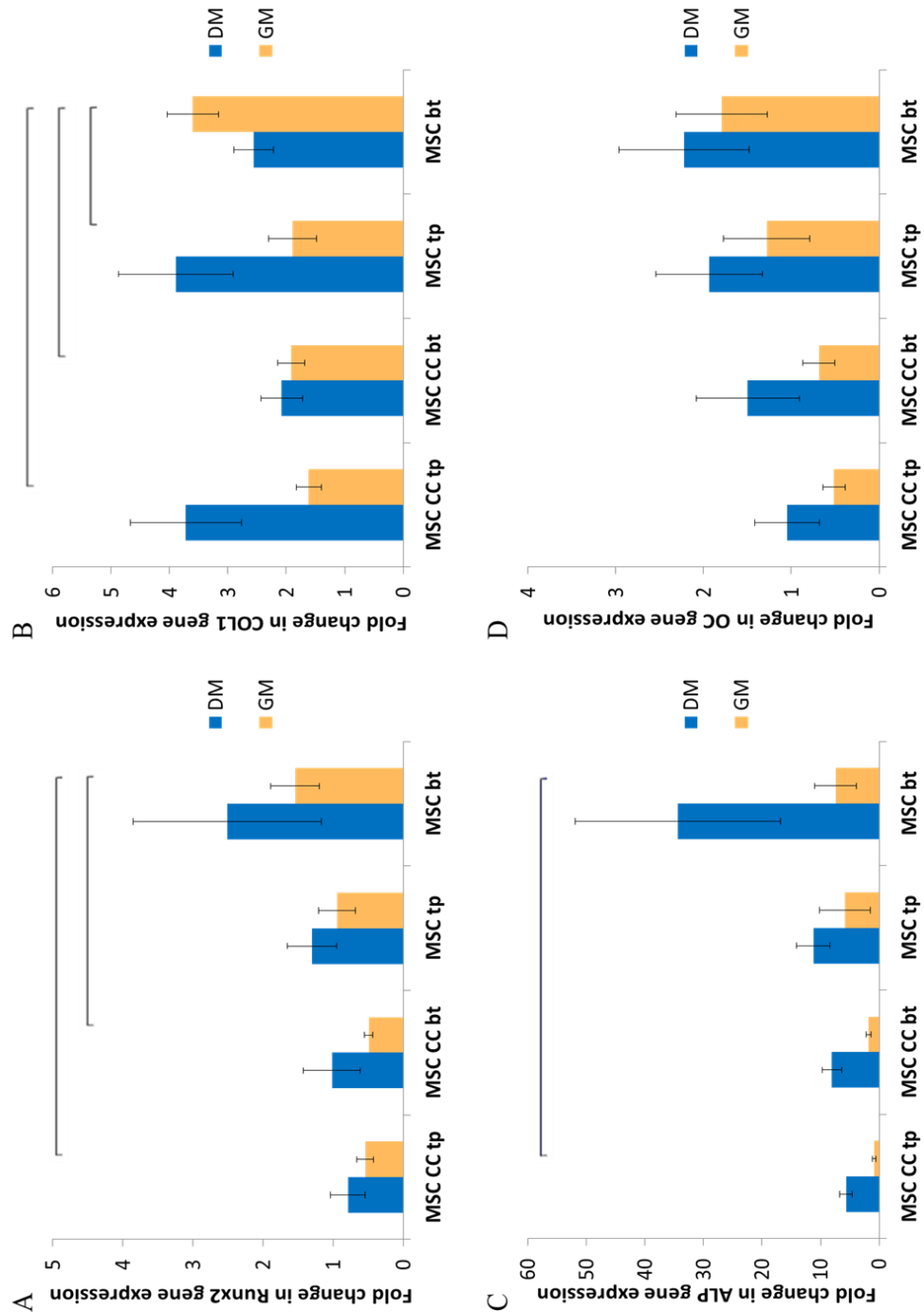


Figure 4.1. Comparative real-time PCR results of Runx2 (A), type I collagen (B), ALP (C) and OC (D) genes expression in MSC at day 21 of indirect co-culture with MG63 in monolayer. Diagrams show the mean fold change in gene expression with the standard error of the mean (3 experiments, n=9). Gene expression was normalised to 18S rRNA and made relative to gene expression in MSC cells at day 0. A, B, D: Data normally distributed, one-way ANOVA with Games-Howell. C: Data not normally distributed: Kruskal-Wallis and Mann-Whitney with Bonferroni correction. Statistical significance was determined as $p < 0.05$. MSC CC bt: MSC cells co-cultured with MG63 in the bottom of the plate; MSC CC tp: MSC cells co-cultured with MG63 in the cell culture insert; MSC bt: MSC cells in the bottom of the plate; MSC CC tp: MSC cells in the cell culture insert.

4.2.1.2. The effect of monolayer co-culture on MSC functionality

The co-culture of MSCs with MG63 cells had no significant effect on ALP protein activity in MSCs compared to MSCs cultured alone (Fig.4.2). For cells maintained in DM, enzyme activity was at the same level in all groups. Similar results were obtained for MSCs located in the well which were co-cultured with MG63 and single cell type culture of MSCs plated in the well and maintained in GM. For MSCs in cell culture inserts, the ALP activity was slightly higher for co-cultured MSCs in the insert group in GM than for control MSC in the insert maintained in GM (Fig.4.2).

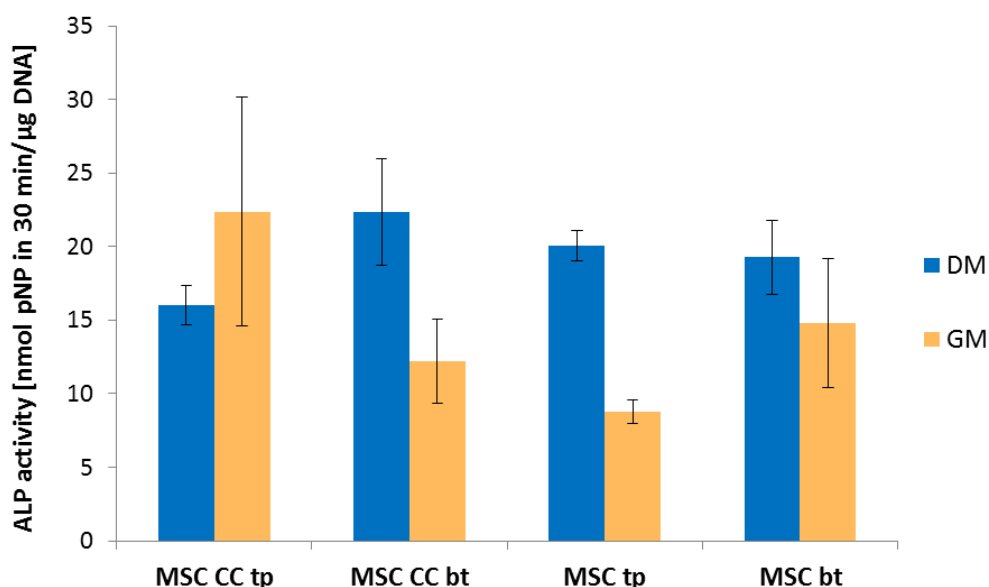


Figure 4.2. Diagram shows the mean of alkaline phosphatase (ALP) protein activity in 30 minutes relative to the amount of DNA at day 14 with the standard error of the mean (3 experiments, n=9). MSC and MG63 in monolayer indirect co-cultures or single cell type cultures were maintained in differentiation medium (DM) or, as control, in growth medium (GM) for 14 days. Data normally distributed, one-way ANOVA with Games-Howell. Statistical significance was determined as $p < 0.05$. MSC CC bt: MSC cells co-cultured with MG63 in the bottom of the plate; MSC CC tp: MSC cells co-cultured with MG63 in the cell culture insert; MSC bt: MSC cells in the bottom of the plate; MSC CC tp: MSC cells in the cell culture insert.

Significant differences were determined between groups for ^{45}Ca incorporation (Fig.4.3). When MSCs were located in the insert and cultured in GM conditions, there was 1.56-fold less calcium detected in co-cultured MSCs compared to control

MSCs group ($p=0.021$). A similar trend was reported in DM conditions for co-cultured and control MSCs seeded on the insert membrane. Moreover, in DM the ^{45}Ca level was decreased in MSC co-cultures in the well compared to MSCs seeded in the well without co-culture ($p=0.014$), whereas it was at the same level for respective GM groups (Fig.4.3). Results indicated that the location of cells in the co-culture system influences the ^{45}Ca uptake into the MSCs culture. Compared to co-cultured MSCs seeded in the well in DM and GM groups there was significantly more

^{45}Ca incorporation than in co-cultured MSCs located in the insert which were maintained in DM ($p=0.033$) and GM ($p=0.001$), respectively (Fig.4.3). Analogous relation was determined for single cell type cultures. In GM conditions, this trend reached significant level for control MSCs in the insert compared MSCs seeded in the well ($p=0.002$) (Fig.4.3).

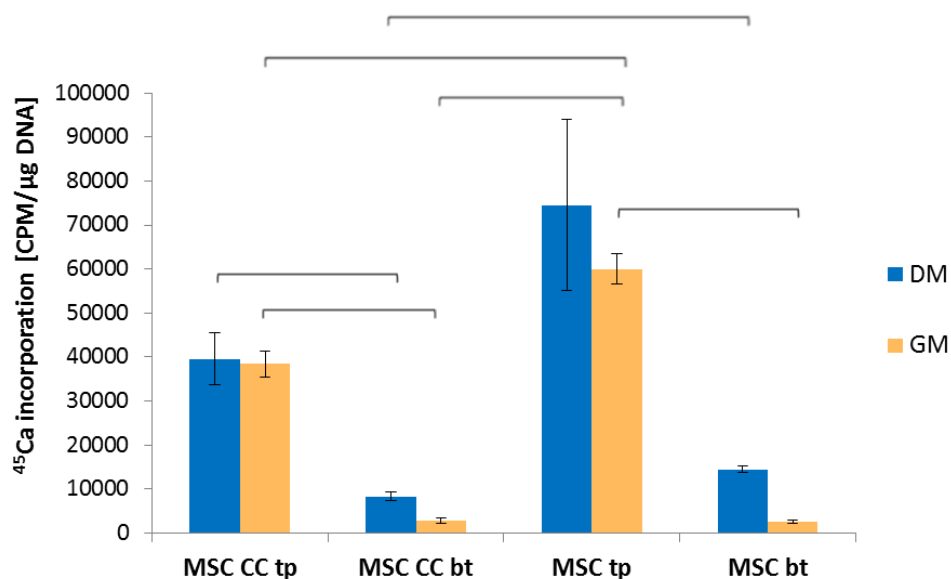


Figure 4.3. Diagram shows the mean of ^{45}Ca incorporation relative to the amount of DNA at day 21 with the standard error of the mean (3 experiments, $n=9$). MSC co-cultured with MG63 or cultured alone were maintained in differentiation medium (DM) or, as control, in growth medium (GM) for 21 days. Data normally distributed, one-way ANOVA with Games-Howell. Statistical significance was determined as $p<0.05$. MSC CC bt: MSC cells co-cultured with MG63 in the bottom of the plate; MSC CC tp: MSC cells co-cultured with MG63 in the cell culture insert; MSC bt: MSC cells in the bottom of the plate; MSC CC tp: MSC cells in the cell culture insert.

4.2.1.3. The effect of monolayer co-culture on osteogenic gene expression in osteoblast (MG63) cells

The analysis of Runx2, COL1, ALP and OC gene expression in MG63 cells co-cultured with MSCs in monolayer showed a similar expression pattern for Runx2, COL1, ALP (Fig.4.4). Moreover, the highest gene expression level for the aforementioned genes was reported for MG63 cells in the cell culture insert when in co-culture with MSCs in differentiation medium (MG63 CC tp DM group) (Fig.4.4A-D).

Indirect monolayer co-culture of MSCs with MG63 cells had no significant effect on Runx2 gene expression at day 21 in groups maintained in GM medium (Fig.4.4A.). Moreover, it had no effect on Runx2 expression in these DM groups in which MG63 cells were cultured on the bottom. In the case of MG63 cells cultured on the cell culture insert in DM, Runx2 mRNA expression was 7.3-fold higher in the group of co-cultured MG63, compared to MG63 cells cultured alone ($p=0.032$) (Fig.4.4A.).

Similarly as for Runx2, the COL1 gene expression for MG63 located in the insert and cultured in DM was significantly higher in co-cultured MG63 compared to control MG63 ($p=0.029$), whereas comparing the analogous groups located in the wells the expression was at the same level for MG63 from co-culture and control (Fig.4.4B.). There were no significant differences in Runx2 gene expression between cells co-cultured in the cell culture insert or in the well in GM and their respective controls. Runx2 mRNA expression in co-cultured MG63 located in the wells showed the highest expression compared to other GM groups. This trend reached significance only for control MG63 located in the insert in GM conditions ($p=0.018$) (Fig.4.4B.).

The investigation of ALP gene expression revealed significant, 3.1-fold, higher expression level in differentiation medium for MG63 located in the insert above MSCs group compared to MG63 located in the well below MSCs (Fig.4.4C.). Compared to other DM groups, the ALP mRNA expression was also higher in co-cultured MG63 which were located in the insert (Fig.4.4C.). However, these

differences did not reach significance. Expression of ALP was similar in all GM groups. Moreover, it was at a similar level as in DM groups except of co-cultured MG63 above MSCs in GM conditions. In this group, a trend of lower ALP expression than in analogous DM group was detected (Fig.4.4C.).

Significant differences between groups in DM were determined for the gene expression of OC, the late osteoblastic marker (Fig.4.4D.). Similarly as for other genes, the OC mRNA expression was the highest for MG63 cultured on the insert membrane above MSCs in differentiation medium. Comparing MG63 DM groups the OC expression was 2.45-, 2.17- and 1.83-fold higher in co-cultured MG63 located in the insert than in co-cultured cells in the well ($p=0.002$), single cell type cultures located on the bottom ($p=0.003$) and single cell type cultures in the insert ($p=0.048$), respectively (Fig.4.4D.). In GM conditions, the expression of OC mRNA was at similar level in all groups. Interestingly, in GM conditions for co-cultured MG63 located in the well and in single cell type cultures of MG63 seeded in the well or in the insert the OC gene expression was higher than in the respective DM groups (Fig.4.4D.).

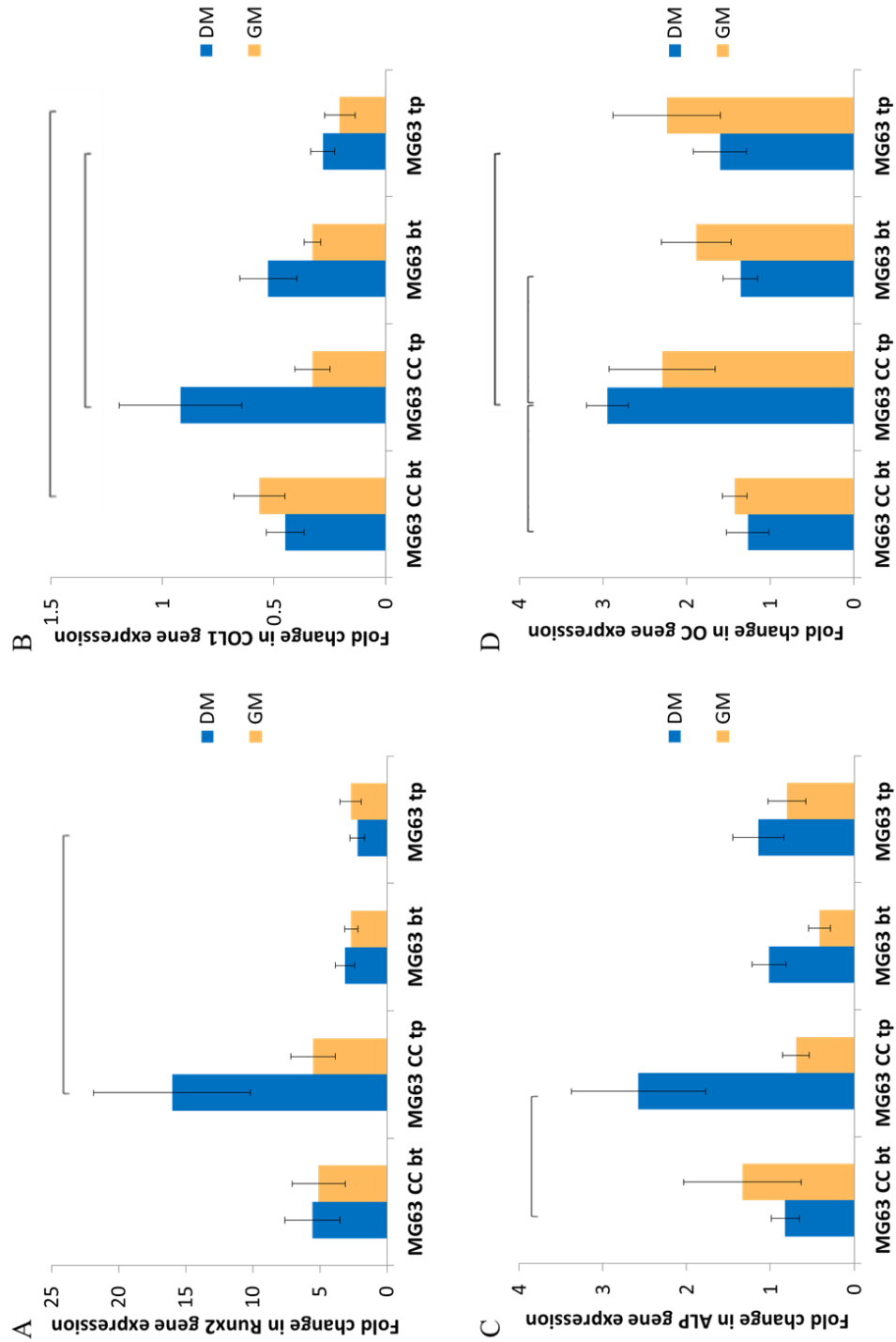


Figure 4.4. Comparative real-time PCR results of Runx2 (A), type I collagen (B), ALP (C) and OC (D) genes expression in MG63 at day 21 of co-culture with MSC in monolayer. Diagrams show the mean fold change in gene expression with the standard error of the mean (3 experiments, n=9). Gene expression was normalised to 18S rRNA and made relative to gene expression in MG63 cells at day 0. Data normally distributed, one-way ANOVA with Games-Howell. Statistical significance was determined as $p < 0.05$. MG63 CC bt: MG63 cells co-cultured with MSC in the bottom of the plate; MG63 CC tp: MG63 cells co-cultured with MSC in the cell culture insert; MG63 bt: MG63 cells in the bottom of the plate; MG63 CC tp: MG63 cells in the cell culture insert.

4.2.1.4. The effect of monolayer co-culture on osteoblast (MG63) functionality

ALP protein activity was analysed in MG63 cultured with or without MSCs in growth or differentiation medium at day 14 and made relative to the amount of DNA at the same time point. For sample harvesting, inserts were transferred to the wells containing no cells to allow the precise analysis of ALP protein activity and quantitation of DNA in both cell types.

The investigation of ALP protein activity in monolayer co-cultures revealed no significant differences between groups (Fig.4.5). Nevertheless, a trend of higher enzyme activity was observed for MG63 cells co-cultured with MSCs in DM compared to MG63 cells cultured alone. Additionally, ALP protein activity was higher in DM groups than in GM groups, except of control MG63 group located in the insert and maintained in DM and GM. In these control groups the enzyme activity was at the same level (Fig.4.5).

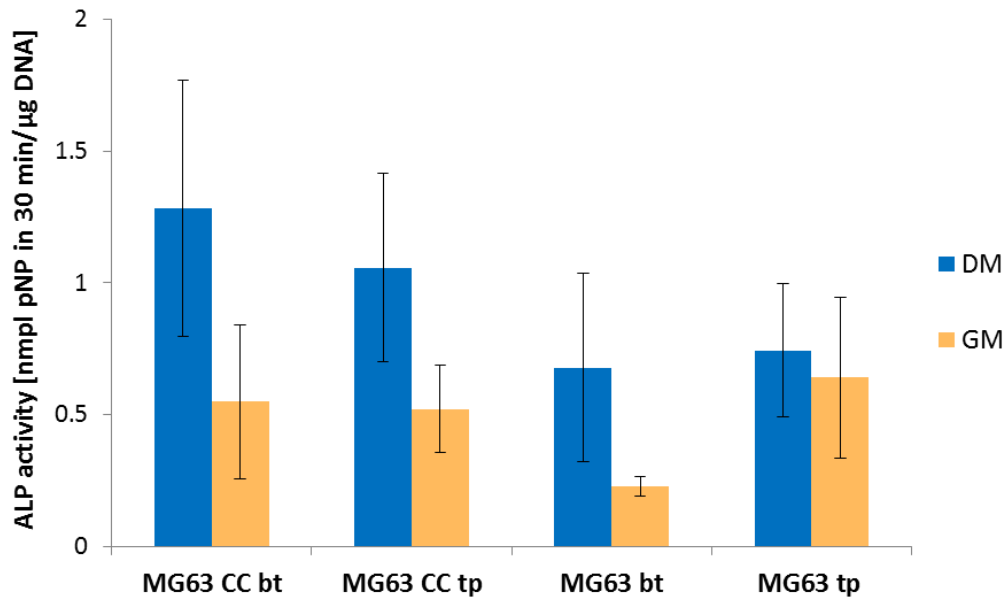


Figure 4.5. Diagram shows the mean of alkaline phosphatase (ALP) protein activity in 30 minutes relative to the amount of DNA at day 14 with the standard error of the mean (3 experiments, n=9). MSC and MG63 in monolayer co-cultures or single cell type cultures were maintained in differentiation medium (DM) or, as control, in growth medium (GM) for 14 days. Data not normally distributed Kruskal-Wallis and Mann Whitney with Bonferroni correction. Statistical significance was determined as $p < 0.05$. MG63 CC bt: MG63 cells co-cultured with MSC in the bottom of the plate; MG63 CC tp: MG63 cells co-cultured with MSC in the cell culture insert; MG63 bt: MG63 cells in the bottom of the plate; MG63 CC tp: MG63 cells in the cell culture insert.

Mineral incorporation in the newly formed ECM was investigated by ^{45}Ca uptake and made relative to the amount of DNA at day 21. As with ALP protein activity analysis, co-cultures were separated for each assay. The analysis of ^{45}Ca uptake revealed significant differences between groups (Fig.4.6). For both, cells in co-culture and single cell type cultures, the Ca^{45} uptake was higher for MG63 cultured in the cell culture insert (Fig.4.6).

Comparing co-cultured DM groups, ^{45}Ca incorporation was 13.2-fold higher for MG63 seeded in the insert than for MG63 seeded in the well ($p=0.034$). This comparison for single cell type cultures revealed 9.7-fold difference between control MG63 cultured in the insert and control MG63 located on the bottom ($p=0.022$) (Fig.4.6). In both DM groups of co-cultured MG63 and control MG63 in the well the ^{45}Ca uptake was at the same level. Although, for the DM groups with cells

in the cell culture insert ^{45}Ca incorporation was 1.75-fold higher in co-cultured MG63 than single cell type MG63 cultures, the co-culture with MSCs had a significant effect on ^{45}Ca incorporation in MG63 cells when these cells were cultured in the insert. A similar pattern of ^{45}Ca incorporation was reported for GM groups (Fig.4.6). Higher results were detected for groups with MG63 cells in the cell culture inserts. For cells maintained in GM, the ^{45}Ca uptake was 3.8-fold higher in co-cultured MG63 insert group than in co-cultured MG63 located in the well ($p=0.007$) and 4.56-fold higher in the control MG63 in the insert than the control MG63 in the well ($p=0.002$) (Fig.4.6). Even though not significant, the ^{45}Ca uptake was lower in GM groups with MG63 in the insert than in the respective DM groups (Fig.4.6).

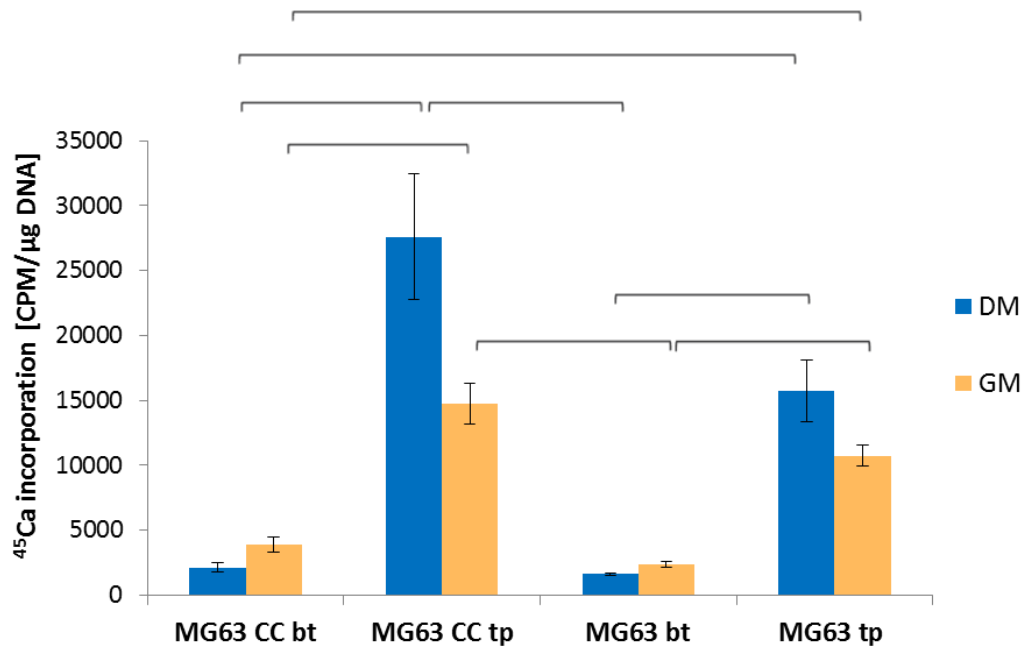


Figure 4.6. Diagram shows the mean of ^{45}Ca incorporation relative to the amount of DNA at day 21 with the standard error of the mean (3 experiments, $n=9$). MG63 indirectly co-cultured with MSC in monolayer or cultured alone were maintained in differentiation medium (DM) or, as control, in growth medium (GM) for 21 days. Data normally distributed, one-way ANOVA with Games-Howell. Statistical significance was determined as $p<0.05$. MG63 CC bt: MG63 cells co-cultured with MSC in the bottom of the plate; MG63 CC tp: MG63 cells co-cultured with MSC in the cell culture insert; MG63 bt: MG63 cells in the bottom of the plate; MG63 CC tp: MG63 cells in the cell culture insert.

4.2.2. Indirect co-culture of MSCs and MG63 in micromass and its effect on the osteogenic phenotype of cells

A micromass culture model was investigated for its potential use as a 3D co-culture model for MSCs and osteoblasts. This model, consisting of a high number of cells plated on the culture surface, is supported exclusively by the ECM produced by cultured cells. We aimed to investigate paracrine communication between MSC and osteoblast cells in 3D environment which provides a physiologically relevant context and promotes cell differentiation and maturation. The micromass co-culture was prepared as described in paragraph 2.2.11.2. Briefly, a micromass consisted of 100000 cells suspended in 5 μ l medium. For co-cultures and single cell type cultures, micromasses of each cell type were seeded in the well of 24-well plate ensuring that the distance between them and the edge of the well is the same in each sample. Cultures were maintained in growth medium (GM) as control or differentiation medium (DM). Growth medium consisted of DMEM (1g glucose/L), 10% FBS and 1% Penicillin-Streptomycin. Differentiation medium had the same components as GM and was supplemented with 50 μ g/ml L-ascorbic acid 2-phosphate sesquimagnesium salt hydrate, 10nM dexamethasone and 5mM β -glycerolphosphate.

The investigation of gene expression included four groups in DM and four in GM conditions (Tab.4.2). The ALP activity, DNA and ⁴⁵Ca incorporation were analysed in six groups out of which three groups were maintained in DM and three in GM (Tab.4.2).

Groups for gene expression analysis	
<i>Group name</i>	<i>Description</i>
MSC CC	MSCs co-cultured with MG63
MG63 CC	MG63 co-cultured with MSCs
MSC	single cell type culture of MSCs = control MSCs
MG63	single cell type culture of MG63 = control MG63

Groups for ALP activity, DNA, ⁴⁵Ca incorporation	
<i>Group name</i>	<i>Description</i>
MSCMG63	Two populations of co-cultured cells (MSCs and MG63) together
MSC	single cell type culture of MSCs = control MSCs
MG63	single cell type culture of MG63 = control MG63

Table 4.2. Description of the groups included for analysis of indirect co-culture of MSCs and MG63 in micromass.

4.2.2.1. The effect of micromass co-culture on osteogenic gene expression in MSCs

The results of Runx2 and COL1 gene expression in MSCs co-cultured with MG63 cells or cultured alone indicated no significant differences between groups (Fig.4.7A&B). Nevertheless, the expression of both genes showed a similar trend. In co-cultured MSCs DM and GM groups, gene expression was decreased compared to control MSC DM and GM groups, respectively (Fig.4.7A&B).

The effect of co-culture on MSC cells was more pronounced in the expression of ALP mRNA. Similarly, as for the Runx2 and COL1 expression, the ALP expression was lower in co-cultured MSCs DM and GM groups than in their respective controls (Fig.4.20.C). Specifically, ALP mRNA expression was 2.58-fold lower in co-cultured MSC DM than in control MSCs DM ($p=0.038$), whereas in GM groups it was 22.65-fold lower in co-cultured MSCs comparing to their controls

($p < 0.0001$) (Fig.4.7C). The presence of osteogenic supplements had a significant effect on ALP expression only in MSCs co-cultured with MG63 cells in micromass. This expression was approximately 12-fold higher in co-cultured MSCs in the presence of differentiation supplements than in co-cultured MSCs maintained in GM ($p < 0.0001$) (Fig.4.7C).

The investigation of OC mRNA levels revealed no significant differences between co-cultured MSCs DM and control MSCs DM groups (Fig.4.7D). Interestingly, in co-cultured MSCs GM group the OC expression was 2.38-fold up-regulated compared to control MSCs GM group. There was no significant effect of differentiation supplements on ALP expression in co-culture or single cell type culture groups (Fig.4.7D).

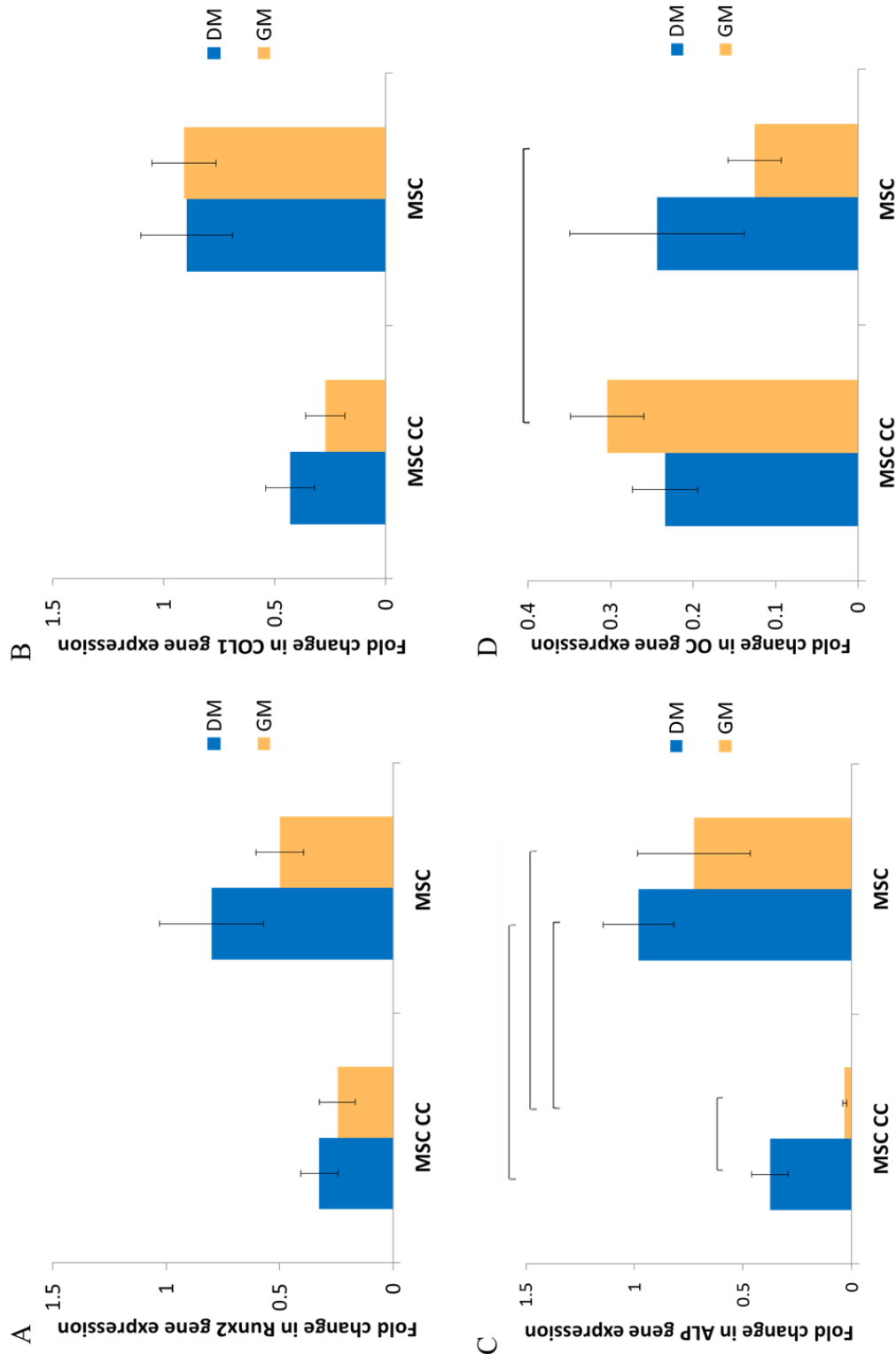


Figure 4.7. Comparative real-time PCR results of Runx2 (A), type I collagen (B), ALP (C) and OC (D) genes expression in MSC at day 21 of co-culture with MG63. Diagrams show the mean fold change in gene expression with the standard error of the mean (3 experiments, n=9). Gene expression was normalised to 18S rRNA and made relative to gene expression in MSC cells at day 0. Data normally distributed, one-way ANOVA with Games-Howell. Statistical significance was determined as $p < 0.05$.

In addition to analyses of osteogenic genes, the ratio between specific genes and Runx2 transcription factor was analysed (Fig.4.8). Runx2 is considered as an early osteoblast marker, whose expression decreases with the progression into the osteoblastic phenotype. Although, Runx2 did not show significant differences by itself, it showed the trend of lower expression in the MSC co-cultured group than in MSC cultured alone. COL1 gene expression relative to Runx2 expression was similar between co-cultured MSCs and control MSCs maintained in differentiation medium, whereas in GM conditions it was significantly lower in co-cultured MSCs than in control MSCs group ($p=0.003$) (Fig.4.8A).

Similar lower relative gene expression results in GM groups were obtained for the ALP/Runx2 ratio ($p=0.005$) (Fig.4.8B). The ALP/Runx2 ratio was decreased in co-cultured MSCs compared to control MSCs when cells were cultured in DM. Although this ratio was 2-fold higher in co-cultured MSCs than in control MSCs in DM conditions, this trend did not reach significance (Fig.4.8B) In addition, the ALP/Runx2 ratio in co-cultured MSCs and control MSCs maintained in GM was lower than in respective GM groups. This difference was found to be significant for co-cultured MSCs in DM and in GM ($p=0.001$) (Fig.4.8B).

The OC/Runx2 ratio showed interesting results. For both DM and GM conditions, the OC/Runx2 was higher for co-cultured MSCs (Fig.4.8C). This ratio was 2.22-fold higher in co-cultured MSCs than in control MSCs. Specifically, when micromass' were cultured in growth medium the OC/Runx2 ratio was 4.5-fold higher ($p=0.02$) in co-cultured MSCs compared to control MSCs (Fig.4.8C).

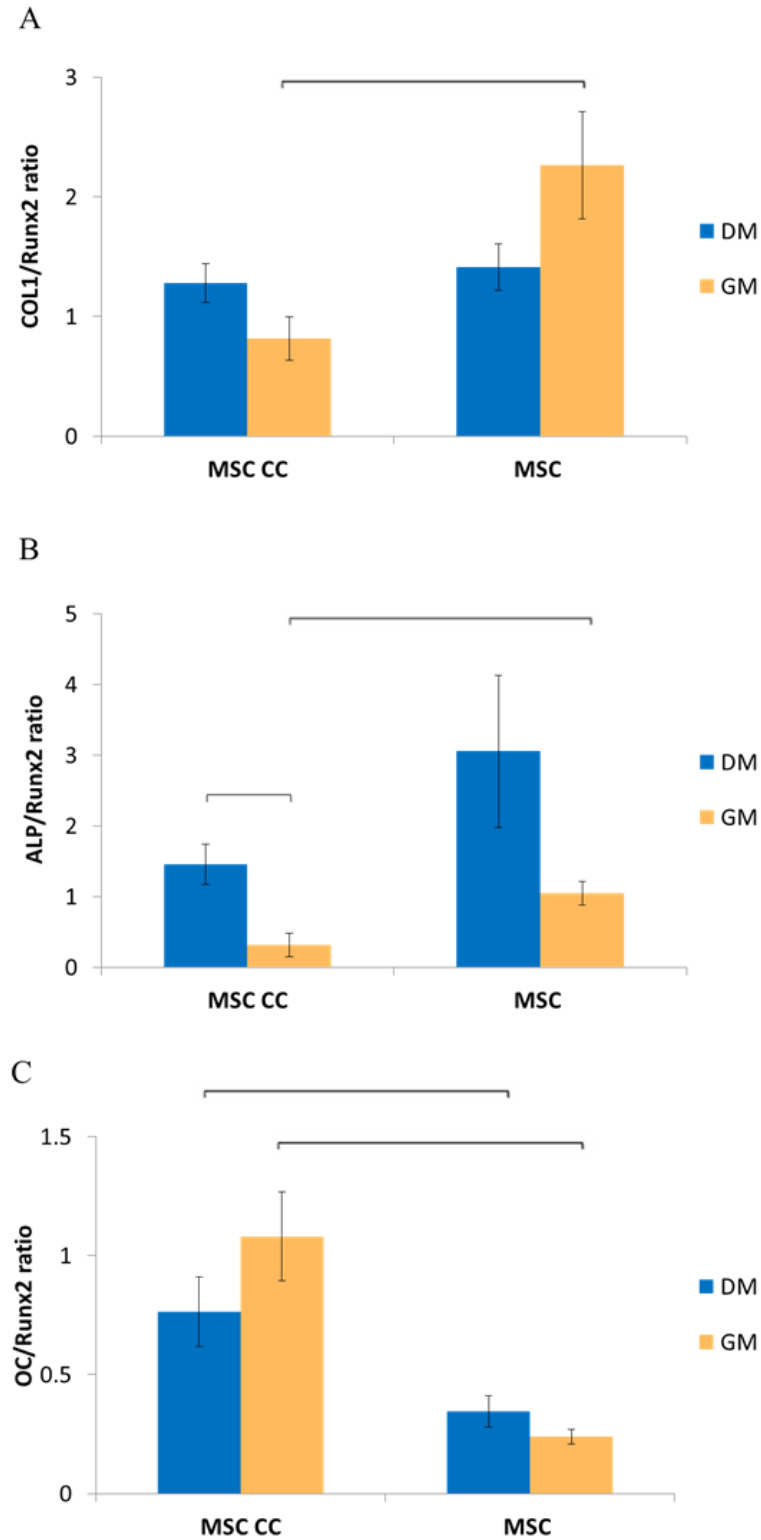


Figure 4.8. Diagrams show the mean of COL1/Runx2 (A), ALP/Runx2 (B) and OC/Runx2 (C) ratio in gene expression at day 21 with the standard error of the mean (3 experiments, n=9). Gene expression was normalised to 18S rRNA and made relative to gene expression in MSC cells at day 0. A, B: Data not normally distributed, Kruskal Wallis, Mann Whitney with Bonferroni correction. C: Data normally distributed, one-way ANOVA with Games-Howell. Statistical significance was determined as $p < 0.05$.

4.2.2.2. The effect of micromass co-culture on osteogenic gene expression in osteoblast (MG63) cells

The effects of co-culture on the osteoblast phenotype were determined by comparative real-time PCR at day 21 of culture.

No significant differences between cells in co-culture and MG63 in single cell type cultures could be detected for Runx2 expression (Fig.4.9A). Gene expression results showed that in growth medium (GM) co-culture has no effect on type 1 collagen (COL1) mRNA expression (Fig.4.9B). On the contrary, a trend of lower COL1 gene expression was reported in MG63 cells from co-culture maintained in differentiation medium (MG63 CC DM group) compared to MG63 from single cell type culture in DM (MG63 DM group). In both culture systems, COL1 mRNA expression was higher in DM groups. For MG63 cultured alone, this difference reached significance ($p=0.005$) (Fig.4.9B).

The ALP expression of MG63 cultured with MSC or alone in micromass was investigated. Significant differences between groups were found only for cells co-cultured in different media (Fig.4.9C). In co-cultured MG63 DM group ALP gene expression was 2.4-fold higher than in co-cultured MG63 GM group ($p=0.025$). ALP expression in MG63 cultured alone in different media was at the same level at day 21 of culture. Compared to the expression of COL1 in co-cultured MG63 and control MG63 maintained in DM, the ALP results showed an opposite trend of higher mRNA expression in co-culture group. Similarly as for COL1, this trend did not reach statistical significance (Fig.4.9C).

The co-culture had no effect on the expression of the late osteoblastic marker gene, OC, in co-cultured MG63 DM and GM groups compared with control MG63 micromass cultures in DM and GM, respectively (Fig.4.9D). In both culture models, the OC mRNA expression was higher in differentiation medium. The difference between DM and GM was significantly higher for groups of co-cultured MG63 (Fig.4.9D).

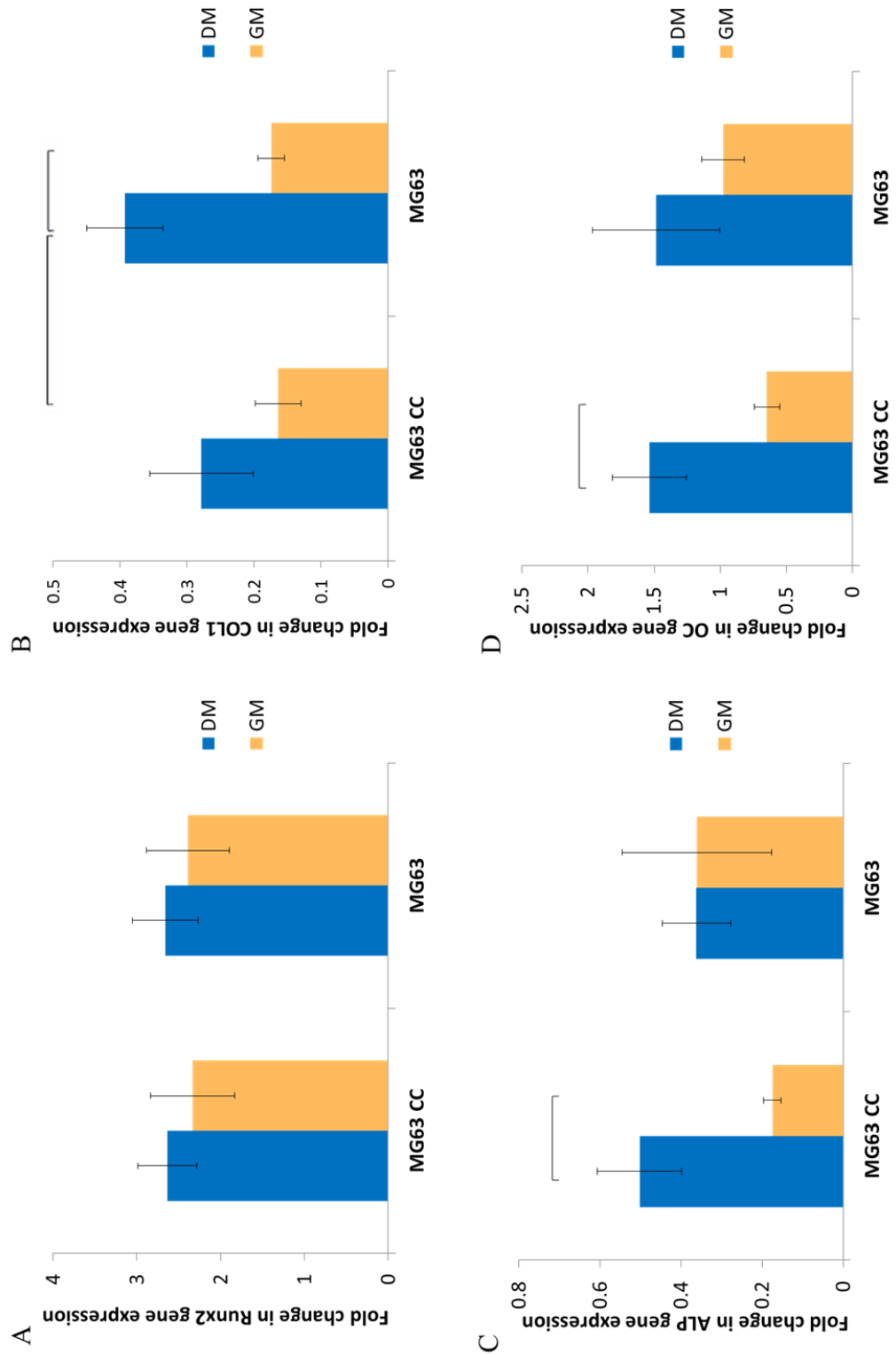


Figure 4.9. Comparative real-time PCR results of Runx2 (A), type I collagen (B), ALP (C) and OC (D) genes expression in MG63 at day 21 of co-culture with MSC. Diagrams show the mean fold change in gene expression with the standard error of the mean (3 experiments, n=9). Gene expression was normalised to 18S rRNA and made relative to gene expression in MG63 cells at day 0. A, B: data not normally distributed: Kruskal-Wallis and Mann-Whitney with Bonferroni correction. C, D: normally distributed, one-way ANOVA with Games-Howell. Statistical significance was determined as $p < 0.05$ (*).

4.2.2.3. The effect of micromass co-culture on ALP and mineralisation

ALP protein activity was analysed in micromass cultures maintained in growth or differentiation medium at day 14 and made relative to the amount of DNA at the same time point. For this analysis co-cultured cell types were not separated hence, the ALP activity in co-cultures was measured in samples harvested from both cell types at the same time (MG63MSC group).

The ALP activity in micromass cultures showed significant differences between co-cultured cells and single cell type cultures (Fig.4.10). The enzyme activity was significantly higher in co-cultured group maintained in DM compared to MG63 cells cultured alone in DM ($p=0.00003$). Conversely, the ALP activity was dramatically lower in MG63MSC co-culture in DM than in single control MSC DM group ($p=0.001$). A similar pattern of ALP activity was reported for cultures in GM, where the co-culture group had a higher enzyme activity than control MG63 ($p=0.017$). At the same time, it was 6-fold lower in co-culture group than in control MSC group ($p=0.04$) (Fig.4.10). The culture conditions of micromass co-cultures and micromass single cell type cultures had significant effects on ALP activity. In general, lower enzyme activity was reported for all groups in GM. Interestingly, for all groups the presence of differentiation supplements in medium had similar effect on ALP activity. Enzyme level was 3.16-fold higher in micromass from co-culture maintained in differentiation medium than in growth medium ($p=0.0002$). For control MG63 micromasses cultured in DM the ALP activity was 3.6-fold greater compared to control MG63 in growth medium ($p=0.018$), whereas for MSCs micromasses this difference equalled 2.85-fold between cultures in differentiation and growth medium ($p=0.01$) (Fig.4.10).

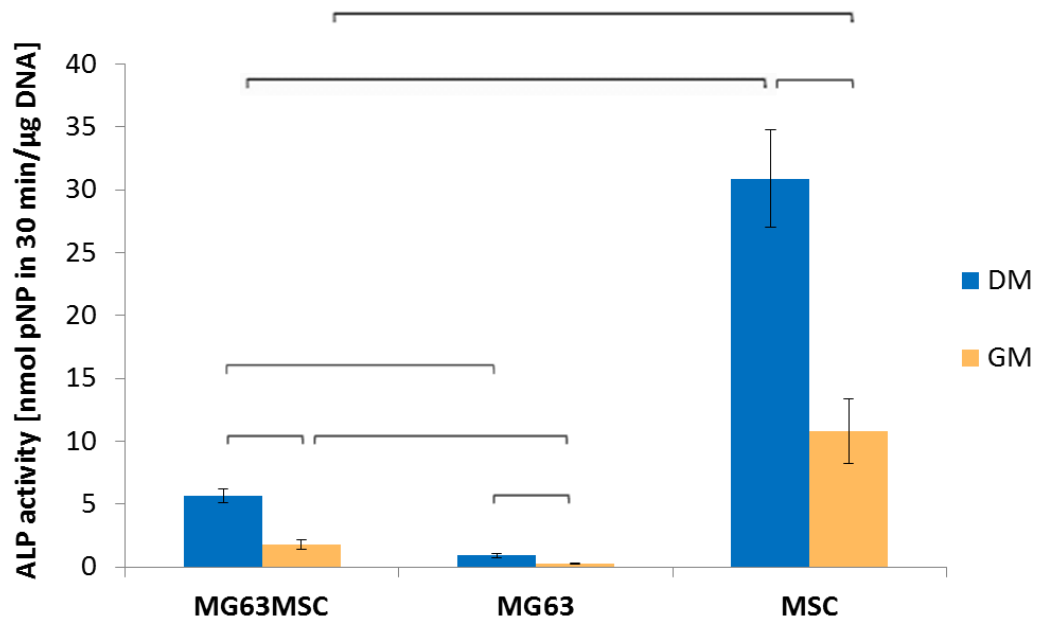


Figure 4.10. Diagram shows the mean of alkaline phosphatase (ALP) activity in 30 minutes relative to the amount of DNA at day 14 with the standard error of the mean (3 experiments, n=9). MSC and MG63 micromass co-cultures (MG63MSC) or single cell type cultures (MG63; MSC) were maintained in differentiation medium (DM) or, as control, in growth medium (GM) for 14 days. Data normally distributed, one-way ANOVA with Games-Howell. Statistical significance was determined as $p < 0.05$.

Mineral incorporation detected by ^{45}Ca uptake at day 21 revealed significant differences between groups (Fig.4.11). In co-cultures the calcium incorporation significantly increased compared to the control MG63 DM group ($p=0.019$). The opposite relation in DM conditions was reported for co-cultures and control MSCs, where the calcium incorporation was 2-fold higher in the control MSCs group ($p=0.002$) (Fig.4.11). There were no significant changes in calcium uptake between GM groups. Moreover, for each culture group there were significant differences between DM and GM groups. Interestingly, for MG63 the calcium incorporation was lower in the DM than the GM group ($p=0.001$), whereas in micromass co-cultures and control MSCs cultures this was higher in DM groups compared to GM groups ($p=0.043$ and $p < 0.0001$, respectively) (Fig.4.11).

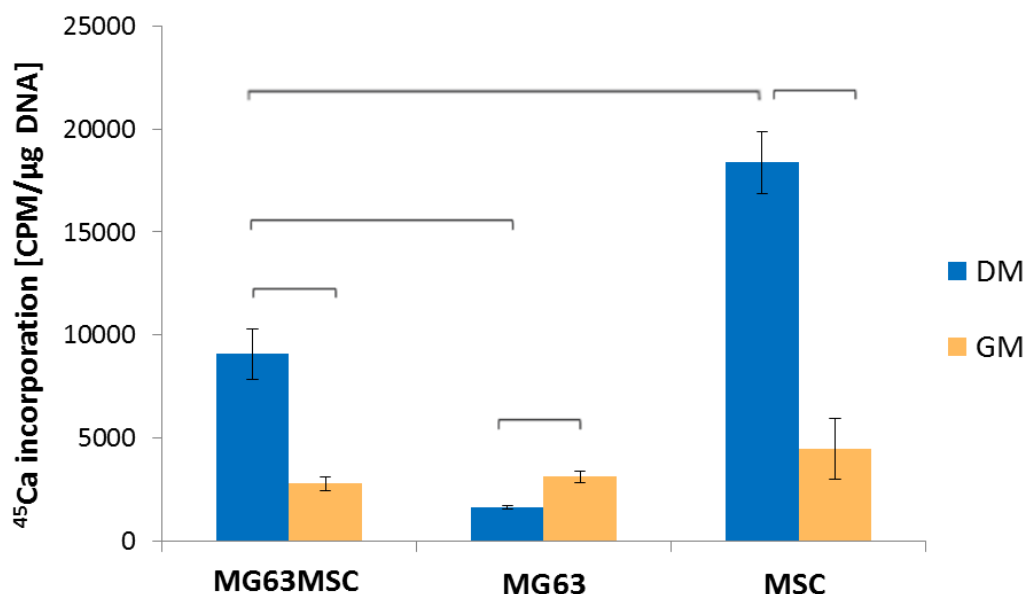


Figure 4.11. Diagram shows the mean of ^{45}Ca incorporation relative to the amount of DNA at day 21 with the standard error of the mean (3 experiments, $n=9$). MSC and MG63 micromass co-cultures (MG63MSC) or single cell type cultures (MG63; MSC) were maintained in differentiation medium (DM) or, as control, in growth medium (GM) for 21 days. Data normally distributed, one-way ANOVA with Games-Howell. Statistical significance was determined as $p<0.05$.

4.2.3. Generation and functionality of MG63 cells expressing GFP

4.2.3.1. Transduction efficacy and cell colonies selection

MG63 cells were selected for transduction with pMX retroviral expression vector containing a GFP insert. When cells reached approximately 80% confluence, the transduction efficiency and selection of GFP positive cells was analysed with fluorescence-activated cell sorting (FACS). The analysed cells had the homogeneous morphology (Fig.4.12) which was the same as for non-transduced MG63 cells (data not shown). For the further analysis of the visualisation of the expression of the fluorescence approximately 96% of cells were included (Fig.4.12A). These cells included two population of cells which were GFP negative and GFP positive (Fig.4.12B&C). From these populations 14.2% of cells were expression GFP. Positive cells were selected. The post-sort analysis of separated populations of cells confirmed the successful separation of GFP negative (Fig.4.13A-C) from GFP positive cells (Fig.4.13D-F). In this analysis, for the selected GFP positive cells there

were 91.3% cells which appeared in the gate of positive cells and 2.4% cells were in the gate of negative cells.

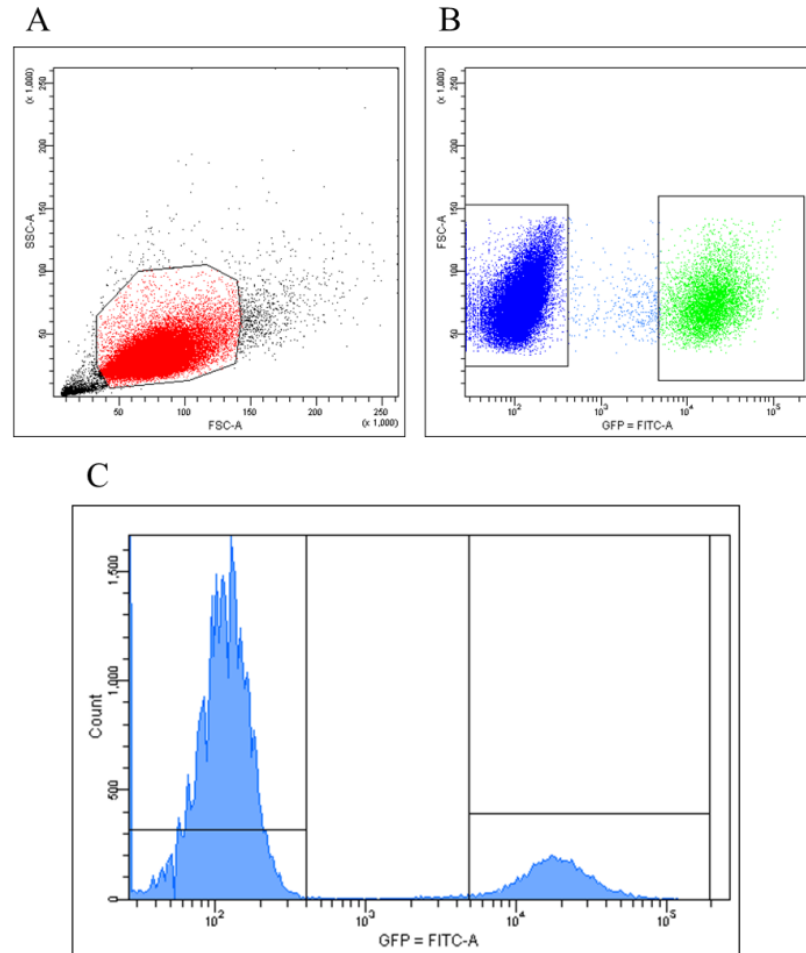


Figure 4.12. Diagrams show the transduction efficiency of MG63 cells with GFP. A: Population of cells selected for the analysis. B: Selection of populations GFP negative (blue) and positive (green) cells. C: Gated populations of GFP negative (left histogram) and positive (right histogram) cells.

The population of GFP positive and negative cells was plated for further expansion. The morphology of both types of cells was the same indicating that the transduction itself does not have any influence on cell morphology (Fig.4.14A-D).

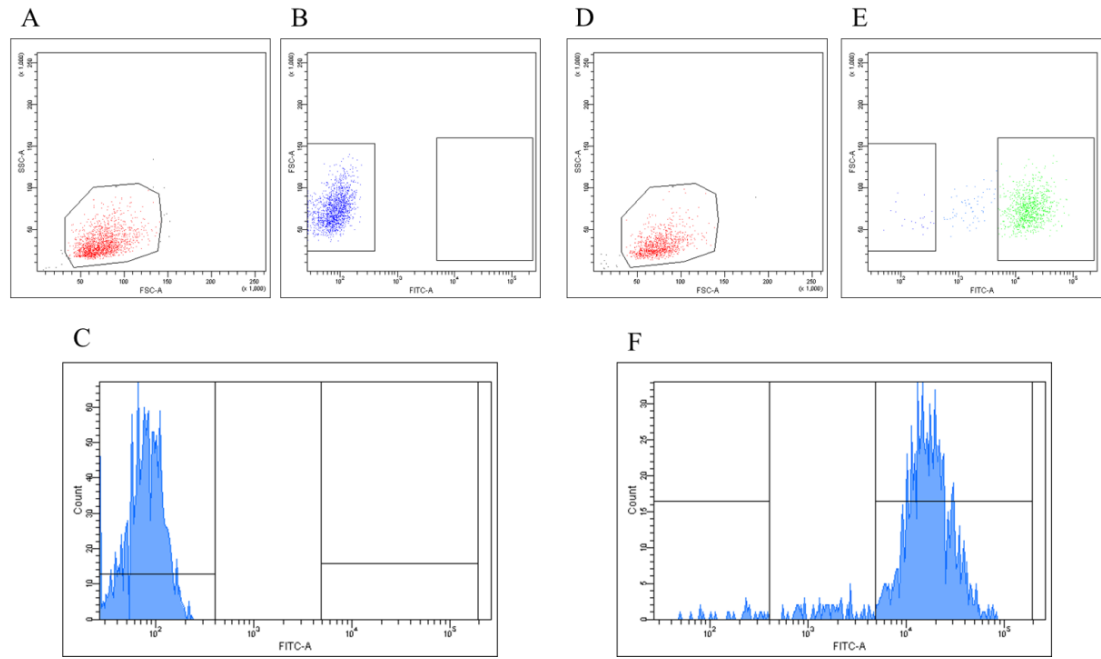


Figure 4.13. Diagrams show the post-sort of cells separated with FACS after the transduction with GFP. Analysis of GFP negative cells population (A-C) and GFP positive cells population (D-F).

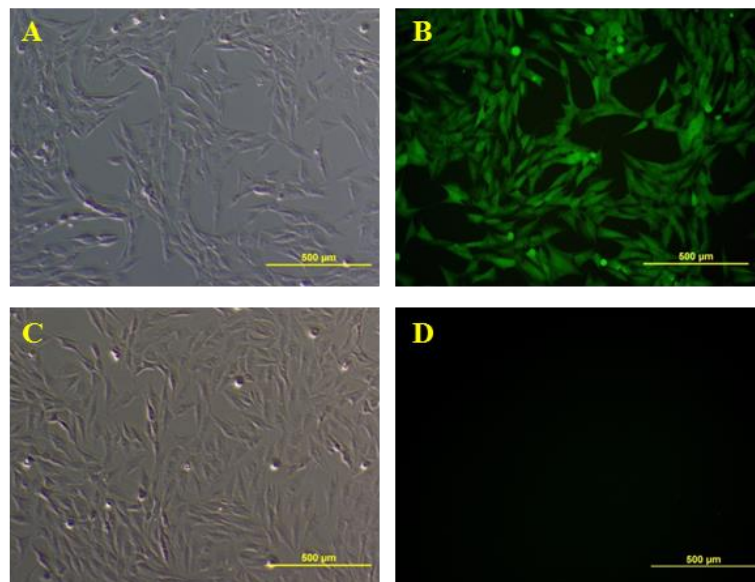


Figure 4.14. Representative microphotographs of MG63 expressing GFP (A, B) and MG63 (C, D) cells in culture. A, C: cultures visualized with phase contrast. B, D: cultures visualised using Olympus CK40 microscope with associated 500-nm emission filter (Olympus CX-DMB-2 cube).

After the expansion, the GFP positive cells were analysed again with FACS (Fig.4.15.A-C). With applying the same gating as previously, 97.5% of cells were included in the gate for/of the positive cells (Fig.4.15.A). To ensure the pure, 100%, population of MG63 expressing GFP cells, single cell colonies were established in a 96-well plate.

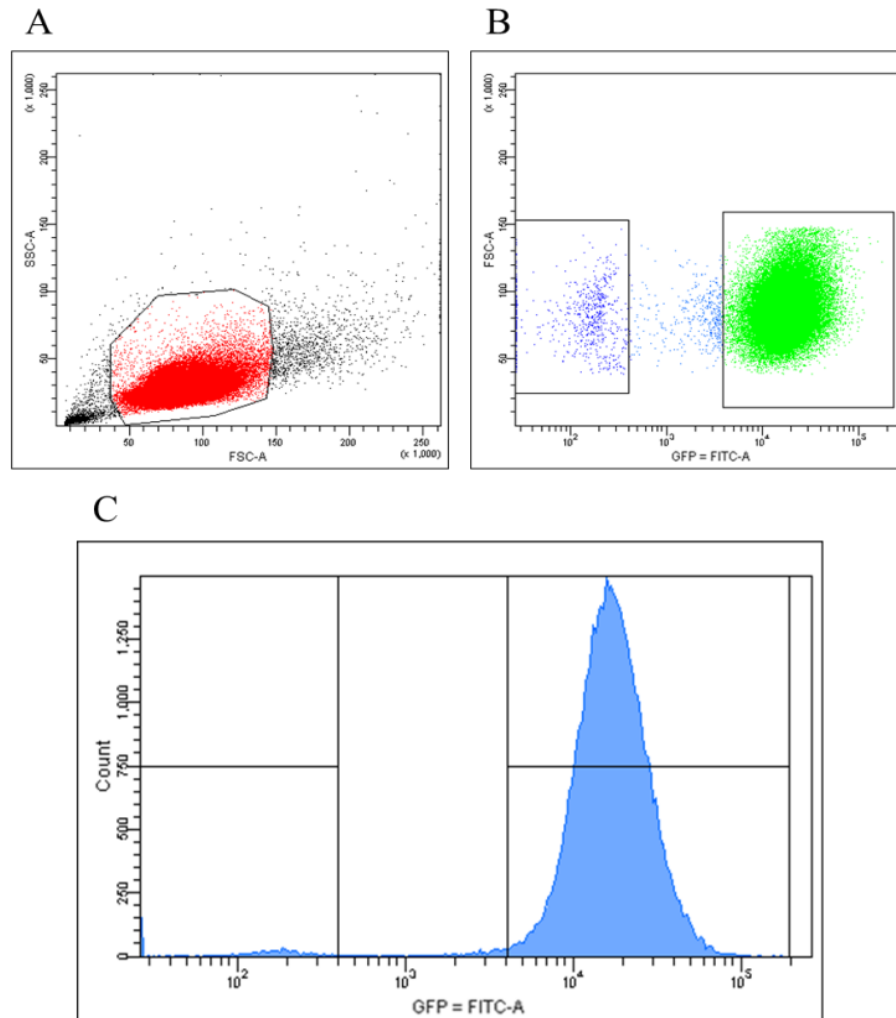


Figure 4.15. Diagrams show the analysis of MG63 cells expressing GFP used for establishing single cell colonies. A: Population of cells selected for the analysis. B: Selection of populations GFP negative (blue) and positive (green) cells. C: Gated populations of GFP negative (left histogram) and positive (right histogram) cells.

Based on the visual assessment of the GFP intensity, six cell colonies were selected and expanded further. All these cell populations originating from single cell colonies were analysed with FACS. The analysis revealed the presence of 99.2-99.6% positive cells. Additionally, expression of GFP different intensity levels by three out

of six colonies was confirmed by FACS (Fig.4.16). The median of GFP intensity in MG63 cells (negative control) was at the level of 138, whereas for GFP expressing cells it was at the level of 18570 (colony 1), 26167 (colony 2) and 40137 (colony 3). Colony with the highest GFP intensity level was named as MGreen63 cells and was selected for the evaluation of the cellular functionality. Furthermore, the phenotype of these cells was compared to the parental MG63 cells.

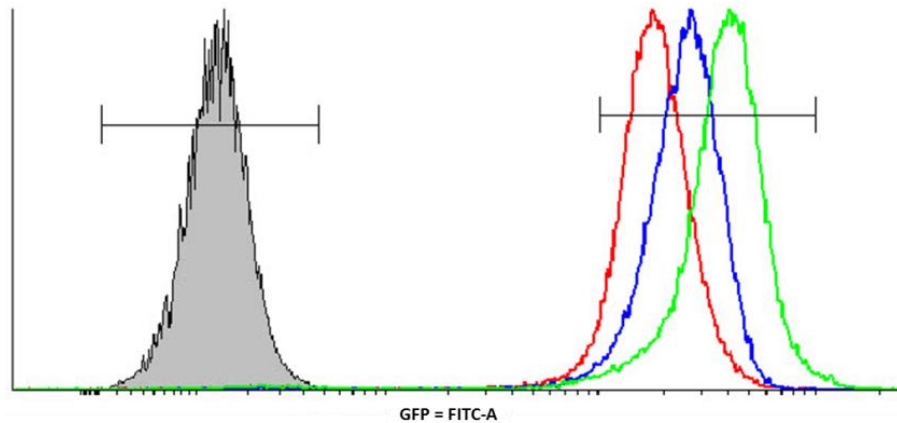


Figure 4.16. Diagram shows the overlay of histograms of GFP intensity of 3 selected colonies obtained after seeding single cell colonies (*red* – colony 1, *blue* - colony 2, *green* - colony 3) and MG63 cells (negative control; grey histogram).

4.2.3.2. Phenotypic assessment of MGreen63 cell line

4.2.3.2.1. Proliferation of MGreen63 cell line

Proliferation of cells was assessed with DNA-binding Hoechst assay. MG63 and MGreen63 presented similar trend of proliferation (FIG). The gradual increase in DNA amount was reported from day 2 to day 10 of cell culture. No significant differences at any time point were detected in growth kinetics between MG63 and MGreen63 (Fig.4.17).

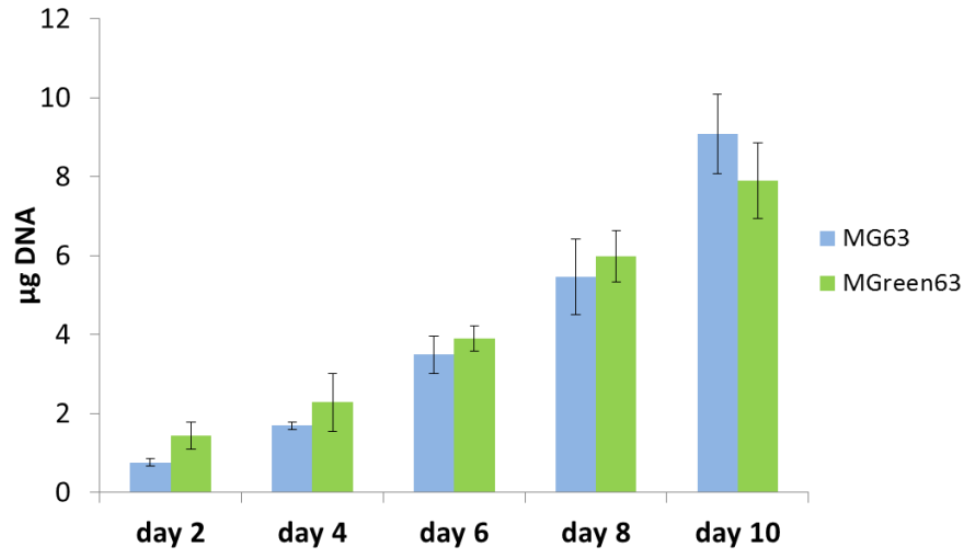


Figure 4.17. The amount of mean DNA quantified during the culture of MG63 and MGreen63 at day 2, 4, 6, 8 and 10. The diagram presents the mean with the standard error of the mean (3 experiments, n=9). Data normally distributed: two-way ANOVA with Least Significant Difference adjustment for multiple comparisons. Statistical significance was determined as $p < 0.05$.

4.2.3.2.2. Analysis of osteoblastic functions (ALP & mineralisation)

The ALP activity was quantitatively detected in MGreen63 and MG63 cells at day 2, 7, 14 and 21. The enzyme activity in MGreen63 in DM and GM was compared to the MG63 DM and GM, respectively.

In vitro ALP activity changed in a time-dependent manner (Fig.4.18). There were no significant differences for enzyme activity at any time point in both cell types maintained in DM medium. Nevertheless, over time the ALP activity decreased in MGreen63 DM, whereas for MG63 DM the decrease (Fig.4.18) was at lower level (Fig.4.18). In GM medium, the ALP activity decreased from day 2 to day 21, while for MG63 ALP was at similar level over time. The ALP activity was higher in MGreen 63 GM at day 2 and 7, with significant level reported for day 2 ($p=0.049$) (Fig.4.18).

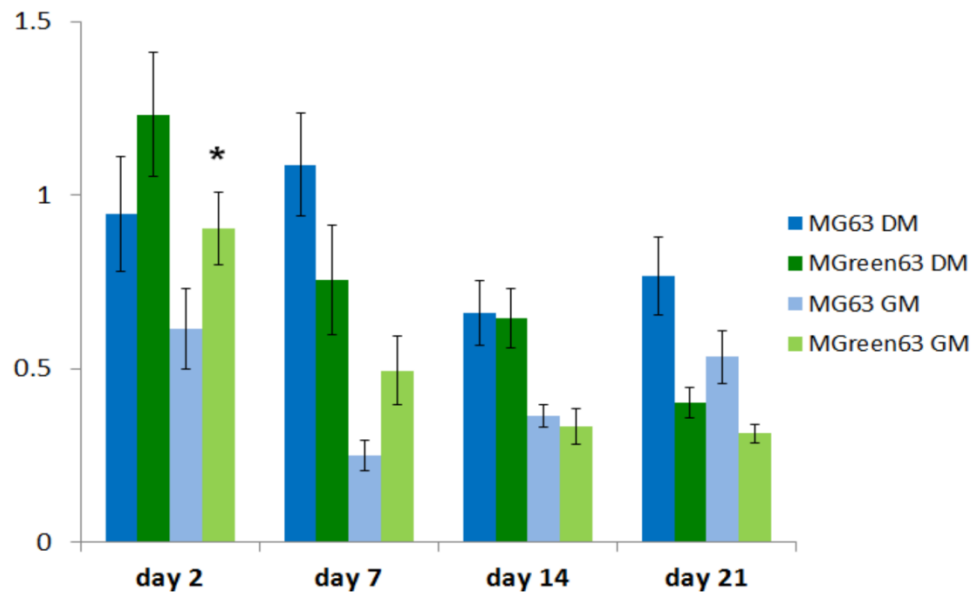


Figure 4.18. Diagram shows the mean alkaline phosphatase (ALP) activity with the standard error of the mean in MG63 and MGreen63 cells cultured in osteogenic (DM) or growth (GM) medium. For each cell type ALP activity was assessed as nmol pNP released in 30 minutes and normalised to the amount of DNA (3 experiments, n=9). Data normally distributed: two-way ANOVA with Least Significant Difference adjustment for multiple comparisons. Statistical significance was determined as $p < 0.05$. *: MGreen63 DM compared to MG63 DM; #: MG63 DM compared to MG63 GM.

The visual detection of mineralisation of MGreen63 and MG63 was assessed using Alizarin Red S (ARS) staining at day 21 of culture. Representative images from three individual experiments performed for each cell type are shown (Fig.4.19). Both cell types maintained in DM and GM were negative for ARS at day 21 (Fig.4.19.E-H).

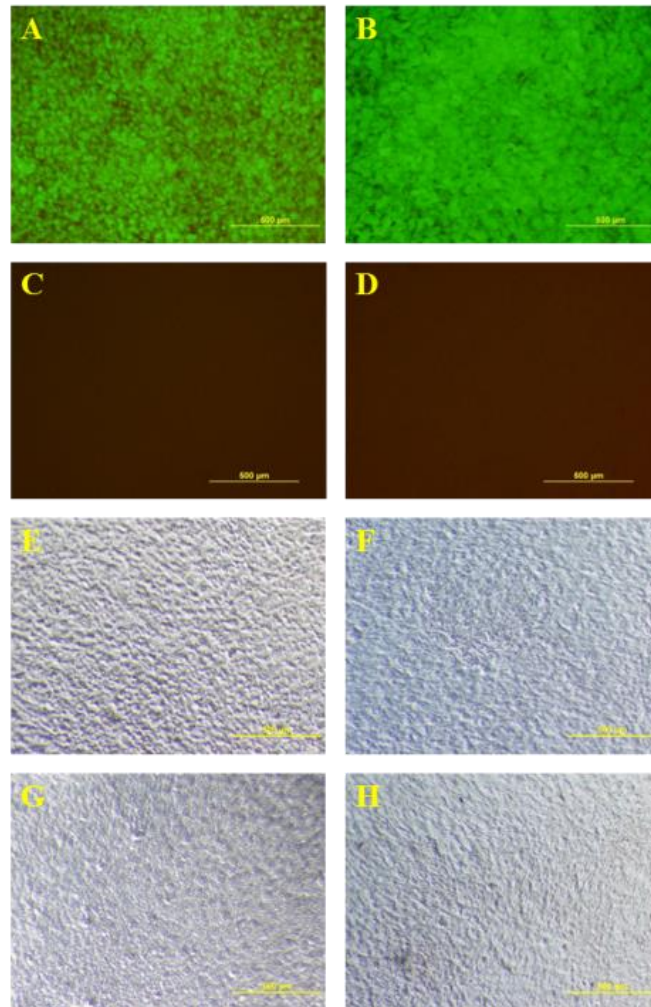


Figure 4.19. Representative microphotographs of MGreen63 (A, B, E, F) and MG63 (B, C, G, H) cells at day 21. Both cell types were maintained in DM (A, C, E, G) or GM (B, D, F, H) medium for 21 days before the analysis. A, B, C, D: cultures visualised using Olympus CK40 microscope with associated 500nm emission filter (Olympus CX-DMB-2 cube). E, F, G, H: cultures visualized with phase contrast after staining with Alizarin Red S.

4.2.3.2.3. Osteogenic genes expression in MGreen63 cell line

The transcriptional changes of early, mid-term and late osteoblast specific genes over 21 days were analysed in MGreen63 and MG63 cells. Gene expression was made relative to the expression of genes in MG63 cells at day 0.

For both cell types in DM and GM groups, the expression of Runx2 showed an increase over time. The expression levels were lower for MGreen63 than MG63 in DM groups (Fig.4.20A). This trend reached significant level at day 7 ($p=0.003$) and day 21 ($p=0.024$). At these time points, the Runx2 expression was 2.6- and 1.5-fold, respectively, lower in MGreen63 DM group compared to MG63 DM group. For cells in GM groups, the Runx2 mRNA expression was significantly higher in MGreen63 compared to MG63 only on day 14 ($p=0.003$) (Fig.4.20A).

Comparable levels of COL1 were observed between Mgreen63 and HOb cells for day 2,14 and 21, however, at day 7 COL1 mRNA levels were observed significantly lower in MGreen63 compared to MG63 ($p<0.001$) (Fig.4.20B). In GM groups, the COL1 gene expression was significantly lower in MGreen63 compared to MG63 only at day 2 ($p=0.018$), whereas at later time points the same levels of COL1 mRNA were observed in both cell types (Fig.4.20B).

The ALP gene expression showed the temporal changes for both cell types, with the highest expression at day 7. For MGreen63 DM group, ALP mRNA level was significantly lower at day 7 ($p=0.004$) compared to MG63 DM group (Fig.4.20C). In GM groups at day 14, the 2.38-fold higher expression of ALP in MGreen63 cells compared to MG63 cells reached the significance ($p=0.022$) (Fig.4.20C).

The expression of OC mRNA expression in MGreen63 DM and GM groups showed similar trend compared to MG63 DM and GM groups, respectively (Fig.4.20D). The only significant difference was determined for lower OC mRNA expression in MGreen63 DM compared to MG63 DM at day 7 ($p<0.001$) (Fig.4.20D).

The expression of E11 was at the same level in MGreen63 and MG63 maintained in DM or GM medium except day 7 for DM groups. At this time point, E11 expression was significantly lower in MGreen63 DM compared to MG63 DM ($p<0.001$) (Fig.4.20E).

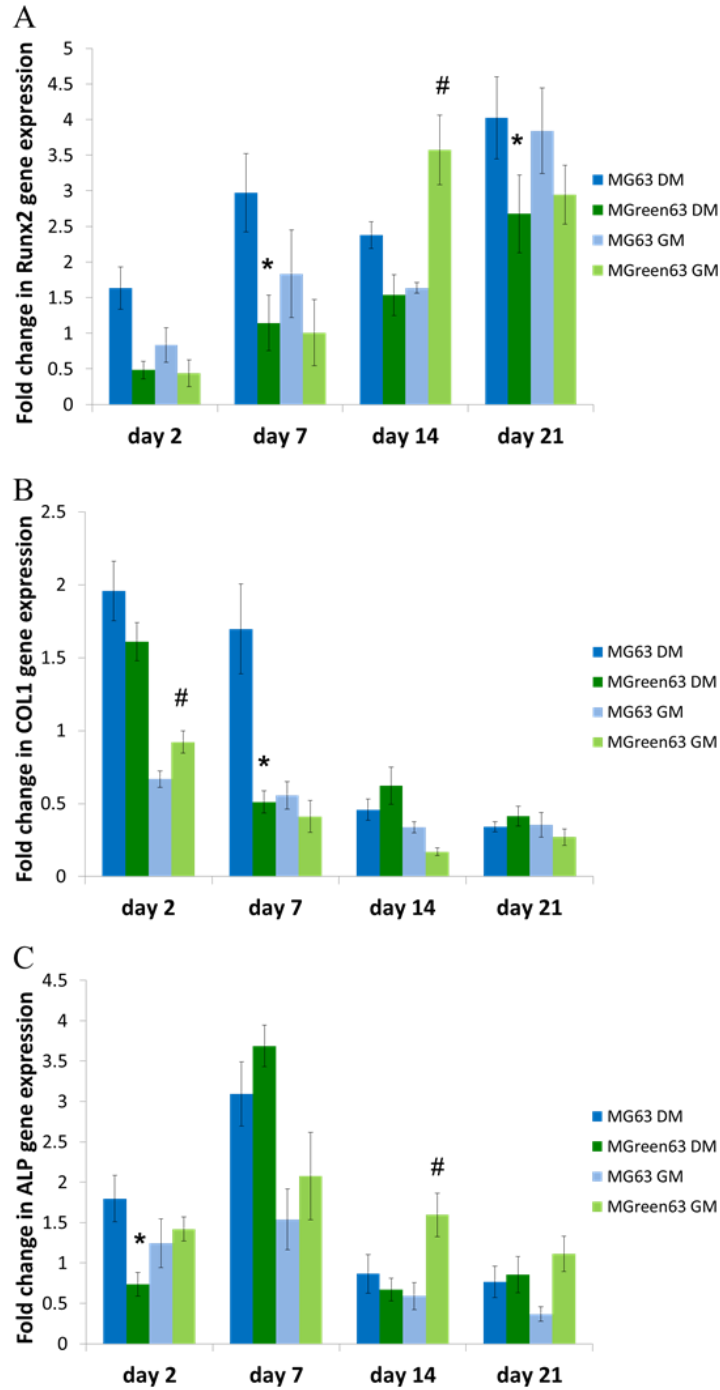


Figure 4.20A-C. Comparative real-time PCR results of Runx2 (A), type I collagen (COL1; B) and ALP (C) was performed at day 2, 7, 14 and 21 of culture period of MG63 and MGreen63 cell lines cultured in osteogenic (DM) or growth medium (GM). Diagrams show the mean fold change in relative gene expression with the standard error of the mean (3 experiments, n=9). Gene expression levels were normalised to RPL13a and were made relative to expression levels in MG63 cells at day 0 of culture. Data normally distributed: two-way ANOVA with Least Significant Difference adjustment for multiple comparisons. Statistical significance was determined as $p < 0.05$. *: MGreen63 DM compared to MG63 DM; #: MGreen63 GM compared to MG63 GM.

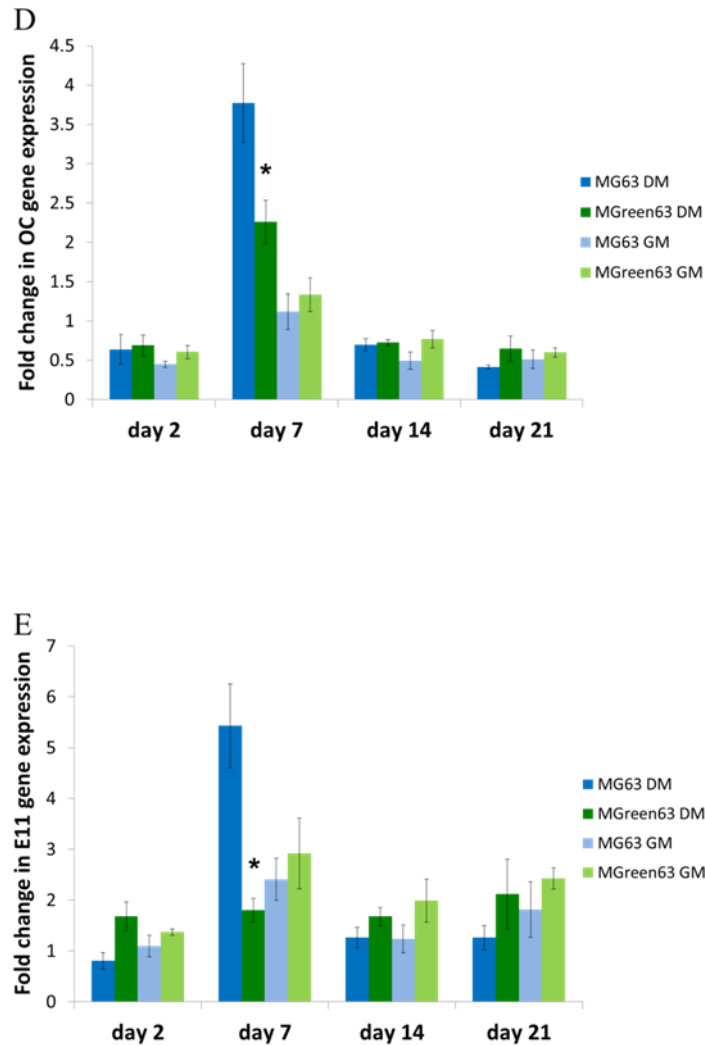


Figure 4.20D-E. Comparative real-time PCR results of osteocalcin (OC; D) and E11 (E) was performed at day 2, 7, 14 and 21 of culture period of MG63 and MGreen63 cell lines cultured in osteogenic (DM) or growth medium (GM). Diagrams show the mean fold change in relative gene expression with the standard error of the mean (3 experiments, n=9). Gene expression levels were normalised to RPL13a and were made relative to expression levels in MG63 cells at day 0 of culture. Data normally distributed: two-way ANOVA with Least Significant Difference adjustment for multiple comparisons. Statistical significance was determined as $p < 0.05$. *: MGreen63 DM compared to MG63 DM; #: MGreen63 GM compared to MG63 GM.

4.3. Discussion

Within this chapter the effects of co-culture of osteoblast lineage cells have been investigated. In particular, indirect co-culture models have been used to evaluate the importance of the mode of cell-cell communication on cell differentiation towards the osteoblast phenotype. This was to determine the effect of two-way communication on the osteoblastic phenotype development within monolayer or micromass co-culture systems.

MSCs co-cultured with MG63 cells in monolayer showed similar ALP enzyme activity in DM at day 14 compared to control cultures. In GM cultures there was a trend of higher ALP activity in cells from co-cultures with MG63, but only in MSCs located on the porous membrane. On day 21 the ALP gene expression was lower in MSCs co-cultured with MG63 cells. Similar trends were reported for Runx2, an early osteogenic marker and master transcriptional factors regulating osteogenic differentiation (Eames et al., 2004). Runx2 is up-regulated during the mesenchymal condensation, which leads to the formation of pre-osteoblasts (Ducy et al., 1997). Osteocalcin is a small calcium-binding protein found predominantly in the ECM of bone and is considered as a late marker for osteogenic differentiation (Poser and Price, 1979; Hauschka et al., 1989). Similarly to ALP and Runx2 mRNA results, the OC gene expression was slightly lower in MSCs from the co-culture group compared to controls. Considering the location of MSCs in co-culture, a trend of lower Runx2, ALP and OC mRNA was reported in cells cultured on the membrane of the insert. The opposite trend was reported for COL1 gene expression in MSCs co-cultured or cultured alone in DM medium, whereas in GM groups it was higher only for the control group with MSCs located in the well. Interestingly, the co-culture of MSCs with MG63 in DM had no effect on COL1 gene expression. For MSC groups cultured in DM or GM on a porous membrane, the ^{45}Ca incorporation was significantly higher than for cells from bottom groups. Moreover, the ^{45}Ca uptake was at a lower level in co-cultured cells compared to their controls in the monolayer co-culture system. Type I collagen is the main protein of the ECM within the bone which synthesis and presence is essential for the deposition of inorganic matrix, with Ca^{2+} being one of the constituent (Lynch

et al., 1995). The lower expression of Runx2, ALP and OC genes in MSCs co-cultured with MG63 is in agreement with the ^{45}Ca uptake results. Altogether, these results suggest a delayed osteogenic differentiation process compared to MSCs cultured alone.

As mentioned above, the location of cells in the co-culture (inserts or wells) had an influence on cell performance. Two factors need to be mentioned here which could be related to the results, such as oxygen diffusion, availability of growth factors and substrate/surface topography. Even though in the MSC-MG63 monolayer co-culture experiments the permeable PET membranes ($0.4\mu\text{m}$ inserts with the pore density ($2\pm 0.2 \times 10^6/\text{cm}^2$)), the penetration and availability of oxygen and growth factors could differ between two compartments of the co-culture system. Single cell type culture of MSCs or MG63 cells in wells concurrent with single cell type cultures on PET located on the bottom of the well would be essential to explore if the differences in cell performance are associated with gas and nutrients diffusion through the membrane. As indicated above, another factor, the topography of the membrane, could be related to the differences in the results from the same type of cells located on the membrane and in the well. The porous PET membrane used within this study with the pore size $0.4\mu\text{m}$ is in the range of spectrum of roughness between $0.2\text{--}2\mu\text{m}$. It has been suggested that this range is sensed by cells as 'rough' which result in reduced cell spreading and induces the expression and function of osteoblastic genes through the conformational changes in focal adhesions (Richards, 2008). Mechanotransduction arising from the nanotopography is the principal mechanism involved in the regulation of the morphological and functional changes in cells. Direct mechanotransduction utilizes changes in focal adhesions and cytoskeletal conformation to pass information about the ECM (or substrate) topography to the nucleus as mechanical signals (Dalby et al., 2005). The information of the nanotopography sensed by cells is transmitted to the nucleus by the tension of the lamina network (Dahl et al., 2004). Compared to smooth topography within the 'rough' surface range, cells showed reduced spreading, a dense lamina network and relaxation of nucleus size and changes in chromosome positioning influencing regulation of genes (Dahl et al., 2004; Dalby et al., 2007).

At day 14, MG63 co-cultured with MSCs in a monolayer in DM showed a trend of higher ALP protein activity compared to MG63 cultured alone. In GM conditions, the enzyme activity was at the same level between groups. For ALP results in DM, the statistical power was not reached. In fact, MG63 present in the early stage of osteoblastic phenotype. As presented in chapter 3 and by others, the ALP enzyme activity is hardly detectable in MG63 cells (Pierschbacher et al., 1988;Czekanska et al., 2013;Saldana et al., 2011). It appears that co-culture with MSCs did not influence this feature of MG63. Interestingly, gene expression results showed higher expression of Runx2, ALP, COL1 and OC in the co-cultured MG63 groups located on the insert membrane and maintained in DM compared to the other MG63 groups. For MG63 cells located in the well there was no influence of co-culture on Runx2, ALP, COL1 and OC gene expression. Similarly, a trend for the ^{45}Ca uptake as for MSC groups was reported for MG63 cells. At day 21, higher ^{45}Ca incorporation was found in MG63 groups cultured on the membrane compared to the groups cultured at the bottom of the wells. For cells located in the well, the ^{45}Ca uptake was at the same level in MG63 with or without MSCs. In the monolayer system, the co-culture of MSCs with MG63 cells positively influenced the expression of osteogenic genes in MG63 cells, whereas it has an opposite effect on MSCs differentiation. In addition, the different response of both cell types associated with the location in the co-culture indicates that not only paracrine factors influence the cell activity.

Following the investigation in monolayer, we investigated if similar effects of co-culture on osteogenic differentiation occur in a micromass system. Similarly as in the monolayer system, at day 21, the expression of Runx2, ALP and COL1 in MSCs co-cultured with MG63 was lower than in MSCs cultured alone. Although, the co-culture had no effect on OC gene expression in DM, the OC/Runx2 ratio was significantly higher in MSCs co-cultured with MG63. In GM medium, both OC mRNA and OC/Runx2 ratio were significantly higher in co-cultured MSCs compared to MSCs cultured alone. This result indicates the positive effect of the co-culture of MSCs with MG63 on osteogenic differentiation of MSCs in the absence of osteogenic supplements. The mRNA results from day 21 with lower Runx2, COL1, ALP and at the same time higher OC/Runx2 ratio in MSCs from co-culture could suggest a more differentiated stage of cells compared to MSCs from single cell

type culture. The micromass co-culture with MSCs had no significant influence on Runx2, ALP, COL1 and OC gene expression in MG63 DM or GM groups compared to their respective controls. In DM conditions, there was a trend of decreased COL1 mRNA and increased ALP mRNA expression in the co-cultured MG63 compared to MG63 alone.

Since the micromass co-cultures were located side-by-side in the wells of the 24-well plate, the ALP activity and ^{45}Ca uptake analysis was performed without the separation of the two cell types of the culture. There were significant differences in ALP activity in the co-cultures and single cell type cultures at day 14 in DM and GM. For co-cultures, enzyme activity was significantly lower than MSCs and higher compared to MG63 cultures. If there was no effect of the co-culture on ALP activity, then the value of the enzyme level for the co-culture would be approximately an average of the results from the single cell type cultures. Here, ALP activity in the co-cultures was much below the expected average of the single cell type cultures suggesting the lower ALP activity of MSCs in the co-cultures than in the single cell type cultures. One possible reason for this is that ALP activity in MSCs peaks earlier in the co-culture than when cells are cultured alone. This is in agreement with gene expression results and supports the hypothesis of stimulated osteogenesis of MSCs in co-cultures. Analysing the ALP activity at earlier time points than day 14 would help to evaluate the validity of this hypothesis.

The ^{45}Ca incorporation data showed significant differences between the co-cultures and single cell type cultures in DM at day 21, whereas it was at the same level in all GM groups. MG63 cells showed little ^{45}Ca uptake compared to co-cultures. The predominant cells in the co-culture responsible for the ^{45}Ca incorporation seem to be MSCs. These cells in the micromass from single cell type cultures incorporated approximately 2-fold more ^{45}Ca than cells in the co-culture group. Even though, there were significant differences between groups, the micromass co-culture of MSCs and MG63 in DM have no effect on ^{45}Ca incorporation at day 21.

Interestingly, for the MSC alone cultures the ALP activity was at similar level in the monolayer and micromass cultures GM groups, whereas it was higher in the micromass than in the monolayer culture in DM medium. For MG63 cells, the cell culture system had no influence on ALP activity, which again supports the previous observations (Saldana et al., 2011;Czekanska et al., 2013) .

For both MG63 and MSC single cell type cultures, the ^{45}Ca incorporation was higher in the monolayer cell culture system. It has to be taken into account that in micromass, where cells are in close cell to cell contact and ECM is dense, the reagent diffusion towards the centre of the micromass is difficult. Moreover, in a dense 3D system, like pellets or micromass, the uptake is limited to the population of cells located on the surface; hence limiting the availability of the reagent for the cells located more in the centre. To overcome this problem, we performed a preliminary experiment to clarify whether 4-hour pre-incubation of cells with medium containing $^{45}\text{CaCl}_2$ at 4°C will have an influence on the final the ^{45}Ca uptake results. This strategy would slow down the metabolic activity of cells on the surface and increase the penetration of the reagent within the micromass. No significant differences were reported between the cultures pre-incubated at 4°C compared to the cultures without pre-incubation (data not shown). Still, we believe that the obtained results are reliable for the comparison of the micromass cultures.

Even though, the MG63 cell line presented fewer similarities with HOb cells than SaOs2 and MC3T3-E1 regarding the development of the osteoblastic phenotype (chapter 3), this cell line was selected for establishing stable and homogeneous cell line expressing GFP. In addition, many studies exploring cell-material interactions utilise various cell types, including MG63, SaOs2 cell lines and primary animal osteoblast cells (Zinger et al., 2005;Bitar et al., 2008;Oh et al., 2006;Hansen et al., 2007). By generating a MG63 cell line expressing GFP, we aimed to establish a cell line which would serve as a cell model for studies aiming to assess the importance of direct cell-cell communication and for the live assessment of cytotoxicity and cytocompatibility of biomaterials. From both a biological and tissue engineering point of view, it is important to track and understand the integrin-mediated cell-surface interactions. It has been shown that MG63 cells express similar integrin

subunits profile, including α_2 , α_5 , α_v , β_1 , β_3 , to HOb cells (Sinha and Tuan, 1996; Clover et al., 1992). An early osteoblastic phenotype, similar morphology and integrin subunits profile to HOb cells, makes MG63 cells an attractive candidate for initial assessment and cytocompatibility of biomaterials. The transduction of MG63 cells with GFP retroviral vector and subsequent selection of cells resulted in generation of cell line with stable expression of GFP. The further approach of proliferating colonies from single cell cultures resulted in selection of highly homogeneous populations of cells. One of these colonies, MGreen63, which was investigated in more details, presented similar characteristics as MG63 cells, including proliferation rate and osteoblastic phenotype development.

Taken together these results suggest there is an active signalling pathway between MSCs and osteoblasts. The direct co-culture of MSCs with newly generated osteoblast cell line expressing GFP, MGreen63, would provide more detailed information regarding the cell-cell communication.

CHAPTER 5

ENHANCING INFLAMMATORY AND CHEMOTACTIC SIGNALS TO REGULATE BONE REGENERATION

Sections of this chapter have been submitted as:

Czekanska E.M., J. R. Ralphs, M. Alini, M. J. Stoddart: Enhancing therapeutical potential of mesenchymal stem cells (MSC) to *European Cells and Materials*

5.1. Introduction

Various strategies have been developed and applied to aid the regeneration process of injured tissue. These include separate or combined implantation of specific cell types, biomaterials and factors. Cell therapy alone, or in combination with supportive biomaterials and factors, is of particular interest for clinical application to treat a wide array of acute or chronic conditions due to the inherent potential of stem cells to differentiate into various cell types (Pittenger et al., 1999). Currently, more than 9600 ongoing cell therapy clinical trials have been registered worldwide (www.clinicaltrials.gov). Specifically, much attention and hope is put in single surgical procedure cell therapies. This strategy integrates the autologous cell harvesting, processing and re-implantation into injured site. Intraoperative autologous stem cell therapy brings advantages regarding the usage of patient's own cells which allows avoiding of the activation of an immune response, extensive *in vitro* cell expansion and manipulation, requirements for Good Manufacture Practice facilities, secondary procedure and potential contamination (Coelho et al., 2012).

In addition to their direct contribution to tissue regeneration as a consequence of differentiation into a specific phenotype, implanted cells aid regeneration by producing various bioactive molecules, including growth factors, cytokines and extracellular matrix molecules (Hsiao et al., 2012; Tsiridis et al., 2007; Zhukareva et al., 2010). These secreted factors act in an auto- and paracrine manner regulating the cell phenotype. The importance of paracrine actions in the host tissue have been studied extensively in repair and regeneration of the central nervous system (Drago et al., 2013), heart (Gnecchi et al., 2006; Hwang et al., 2012) and skin (Schlosser et al., 2012). The indirect action of progenitor cells implanted within a bone healing environment is less understood; nevertheless, the importance of various factors secreted by cells present in fracture milieu is known to have great importance on bone regeneration.

Conventionally, fracture healing is divided into consecutive but overlapping stages, namely inflammation, soft callus formation, hard callus formation and remodelling.

During inflammation many factors are released by various cells present at the injury site. These factors have their role in attracting cells, promoting differentiation of MSCs, initiating angiogenesis and enhancing ECM synthesis. The importance of inflammation occurring after bone fracture has been demonstrated directly by the increased levels of various factors at the molecular and protein level, as well as indirectly by removing the fracture hematoma (Kolar et al., 2011). Combating inflammation and, as a consequence, the wide spectrum of factors secreted by the immune and progenitor cells present at the fracture site has also been shown to have a role (Simon et al., 2002). The local increased levels of mRNA expression of interleukin 8 (IL8), vascular endothelial growth factor (VEGF) together with interleukin 6 (IL6), CXC chemokine receptor type 4 (CXCR4) and secreted phosphoprotein 1 (SPP1) in fracture hematomas indicate their importance for chemotaxis, angiogenesis and osteogenesis (Kolar et al., 2011). The removal of the hematoma, together with the cells contained within, or combating the inflammation with non-steroid anti-inflammatory drugs prolonged the time of fracture healing compared to fracture with hematoma (Kolar et al., 2011; Simon et al., 2002; Mountziaris et al., 2011) .

As shown in the subcutaneous *in vivo* mice models, implantation of a hydroxyapatite (HAP) scaffold with exogenous MSCs resulted in the recruitment of endothelial and osteoprogenitor cells, followed by ectopic bone formation by the host cells (Tasso et al., 2010). In addition, the fact that endothelial cells were identified in implants seeded with MSCs, but not osteoblast cells, indicates that MSCs secrete a more broad range of factors than osteoblast cells (Tortelli et al., 2010). Hence, in a fracture repair setting, MSCs in addition to having a direct role in differentiating into osteoblast lineage cells and forming new bone, also promote new bone formation by indirect cell-cell communication due to a localized release of factors attracting host cells and enhancing their differentiation potential.

To increase the production of specific factors by cells various strategies can be applied including genetic engineering and preconditioning of cells. Since the secretion of trophic factors is modulated *in vivo* by chemotactic and inflammatory factors, the use of these factors could provide a strategy to enhance the

paracrine actions of cells. Driven by this hypothesis, for this study, we selected four factors which are the players in the early stages of bone healing cascade, namely Stem Cell Factor (SCF), interleukin 1 β (IL1 β), stromal cell-derived factor 1 (SDF1) and granulocyte colony-stimulating factor (GCSF). Based on the literature reports, the *in vitro* and *in vivo* research on cell behaviour are currently limited to the direct effects when treating cells with GCSF, SDF1, SCF or IL1 β (McNiece and Briddell, 1995;Pan et al., 2013;Zhou et al., 2007;Kitaori et al., 2009;Hara et al., 2011;Tang et al., 2009;Konig et al., 1988;Boyce et al., 1989;Lee et al., 2010). In addition, from these 4 factors only IL1 β has been given significant attention, whereas the effects and applicability of other factors are overlooked in relation to bone regeneration. To overcome this impediment, we chose these factors, having differential action on cells during tissue regeneration, for assessing their direct and indirect effects on cells. As mentioned above, understanding the mechanisms involved in indirect effects of preconditioning, i.e. due to the enhancement of secretion of trophic factors acting in paracrine manner, would be of great interest for cell-based regenerative therapies. Therefore, we sought to elucidate the cytokine profile of MSCs after stimulation with these factors and the relevance of the secreted factors in supporting MSC proliferation and differentiation towards the osteoblastic lineage.

5.2. Results

5.2.1. Direct influence of MSCs stimulation with cytokines on MSCs

5.2.1.1. Effects of stimulation with cytokines on gene and protein expression profile of MSCs

Mesenchymal stem cells (MSC) for this study were isolated from the bone marrow aspirates of 9 different donors within an average age of 43 ± 21 years-old (age range: 18-65) from the iliac crest or vertebral body (Tab.5.1). Moreover, cells which underwent 6.082 ± 0.83 population doublings after thawing from cryopreservation were used. In the first part, cells were stimulated with 4 different factors (IL1 β , SCF, SDF1 and GCSF) for 2 hours in monolayer cell culture (Tab.5.1). After that time, cells were washed with PBS after which medium containing 10% FBS was added. The effect of the stimulation was assessed at the gene expression level 72 hours later. In the later part, experiments focused on assessing in more detail the effects of short term stimulation with IL1 β and SCF (Tab.5.1.). The experimental design was modified in order to investigate not only the effects of stimulation on gene expression, but also the protein expression. Therefore, after stimulation, cells were maintained in serum free DMEM low glucose with 1% Penicillin-Streptomycin for 48 hours. Stimulation was always performed in medium containing 10% FBS and 1% Penicillin-Streptomycin.

Donor #	Gender	Age	Isolation site	Stimulation				Analysis
				IL1 β	SCF	SDF1	GCSF	
1	female	65	n.k.	x			x	Cytokine gene expression profile
2	male	41	iliac crest		x	x	x	
3	female	64	n.k.	x	x	x	x	
4	female	40	iliac crest	x	x	x	x	
5	female	18	vertebra	x	x			Cytokine gene and protein expression profile
6	female	20	n.k.	x				
7	female	40	iliac crest	x	x			
8	male	41	iliac crest	x				
9	female	55	iliac crest	x	x			

Table 5.1. Details about MSC donor isolation site and short-term stimulation experiment outline; *n.k.* – not known.

5.2.1.1.1. MSCs cytokine gene expression after culture in serum containing medium

Real-time PCR analysis of cytokine and growth factor expression levels in MSC stimulated with different factors revealed that the response to 2 hour stimulation is highly donor dependent. Yet, consistent effects at the mRNA level 72 hours after stimulation were observed. For stimulation with each factor, three different donors were included. Response to the treatment was assessed as positive if up- or down-regulation of a gene occurred in cells obtained from at least 2 donors when compared to untreated controls. Out of the four donors included in the experiment, donor 4 varied the most in response to SCF, SDF1 and GCSF treatment when compared with other donors (Fig.5.1B-D). Interestingly, donor 1 showed the highest response to GCSF and the lowest to IL1 β stimulation (Fig.5.1C&A) whereas cells from donor 3 showed the highest sensitivity to IL1 β in comparison to other donors (Fig.5.1A). Due to differential sensitivity of cells from different donors to the stimulation, results are presented for each individual donor.

Two hour stimulation of cells with 10ng/ml IL1 β resulted in the up-regulation of a wide range of cytokine genes. The highest up-regulation was detected for BMP2, IL8, TNFSF11 and IL6 in cells from all three donors. BMP6 and NODAL were up-

regulated in 2 out of 3 donors. In addition, 2 cytokines, GDF5 and IL17B were down-regulated in response to the treatment in all three donors (Fig.5.1A).

GCSF stimulation resulted in a pronounced up-regulation of mRNA expression of 5 cytokines (BMP2, GDF9, IL8, IL10, NODAL) and down-regulation of one cytokine (INFA1). Cells from all three donors consistently down-regulated INFA1 gene expression compared to unstimulated cells (Fig.5.1B).

As seen with GCSF stimulation, cells from donor 4 stimulated with SCF showed the lowest level of response. MSC stimulation with 100ng/ml SCF resulted in high up-regulation of IL1A and NODAL in all donors. In addition, two of the donors (1&2) positively responded to stimulation by increasing the expression of GDF9 and TNFSF11 compared to unstimulated cells. Interestingly, donor 4, which showed the lowest up-regulation in IL1A and NODAL expression out of all donors, showed an opposite response regarding GDF9 and TNFSF11 in comparison to the 2 other donors (Fig.5.1C).

A high up-regulation of NODAL gene expression was detected in response to SDF1 treatment in all three donors. Additionally, stimulation had positive effects on two other cytokines, BMP8B and IL10, whereas IL1 β was strongly down-regulated in 2 out of 3 donors (Fig.5.1D). The positive response to SDF1 stimulation in IL1 β regulation was reported in cells from donor 3. As previously described, cells from donor 3 were also highly responsive to 10ng/ml IL1 β stimulation.

Out of the effects reported for the 4 factors investigated, IL1 β resulted in the regulation of cytokine genes influencing the broadest range of biological processes. Cytokines, which responded to the IL1 β treatment, take part in bone formation (BMP2, BMP6), angiogenesis (IL6, IL8), osteoclastogenesis (TNFSF11), development (NODAL), chondrogenesis (GDF5) and immunomodulation (IL17B). Specifically, only IL1 β regulated the expression of BMP6, IL6, TNFSF11 and GDF5 (Fig.5.1A). SCF stimulation showed no effect on the gene expression of cytokines implicated in angiogenesis or bone formation, but still it up-regulated genes involved in chondrogenesis (GDF9) immunomodulation (IL1A) and development (NODAL)

(Fig.5.1B). Short-term stimulation of MSCs with GCSF resulted in a positive response on the mRNA level of cytokines involved in bone formation (BMP2), chondrogenesis (GDF9), angiogenesis (IL8, IL10) and development (NODAL) while decreasing the expression of IFNA1, which is involved in immunological responses (Fig.5.1C). SDF1 stimulation of MSCs uniquely regulated gene expression of one bone formation factor (BMP8b) (Fig.5.1D). In addition, it stimulated the expression of an angiogenic factor (IL10) and down-regulated expression of IL1 β cytokine which effects multiple actions on cells (a wide spectrum of actions). Similarly, as with stimulation with other factors, a cytokine involved in developmental processes, NODAL, was up-regulated in response to SDF-1 stimulation (Fig.5.1D).

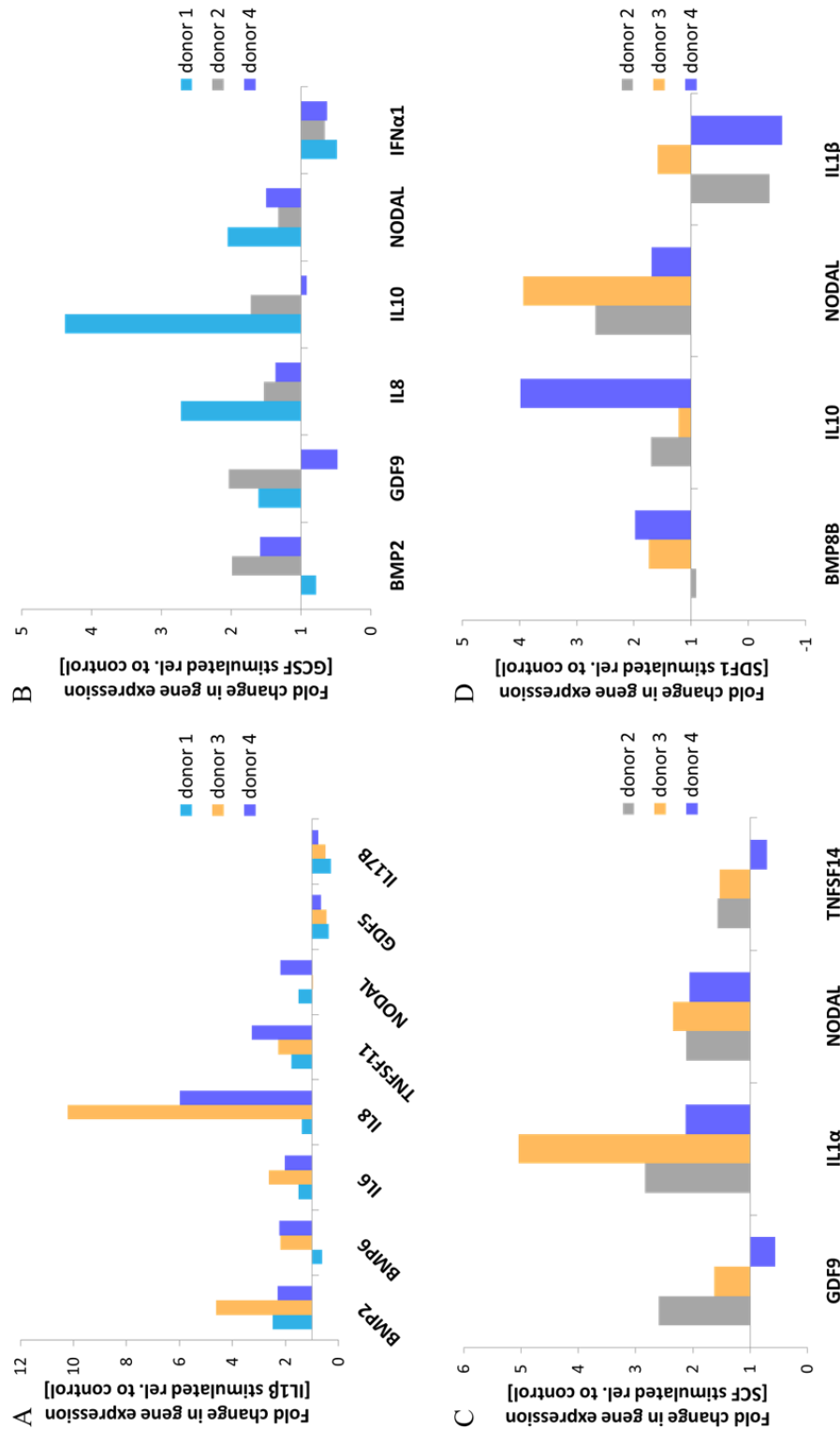


Figure 5.1. Diagrams show the mRNA levels of cytokines in MSC cells stimulated by IL1β (A), SCF (B), GCSF (C) and SDF1 (D). Cells in monolayer were stimulated with specific factor for 2 hours. Cells without any stimulation were included as controls for assessing regulatory effects of stimulation. Gene expression level in stimulated cells was made relative to control samples.

5.2.1.1.2. MSCs cytokine gene expression after culture in serum-free medium

The effect of IL1 β or SCF stimulation on mRNA levels was analysed in MSCs (n=5 donors) 48 hours after exposure. In the time between stimulating the cells with either IL1 β or SCF and mRNA sample collection, cells were maintained in DMEM medium supplemented only with 1% penicillin-streptomycin. No serum was included in the medium in order to eliminate any potential synergic or antagonistic effects of selected factors with any protein present in the serum. Forty-eight hours after the stimulation with IL1 β , mRNA expression of 20 cytokine genes were similarly regulated in at least of 3 out of 5 donors (Fig.5.2). In addition, 3 out of 5 donors (5, 6 and 7) showed the most similar trend in the response to the treatment with IL1 β . Cells isolated from donor 8 responded to the IL1 β stimulation by increasing the greatest number of genes compared to other donors, whereas cells from donor 9 showed the opposite trend. In general, cells from donor 5 showed the highest fold change in cytokine mRNA expression relative to unstimulated cells in comparison to MSCs from other donors.

Stimulation of MSCs with IL1 β resulted in an up-regulation of TNFRSF11B and IL1 β and a down-regulation of GDF5 gene expression in all 5 donors (Fig.5.2). An increased mRNA expression in stimulated cells was detected for: BMP6, CD70, IL1a, IL6, IL8 and IL12A in 4 out of 5 donors. On the other hand, various BMP-family members (BMP3, 4, 5 and 7), TGF β 3, GDF8, LTA and IL5 were down-regulated in 4 donors. A positive response in GDF9 and GMCSF gene regulation was detected in cells from 3 donors. Similarly, 3 from 5 donors down-regulated BMP2 gene expression after 2 hours stimulation with IL1 β (Fig.5.2).

MSCs from 3 donors were treated for 2 hours with SCF. As a result, 12 cytokine genes showed response to the stimulation in at least 2 donors (Fig.5.3). Eight of these genes were up-regulated in cells from all 3 donors. More specifically, the mRNA level in stimulated cells relative to unstimulated cells was higher for BMP4, TNFRSF11B, TNFSF14, TGF β 2, INHBA, NODAL, IL1A and IL18. Due to an opposite response in regulation of TNFSF4, IL1 β , IL17b and IL21 in cells from

donor 5 or 9 (compared to other donors), these genes were up-regulated in 2 out of 3 donors (Fig.5.3).

It has to be highlighted that overall the magnitude of the response was lower compared to the effect of IL1 β on cytokine gene regulation. Approximately a 2-fold increase in gene regulation, relative to unstimulated controls, was detected after SCF stimulation. As an exception, cells from donor 7 were the most sensitive to SCF stimulation, which was marked by the highest increase of TNFSF14, IL1a, IL1 β , IL18, IL21 and TNFSF4 mRNA level among all 3 donors (Fig.5.3).

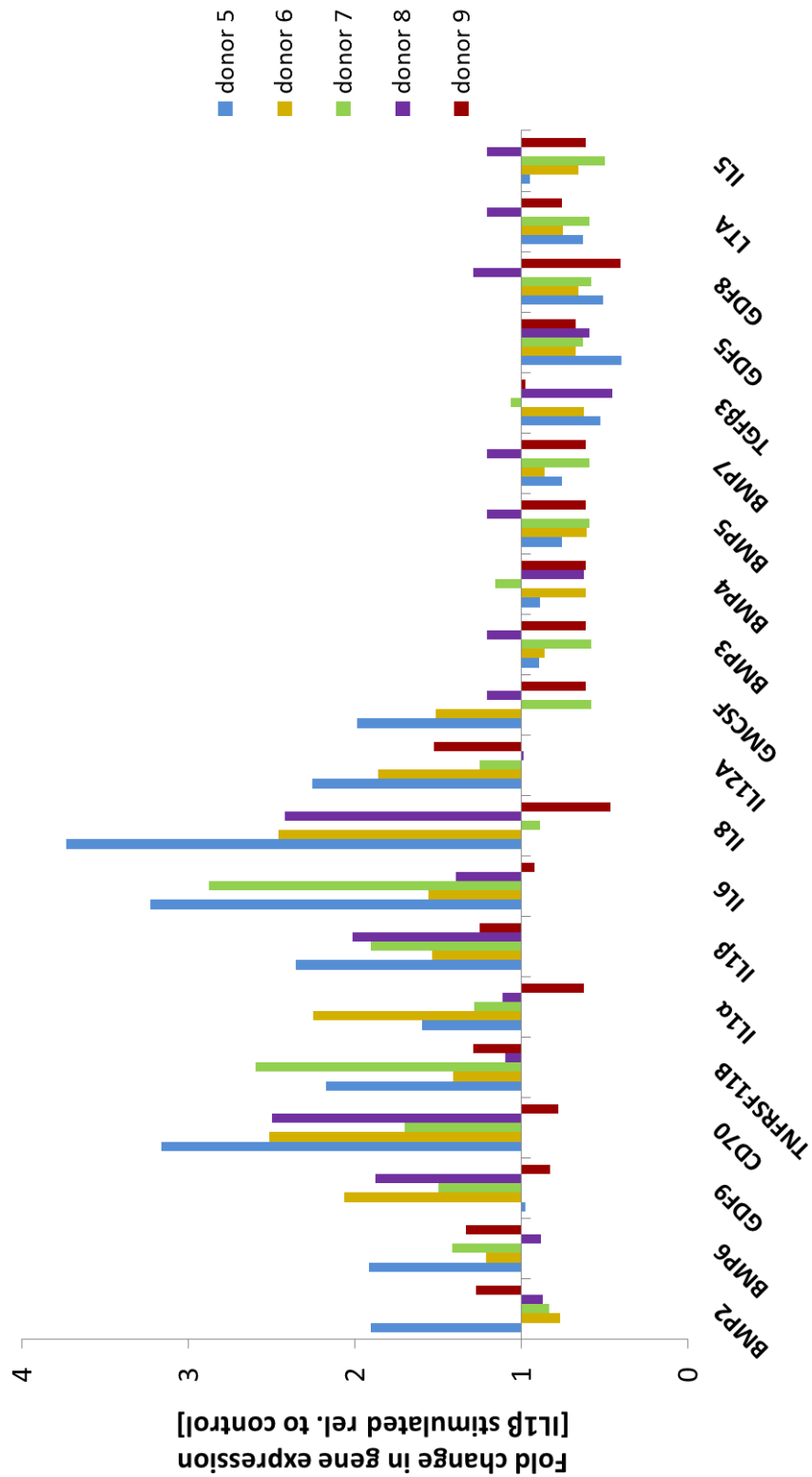


Figure 5.2. Gene expression levels of cytokines in MSC cells stimulated with IL1 β . Cells in monolayer were stimulated with 10ng/ml IL1 β for 2 hours. Cells without any stimulation were included as controls for assessing regulatory effects of stimulation. The gene expression level from stimulated cells was made relative to control samples.

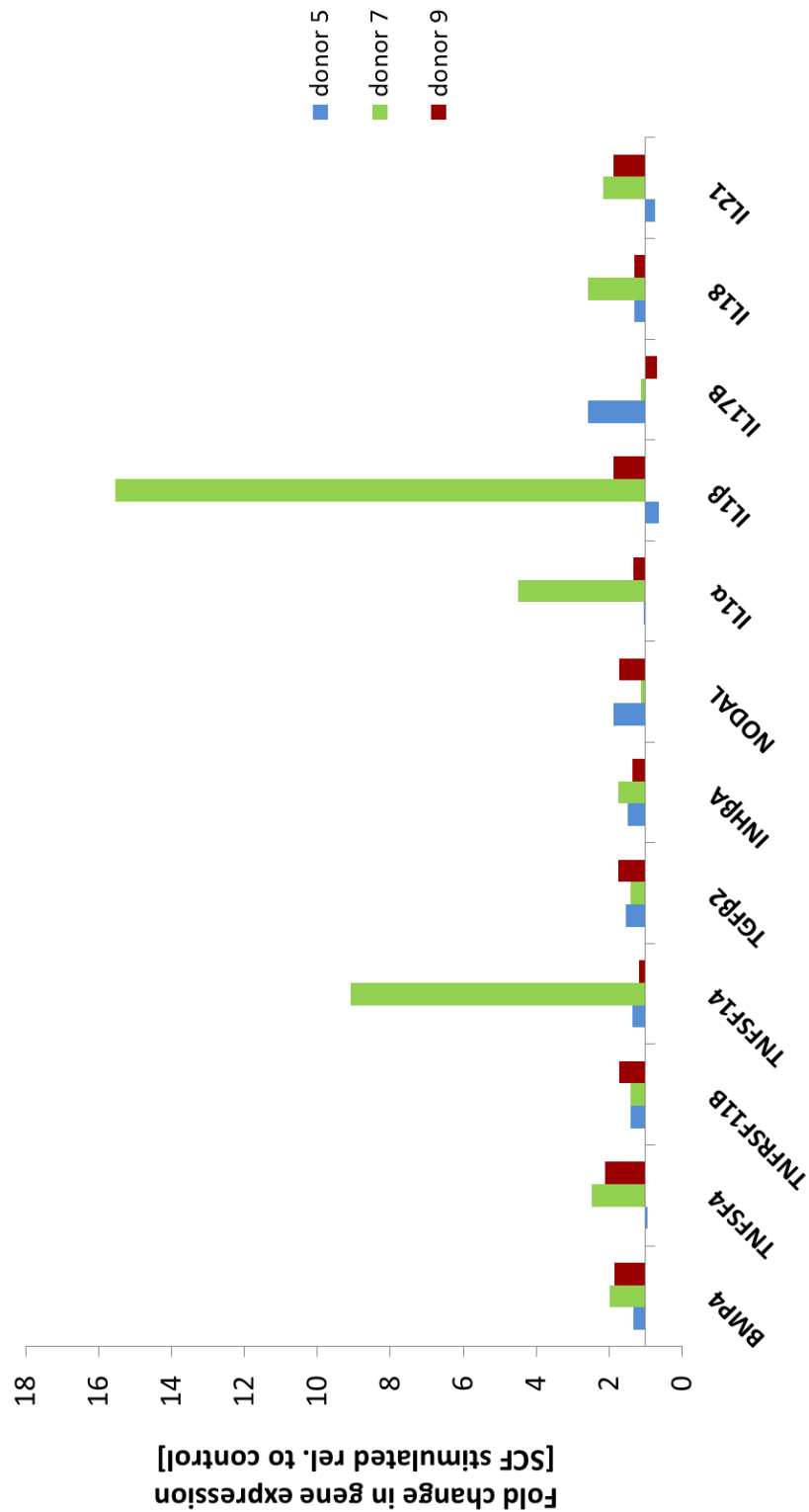


Figure 5.3. Gene expression levels of cytokines in MSC cells stimulated with SCF. Cells in monolayer were stimulated with 100ng/ml SCF for 2 hours. Cells without any stimulation were included as controls for assessing regulatory effects of stimulation. The gene expression level from stimulated cells was made relative to control samples.

5.2.1.1.3. Regulation of osteogenic and Wnt signalling genes in stimulated MSCs

In addition to array analysis of a wide array of cytokine genes regulated in response to the stimulation with IL1 β and SCF, gene expression was assessed with real-time PCR using the TaqMan real-time PCR method. In this analysis the expression of IL6, IL8, BMP2, RANKL was included to confirm the results obtained from RT² PCR array analysis. Additionally, the direct influence of IL1 β and SCF stimulation on components of the canonical and non-canonical Wnt signalling pathways and osteogenic markers was assessed at the gene expression level. Similarly to results from the cytokine gene expression arrays, the gene regulation in response to the stimulation was donor dependent. From 5 number of donors, cells from donor 9 showed the opposite response to IL1 β treatment than cells from other donors included in the analysis (Fig.5.4A&C). Cells from donors 5-8 showed a similar trend in the response to IL1 β . Hence, donor 9, as an outlier, was excluded from the statistical analysis. For stimulation with SCF, cells from all donors were included for the analysis of any significant differences in response to the stimulation.

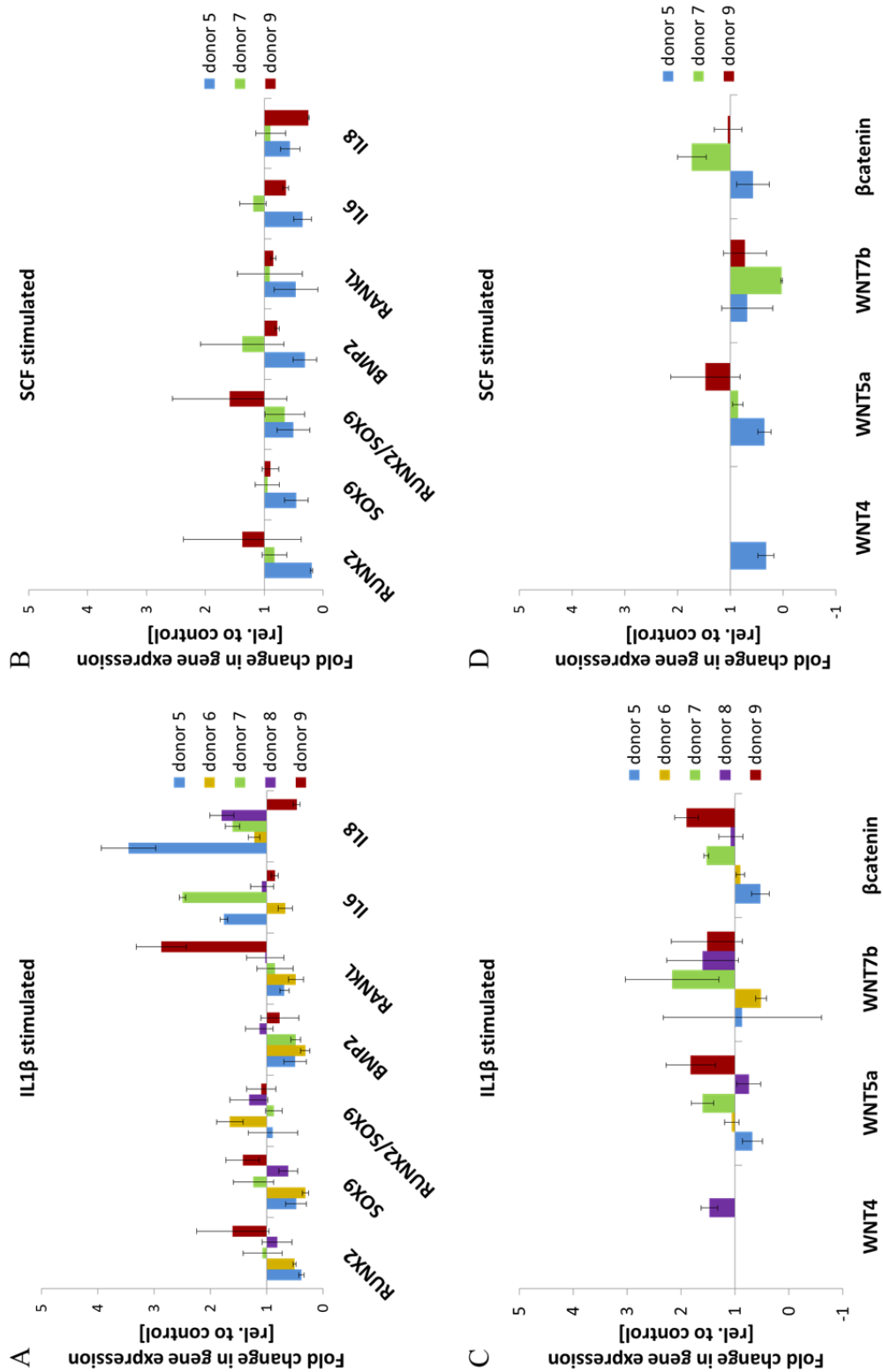


Figure 5.4. Diagrams show the fold change gene expression in relative to control from each donor with the standard deviation, quantified by real-time PCR 48 hours after the stimulation of MSC with IL1 β or SCF for 2 hours. A& C: Cells stimulated with IL1 β ; B&D: Cells stimulated with SCF. Cells from 5 and 3 donors were stimulated with IL1 β or SCF, respectively.

IL1 β stimulation significantly down-regulated mRNA expression of bone markers, including Runx2 (p=0.02), Sox9 (p=0.02), BMP2 (p=0.01) and RANKL (p=0.01) (Fig.5.5A). Even though there were significant changes in Runx2 and Sox9 gene expression, IL1 β stimulation had no effect on the overall Runx2/Sox9 ratio compared to unstimulated cells (p=0.468). Treatment with IL1 β increased the expression of IL6 and IL8. Yet, this increase was significant only for IL8 (p<0.001). Stimulation with SCF showed a negative effect on the regulation of Runx2, Sox9, BMP2, RANKL, IL6 and IL8 genes (Fig.5.4B&5.5A). However, this decreased expression compared to the untreated cells only reached significance for Sox9 (p=0.05), RANKL (p=0.004) and IL8 (p=0.004) (Fig.5.5A).

It was only possible to detect Wnt4 expression in cells from donor 8 and in donor 5 after the stimulation with IL1 β and SCF (Fig.5.4C&D). Moreover, mRNA expression of Wnt3 was not detected in any donor. Although, there were no significant differences in gene expression of Wnt5a (p=0.748), Wnt7b (p=0.3) or β catenin (p=0.748) between stimulated with IL1 β and unstimulated cells, there was a trend of higher expression of Wnt7b compared to control (Fig.5.5B). Stimulation of MSCs with SCF had no influence on the mRNA expression of Wnt5a (p=0.256) or β catenin (p=0.73), whereas it significantly decreased Wnt7b expression (p=0.008) compared to control (Fig.5.5B).

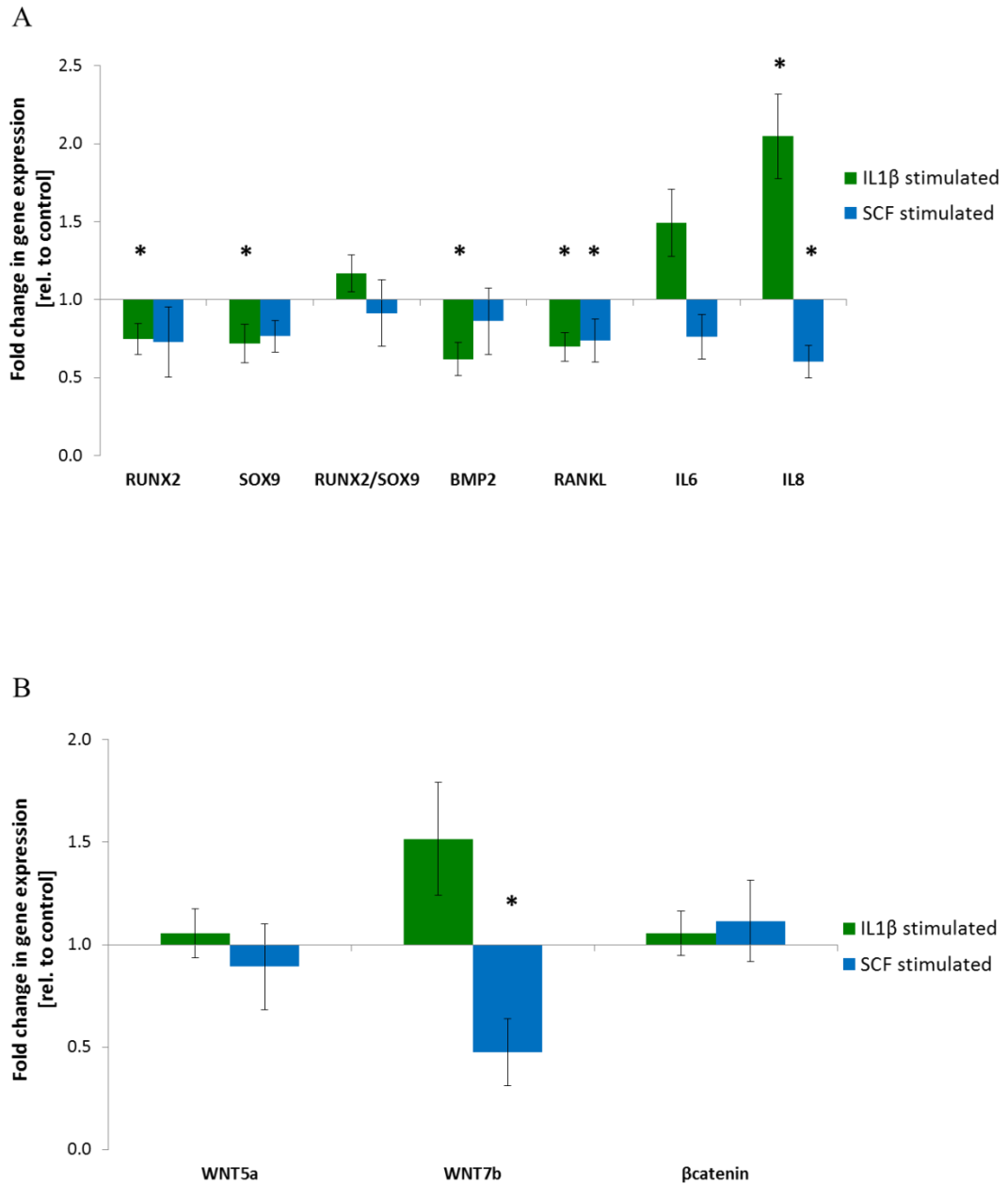


Figure 5.5. Diagrams show the mean fold change gene expression relative to control with the standard error of the mean, quantified by real-time PCR 48 hours after the stimulation of MSC with IL1 β or SCF for 2 hours. A: Expression of genes: Runx2, Sox9, Runx2/Sox9, BMP2, RANKL, IL6, IL8; B: Expression of Wnt5a, Wnt7b and β catenin. Gene expression was normalised to RPL13a and made relative to expression of genes in unstimulated cells. Statistical significance at $p < 0.05$ (*) of genes compared to unstimulated cells was determined with Mann-Whitney U test.

5.2.1.1.4. Influence of stimulation on cytokine protein secretion by MSCs in serum-free medium cell culture

Similarly to results from gene expression arrays, the regulation of 174 cytokine proteins in response to IL1 β or SCF stimulation was highly donor dependent. As a consequence, for each donor secretion of each protein was regulated to a different extent, which prevented presentation of the averaged results. Nevertheless, it was possible to analyse results in a similar manner to the gene expression results.

The initial analysis of the fluorescence intensity of the medium samples collected from unstimulated cells revealed that of 174 cytokine proteins assessed, 139 proteins were secreted by cells from donor 5, 152 from donor 6 and 9, 154 from donor 7 and 153 from donor 8 (Appendix 4). For both treatments, the expression of proteins in conditioned medium was made relative to protein secretion into medium by unstimulated (control) cells. In case of IL1 β stimulation, if cells from at least 3 out of 5 donors showed similar regulation of proteins, the effect of stimulation was assessed as positive (Fig.5.6). Similar conclusions were made for SCF stimulation, when cells from at least 2 out of 3 donors responded to stimulation in a similar fashion (Fig.5.7). All regulated cytokine proteins were grouped depending on their function (Tab.5.2.). This showed that 2 hour stimulation with IL1 β mostly influenced the secretion of proteins involved in chemotaxis, inflammation, angiogenesis and bone formation. On the other hand, stimulation with SCF affected mitogenic, ECM and differentiation markers.

Function	Cytokine
Chemotactic	GCP2, RANTES, MIP1 β , MIP3 α , IL2R α , ENA78, IL8, MDC, B7-1
Mitogenic	Amphiregulin, NAP2, IGFBP3, basic FGF, FGF4, sTNFRII
Proinflammatory	GRO, I309, GRO α , ICAM3
Immunoregulation	MIF, IL8, IL2R α , GITR, LIGHT
Bone formation	FGF4, Amphiregulin, Activin A, IL6, IGFBP3
Angiogenesis	GCP2, FGF9, IL6, IL8, RANTES, ENA78 (indirectly)
Chondrogenesis	BMP6
ECM regulation	TIMP1, TIMP4

Table 5.2. Functional grouping of cytokines regulated by 2 hour stimulation of bone marrow derived MSC cells with 10ng/ml IL1 β or 100ng/ml SCF. Colours indicate response to the stimulation: dark green - up-regulation after stimulation with 10ng/ml IL1 β , light green – down-regulation after 10ng/ml IL1 β stimulation, dark blue – up-regulation after stimulation with 100ng/ml SCF, light blue – down-regulation, dark brown – up-regulation by 10ng/ml IL1 β and 100ng/ml SCF, light brown - down-regulation by 10ng/ml IL1 β and 100ng/ml SCF. B7-1=CD80 - cluster of differentiation 80; basic FGF - basic fibroblast growth factor; BMP4 – bone morphogenic protein 4; BMP6 - bone morphogenic protein 6; ENA78/CXCL5 - epithelial-derived neutrophil-activating peptide 78; FGF4 – fibroblast growth factor 4; GCP2 - granulocyte chemotactic protein; GITR/TNFRSF18 - glucocorticoid induced tumour necrosis factor receptor family related gene; GRO - growth-related oncogene; GRO α - growth-related oncogene alpha; I309=CCL1 - chemokine (C-C motif) ligand 1; ICAM3/CD50 - intercellular adhesion molecule 3; IGFBP3 - insulin-like growth factor binding protein-3; IL2R α - interleukin 2 receptor alpha; IL1 β – interleukin 1 beta; IL6 – interleukin 6; IL8 – interleukin 8; LIGHT=TNFSF14 - tumour necrosis factor ligand superfamily member 14; MIF - Macrophage migration inhibitory factor; MIP1 β /CCL4 - Macrophage inflammatory protein-1 beta; MIP3 α - Macrophage inflammatory protein-3alpha; NAP2 - neutrophil-activating protein-2; RANTES/CCL5 - regulated on activation, normal T cell expressed and secreted; SCF – stem cell factor; sTNFRII - soluble tumour necrosis factor receptor type II; TIMP1 - tissue inhibitor of metalloproteinase-1; TIMP4 - tissue inhibitor of metalloproteinase-4.

Stimulation with IL1 β influenced protein synthesis and secretion in MSC cells. In detail, 18 out of 174 analysed proteins were up-regulated in the conditioned medium collected 48 hours from cells stimulated with IL1 β in comparison to conditioned medium from unstimulated cells (Fig.5.6). At the same time, a lower secretion of 2 proteins, namely B7-1 and MIF was observed in response to IL1 β stimulation. Out of the up-regulated 18 proteins, 9 of them, namely GCP2, GRO, ICAM3, IL8, MIP3 α , RANTES, I309, IL6, IL2R α and MCP3, were up-regulated in cells isolated from all 5 donors. This strongly indicates the regulatory role of IL1 β on these cytokines. An increased expression of a further 9 proteins, including Activin A, Amphiregulin, ENA78, FGF4, FGF9, GRO α and LIGHT, was detected 48 hours after IL1 β stimulation in at least 3 of 5 donors (Fig.5.6).

Among 174 proteins analysed from medium conditioned by MSCs stimulated with SCF, secretion of 15 of them were specifically regulated in response to the stimulation (Fig.5.7). In relation to results from controls, SCF stimulation showed a negative effect on B7-1, sTNFRII and TIMP4 protein secretion in cells from all 3 donors. On the other hand, all donors showed a positive response to SCF stimulation by increased secretion of Amphiregulin, NAP2, FGF4, GITR, IGFBP3, LIGHT, MDC, TIMP1. Basic FGF, BMP6, MIP1beta and TRAILR3 were up-regulated in 2 out of 3 donors, with Donor number 9 being the exception (Fig.5.7).

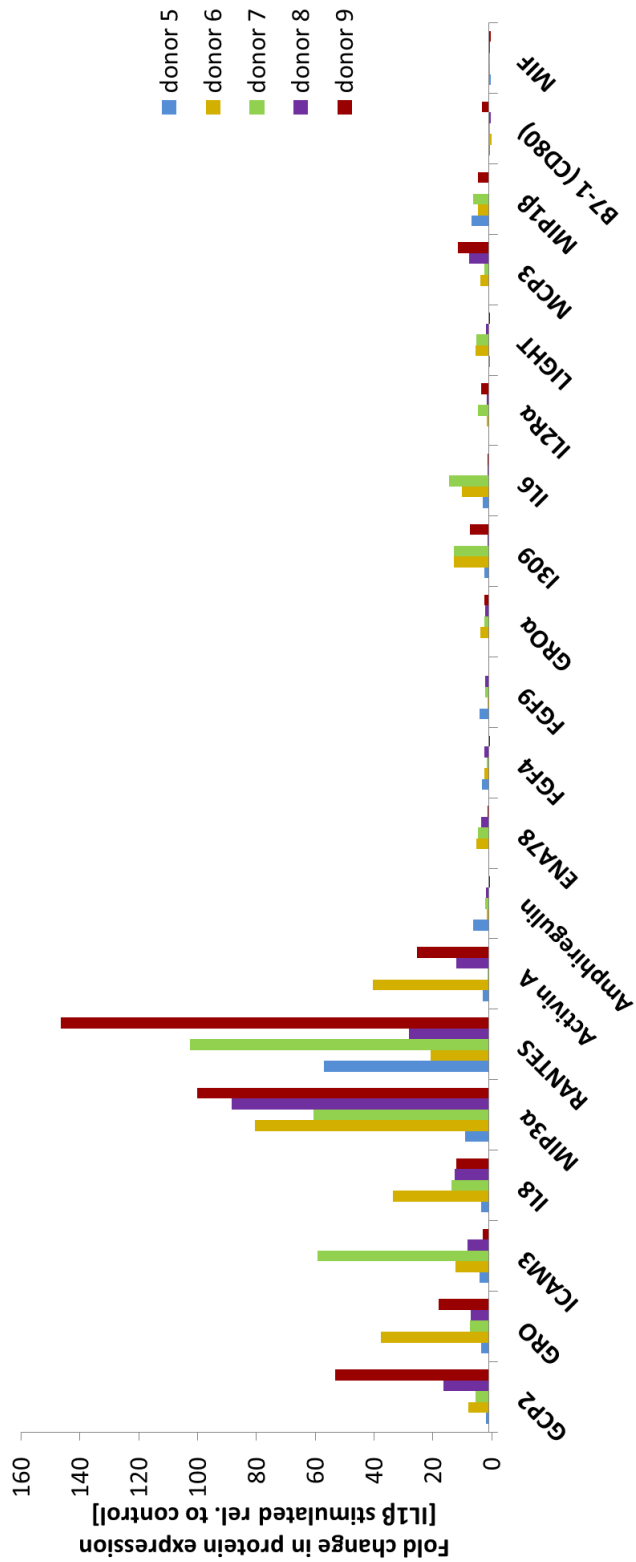


Figure 5.6. Protein levels of cytokines in medium conditioned by MSCs stimulated with IL1β. Monolayer cells were stimulated for 2 hours with 10ng/ml IL1β. After stimulation, cells were washed with DMEM and maintained in DMEM with 1% Penicillin-Streptomycin for 48 hours. After that time conditioned medium was collected for the analysis of secreted proteins.

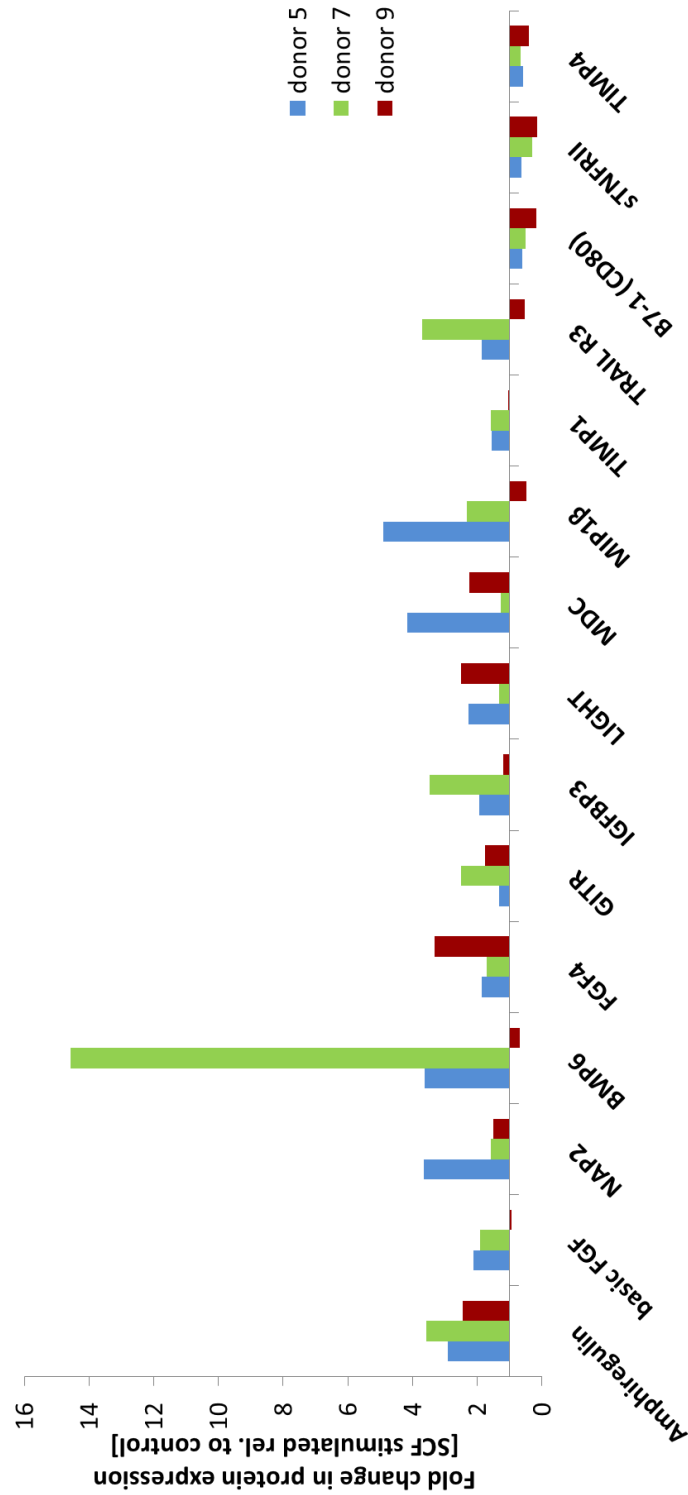


Figure 5.7. Protein levels of cytokines in medium conditioned by MSCs stimulated with SCF. Monolayer cells were stimulated for 2 hours with 100ng/ml SCF. After stimulation, cells were washed with DMEM and maintained in DMEM with 1% Penicillin-Streptomycin for 48 hours. After that time conditioned medium was collected for the protein secretion analysis.

5.2.2. Indirect effects of MSCs stimulation with cytokines on osteogenic differentiation of MSCs

To investigate the functional effects on cell proliferation of the secreted proteins, modulated in response to stimulation, an experiment with conditioned medium was performed. Unstimulated MSCs collected from one donor (6) were cultured in two types of media. As control medium (growth medium; 'GM'), 50% of conditioned medium from unstimulated or stimulated cells mixed with 50% of growth medium composed of DMEM supplemented with 1% Penicillin-Streptomycin and 2% FBS was used. The differentiation medium ('DM') was composed of 'GM' supplemented with 50 μ g/ml ascorbic acid, 10nM dexamethasone and 5mM β -glycerolphosphate.

5.2.2.1. Conditioned medium from stimulated cells inhibits the proliferation of MSCs

The analysis of the amount of DNA from cell cultures revealed the inhibition of proliferation when cells were cultured in conditioned medium harvested from IL1 β or SCF stimulated cells. Compared to day 2, there was a 58% increase in DNA amount at day 10, whereas in IL1 β and SCF groups this increase was 16% and 25%, respectively. The highest increase between control, IL1 β and SCF groups was reported from day 8 to day 10. Indeed, at day 10 the amount of DNA was significantly higher in the control group compared to IL1 β (p=0.018) and SCF (p=0.034) groups (Fig.5.8).

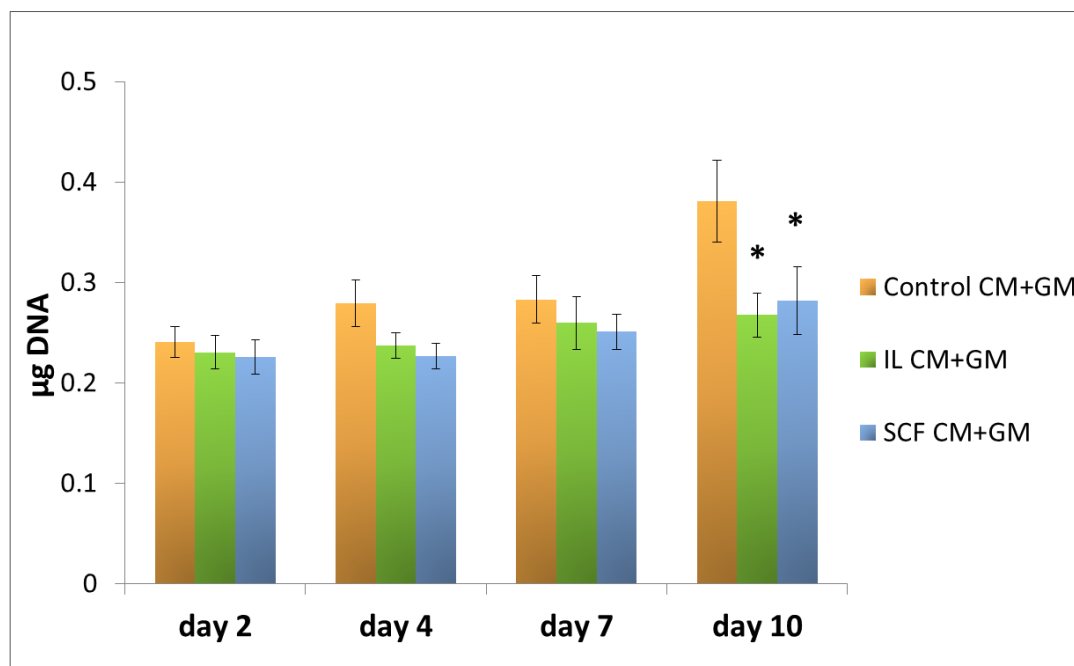


Figure 5.8. Diagram showing the amount of mean DNA (Hoechst) with the standard error of the mean, quantified during the culture of MSC cells in GM medium with the addition of conditioned medium collected 48 hours after the stimulation with 10ng/ml IL1 β or 100ng/ml SCF. As control, conditioned medium from unstimulated cells was used. DNA results were normally distributed and significance between control and IL1 β or SCF groups was determined at $p < 0.05$ (*) using one-way ANOVA with Games-Howell.

5.2.2.2. Regulation of osteogenic genes in response to co-culture with conditioned media

The relative gene expression of Runx2, Sox9, ALP, type I collagen (COL1) and osteocalcin (OC) was investigated during monolayer cell culture of MSCs in conditioned medium. In addition to this, the relation of Runx2/Sox9 as well as ALP/Runx2, COL1/Runx2, OC/Runx2 was assessed.

Culturing cells with conditioned media from stimulated cells had no effect on Sox9 gene expression when compared to the results from the control groups (Fig.5.9A). In fact, the level of Sox9 mRNA at day 7 was similar among DM and GM groups. At this time point, only IL CM+DM group had significantly higher expression of Sox9 when compared to IL CM+GM ($p=0.035$). Moreover, even though not significant, IL CM+DM showed a slightly higher level of Sox9 mRNA compared to Control CM+DM group. There was higher increase in Sox9 gene expression between day 7 and day 14 for all 'DM' groups. Furthermore, at day 14, a trend

for higher Sox9 expression in 'DM' groups over their respective 'GM' controls was detected (Fig.5.9A).

At day 7 the expression of Runx2 mRNA was at the same level among DM groups as well as among GM groups (Fig.5.9B). Yet, the Runx2 gene expression was significantly higher in Control CM+DM ($p=0.009$) IL CM+DM ($p=0.041$) and SCF CM+DM ($p=0.034$) when compared to its 'GM' controls. There were no significant changes in Runx2 gene expression at day 14.

Type I collagen expression at day 7 was lower in GM groups compared to DM groups (Fig.5.9C). There were no differences in COL1 expression between Control DM+GM and IL1 CM+DM or SCF CM+DM groups at day 7 and 14. Similar results were reported for day 14. Only at day 7, the COL1 expression between Control CM+DM ($p=0.001$), IL1 CM+DM ($p=0.002$) and SCF CM+DM ($p=0.001$) and respective GM groups reached statistical significance. The expression of COL1 in IL CM+DM and SCF CM+DM decreased from day 7 to day 14, whereas for the Control CM+DM group it remained at the same level.

The gene expression of ALP at day 7 was significantly higher in all DM groups compared to their specific GM controls ($p<0.001$) (Fig.5.9D). Yet, the combination of DM or GM medium with conditioned medium from stimulated cells had no influence on ALP mRNA expression at that time point compared to Control CM+DM or Control CM+GM groups, respectively. There was a decrease in ALP mRNA gene expression between day 7 and 14 in all DM groups. At the same time, it showed slight increase in GM groups (Fig.5.9D).

The gene expression of the late osteoblast marker, osteocalcin (OC), was higher in GM groups at day 7 and day 14 (Fig.5.9E). At the former time point, the expression of OC mRNA was significantly higher in Control CM+GM ($p=0.028$) and SCF CM+GM ($p=0.012$) groups compared to Control CM+DM and SCF GM+DM groups, respectively. Additionally, at day 7 the OC gene expression was higher in IL CM+DM ($p=0.049$) than Control CM+DM. At day 14, the OC gene

expression was at the same level as at day 14 except IL CM+ GM group. For this group the gene expression increased from day 7 to day 14.

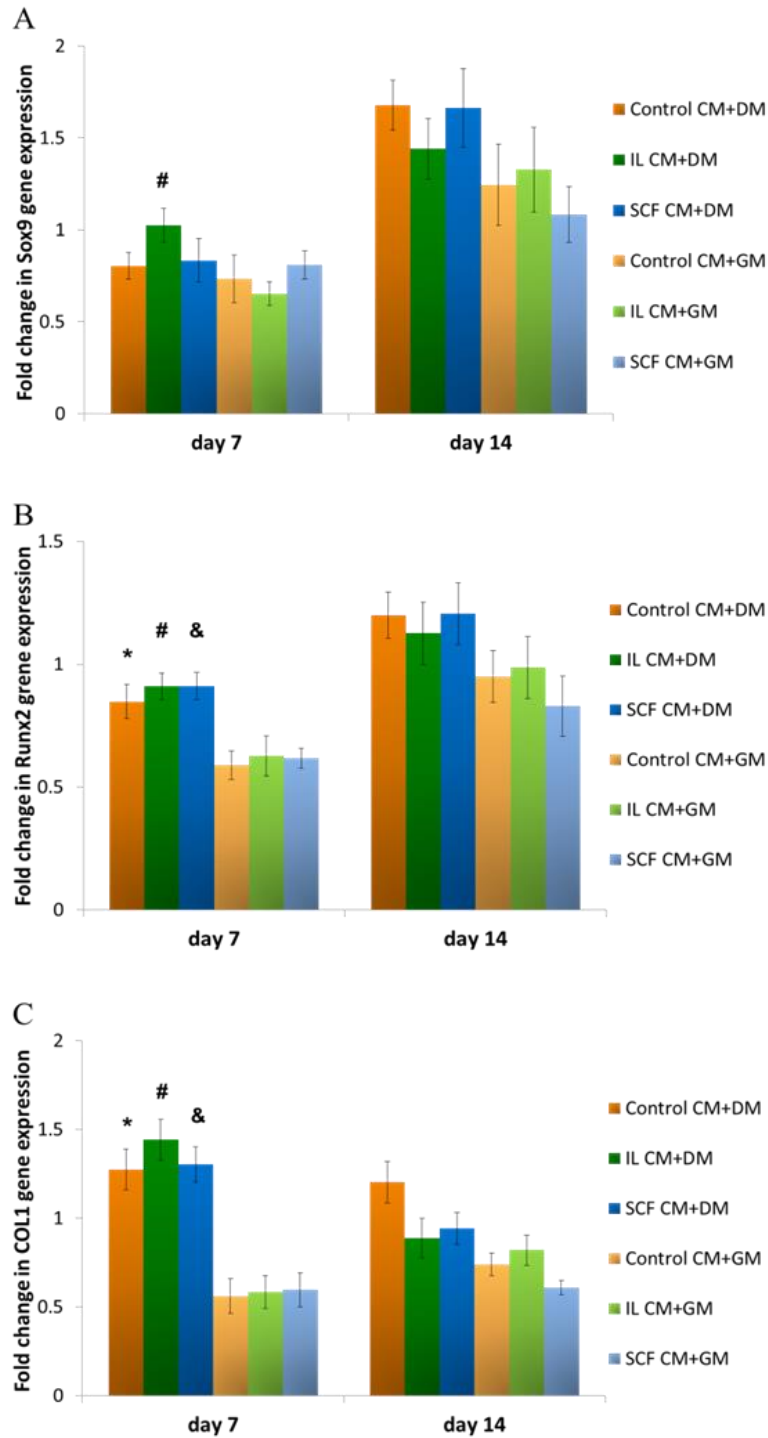


Figure 5.9A-C. Diagrams show the mean fold change in expression of Sox9 (A), Runx2 (B) and type I collagen (C) genes at day 7 and 14 in relative to Control CM+GM at day 2 with the standard error of the mean (3 experiments, n=9). Gene expression was normalised to RPL13a. Statistical significance at $p < 0.05$ was determined using one-way ANOVA with Games-Howell. *: compared to Control CM+GM; #: compared to IL CM+GM; &: statistically significant compared to SCF CM+GM; a: compared to Control CM+DM.

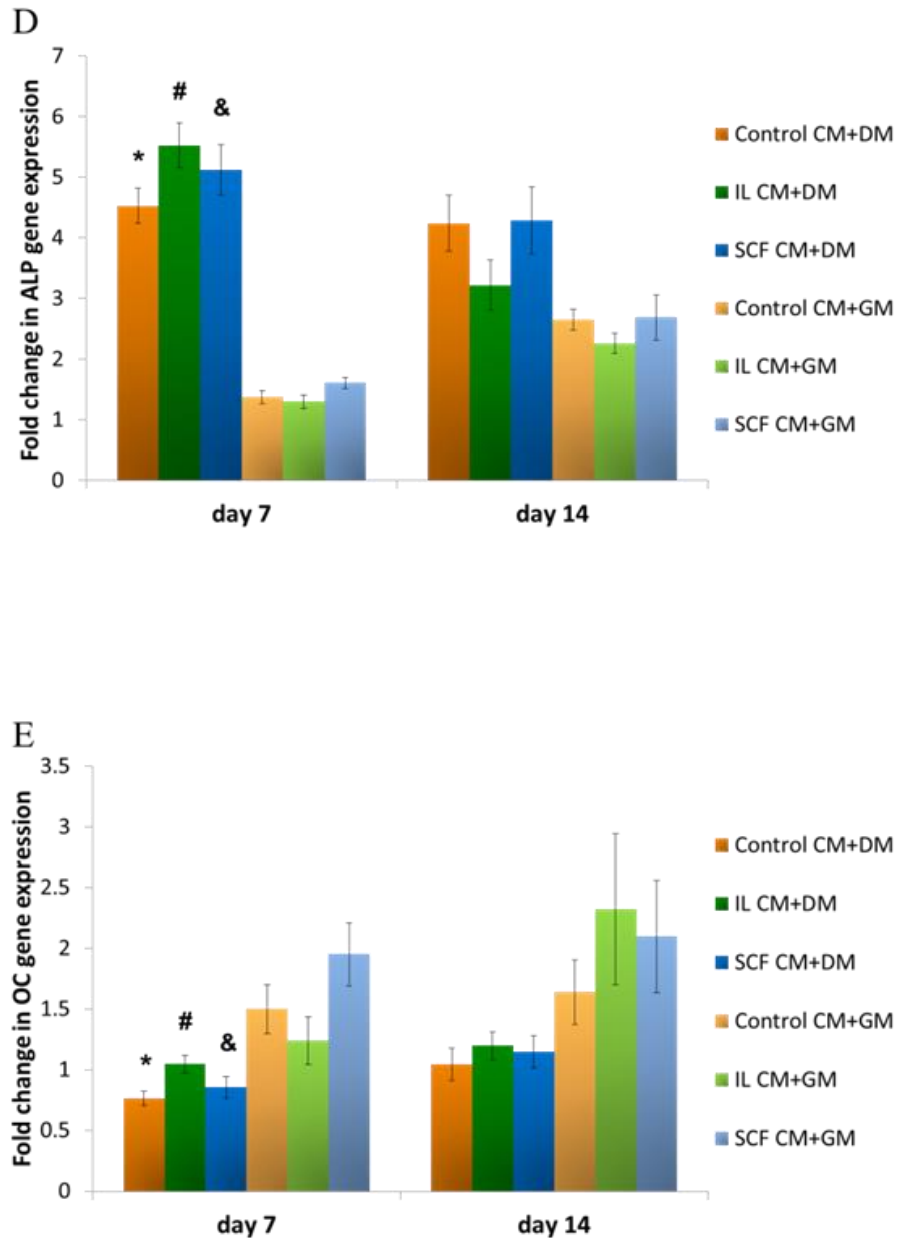


Figure 5.9D-E. Diagrams show the mean fold change in expression of ALP (D) and OC (E) genes at day 7 and 14 in relative to Control CM+GM at day 2 with the standard error of the mean (3 experiments, n=9). Gene expression was normalised to RPL13a. Statistical significance at $p < 0.05$ was determined using one-way ANOVA with Games-Howell. *: compared to Control CM+GM; # compared to IL CM+GM; &: statistically significant compared to SCF CM+GM; a: compared to Control CM+DM.

In addition to osteogenic genes, the ratio between specific genes and Runx2 transcription factor or between transcription factors, Runx2 and Sox9, were analysed (Fig.5.10.).

The analysis of Runx2 to Sox9 ratio, indicating the osteogenic potential of cells, showed similar results at day 7 and 14 for IL CM+DM and SCF CM+DM or IL CM+GM and SCF CM+GM to Control CM+DM and Control CM+GM groups, respectively (Fig.5.10A). Yet, the Runx2/Sox9 was significantly higher in SCF CM+DM ($p=0.034$) than in SCF CM+GM at day 7. Interestingly, the ratio decreased in DM groups from day 7 to day 14, whereas in GM it stayed at the same level over time. The expression of ALP relative to Runx2 was higher in all DM groups at day 7 and decreased by day 14 (Fig.5.10B). At the later time point, ALP/Runx2 was at the same level in DM and GM groups. At day 7, the ratio in Control CM+DM ($p<0.001$), IL CM+DM ($p<0.001$) and SCF CM+DM ($p<0.001$) was significantly higher than in respective GM groups. There were no differences in COL11/Runx2 between groups at any time point. Although, at day 7 the ratio was higher in DM groups compared to their respective GM controls, this trend did not reach statistical significance (Fig.5.10C). The OC/Runx2 ratio at day 7 and 14 in IL CM+DM and SCF CM+DM was the same as for Control CM+DM (Fig.5.10D). At both time points, the OC/Runx2 was lower in Control CM+DM ($p<0.001$ for d7 and $p=0.003$ for d14) and SCF CM+DM ($p<0.001$ for d7&d14) compared to the respective GM groups. For IL CM+DM group at day 7, the OC/Runx2 ratio was significantly lower ($p=0.039$) compared to IL CM+GM. Moreover, at this time point, the IL1 CM+DM group showed lower OC/Runx2 results compared to Control CM+GM. Interestingly, the ratio remained at the same level for this group at day 7 and 14, whereas it decreased over time for Control CM+GM and SCF CM+GM (Fig.5.10D).

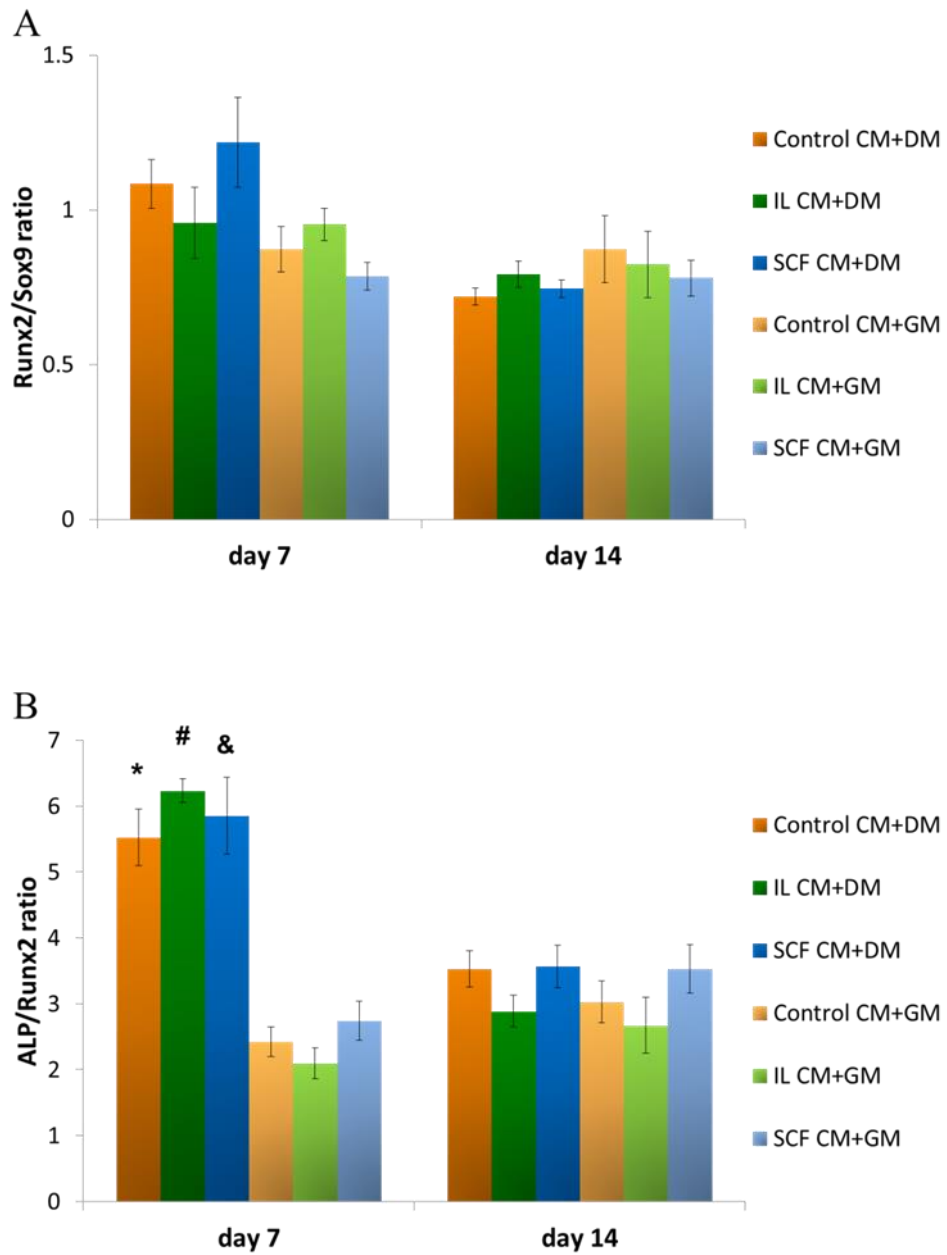


Figure 5.10A-B. Diagrams show the gene expression ratio of Runx2/Sox9 (A) and ALP/Runx2 (B) at day 7 and 14 with the standard error of the mean. Gene expression was normalised to RPL13a and made relative to Control CM+GM at day 2 (3experiments, n=9). Statistical significance at $p < 0.05$ was determined using one-way ANOVA with Games-Howell. *: compared to Control CM+GM; # compared to IL CM+GM; &: compared to SCF CM+GM.

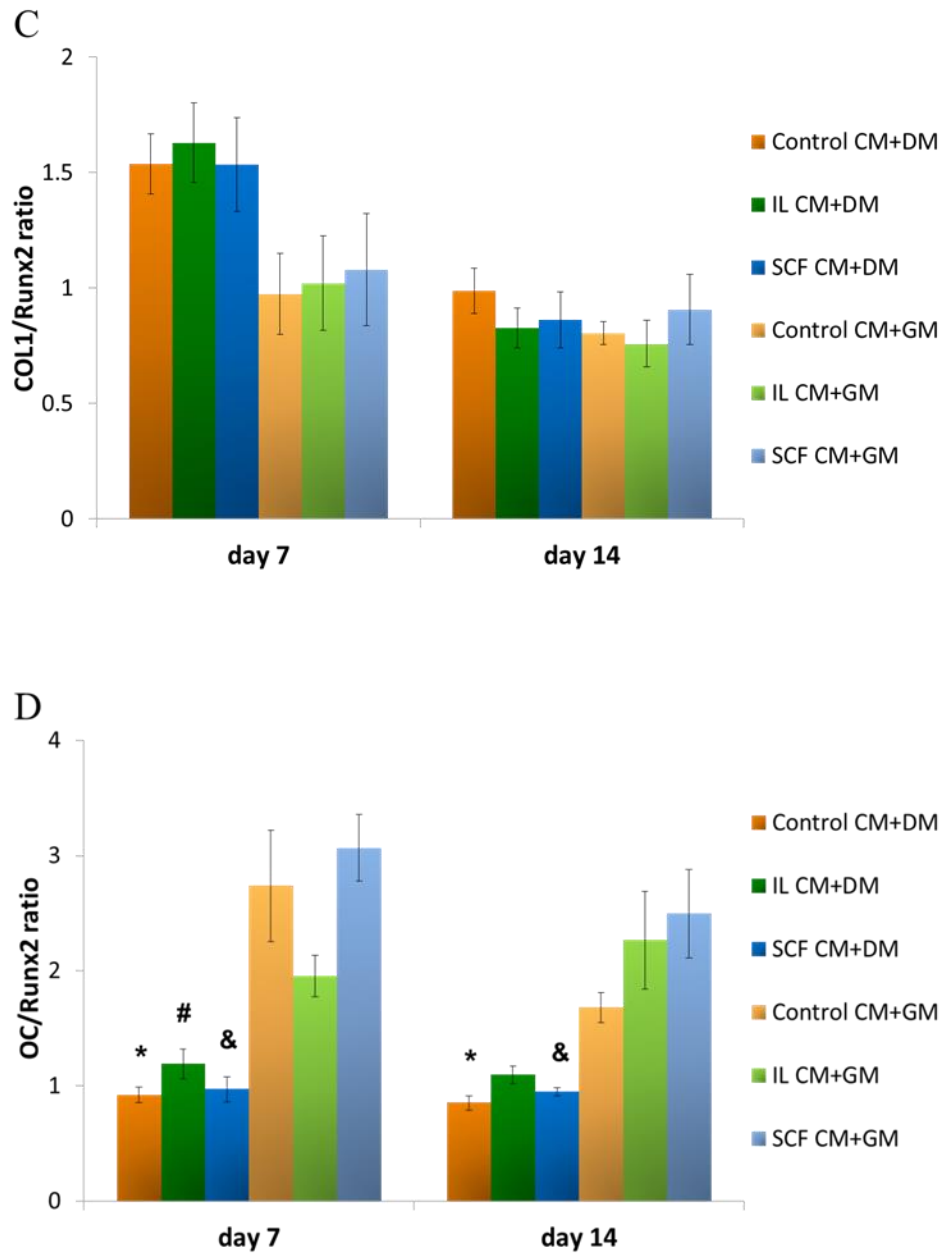


Figure 5.10C-D. Diagrams show the gene expression ratio of COL1/Runx2 (C) and OC/Runx2 (D) at day 7 and 14 with the standard error of the mean. Gene expression was normalised to RPL13a and made relative to Control CM+GM at day 2 (3experiments, n=9). Statistical significance at $p < 0.05$ was determined using one-way ANOVA with Games-Howell. *: compared to Control CM+GM; #: compared to IL CM+GM; &: compared to SCF CM+GM.

5.2.2.3. Influence of MSCs co-culture with conditioned media on cell functionality (ALP activity and mineral deposition in newly formed ECM)

In addition to investigating the expression of bone related genes, ALP protein activity was analysed in MSCs cultured with 50% of conditioned medium.

The analysis of ALP activity at day 7 and 14 revealed no significant differences between stimulated and control 'DM' or 'GM' groups (Fig.5.11). At day 7, the enzyme activity showed a trend of lower level in IL CM+DM ($p=0.487$) and SCF CM+DM ($p=0.516$) groups compared to Control CM+DM group. At both time points, the enzyme activity was significantly higher in cells cultured in DM medium compared to results from GM groups. There was 2.7-fold higher ALP level in Control CM+DM group than in Control CM+GM group ($p=0.006$) at day 7. Similarly, a 2.6- and 3.2-fold difference, was detected for IL CM+DM vs IL CM+GM groups ($p=0.002$) and SCF CM+DM vs SCF CM+GM ($p=0.020$) groups, respectively (Fig.5.11).

At day 14 there were no differences when comparing Control CM+DM and IL CM+DM ($p=0.920$) or SCF+DM ($p=0.929$) groups (Fig.5.11). Similarly, the ALP activity was at the same level in all 'GM' groups ($p>0.7$ for all comparisons). The ALP activity in DM groups was significantly higher than respective GM groups at day 14. The increase between DM and GM was similar for all treatments. Specifically, it was 1.74-, 1.80- and 1.62-fold higher between Control CM+DM and Control CM+DM ($p=0.003$), IL CM+DM and IL CM+DM ($p=0.001$), SCF CM+DM and SCF CM+DM ($p=0.020$), respectively.

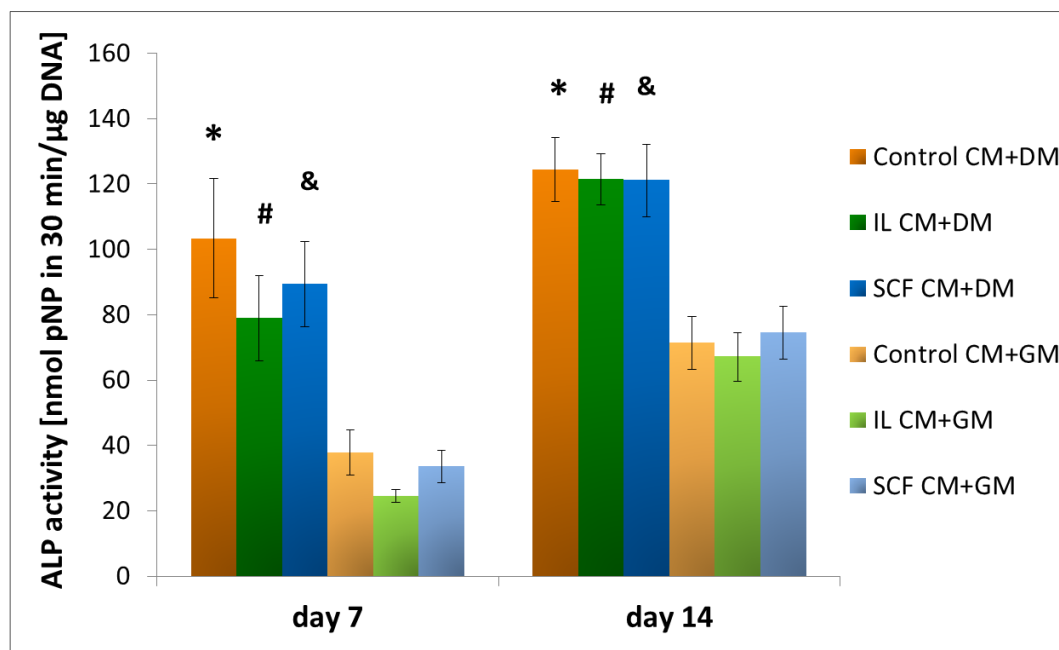


Figure 5.11. Diagram shows the mean alkaline phosphatase (ALP) activity in 30 minutes relative to the amount of DNA with the standard error of the mean (3 experiments, n=9). Statistical significance at $p < 0.05$ was determined using Kruskal-Wallis with Mann Whitney test for pairwise comparisons. *: compared to Control CM+GM; # compared to IL CM+GM; &: compared to SCF CM+GM.

The mineralisation of newly *in vitro* formed ECM was determined with Alizarin Red S staining and quantitation assay as described in paragraph 2.2.15.1 and 2.2.15.2. The amount of bound ARS to calcium was evaluated relative to the amount of DNA. MSC cells from one donor were cultured with conditioned medium from unstimulated or stimulated cells harvested from MSC cells from 3 different donors (#5, #7 and #9). After 2 weeks of *in vitro* cell culture with conditioned medium from donor 5, monolayer cultures tend to contract and fold preventing the analysis of ECM mineralisation in these cell cultures.

The ARS staining at day 28 of cell culture was positive in all cultures maintained with the addition of differentiation supplements (DM medium) (Fig.5.12A-C). Interestingly, in IL CM+DM and SCF CM+DM groups cells developed regions with thicker multilayer and larger nodules compared to the Control CM+DM group. In the latter, mineral deposition was more scattered throughout the whole cell layer (Fig.5.12). Although, the staining results could indicate higher mineralisation in cultures with the addition of conditioned medium from stimulated cells,

the quantitation analysis relative to the amount of DNA revealed no significant differences in the ARS bound to the ECM relative to DNA (Fig.5.13). The amount of bound ARS for all DM groups was in the range 4.60-4.98nmol bound ARS per μ g DNA. MSCs maintained in GM with the addition of different conditioned media developed nodules (Fig.5.12D-F). Yet, it seemed that similarly to DM groups, this was more advanced in cultures with the addition of IL CM and SCF CM. However, in any GM group no calcium deposition within the ECM was reported with ARS staining. The quantification analysis showed no difference between Control CM+GM and IL CM+GM or SCF CM+GM groups (Fig.5.13).

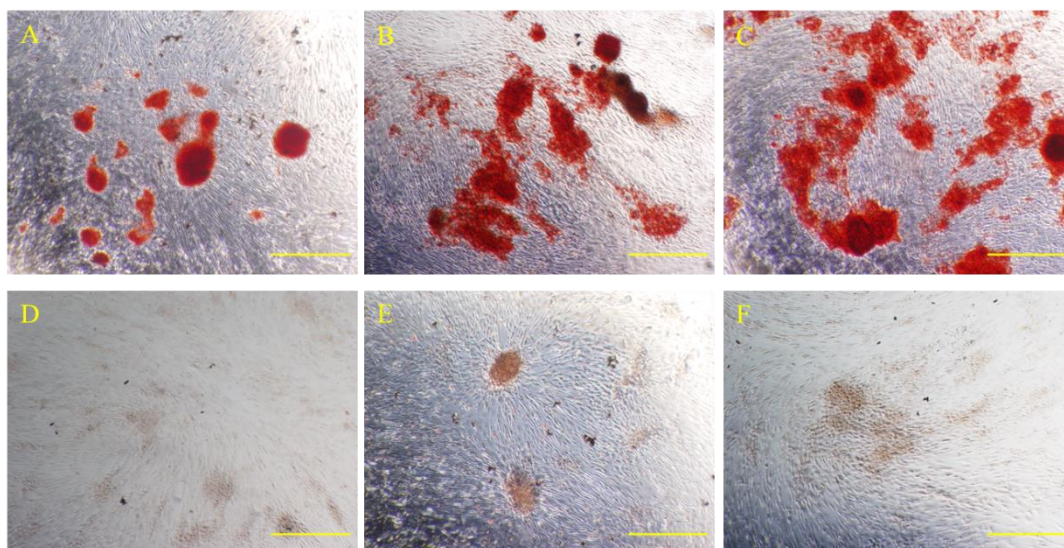


Figure 5.12. Representative images of Alizarin Red S staining of MSC at day 28. Cells were cultured in conditioned medium with the addition of DM (A-C) or GM (D-F); Conditioned medium was collected from unstimulated cells (A, D) and cells stimulated with 10ng/ml IL1 β (B, E) and 100ng/ml SCF (C, F). Scale bar 1 mm.

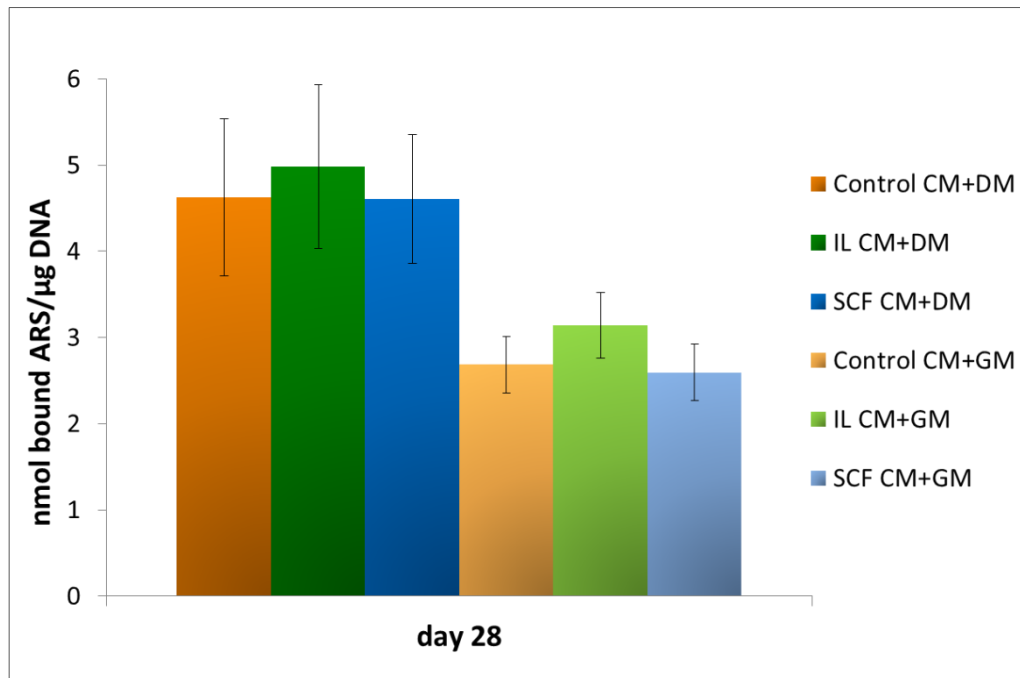


Figure 5.13. Diagram shows the mean amount of bound Alizarin Red S (ARS) with the standard deviation of the mean (n=6), at day 28 the culture of MSC cells in DM or GM medium with the addition of conditioned medium collected 48 hours after the stimulation with 10ng/ml IL1 β or 100ng/ml SCF. As control, conditioned medium from unstimulated cells was used.

5.3. Discussion

Investigations within this chapter focused on the influence of one-way cell-cell communication on MSCs differentiation into osteoblastic phenotype and whether this differentiation can be enhanced indirectly. In addition, the direct effects of cells stimulation with chemotactic and inflammatory factors were investigated. Preconditioning of cells and genetic engineering are two approaches to increase the production of specific factors by cells. We hypothesised that since the secretion of tropic factors is modulated *in vivo* by chemotactic and inflammatory factors, the use of these factors could provide a strategy to enhance the paracrine actions of cells. Four factors, which are the players in the early stages of bone healing cascade, namely Stem Cell Factor (SCF) and interleukin 1 β (IL1 β), stromal cell-derived factor 1 (SDF1) and granulocyte colony-stimulating factor (GCSF), were included for this analysis.

At first, the effect of all 4 factors, IL1 β , SCF, GCSF and SDF1, on cytokine gene expression in MSCs was analysed. Only 2 hours stimulation of cells with each of these factors resulted in a cell response which was still pronounced 72 hours after the treatment. Compared to other factors, the stimulation with IL1 β regulated the mRNA expression of the highest number of cytokine genes emphasising the multifunctional role of this cytokine. Interestingly, only one cytokine gene, NODAL, was up-regulated by all 4 factors. The functional analysis regulated factors demonstrated that, on a gene expression level, IL1 β , SCF, GCSF and SDF1 influence the expression of cytokines important at different stages of the bone healing process. The widest range of genes was regulated by IL1 β . This cytokine induced regulation of genes involved in bone formation, osteoclastogenesis, chondrogenesis and immunomodulation indicating its multiple actions and importance in bone healing process. Similarly, the results obtained from cells stimulated by GCSF indicated the influence of this cytokine on differentiation pathways, such as osteogenic, chondrogenic and angiogenic. Except for NODAL gene expression, SCF and SDF1 stimulation resulted in regulation of different cytokine genes compared to response of IL1 β treatment. Interestingly, the synergic effects of SCF and GCSF on stimulating proliferation and inhibiting differentiation of rabbit MSCs have been

reported (Tang et al., 2009). Hence, it would be of interest to analyse whether the combined stimulation of MSCs with all or some of factors included in this study synergises and results in stronger response.

Due to the high interest in IL1 β -regulated osteogenic differentiation (Ferreira et al., 2012; Sonomoto et al., 2012; Mumme et al., 2012; Lee et al., 2010) and recent promising influences of SCF on tissue regeneration (Kim et al., 2011; Pan et al., 2013), our further investigations focused on a more detailed analysis of the direct and indirect effects of these two cytokines. Interestingly, 48 hours after the stimulation, the treatment with IL1 β or SCF showed more pronounced effects on the cytokine gene expression compared to results of the analysis made 72 hours after the stimulation. After IL1 β stimulation, 11 cytokine genes were up-regulated and 9 cytokine genes were down-regulated, whereas SCF resulted in the up-regulation of 13 cytokine genes. BMP2, BMP6, IL6, IL8 and GDF5 showed the same response to IL1 β treatment 48 and 72 hours after the stimulation. No effect on TNFSF11, NODAL and IL17b was found 48 hours after IL1 β treatment, but the up-regulation of TNFSF11, NODAL and down-regulation of IL17b was detected after an additional 24 hours, suggesting these may be downstream events. Similarly, only TNFSF14 and IL1 α , but not GDF9 and NODAL gene expression were up-regulated 48 hours after SCF stimulation, whereas all of these cytokines were up-regulated 72 hours after the SCF treatment. These partial variances in the response to the IL1 β and SCF stimulation could be attributed to the differences in the experimental setting. First of all, the effect of IL1 β and SCF treatment on cells was evaluated after 48 or 72 hours. It is highly probable that the expression of some of the genes increases or diminishes in the 24 hour frame between both time points, especially as some genes may be induced by the factors induced during the early time points and may not be directly responsive to the cytokine used. It also has to be emphasised that the stimulation with 10ng/ml IL1 β and 100ng/ml SCF was performed in the same conditions (DMEM, 10% FCS and 1% penicillin-streptomycin), but following the stimulation cells were maintained for 48 hours in medium without serum and for 72 hours in medium with serum.

Serum contains a wide range of minor components including nutrients, hormones, growth factors, minerals and lipids. Although, serum has been globally used in cell culture protocols, the concentrations and actions of all these components are not fully determined and the existence of variations between batches of serum is known. The latter issue may result in significant variation in MSCs properties and osteogenic differentiation behaviour. The presence of the serum constituents could affect the regulation of various signalling pathways and the expression of cytokine genes. Although, within this study, all the analysis of the direct effects of short term stimulation with different factors was made relative to the untreated cells, it would be interesting to directly assess/evaluate to what extent the stimulation of MSCs with different factors is affected by the serum.

However, our initial approach was to analyse the direct effects of stimulation of MSCs, regarding the indirect effects of short-term stimulation of MSCs with IL1 β and SCF. Being aware of the potential influence that the serum can cause, the further analysis of gene expression and protein secretion by cells in response to IL1 β and SCF was analysed in cultures maintained in a serum-free medium.

IL1 β and SCF regulated the expression of members of interleukin family, including IL1 α , IL1 β , IL5, IL6, IL8, IL12A, IL17, IL18, IL21 and IL2R α . These cytokines have been recognized for their proinflammatory role and destructive effects on bone in pathological conditions including OA (Kapoor et al., 2011; Fernandes et al., 2002). Paradoxically, in the context of bone regeneration, the presence of some of these proinflammatory cytokines promotes the bone regeneration in multiple ways. Importantly, this positive effect strongly depends on the timing of their expression. Both, IL12 and IL18 have been shown to inhibit *in vitro* osteoclast differentiation. In addition, IL18 directly induces IL6 production, which is known for its potent roles at early stages of the bone healing process (Gracie et al., 2003). In fact, IL6 together with IL8 are the major angiogenic factors stimulating vascular endothelial growth factor (VEGF) during fracture healing (Martin et al., 2009; Kolar et al., 2011). IL1 β treatment increased the gene and protein expression of IL6 and IL8, whereas SCF had an opposite effect on gene expression of these cytokines (Fig.4.5A) suggesting the involvement of IL1 β , but not SCF, in triggering angiogenesis. On the other hand,

the SCF stimulatory effects on angiogenesis could be mediated through the up-regulation of IL18 cytokine gene expression which induces production of IL6 (Gracie et al., 2003).

The gene expression of osteoblastic phenotype regulatory factors, such as BMP2, BMP3, BMP4, BMP5, BMP7, TGF β ₃, GDF5 and GDF8, was lower in cells after IL1 β treatment. BMPs are important for proliferation, osteoblastic and chondrogenic differentiation, morphogenesis and apoptosis. A heterodimeric association of BMP4/7 and BMP2/7 regulates the proliferation of MSCs and induces the differentiation of MSCs into osteoblastic lineage (Tsiridis et al., 2007). Similarly, BMP5 and TGF β ₃ possess osteoinductive properties (Wozney, 2002). At the same time, BMP6, a factor implicated in chondrocyte maturation, was up-regulated after the stimulation with IL1 β . GDF5 and GDF8 are involved in chondrogenesis and callus formation. GDF8, a known negative regulator of skeletal muscle growth, stimulates the adipogenic differentiation in mesenchymal stem cells whereas its absence increases osteogenic differentiation (Artaza et al., 2005; Hamrick et al., 2007). Interestingly, Kellum and co-workers reported a positive correlation of GDF8 deficiency and fracture callus size in a mouse *in vivo* model (Kellum et al., 2009). The down-regulation of BMP together with the down-regulation of Wnt molecules upon stimulation suggest the inhibitory effects of IL1 β on osteogenic differentiation of MSCs. On the other hand the increased expression of chondrogenic messengers recapitulates the sequence of early events occurring during fracture healing where fracture callus formation and angiogenesis precede osteogenesis.

In addition to the assessment of cytokine genes in response to 2 hours stimulation of cells with IL1 β and SCF, the expression of Wnt signalling pathway components and their relation to Sox9 and Runx2 transcription factor gene expression was analysed 48 hours after the treatment. The analysis of Wnt 3a, 4, 5a, 7b and β catenin mRNA expression in cells stimulated with IL1 β or SCF relative to untreated cells was strongly donor dependent. Interestingly, in the experimental setting within this study, the expression of Wnt3a was not detected in cells, neither with nor without the stimulation with IL1 β or SCF. In cells from 2 donors (#5 and # 8) the Wnt4 gene expression was detectable in control samples and in treated cells; whereas Wnt5a, 7b

and β catenin were expressed in stimulated and unstimulated cells. Both, Wnt3a and Wnt4 together with β catenin are involved in the canonical Wnt pathway which is known to stimulate the expression of important osteogenic molecules, such as alkaline phosphatase (ALP), osteocalcin (OC), bone morphogenic protein 2 (BMP2) and the transcriptional factor Runx2 (Kim et al., 2013), and inhibit the non-canonical pathway (Boland et al., 2004). Importantly, the effect of canonical Wnt signalling on osteogenesis is highly dependent on the stage of target cells (Ling et al., 2009). Wnt5a and Wnt7b activate the non-canonical Wnt signalling pathway which induces several cascades, including planar-cell polarity (PCP), c-Jun N-terminal kinase (JNK), Nemo-like kinase (NLK) and Rho-associated kinase (ROK) signalling (Ling et al., 2009).

Results within this chapter indicated that although the stimulation with IL1 β had no significant effect on Wnt5a, Wnt7b and β catenin gene expression, Wnt7b showed a trend of increased expression upon the treatment with IL1 β (Fig.4.5). This was in conjunction with significant decrease in Runx2 and Sox9 gene expression (Fig.4.5). The treatment with SCF showed a similar trend in Wnt5a, Wnt7b, Runx2 and Sox9 gene expression as reported for IL1 β stimulation. However, in case of SCF stimulation, the expression of Wnt7b was significantly down-regulated. Based on research evidence, the canonical Wnt signalling stimulates the differentiation of MSCs which are committed to osteogenic lineage, whereas it suppresses the terminal differentiation of mature osteoblasts (Ling et al., 2009). The former process is promoted through the up-regulation of Runx2, which along with Sox9, is a transcriptional effector of the canonical Wnt signalling (Parr et al., 1993;Eames et al., 2004). Interestingly, Runx2 expression is also regulated by Wnt5a in the non-canonical Wnt pathway (Arnsdorf et al., 2009). Although, the expression of Runx2 and Sox9 was down-regulated upon the stimulation of MSCs with IL1 β or SCF, the Runx2/Sox9 ratio remained at the same level.

In fact, experiments within our group showed the chronic stimulation of cells with IL1 β induces proliferation and osteogenic differentiation of MSCs with subsequent promotion of ECM mineralisation (Loebel et al., 2014b). The promotion of osteogenic differentiation by IL1 β is dependent on the non-canonical Wnt pathway

stimulating Runx2 gene expression (Sonamoto et al., 2012). Results presented within this chapter and our further observations showed that the short term treatment induces other mechanisms and outcomes in MSCs osteogenic differentiation in a monolayer cultures. The direct two hours treatment with IL1 β was not sufficient to induce the same effects on the MSCs osteogenic differentiation as the chronic treatment (unpublished results). Moreover, as presented in this chapter, both IL1 β and SCF inhibit mRNA expression of molecules involved in the induction of osteogenic differentiation, including components of the canonical and non-canonical Wnt and BMP2. There is no previous evidence comparing the short and chronic effects of SCF on the osteogenic differentiation. Hence, it is difficult to speculate whether SCF has any influential direct role on the osteogenic differentiation. Nevertheless, the protein analysis of conditioned medium revealed the increased secretion by MSCs of a number of proteins involved in the bone formation process (Tab.4.2) in response to the short term stimulation with IL1 β or SCF. In line with mRNA results, no BMP2 was present in the condition medium. Instead, IL1 β promoted the secretion of wide range of proteins with chemotactic, proinflammatory and angiogenic properties, whereas SCF regulated the expression of proteins involved in proliferation, chondrogenesis and ECM regulation.

Interestingly, the presented results from post-stimulation serum-free cultures showed the mRNA expression of receptor activator of NF- κ B ligand (RANKL) was down-regulated, whereas at the same time TNFRSF11b was up-regulated in response to the stimulation with IL1 β or SCF. RANKL is a paracrine factor involved in osteoblast-osteoclast progenitor cells cross-talk. Secreted RANKL protein binds to RANK receptor on the osteoclast progenitor cell surface activating the differentiation of the osteoclast phenotype (Udagawa et al., 1999).TNFRSF11b is gene coding the osteoprotegerin (OPG) protein known as inhibitor of osteoclastogenesis and activation of mature osteoclasts. In detail, OPG is the decoy receptor for RANKL expressed and secreted by osteoblasts and osteoprogenitor cells. Moreover, studies showed the regulation of OPG and RANKL is Wnt signalling dependent (Maeda et al., 2013;Maeda et al., 2012). Although, the protein level of OPG in the conditioned medium 48 hours after the stimulation of MSCs with IL1 β or SCF was at the same level as in untreated cells

(data not shown), based on the mRNA expression level results, short term stimulation with IL1 β or SCF suggest the indirect inhibitory effects of IL1 β and SCF on the differentiation of osteoclasts. Additionally, Wnt gene expression results indicated that the regulation of OPG and RANKL in response to IL1 β and SCF is independent on the Wnt pathway. Together with results regarding OPG and RANKL, the mRNA expression of additional factors inhibiting osteoclastogenesis was positively regulated in response to the stimulation with IL1 β and SCF. The latter up-regulated the expression of IL18, stimulating the production of osteoclast differentiation inhibitor, granulocyte macrophage colony-stimulating factor (GM-CSF), by T-cells (Horwood et al., 1998;Gracie et al., 2003). In case of short-term stimulation of MSCs with IL1 β , the expression of GM-SCF gene was directly up-regulated after the treatment.

Understanding the mechanisms involved in the indirect effects of preconditioning, i.e. due to the enhancement of the secretion of trophic factors acting in a paracrine manner, would be of great interest for cell-based regenerative therapies. Therefore, the relevance of the secreted factors, in supporting MSC proliferation and differentiation towards the osteoblastic lineage, was analysed. In order to reduce the influence of proteins present in the medium on osteogenic differentiation, the final concentration of FBS included in medium was 1%. Moreover, being aware of the donor variability, all repeats of the conditioned medium (CM) experiments were performed with cells obtained from one MSCs donor, which was previously evaluated in our laboratory as positive for undergoing osteogenic differentiation. For proliferation and differentiation evaluation these cells were cultured in CM collected from cells isolated from a bone marrow harvested from 3 donors.

Within the monolayer indirect co-culture system, the conditioned medium collected from unstimulated (Control CM+GM) and stimulated cells with IL1 β (IL1 CM+GM) or SCF (SCF CM+GM) had a significant effect on MSC proliferation. Although, stimulation of MSCs with SCF or IL1 up-regulated some mitogenic proteins, IL1 CM+GM and SCF CM+GM had an inhibitory effect on MSC proliferation during the 10 day culture period. In Control CM+GM group an increase of DNA amount was observed from day 2 to day 10.

Further investigations were made to analyse the osteogenic differentiation of MSCs cultured in the conditioned medium with the addition of growth or differentiation media.

The differentiation of MSCs is regulated by the transcription factors which 'switch on' the specific differentiation programme. Runx2 has been described as an early osteogenic differentiation marker as it is up-regulated during the mesenchymal condensation, which leads to the formation of pre-osteoblasts (Ducy et al., 1997). Sox9 activates the expression of genes specific for cartilage phenotype, including type II collagen and aggrecan. The results from *in vivo* investigations indicated that in endochondral ossification Sox9 expression precedes the expression of Runx2 (Eames et al., 2004). The recent results from our laboratory indicated that *in vitro* the osteogenic differentiation of cells correlated with the relative expression of Runx2 to Sox9 ratio within 7 days of culture (Loebel et al., 2014a). The gene expression analysis of Sox9, Runx2 and Runx2/Sox9 revealed no differences between groups maintained in different CM with DM or CM with GM. Although, there was an increase in gene expression from day 7 to day 14 for both Runx2 and Sox9, there were no significant differences in Runx2/Sox9 ratio for all groups at either time point. The expression of later osteogenic markers, type I collagen, ALP and osteocalcin was at a similar level in IL CM and SCF CM compared to the respective control CM DM or GM groups. ALP/Runx2, COL1/Runx2 and OC/Runx2 ratios were analysed as differentiation index indicative of more advanced osteogenic differentiation with the higher ratio values. The differentiation indexes showed similar results between IL CM and SCF CM and the respective control CM DM or GM groups. The Alizarin Red S staining results could suggest that culturing MSC cells in DM with the addition of IL CM and SCF DM promotes the nodule formation compared to DM with control CM. However, there was no correlation of these observations with the quantitative results relative to the DNA amount. Similarly, no differences were reported for ALP activity in cultures maintained in the DM or GM media containing control CM, IL CM or SCF CM. According to the results from the CM co-culture model, the range of proteins produced by cells in response to IL1 β or SCF treatment has no pronounced effects

on the osteogenic differentiation of MSCs over the effects of proteins secreted by the unstimulated cells.

Regarding gene expression analysis, the OC mRNA was reported at a higher level in GM than DM conditions, whereas an inverse relation was reported for other osteogenic differentiation markers. It has been suggested that the supplementation of cell culture medium with dexamethasone, 1,25(OH)₂D₃, β-glycerophosphate, ascorbic acid and BMPs, is effective in directing osteoblast mineralisation (Arnett, 1990;Jorgensen et al., 2004). It has been shown that dexamethasone, in a physiological range 10⁻⁷ to 10⁻⁹ M promotes more differentiated osteoblast cells phenotype and nodule formation (Yang et al., 2003;Bellows et al., 1987). Nevertheless, the conflicting results regarding cell proliferation, ALP activity, type I collagen synthesis and osteocalcin have been reported (Yang et al., 2003;Sutherland et al., 1995;Wong et al., 1990;Lian et al., 1997;Chen and Fry, 1999;Kim et al., 1999). One of the reasons to which these differences are related is the origin of cells. In contrary to observations from rat osteoblast cell cultures, the chronic exposure of mouse osteoblast cells to dexamethasone initiated during the proliferation period, blocked osteoblast differentiation indicating differential species-specific mechanisms of response to dexamethasone administration (Lian et al., 1997;Chen and Fry, 1999). Similarly, the dexamethasone supplementation of cell culture medium for MSCs decreased proliferation rate, type I collagen mRNA and protein expression and osteocalcin production (Kim et al., 1999;Jorgensen et al., 2004). Similar results regarding osteocalcin production were seen for primary human osteoblasts (Viereck et al., 2002). The here reported lower expression of OC in medium supplemented with dexamethasone supports previous observations and suggest negative effect of this glucocorticoid on the development of the mature osteoblastic phenotype.

It has to be mentioned that for the CM study, the monolayer culture system was applied which may not be the best and can sorely affect results. SCF and IL1β are released at the inflammation phase of secondary bone healing analogous to endochondral bone formation (Shapiro, 2008). It is challenging to recapitulate endochondral ossification in an *in vitro* culture. However, the controlled stimulation of the chondrogenic differentiation followed by the osteogenic differentiation

of MSCs in a 3D *in vitro* culture results in formation of bone tissue *via* an endochondral ossification (Muraglia et al., 2003;Scotti et al., 2010). Differentiation of MSCs in monolayer cell culture focuses on the direct stimulation of osteogenesis which is alike intramembranous ossification. *In vivo* this process is related to the primary bone healing in which hematoma does not occur (Kolar et al., 2011;Giannoudis et al., 2007). As consequence, the influx of inflammatory cells and the release of the inflammatory and chemotactic factors are absent. Hence, the primary bone healing is not affected by inflammation causing changes in cells present at the fracture site. Furthermore, the parameters, such as surface roughness, are critical for cell behaviour. The recent research evidences regarding the short term stimulation of human adipose derived stem cells to enhance osteogenic differentiation showed superior results in a 3D biphasic calcium phosphate scaffold (pore size 100-500um) compared to a 2D culture on tissue polystyrene (Overman et al., 2013a). Moreover, in response to short term pre-treatment of cells with BMP2 the gene expression of trophic factors was differentially regulated in cells cultured in 3D compared to monolayer (Overman et al., 2013b). With respect to these results, a monolayer culture system is a clear limitation of our study. Therefore, it seems that the analysis of the indirect effects of MSCs stimulation with IL1 β or SCF in a 3D *in vitro* model investigating endochondral ossification rather than osteogenesis would provide more relevant and unambiguous results.

Taken together the secretome of MSCs can be modified over longer periods by way of a short stimulation which could be performed intra-operatively. However, to investigate these effects more reliably a 3D endochondral model may be more suitable.

CHAPTER 6

THE EFFECT OF DIFFERENT 3D CELL CULTURE SYSTEMS ON MSC CELLS

6.1. Introduction

Since the first attempt of isolation and *in vitro* culture of osteoblast cells from adult human bone (Bard et al., 1972), a great improvement in the knowledge of the biology of bone and, in particular, osteoblastic cells has been made. Most of this has been achieved through the analysis of various aspects of bone cell phenotype in an *in vitro* monolayer cell culture. In fact, this simplified system is considered as the gold standard *in vitro* culture model as it ensures the controlled culture environment. Nevertheless, within bone, cells are embedded in a mineralised organic matrix composed of type I collagen, non-collagenous proteins and hydroxyapatite. In this milieu, bone cells interact with each other and with the ECM through soluble factors or direct cell-cell and cell-matrix interactions. Having this in mind, it is evident that in monolayer culture system many of these interactions occurring *in vivo* are neglected.

For a better understanding of the processes occurring in bone, the requirement of a reliable *in vitro* cell culture model is critical. When considering the composition of bone, it is clear that formulating an *in vitro* cell culture model based on naturally occurring components would be the most advantageous. In this chapter the focus is directed towards the osteogenic differentiation of bone progenitor cells in order to compare this process in a 2D monolayer and two types of 3D *in vitro* culture models, with the emphasis on 3D models which are supported by the naturally occurring components in the bone. The following paragraphs of this introduction bring the concept of the influence of the *in vitro* cell culture environment on the osteoblast-like phenotype.

In vitro differentiation of osteoblast cells has been extensively studied in 2D monolayer conditions. Indeed, the full differentiation process, from proliferation to mineral deposition can be recapitulated in monolayer cell culture for osteogenic cells. The generally accepted temporal sequence of expression osteoblast markers during cell phenotype development was established in low-density seeded monolayer culture of rat calvaria derived cells by Lian and Stein (Lian and Stein, 1992). A similar progression in phenotype has been

reported for cells from other origins including primary cells from animals and some cell lines (Wang et al., 1999;Buttery et al., 2001). Although, primary human osteoblast cells of foetal origin undergo a progress similar to rat osteoblast cells from proliferation, through matrix production and maturation, to mineralisation of ECM; it has been shown that adult human derived HOB's not always are able to complete osteogenesis up to mineral deposition *in vitro* in monolayer cell culture (Hughes and Aubin, 1998;Di Silvio and Gurav, 2001). These findings emphasise the limitation of the monolayer culture systems in studying the late stages of osteogenesis. It is also evident that monolayer cell culture system is not physiologically relevant.

To overcome this limitation, and provide a physiologically more relevant context, culturing osteoblast cells in a 3D environment has attracted a lot of interest. Maintaining cells in 3D systems, such as spheroids, micromass and pellets, promotes progression in osteoblastic differentiation leading to osteoblast cell maturation (Kale et al., 2000;Gerber and ap Gwynn, 2002;Jahn et al., 2010). These simple 3D models are supported by the ECM produced by cultured cells and were utilised for culturing primary human or rat osteoblast cells. Results from 3D high density cell cultures revealed considerable differences compared to standard monolayer conditions. Cells in micromass promote earlier differentiation by increasing collagen production, together with decreasing proliferation due cell-cell contact being established early (Gerber and ap Gwynn, 2002). Similarly, osteoblast cell phenotype progression was observed for human osteoblast cells in pellet and spheroids cultures compared to monolayer cultures (Kale et al., 2000;Jahn et al., 2010). Human bone precursor or osteoblast cells in spheroids, formed by induction with TGF β ₁, had increased osteonectin and alkaline phosphatase gene expression and collagen synthesis compared to monolayer cells (Kale et al., 2000). Moreover, 3D bone cell cultures based on high cell numbers contributed to the establishment of a more complex model for endochondral bone development. Formation of osteochondral structures within pellets was achieved from bone-derived MSC cells and cells from human foetal femurs (Muraglia et al., 2003;El-Serafi et al., 2011;Tortelli et al., 2010).

Bone tissue engineering approaches focus on combining stem cell therapy with scaffolds, membranes, sponges, natural and synthetic hydrogels, which can be implanted into the body and would enhance tissue regeneration process. Type I collagen is the major component of ECM, constituting 90% of the organic material in bone (Currey, 2008). Therefore, a huge attention has been directed towards the use of the collagen gels as biomimetic substrates or scaffolds in cell-driven remodelling events. Type I collagen can be extracted from various sources, including rat, bovine and equine tendon, porcine skin, and human and ovine placenta. Commercially available products, such as Collapat II (BioMet, Inc), Healos (Deputy Spine, Inc), Collagraft (Neucoll, Inc; Zimmer, Inc) or Biostate (Vebas, s.r.l), for hard tissue repair are based on bovine and equine type I collagen components (Wahl and Czernuszka, 2006).

Type I collagen has been shown to be fundamental for the developmental expression of the osteoblast phenotype and the formation of mineralised matrix (Owen et al., 1990; Lynch et al., 1995). Culturing cells on type I collagen enhances expression of osteoblastic markers and results in uniform mineralisation of ECM (Lynch et al., 1995). Interaction of type I collagen with $\alpha_2\beta_1$ integrin on the cell surface is crucial for initiation of osteoblastic phenotype differentiation. Upon interaction the mitogen-activated protein kinase (MAPK) pathway is activated. This activation results in phosphorylation and activation of Runx2 (Wenstrup et al., 1996), which is required for the activation of the osteocalcin promoter within the nucleus (Xiao et al., 1998). The discrepancies in the response of cells in monolayer or type I collagen gels are evident. The typical temporal monolayer cultures pattern of specific gene expression, is shifted in cells cultured on collagen gels (Lian and Stein, 1995). ALP activity was observed before the proliferation phase of cells cultured on collagen gels was completed (Lian and Stein, 1995; Lynch et al., 1995). Recent results, showed that murine osteoblast cells seeded on top of type I collagen gel were able to migrate into the collagen gel and differentiate towards an osteocyte-like phenotype (Uchihashi et al., 2012). Similar stimulation of differentiation towards mature osteoblasts and osteocytes was reported for cells within dense type I collagen gel achieved by plastic compression (Buxton et al., 2008).

This chapter will investigate the influence of the *in vitro* cell culture environment on the osteoblast-like phenotype. Specifically, monolayer culture will be compared with 3D culture models. Two 3D culture models will be used, including standard high density micromass culture and a novel type I collagen-hydroxyapatite hydrogel. Through employing two different systems, the importance of the ECM for osteoblast and bone derived MSC cell phenotype development will be investigated. We aim to establish a 3D osteoblast cell model resembling a more natural milieu allowing for a better understanding of osteoblastic cell development.

6.2. Results

6.2.1. Type I collagen gel-hydroxyapatite gel formulation and optimisation process

Prior the culturing of cells within 3D type I collagen system, the collagen hydrogel polymerisation and stability were optimised (Tab.6.1.). Specifically, the concentration had a huge impact on polymerisation efficacy. In addition, since the gel was not cross-linked with any agent, the stability of gel with cells was low. Gel shrinkage in DMEM culture medium was observed from day 5. The addition of 1mg hydroxyapatite (HAP) particles (80-200 μ m) per 1ml of the gel dramatically improved gel stability. In order to prevent the formation of a cell monolayer below the gel, the collagen-hydroxyapatite (CHAP) gels containing cells were placed on the surface pre-coated with 2% agarose. However, due to compromised gel stability during long-term cell culture, pre-coating the tissue culture polystyrene with type I collagen gel was investigated and dramatically improved long term stability of CHAP (Tab.6.1).

Step	Description	Observations and Results
Preparing the gel mixture	Manufacturer's instruction followed: 83% type I collagen gel, 10% 10xPBS, 2.5% 1N NaOH, 4.5% DMEM	Gelation within 30 min, but some liquid below the gel occurred
Optimising salt concentration	83% type I collagen gel, 5% 10xPBS, 2.5% 1N NaOH, 9.5% DMEM	Successful gelation within 40 min at 37°C
Cells + type I collagen gel	Cells were resuspended in small volume of DMEM and mixed with type I collagen gel mixture	Gel shrinkage and degradation within 5 days
Cells + type I collagen gel + HAP	<p>1) Cells were resuspended in small volume of DMEM and mixed with hydroxyapatite (HAP) at different concentrations (0.2 µg/ml, 0.4 µg/ml; 1 µg/ml, 2 µg/ml)</p> <p>2) Cells mixed with HAP were added to type I collagen gel</p>	Improved stability; cell drooping on the bottom of the well
Pre-coating of the well with agarose	Before placing the gel, the bottom of the well was pre-coated with 2% agarose to prevent the attachment and proliferation of cells on the bottom of the well	Gel detachment and shrinkage
Pre-coating of the well with type I collagen gel	Before placing the gel, the bottom of the well was pre-coated with 2.5 mg/ml type I collagen to maximise collagen-integrin interaction	Improved stability (up to 14-21 days); good cell viability

Table 6.1. The description of the type I collagen-hydroxyapatite optimisation process. HAP-hydroxyapatite.

The initial experiments focusing on the qualitative analysis of human MSC viability within CHAP gels revealed no negative influence of type I collagen-hydroxyapatite gel on MSC cell viability (Fig.6.1.). At day 2, cells were alive and started spreading on the collagen (Fig.6.1.). Additionally, the high level of viability is sustained up to day 37 of culture. At this time point, cells had spindle morphology and were well interconnected (Fig.6.1.).

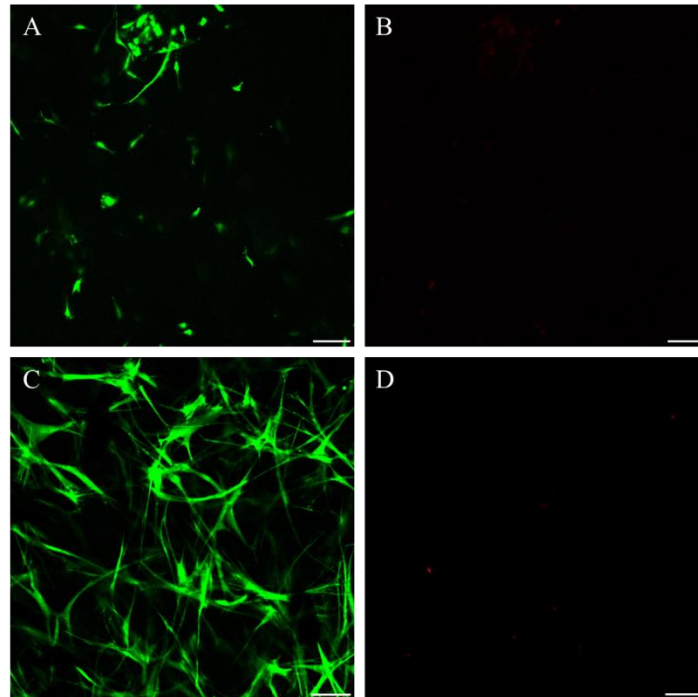


Figure 6.1. Representative microphotographs showing the viability of MSCs cultured within type I collagen-hydroxyapatite gel (CHAP) at day 2 (A, B) and day 37 (C, D). A&C: live (green) cells labelled with calcein AM, B&D: dead (red) cells labelled with ethidium homodimer-1. Scale bar 100µm.

6.2.2. Comparison of *in vitro* culture systems

6.2.2.1. ALP activity & immunolabelling

The ALP protein activity was analysed in human MSCs cultured in monolayer, micromass and type I collagen-hydroxyapatite gel in differentiation (DM) or growth (control; GM) medium. The composition of 'GM' medium was the same as indicated in paragraph 2.2.1.1. The 'DM' medium was composed of 'GM' supplemented with 50µg/ml ascorbic acid, 10nM dexamethasone and 5mM β -glycerolphosphate.

The analysis of ALP activity at day 2, 7, 14 and 21 revealed no significant differences between MSCs cultured in micromass or type I collagen-hydroxyapatite compared to cells monolayer in DM (Fig.6.2). In DM conditions, micromass and type I collagen-hydroxyapatite demonstrated a trend of lower ALP activity compared to monolayer at day 2. An interesting trend was observed for the enzyme activity for DM groups at day 14. At that time point, ALP reached its maximum level in all culture systems. This level was the same for monolayer and type I collagen-hydroxyapatite cultures, whereas it was 1.65-fold higher for micromass (Fig.6.2). At day 7 and 21 the ALP activity was at the same level in all DM groups (Fig.6.2).

Similarly as for DM groups, the maximum ALP activity for cells in different culture systems maintained in GM was reported at day 14 (Fig.6.2). In these conditions, the enzyme activity was lower in micromass and type I collagen-hydroxyapatite cultures compared to monolayer at day 2. Similar results were reported at day 14 and 21. At day 14 the ALP activity in MSCs cultured in micromass in GM was 2.9-fold lower compared to monolayer GM group ($p=0.018$) (Fig.6.2).

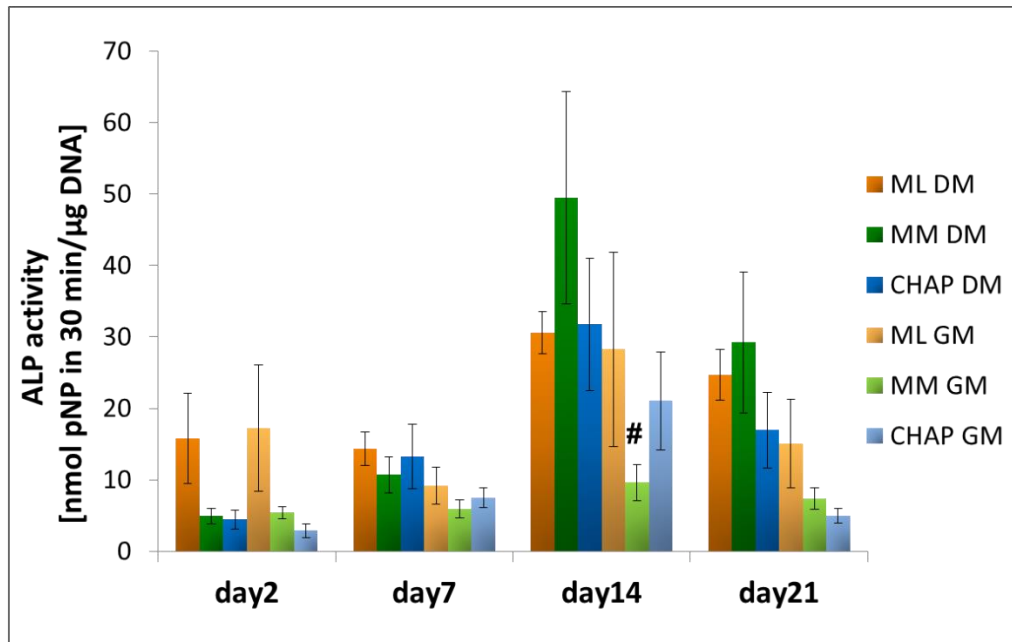


Figure 6.2. Diagram shows the mean alkaline phosphatase (ALP) activity in 30 minutes relative to the amount of DNA with the standard error of the mean (3 experiments, $n=9$). MSCs were cultured in monolayer (ML), micromass (MM) and type I collagen-hydroxyapatite gel (CHAP) in differentiation medium (DM) or growth medium (GM) for 2, 7, 14 and 21 days. Statistical significance at $p<0.05$ was determined using two-way ANOVA with Least Significant Difference adjustment for multiple comparisons. *: compared to ML DM at that time point; #: compared to ML GM compared at that time point.

In addition to the quantitative analysis, the location of ALP activity within micromass and type I collagen-hydroxyapatite gel cultures at day 14 of culture in DM and GM was determined by immunohistochemistry. A uniform labelling throughout micromass and type I collagen-hydroxyapatite was demonstrated at day 14 (Fig.6.3). Compared to GM groups, immune-labelling was more intense in DM for both, micromass and type I collagen-hydroxyapatite groups indicating higher ALP activity in DM groups. Lower activity was observed for type I collagen-hydroxyapatite groups compared to micromass groups (Fig.6.3). These observations are consistent with the protein activity data at the same time point (Fig.6.2).

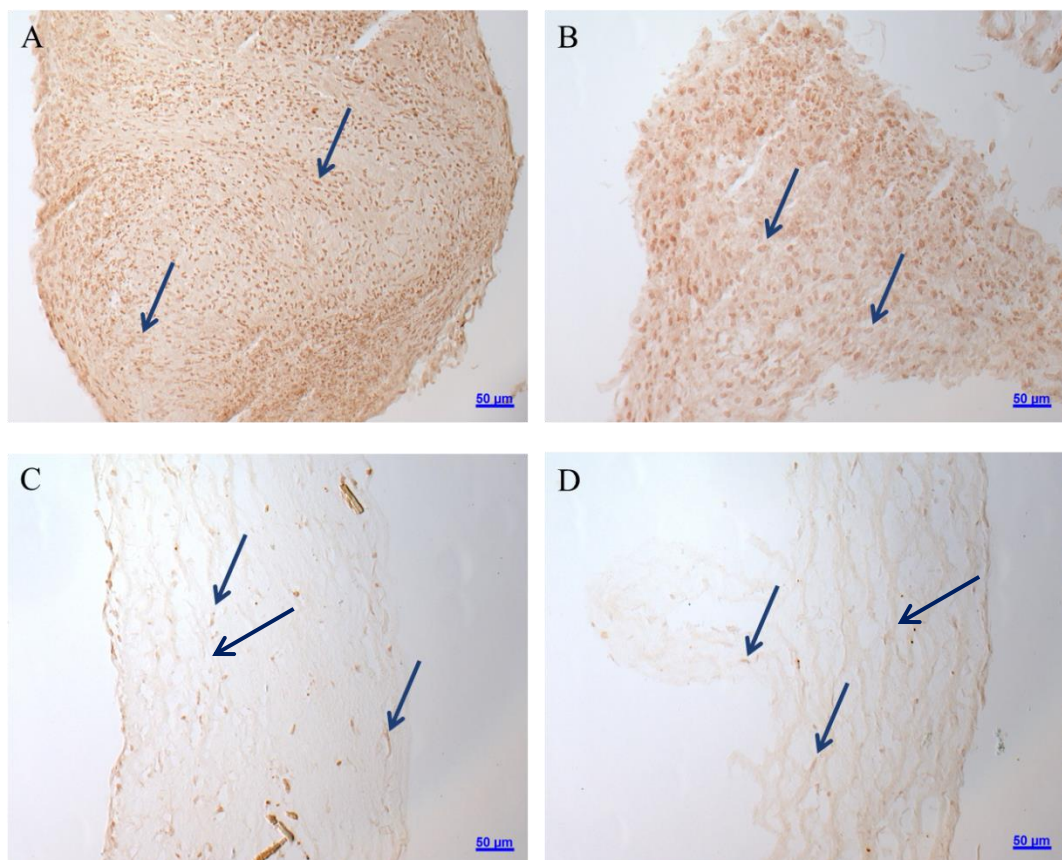


Figure 6.3. Micrographs show immuno-labelling of alkaline phosphatase detected within micromass (A, B) and type 1 collagen-hydroxyapatite (C, D) of MSCs (♂ 22 years old) at day 14 of culture in differentiation medium (A, C) and growth (control) medium (B, D). ALP positive cells are indicated by blue arrow.

Immunolabelling of osteocalcin protein within ECM during micromass and type I collagen-hydroxyapatite culture of MSCs was performed. When maintained in DM, cells remained in spherical shaped micromass, whereas MSCs cultured in GM tend to spread out and form more a loosely connected sphere-like structure (Fig.6.4). For micromass, the OC labelling was more pronounced in GM groups compared to DM. More intense cellular and ECM labelling was demonstrated for micromass groups than type 1 collagen-hydroxyapatite groups (Fig.6.4). Similar osteocalcin labelling was detected between CHAP GM and CHAP DM groups (Fig.6.4).

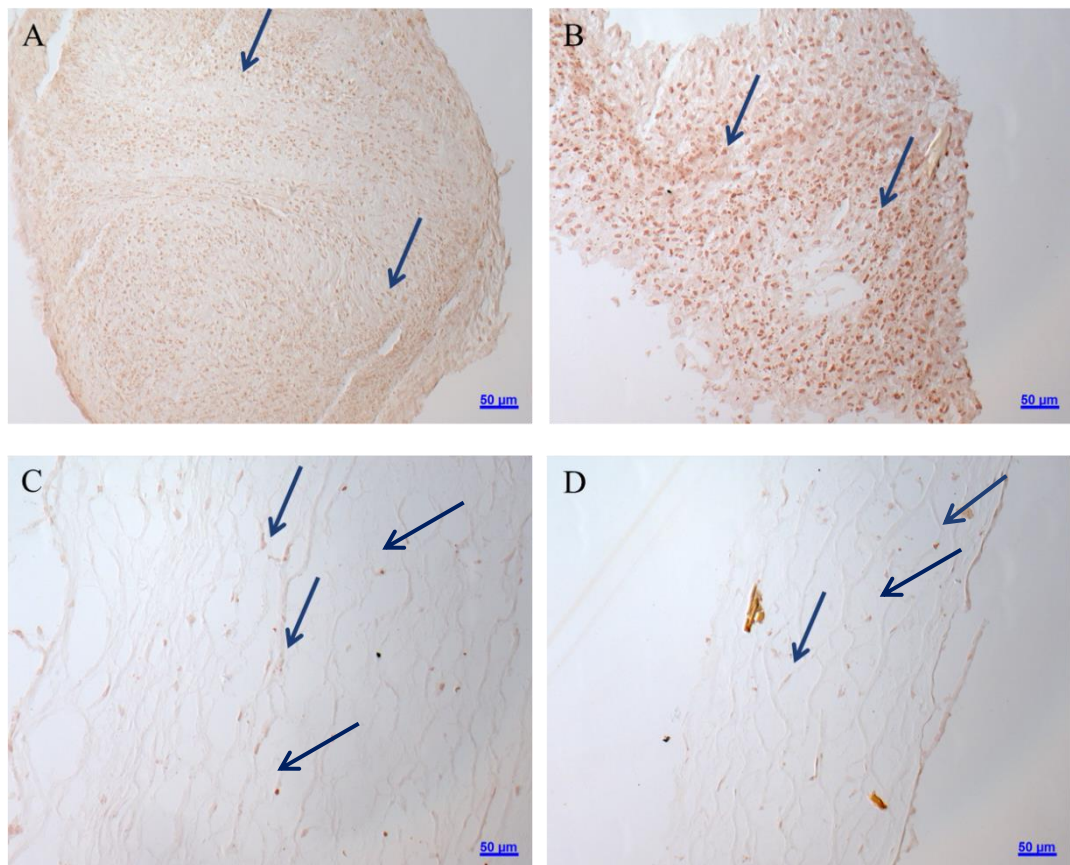


Figure 6.4. Micrographs show immuno-labelling of osteocalcin detected within micromass (A, B) and type 1 collagen-hydroxyapatite (C, D) of MSCs (♂ 22 years old) at day 14 of culture in differentiation medium (A, C) and growth (control) medium (B, D). Osteocalcin positive cells are indicated by blue arrow.

6.2.2.2. Expression of osteogenic genes in MSCs cultured in 2D and 3D

The analysis of the expression of osteoblastic genes in MSCs cultured in the different culture systems revealed high variation between cells obtained from different donors. These donors presented differing magnitudes of regulation of osteoblastic genes

(Appendix 5). Nevertheless, it was possible to perform statistical analysis of the gene expression of osteogenic markers.

In MSC monolayer cultures, maintained in differentiation or growth medium (DM and GM, respectively), Sox9 gene expression remained at the same level until day 14 (Fig.6.5A). Micromass (MM) culture gene expression levels were similar to that of monolayer. Interestingly, significant differences in Sox9 mRNA expression were detected between MSCs cultured in type I collagen gel-hydroxyapatite (CHAP) and in monolayer (ML) after 7 days of culture (Fig.6.5A). In detail, when MSCs were cultured in DM, 4.17- ($p=0.003$) and 5.2-fold ($p<0.0001$) higher Sox9 mRNA level was demonstrated for CHAP compared to monolayer at day 7 and day 14, respectively (Fig.6.5A). A similar trend was reported for MSCs cultured in these models in GM conditions with significantly higher level of Sox9 in CHAP cultures compared to monolayer at day 7 ($p<0.0001$) and 14 ($p=0.003$) (Fig.6.5A).

The culture environment has significant influence on the expression of early osteogenic marker, Runx2 (Fig.6.5B). In the presence of differentiation supplements in the medium, significant up-regulation of Runx2 mRNA was demonstrated for MSCs cultured in micromass ($p=0.01$) compared to cells in monolayer at day 2 (Fig.6.5B). Although, at later time points Runx2 expression decreased in micromass, a trend of higher mRNA expression level of this transcription factor was reported. In contrast, similar Runx2 gene expression over the culture time was reported for MSCs in monolayer and micromass cultures which were maintained in GM (Fig.6.5B). A higher level of Runx2 gene expression was demonstrated for MSCs cultured in type I collagen-hydroxyapatite in DM and GM conditions. At day 2, significant up-regulation of Runx2 mRNA was revealed for CHAP group ($p<0.0001$) compared to monolayer maintained in GM, whereas in DM the significant level was demonstrated for these groups at day 7 ($p<0.0001$) and 14 ($p=0.039$) (Fig.6.5B).

The Runx2 to Sox9 ratio, which was assessed to indicate the early osteogenic potential of MSCs, showed similar results between DM or GM groups at day 7 and 14 for cells in different culture systems (Fig.6.5C). At day 2 for MSCs in GM, the Runx2/Sox9 ratio was significantly higher in micromass ($p<0.0001$) and type

I collagen-hydroxyapatite gel ($p=0.001$) compared to monolayer (Fig.6.5C). Similarly as for GM groups, in differentiation medium, the Runx2/Sox9 ratio was higher in MSCs cultured micromass and type I collagen-hydroxyapatite than in monolayer (Fig.6.5C). However, this trend did not reach statistical significance. The ratio decreased in all DM groups with the culture time (Fig.6.5C).

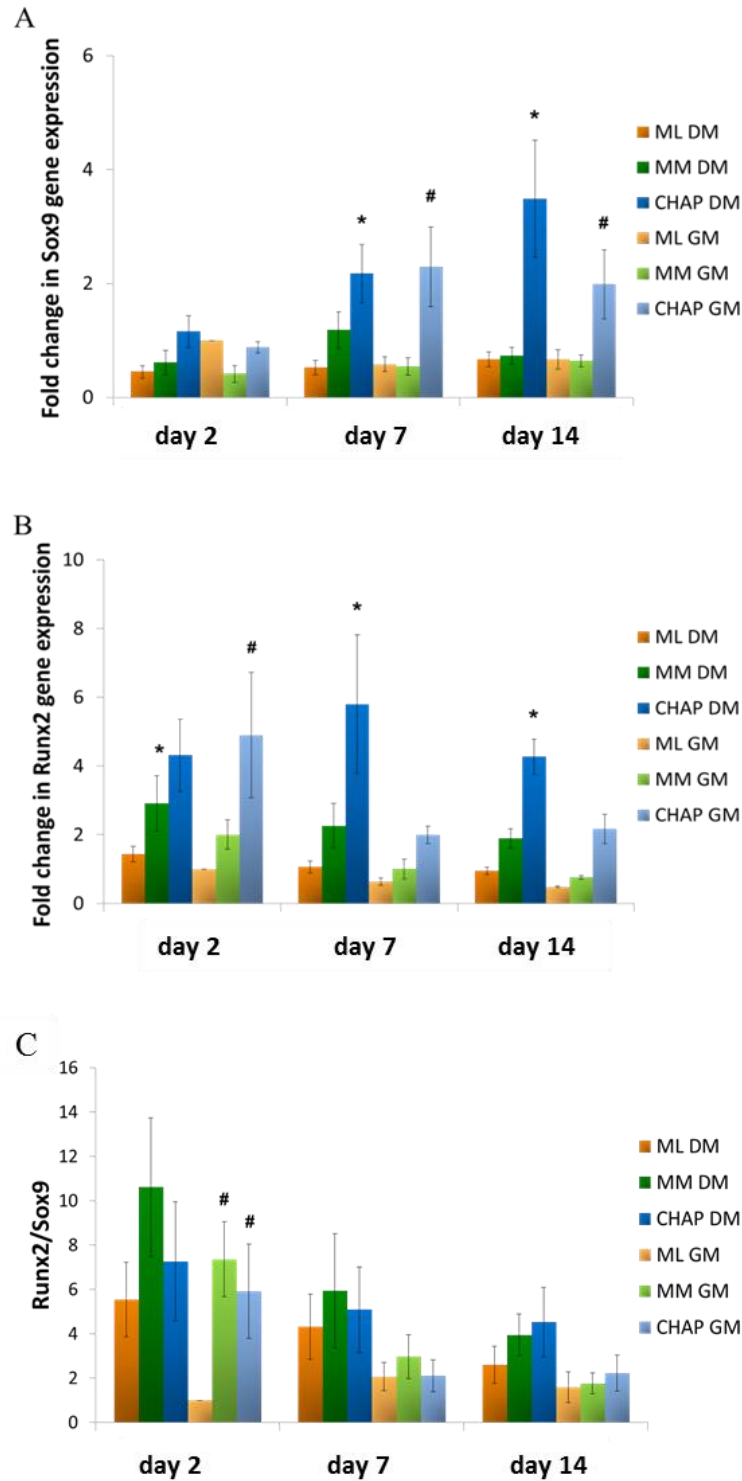


Figure 6.5. Diagrams show the gene expression of Sox9 (A), Runx2 (B) and Runx2/Sox9 ratio (C) with the standard error of the mean. MSCs were cultured in monolayer (ML), micromass (MM) and type I collagen-hydroxyapatite gel (CHAP) in differentiation medium (DM) or growth medium (GM) for 2, 7 and 14 days. Gene expression was normalised to RPL13a and made relative to ML GM at day 2 (3 experiments, n=9). Statistical significance at $p < 0.05$ was determined using two-way ANOVA with Least Significant Difference adjustment for multiple comparisons. *: compared to ML DM at that time point; #: compared to ML GM compared at that time point.

The expression of type I collagen (COL1) in MSCs cultured in three different culture models revealed no significant differences in the expression level in cells cultured in monolayer and micromass (Fig.6.6A). In addition, the expression of this gene was independent from the influence of the differentiation supplements in these culture models, which was indicated by the similar level of COL1 mRNA expression in DM and GM. On the other hand, COL1 gene expression was differentially regulated in DM and GM when MSCs were cultured in type I collagen-hydroxyapatite gel. Importantly, when MSC cultured CHAP and maintained in differentiation medium the expression of COL1 was 2.45-, 8.18- and 6-fold higher compared to monolayer at day 2, 7 and 14, respectively (Fig.6.6A). The significant differences were determined between these groups for day 7 ($p<0.0001$) and 14 ($p=0.02$). In GM conditions, the COL1 mRNA was significantly higher at day 2 ($p=0.0001$) and 14 ($p=0.046$) in MSCs cultured in type I collagen-hydroxyapatite gel compared to monolayer (Fig.6.6A).

Gene expression analysis demonstrated an increase in ALP mRNA level by day 7 in monolayer MSCs cultures maintained in DM, while in micromass the gene expression showed constant increase throughout the 14 day culture period (Fig.6.6B). These results obtained for MSCs in micromass are consistent with the ALP protein data (Fig.6.2). The statistical analysis of the results revealed no significant differences in gene expression between monolayer and micromass culture models in DM conditions. Moreover, in these culture models of MSCs maintained in growth medium, ALP mRNA remained at the same level during the whole culture time, which in the case of MM GM group deviates from the protein data (Fig.6.6B&6.2). MSCs in the gel showed a similar pattern of ALP gene expression in DM conditions as MSCs in monolayer. Although, the magnitude of the gene regulation was higher in CHAP group compared to monolayer, there were no significant differences reported (Fig.6.6B). Interestingly, when cells were maintained in GM conditions, significant up-regulation of ALP gene expression was revealed in the CHAP group compared to ML group. In detail, the ALP mRNA level was 7.05- ($p=0.002$), 23.55- ($p<0.0001$) and 40.27-fold ($p=0.0026$) higher in CHAP GM at day 2, 7 and 14, respectively (Fig.6.6B). These results deviate from ALP protein activity data (Fig.6.6B&6.2).

Significant differences in the expression of the late osteoblast phenotype marker, osteocalcin (OC), were reported between MSCs in type I collagen-hydroxyapatite and monolayer DM and GM groups (Fig.6.6C). In both conditions, the up-regulation of OC mRNA to a high extent was demonstrated for MSCs in CHAP groups. At day 2 and 14, 2.74- ($p=0.008$) and 3.31-fold ($p=0.0001$), respectively, up-regulation was reported for MSCs in CHAP DM compared to cells in ML DM (Fig.6.6C). At the same time, MSCs in type I collagen-hydroxyapatite in GM conditions had the highest up-regulation of OC mRNA on day 2, which was 4.9-fold ($p<0.0001$) higher compared to MSCs in monolayer (Fig.6.6C). While the expression decreased at later time points in CHAP GM groups, it was still significantly higher compared to ML GM groups ($p=0.0001$ for day 7 and $p=0.002$ for day 14) (Fig.6.6C).

Gene expression of E11, which is considered to be expressed by mature osteoblast cells and osteocytes (Aubin, 1998), was significantly up-regulated in both 3D culture models compared to ML (Fig.6.6D). The gene expression was at similar level for micromass cultures in DM and GM and type I collagen-hydroxyapatite gel in both culture conditions. During the whole culture time, E11 expression remained at the same level in micromass groups, which was approx. 5-fold higher compared to monolayer groups. E11 up-regulation was demonstrated when comparing the results obtained from micromass and monolayer cultures in DM at day 2 ($p=0.021$), 7 ($p=0.023$) and 14 ($p<0.0001$), respectively (Fig.6.6D). Similar results were reported for these groups during the culture in GM conditions ($p=0.045$ for day 2, $p=0.016$ for day 7 and $p=0.004$ for day 14) (Fig.6.6D). In CHAP groups, the expression of E11 mRNA reached the maximum level at day 7. Specifically, at this time point 50.76- and 25.48-fold higher expression was reported for CHAP DM ($p<0.0001$) and CHAP GM ($p<0.0001$) compared to the respective monolayer groups (Fig.6.6D). In addition, the statistical analysis of the E11 gene expression results obtained from MSCs cultured in the gel and in the monolayer, indicated the up-regulation of E11 mRNA at significant level in CHAP groups at day ($p=0.012$ for DM and $p=0.0001$ for GM) and day 14 ($p<0.0001$ for DM and $p=0.004$ for GM) (Fig.6.6D).

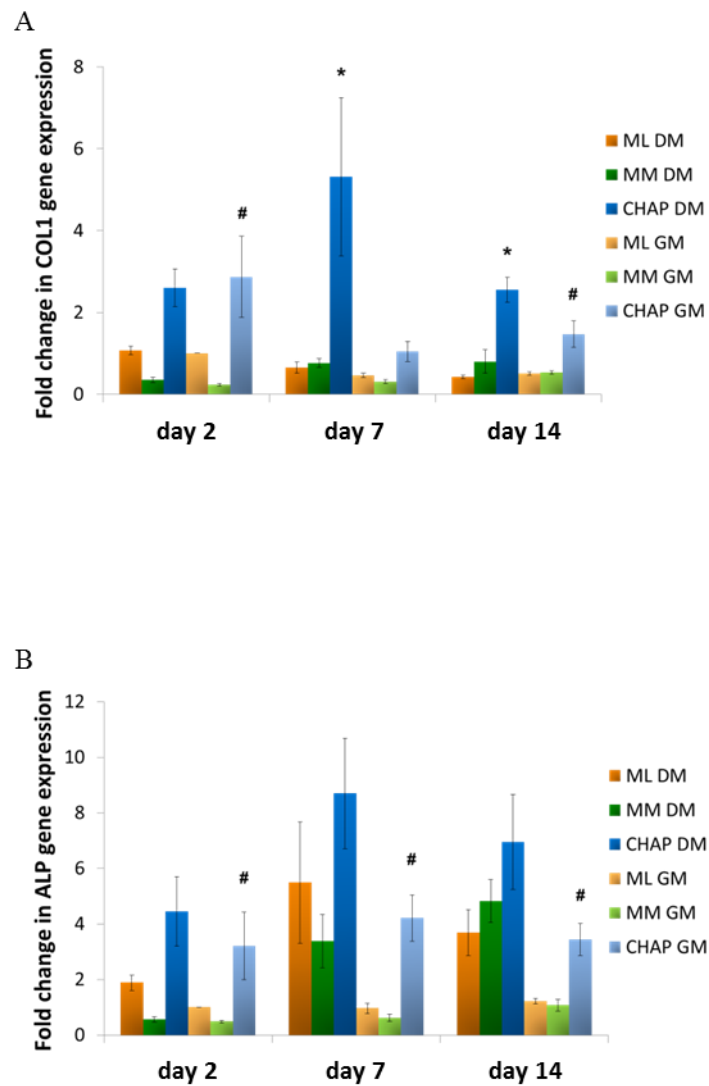


Figure 6.6.A-B. Diagrams show the gene expression of COL1 (A) and ALP (B) with the standard error of the mean. MSCs were cultured in monolayer (ML), micromass (MM) and type I collagen-hydroxyapatite gel (CHAP) in differentiation medium (DM) or growth medium (GM) for 2, 7 and 14 days. Gene expression was normalised to RPL13a and made relative to ML GM at day 2 (3 experiments, n=9). Statistical significance at $p < 0.05$ was determined using two-way ANOVA with Least Significant Difference adjustment for multiple comparisons. *: compared to ML DM at that time point; #: compared to ML GM compared at that time point.

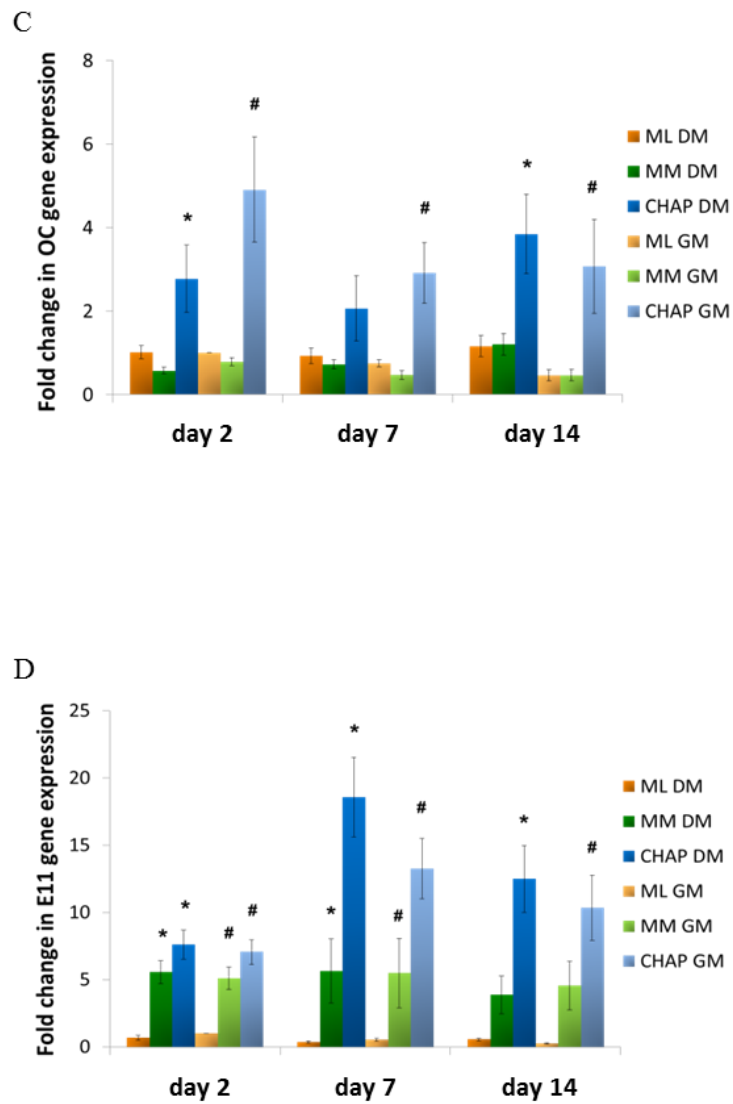


Figure 6.6.C-D. Diagrams show the gene expression ratio of OC (C) and E11 (D) with the standard error of the mean. MSCs were cultured in monolayer (ML), micromass (MM) and type I collagen-hydroxyapatite gel (CHAP) in differentiation medium (DM) or growth medium (GM) for 2, 7 and 14 days. Gene expression was normalised to RPL13a and made relative to ML GM at day 2 (3 experiments, n=9). Statistical significance at $p < 0.05$ was determined using two-way ANOVA with Least Significant Difference adjustment for multiple comparisons. *: compared to ML DM at that time point; #: compared to ML GM compared at that time point.

6.3. Discussion

Studies on the influence of the *in vitro* cell culture environment on the osteoblast-like phenotype were performed in this chapter. The differentiation of MSCs was analysed in monolayer (ML), micromass (MM) and type I collagen-hydroxyapatite (CHAP) culture systems.

The main objective of this study was to assess the osteogenic differentiation of MSCs in a 3D environment *in vitro* which would be physiologically relevant. Hence, the *in vitro* cell culture model utilising type I collagen and hydroxyapatite was established at the early phase of this study. After the successful initial optimisation of the formulation of the gel, hydroxyapatite concentration and retained cellular viability in the gel by day 37, it was used for further analysis of MSC differentiation. Based on the fact that the micromass, a high density cell culture, is supported by the proteins secreted by the cells which remain in the close cell-cell contact, it was employed as a second 3D *in vitro* model. The results obtained for MSCs cultured in these culture systems were compared to those from MSCs cultured in monolayer. For decades, the monolayer culture model has been used to investigate the osteogenic differentiation of various MSCs and osteoblasts cell models. Therefore, to relate and compare results from 3D culture models, the monolayer culture was used as a control in this study.

The results presented in this chapter indicated a strong influence of the culture model on the MSCs osteogenic differentiation. Specifically the 3D environment stimulated the osteogenic potential of MSCs compared to monolayer. Sox9 gene expression showed strong up-regulation in MSCs cultured in type I collagen-hydroxyapatite gel and Runx2 in both 3D culture models. The further analysis of the Runx2/Sox9 ratio at day 2 obtained in this study indicate the promotion of the osteogenic potential of MSCs to the higher extent in micromass and type I collagen-hydroxyapatite gel compared to monolayer. Based on recent evidence, the importance of the Runx2/Sox9 ratio for the prediction of MSCs differentiation and ECM mineralisation was shown for MSCs in monolayer cell culture. In detail, improved osteogenic differentiation of MSCs can be expected in cells with high Runx2/Sox9

ratio at the early stages of cell culture (Loebel et al., 2014a). Moreover, the reported high difference in Runx2/Sox9 ratio reported for monolayer in DM and GM and, at the same time, minimal differences in results for 3D cultures in DM and GM suggest the necessity of strong stimulus for triggering the MSCs' osteogenic potential in monolayer culture.

The further results from the analysis of the expression of osteoblast markers support the conclusions drawn from the assessment of the Runx2/Sox9 ratio. Interestingly, the expression of early and mid-term, type I collagen and ALP genes, respectively, but not late osteogenic genes, including OC and E11, demonstrated the temporal changes during 14 day culture of MSCs in monolayer. At the same, late osteogenic genes were regulated over 14 days in micromass and type I collagen-hydroxyapatite gel cultures of MSCs. In addition, the magnitude of gene expression was dramatically higher in MSCs cultured in type I collagen-hydroxyapatite gel compared to MSCs in monolayer.

In detail, in monolayer culture of MSCs type I collagen gene expression decreased with culture time in differentiation medium, which was positively correlated with the increase in of the ALP gene and protein expression in monolayer culture. There were only small changes in COL1 and ALP gene expression for MSCs in monolayer cultured in the absence of the differentiation supplements. In contrast, the expression of COL1 gene expression demonstrated a small increase in MSCs cultured in micromass in both type of media. This increase in differentiation medium was positively correlated with the ALP gene expression and protein activity by day 14, while in micromass maintained in growth medium, the ALP expression and activity showed only little up-regulation with time of culture. The highest enzyme activity was demonstrated for MSCs cultured in micromass in differentiation medium compared to the other groups in both, differentiation and growth, media types. Interestingly, the enzyme activity was lower for MSCs cultured in type I collagen-hydroxyapatite gel than in monolayer. The qualitative analysis of ALP protein distribution performed for micromass and type I collagen-hydroxyapatite groups confirmed

the quantitative results regarding the extent of the ALP activity in micromass and lower in type I collagen-hydroxyapatite gel.

The ALP activity demonstrated by the immunolabelling in CHAP cultured in DM and GM demonstrated stronger intensity in DM groups. Interestingly, on the gene expression level ALP and COL1 were strongly up-regulated in MSCs cultured in CHAP in medium with and without differentiation supplements. In fact, in significant up-regulation of ALP and COL1 genes was demonstrated for CHAP in GM compared to ML. It has been suggested that dexamethasone stimulation of cells stimulates the osteogenic differentiation of cells in *in vitro* culture through up-regulation of ALP gene and protein expression (Wong et al., 1990). Since that time the formulation of medium used for osteogenic differentiation includes dexamethasone in the 10-100nM concentration range (Wong et al., 1990; Bellows et al., 1994; Yang et al., 2003). Our results suggest that the interaction of MSCs with the ECM protein, type I collagen, is as powerful a stimulus to induce ALP gene expression in MSCs as dexamethasone. Although, ALP protein activity was similar in both type I collagen-hydroxyapatite and monolayer culture, this could be due to the differential post-translational processes in 2D and 3D culture or the incomplete lysis of the samples collected for ALP assay. Indeed, the same protocol was used for monolayer, micromass and type I collagen-hydroxyapatite to extract samples for the assay. It remains to be evaluated whether a prolonged lysis over 3 hours has an influence on the assay results.

The mRNA results of OC and E11 expression clearly demonstrated the differential regulation in 2D and 3D cultures. OC is considered as late osteoblast marker since its accumulation in ECM of the bone was timed after the initiation of mineral deposition (Price et al., 1981; Owen et al., 1990). The expression of E11 is considered as reflecting an even more advanced stage of osteogenic differentiation and formation of cell processes associated with osteoblast-osteocyte transformation (Zhang et al., 2006; Franz-Odenaal et al., 2006). In our culture systems, the significant up-regulation of OC compared to monolayer was reported during the whole culture time for MSCs cultured in CHAP but not in micromass. Although, there was no difference in OC gene expression in micromass cultured

in differentiation and growth medium, a more intense staining was observed for cultures in growth medium, while similar expression of OC in both types of media was observed for MSCs cultured in the gel. At the same time, in both 3D culture models, E11 gene expression was up-regulated. These results clearly indicate that the regulation of E11 gene is induced in 3D culture, but OC gene expression is specifically regulated only in type I collagen-hydroxyapatite culture. Based on the previous evidence, the osteogenic differentiation of cells in monolayer progress towards maturation after matrix synthesis, and it can be stimulated in monolayer culture when the substrate is coated with the ECM protein (Lian and Stein, 1995; Lynch et al., 1995). Our results support this observation, indicating that the expression and synthesis of type I collagen, the main bone ECM protein, is essential to induce expression of the late osteoblast marker gene, osteocalcin.

Interestingly, a clear correlation in the decrease of OC and increase of E11 gene expression for type I collagen-hydroxyapatite (CHAP) and micromass was evident, while the expression of both genes remained at the basic level during the whole culture time in monolayer. In addition, the expression of both OC and E11 demonstrated time-dependent expression changes in the only in CHAP samples, indicating the active regulation of these genes in the gel culture model. Altogether, the presented results suggest strong stimulatory effect of the interaction of MSCs with type I collagen on the osteogenic differentiation of MSCs. This is emphasised by the fact that when MSCs were maintained in medium without any exogenous supplements the expression of osteogenic markers was significantly higher in type I collagen-hydroxyapatite than in monolayer culture. We did not focus on the statistical analysis of the results between micromass and type I collagen-hydroxyapatite culture *per se* as our aim was to directly compare 3D models with monolayer culture which is a standard model for investigating osteogenic differentiation of cells but it could be observed that the differentiation of MSCs can reach more advanced stage in type I collagen-hydroxyapatite than micromass by day 14.

It would be of interest to investigate the osteogenic differentiation of MSCs in different culture models in more details including the analysis of events at later

time points than day 14. Regarding the osteogenic differentiation *in vitro* the temporal analysis progression of differentiation is conducted during 28 days' time frame. With the extension of the investigations, a more detailed analysis focused on the elucidation of processes associated with maturation of cells could be included. In particular, it is not clearly known how primary human cells undergo the transition towards mature osteoblast cells and differentiate further into osteocytes. It is known that the investigations of these processes are not possible in monolayer cell culture model. We believe that by applying the introduced in this chapter type I collagen-hydroxyapatite gel a more detailed analysis of the late stages of differentiation would be possible. In fact, in a similar model based on type I collagen, as presented in this chapter, osteoblast cells were able to migrate in the collagen gel and expressed osteocyte specific genes, including sclerostin (SOST), phosphate-regulating neutral endopeptidase X-linked (PHEX), dentin matrix acidic phosphoprotein 1 (DMP1) after 21 days of culture (Uchihashi et al., 2012). Yet, in the aforementioned study the murine osteoblast cells, MC3T3E1, were used which raise the concern regarding the species associated differences. In fact, most evidences on the subject of terminal differentiation of osteoblasts originate from the analysis performed using *in vitro* rodent cell models. Therefore, the analysis based on the results from primary human cells would bring a great value to the current state of knowledge. In addition, the comparative analysis of differentiation in micromass and CHAP could elucidate on the appropriateness of the culture model to investigate the specific type of ossification process.

In summary, the results presented in this chapter demonstrated three different patterns of MSC differentiation in all three cell culture models. The comparison of the osteogenic potential and progression in osteogenesis based on gene expression and protein analysis revealed strong influence of culture model on MSCs differentiation (Fig.6.7). Each culture model triggered the gene regulation in a different manner. Based on these results, a careful consideration of selection of the culture model prior any future *in vitro* studies is strongly advised.

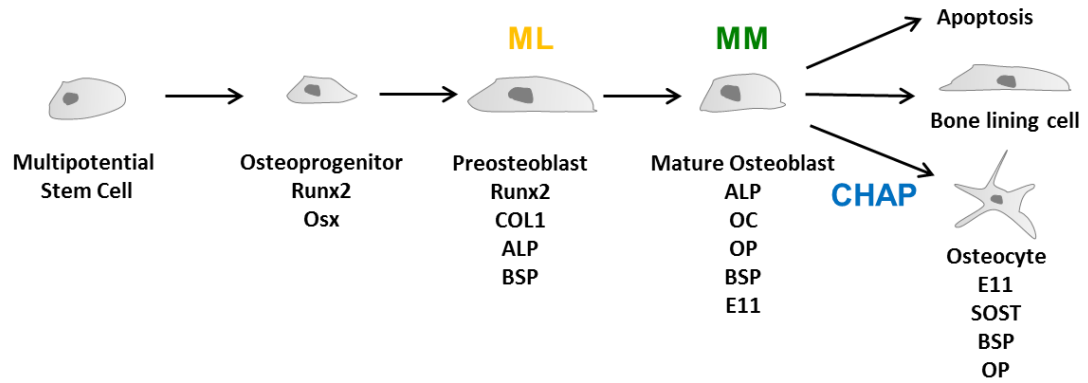


Figure 6.7. Stages of osteoblast lineage cells differentiation implying the results obtained from MSCs cultured in monolayer (ML), micromass (MM) and type I collagen-hydroxyapatite (CHAP) for 14 days. Based on the analysis of gene (Sox9, Runx2, ALP, COL1, OC, E11) and protein (ALP, OC) expression, it is proposed that MSCs cultured in monolayer undergo differentiation process up to the stage of preosteoblasts, while in micromass MSCs reach the stage of mature osteoblast phenotype. In CHAP, MSCs could reach a more differentiated stage leading to osteocyte phenotype. Runx2 – runt-related transcription factor 2, Osx – osterix (=Sp7), COL1 – type I collagen, ALP – alkaline phosphatase, OC – osteocalcin, OP – osteopontin, BSP – bone sialoprotein, E11=podoplanin, SOST – sclerostin.

CHAPTER 7

GENERAL DISCUSSION

Bone is a unique tissue with high potential for self-regeneration. Yet, the treatment of traumatized and degenerated tissue is still a major clinical need. Tissue engineering and stem cell therapy are a big hope to support the regeneration process of bone. However, before clinical application, a detailed *in vitro* analysis and understanding of the processes occurring *in vivo* is required. This thesis highlights the importance of reliable and physiologically relevant *in vitro* cell and culture models. Its main objective is to support the development of new strategies for bone regeneration through defining and evaluating the relevancy of *in vitro* models. For this, the first part of this thesis aimed to investigate different osteoblast cell lines which are currently widely used to determine their relevance in bone-related research, including the evaluation of novel biomaterials. The second part focuses on the evaluation of various *in vitro* 3D culture models to determine the relevance of *in vitro* culture models in relation to the regulation of osteogenic differentiation of osteoblastic lineage cells. Finally, the role of paracrine signalling by MSCs was investigated for determining the potential role of these cells in directing bone regeneration.

7.1. Cell culture models

Within this thesis, four types of osteoblast cells were investigated, including primary human long bone osteoblast cells, SaOs2, MG63 and MC3T3E1. All of these cell types are generally used as osteoblast cell culture models in many areas of bone research, such as developmental, pharmacological, pathophysiology and biomaterial investigations (Zinger et al., 2005; Bitar et al., 2008; Peter et al., 2005; Nakayama et al., 2004; Siddiqi et al., 2014). It becomes evident that for studies focusing on human bone biology, the use of human osteoblast cells is the most relevant. Nevertheless, the limited availability and donor-related variations in osteoblast phenotype, contributed to the development of various osteoblast cell lines from different origins. These cell lines have been well characterised; however, few studies have directly compared the phenotype of these cells to primary human osteoblasts (Pautke et al., 2004; Saldana et al., 2011; Clover and Gowen, 1994). Hence, as a response to this, SaOs2, MG63 and MC3T3E1 cells were compared with primary human osteoblast

cells in chapter 3. We based our investigations on the previously established and accepted model of primary osteoblast cell phenotype progression in monolayer culture (Lian and Stein, 1992).

SaOs2, MG63 and MC3T3E1 cell lines were selected for comparison of their phenotype with primary human osteoblast cells due to their presence as osteoblast cell models in an increasing number of scientific reports focused on the evaluation of novel biomaterials for bone research (Degasne et al., 1999; Lincks et al., 1998; Maekawa et al., 2008; Zinger et al., 2005). It is of utmost importance to provide a reliable and adequate cell culture model which would closely resemble the behaviour of primary human osteoblast cells.

Differences in the growth kinetics, ECM mineralisation and regulation in osteoblast specific genes between cell types were evident. From all included cell lines, MC3T3E1, immortalised mouse calvarial osteoblasts, displayed similar proliferation kinetics to HOB's. MG63 and SaOs2 displayed a greater deviation from HOB proliferation kinetics. MG63 showed similar pattern of growth kinetics, but at much higher rate than HOB's. In case of SaOs2, cells did not reach plateau. Instead a sustained phase of exponential growth was reported. Considering these differences in results, the origin of cells has to be kept in mind. Both MG63 and SaOs2 are cell lines of human origin from osteosarcoma in which cells proliferation capability is infinite due to defective control on their cell cycle (Read and Strachan, 1999).

Primary human cells that were used in this study developed a mature phenotype, which was confirmed by mineral deposition within the ECM after 3 weeks of culture. The mineralisation was preceded by an increase in ALP protein activity which reached a maximum at day 14 of cell culture. Interestingly, the expression of type I collagen (COL1) showed temporal changes in the analysed population of primary human osteoblast cells, while Runx2, ALP and OC mRNA expression remained constant in these cells. The analysis ALP protein and ECM mineralisation indicated differences in the regulation of gene expression and mineralisation potential of SaOs2, MG63 and MC3T3E1. Ultimately, results from chapter 3 indicated that SaOs2 cells were shown to behave in the most similar way regarding the regulation

of gene expression and ALP activity, while MC3T3E1 mineralisation potential was similar to HOb's. MG63 cells presented the least similarities regarding the osteogenic gene expression and mineralisation potential compared to mature HOb's.

There is vast knowledge regarding the maturation of MC3T3E1; however, to our knowledge, the side-by-side comparison to the primary human osteoblast cells has not been performed. Our results indicated the similarities of these cells regarding the proliferation of cells and mineralisation potential. Although, the responsiveness to dexamethasone was distinct for MC3T3E1 from results obtained for human cells (Lian et al., 1997; Haynesworth et al., 1992), the mineralisation potential of MC3T3E1 was not compromised compared to primary human osteoblast cells (chapter 3). In fact, there was a similar mineralisation potential of these cells compared to primary HOb's after 21 days in culture when both cell types were plated at the same initial cell density (5000 cells per cm²) and cultured in the presence of dexamethasone. However, it would be of interest to further analyse this similarity of HOb's and MC3T3E1 regarding the nature of deposited substrate. While MC3T3E1 cells were shown to mineralise their matrix (Sudo et al., 1983; Franceschi and Iyer, 1992), detailed Fourier transform infrared spectroscopy (FTIR) analysis of the deposits demonstrated a lack of calcium phosphate mineralisation and the presence of dystrophic mineralization of unknown origin (Bonewald et al., 2003).

The obtained results regarding the osteogenic phenotype of primary human and osteosarcoma cells are in agreement with previously published reports (Clover and Gowen, 1994; Pautke et al., 2004; Saldana et al., 2011). Similarly as presented in chapter 3, the high ALP activity and mineralisation potential of SaOs2 has been previously demonstrated (Rao et al., 1996; Rodan et al., 1987; Saldana et al., 2011). Moreover, similar growth inhibition and ALP activity in SaOs2 and HOb's on a clinically relevant material Titanium-6% Aluminium-4% Vanadium (Ti6Al4V) alloy and Ti particles indicates the potential of this cell type in the assessment of biomaterials (Saldana et al., 2011). However, compared to HOb's, gene expression, differences in SaOs2 were demonstrated for Runx2, COL1 and OC. It has to be noted that for COL1 and Runx2 these differences were significant only

for later time points. Runx2 demonstrated an evident trend of higher expression in SaOs2 compared to HOb's with statistical significance at day 21. These results suggest a more mature phenotype of SaOs2 cells than the HOb population used in this study. In fact, with the Alizarin Red S staining for mineral deposition, a more advanced formation of nodules was reported for SaOs2 compared to HOb's. This conclusion supports previously published work (Pautke et al., 2004; Rao et al., 1996; Rodan et al., 1987). Since SaOs2 cells have a mature osteoblastic phenotype and possess high matrix mineralisation capacity, they should not be used for studies determining the progression in osteoblastic phenotype or assessing material osteoconductivity.

MG63 cells displayed opposite results than SaOs2 cells compared to HOb's. The ALP activity was marginal in this cell type. With increasing time only a small population of cells was ALP positive. These results were reflected at the gene expression level. During the time course of this study, ALP gene expression was lower in MG63 than in HOb's. Similar trends were reported for COL1 and OC gene expression. In the former, this trend only became significant on day 21. Interestingly, an opposite trend to COL1 was detected for Runx2, where Runx2 was up-regulated compared to HOb's except on day 21. In addition, the lower expression of osteoblast specific proteins, such as ALP and type I collagen, has been recognised before (Pautke et al., 2004). These results suggest a differential regulation of more mature osteoblast genes in MG63 and HOb's, which is not necessarily directed by Runx2, known as master transcription factor for osteoblast differentiation (Ducy, 2000). In addition, on both, tissue culture polystyrene and Ti6Al4V, the regulation of ALP activity up to day 7 was at lower level in MG63 compared to HOb's (Saldana et al., 2011). Within chapter 3, MG63 presented a very immature phenotype compared to HOb's; this was emphasised by the lack of calcium deposition. Therefore, MG63 cells are only a suitable cell model to examine closer the processes directing osteoblastic differentiation of cells over time and factors stimulating this process. Having this in mind, we used this cell line for investigations whether the interaction of MG63 and MSCs has a mutual influence on the development of more mature osteoblastic phenotype (chapter 4). In addition, due to the fact that MG63 has similarities

to primary human osteoblast cells regarding the expression of integrin subunits, including α_2 , α_5 , α_V , β_1 , β_3 , (Sinha and Tuan, 1996; Clover et al., 1992), they may be a good alternative for studies interested in initial attachment to various materials. Although, in this thesis, we focused on indirect cell-cell communication (chapter 4), the further analysis of the direct cell-cell contact on osteogenic differentiation would bring more information regarding the signalling pathways regulation of osteogenesis in different cell-cell contact modes.

Therefore, we developed an osteoblast cell line with a stable and homogeneous expression of green fluorescent protein (GFP; chapter 4), which was based on MG63 cells. With the approach of selecting colonies from single cell cultures we obtained highly homogeneous populations of cells. In result, similar characteristics, including proliferation rate and osteoblastic phenotype development, of these cells compared to the 'mother cell line' MG63 were confirmed. This cell line provides the opportunity to discriminate two cell types in direct monolayer or 3D co-culture for subsequent analysis. In addition, MGreen63 cell line could serve as a reliable model for non-destructive, on-line monitoring of cytotoxicity and cytocompatibility of biomaterials over time. In addition, it allows the analysis of direct cell-cell communication with proper discrimination between two cell populations to be performed. The same approach can be applied to a more mature osteoblast cell line to enable mineralization studies to be performed.

It has to be mentioned that even though the direct comparison of cell lines was performed with primary human osteoblast cells, limitations of this study are present which leaves room for further investigations. One of these is related to HOb's which were used as reference cell type for our investigations. Precisely, primary osteoblast cells from one donor were included for comparison with SaOs2, MG63 and MC3T3E1 cell lines. It has been recognised that the phenotype and activity of primary human osteoblast cells is highly dependent on such parameters as age, gender, origin site/site of origin and the isolation method (Battmann et al., 1997;Katzburg et al., 1999;Zhang et al., 2004;Jonsson et al., 1999). Therefore, rather than postulating on existing differences between cell lines and primary human osteoblast cells from human population from our results, it is more relevant in this

case to refer to specific population of primary osteoblast cells. Specifically, HOb's used in this study were isolated from proximal tibia of 6 years old female donor. We believe that these osteoblast cells are represent population of highly active osteoblast cells and therefore are relevant for this study. However, it is evident that including osteoblast cells from more donors, particularly adult cells, would be beneficial for this study considering the significant analysis of statistical population and biological relevance of obtained results. In addition, including cells obtained from donors with pathological conditions, such as osteoporosis or osteoarthritis, would help to select the cell models which could be used for screening of new pharmacological agents.

In addition, the formulation of culture medium for each cell type differed from that used for HOb's. In detail, for each cell type medium included the supplementation with the same concentration of ascorbic acid (50 μ g/ml), but differed in the concentration of dexamethasone and b-glycerolphosphate (β GP). Results from the initial experiments, in which cell lines were maintained in the medium with the same formulation as the one for HOb's, demonstrated a negative effect of medium supplement, β GP, on SaOs2 viability even at a low dose of 2 mM (data not shown). Previous reports demonstrated the supplementation of medium with β GP in small doses for cells with high osteogenic potential (Orriss et al., 2012). Since this strategy did not bring any benefit/improvement for SaOs2 cells viability, the comparison of cell phenotype was conducted in the conditions supporting the viability and behaviour of each cell type in the best way (reviewed in (Czekanska et al., 2012)).

7.2. *In vitro* 2D and 3D co-culture models

Part of the studies for this thesis concentrated on the investigation of cell differentiation (chapter 6) and communication (chapter 4&5) of bone cells. The analysis of the indirect communication of osteoblast with progenitor cells was motivated by the fact that currently there are limited and conflicting evidence regarding the influence of crosstalk between these cells on their osteogenic phenotype development (Csaki et al., 2009;Buttery et al., 2001;Tsai et al., 2012;Kim

et al., 2003). What is more, out of these reports, only few investigate the effects of crosstalk between human MSCs and osteoblasts (Ilmer, Seto). This limits the discussion of our results in relation to the previously published data, but at the same time indicates the need for further exploration of MSCs-osteoblast crosstalk effects.

The first set of experiments focused on analysing of the influence of cell crosstalk in indirect monolayer co-culture followed by investigations in high density (micromass; MM) indirect co-culture.

The results from the ALP protein activity assay at day 14, gene expression analysis, and Ca incorporation assay suggested the delayed osteogenic differentiation in MSCs co-cultured with MG63, compared to single cell type cultures (control) of MSCs in monolayer. In more detail, while the ALP protein activity was at the same level in co-cultured and control MSCs at day 14, the mRNA level at day 21 of Runx2, ALP and OC was lower in co-cultured MSCs. At the same time Ca incorporation showed a trend of lower uptake in MSCs from co-cultures than in control MSCs cultures.

A more pronounced effect of the co-culture of MSCs with MG63 was reported on the osteoblast cells. When MG63 cells were located on the insert membrane in differentiation medium, the expression of Runx2, ALP, COL1 and OC mRNA as well as and Ca incorporation at day 21 were at higher level in co-cultured cells than in MG63 cultured alone. For cells located in the well no influence of the co-culture on MG63 phenotype was reported. In both configurations of the co-culture, i.e. when MG63 cells were cultured on the membrane or in the well, the ALP activity was at the same level in co-cultured cells as in single cell type cultures. As presented in chapter 3 and in other reports, MG63 cells demonstrate low ALP protein activity (Pierschbacher et al., 1988;Saldana et al., 2011;Czekanska et al., 2013). Hence, the indirect co-culture of MG63 with MSCs is not a sufficient stimulus to regulate the ALP activity in MG63 cells. The obtained results from indirect monolayer co-culture indicated a positive influence on osteogenic gene expression and ⁴⁵Ca uptake in MG63 cells, whereas it has an opposite effect on MSCs.

Following the investigation of cell crosstalk in monolayer, the attention was directed towards indirect cell-cell communication in a micromass culture system. Our objective was to analyse the cell crosstalk in a 3D culture system which would be a step closer and, therefore, more relevant to the cells natural *in vivo* environment.

Additionally, in the setting of micromass co-culture side-by-side in the well we could exclude the potential variables related to the different location and growth surface parameters, which had a prominent effect in monolayer co-culture.

In contrary to the results obtained for MG63 cell in monolayer co-cultures, no differences in the expression of osteoblast genes, including Runx2, COL1, ALP and OC, were observed in MG63 cells co-cultured with MSCs at day 21. At the same time, differences were demonstrated for MSCs co-cultured with MG63 cells compared to single cell type MSCs culture. Specifically, in DM and GM conditions the ALP mRNA expression was significantly lower in co-cultured MSCs, while the expression of Runx2 and COL1 showed a trend of lower expression in co-cultured MSCs compared to single cell type culture of MSCs. The OC gene expression was significantly higher in MSCs co-cultured with MG63 cells compared to control MSCs micromass in growth medium, whereas no differences were reported between these groups in differentiation medium.

To relate the differences in osteoblastic gene expression to the phenotypic stage of cells, the analysis of COL1/Runx2, ALP/Runx2, OC/Runx2 ratios was performed. We postulate that by relating the mRNA of the COL1, ALP, OC to Runx2 the magnitude of the progression of the osteogenic differentiation can be demonstrated. This assumption is based on the importance of Runx2 at the early stages of osteoblast differentiation (Ducy, 2000;Zhou et al., 2006). It is considered that this transcription factor is crucial for osteogenic differentiation of progenitor cells by inducing the expression of osteoblast specific genes, such as ALP, OC, BSP (Komori, 2010). Runx2 gene expression regulation in primary osteoblasts is species specific. Conversely to primary rat osteoblasts *in vitro* culture, the Runx2 gene expression in human primary osteoblasts remains at the same level over time (Lian

and Stein, 1995;Czekanska et al., 2013). Hence, the gene expression ratios give the valuable information regarding the differentiation stage for ostoprogenitor cells in which Runx2 is decreased at the later stages of differentiation (Komori, 2010). The analysis of the genes' ratio indicated significant differences between MSCs co-cultured with MG63 and single cell type cultures in cultures maintained in GM. The COL1/Runx2 and ALP/Runx2 were lower while OC/Runx2 ratio was higher in co-cultured MSCs compared to MSCs cultured alone. Similar relations were demonstrated for OC/Runx2 and ALP/Runx2 in co-cultured or control MSCs micromasses in differentiation medium, whereas the COL1/Runx2 was at the same level in these conditions for both groups.

The results indicate a lower activity of ALP when MSCs were co-cultured with MG63 cells. Further analysis of the ^{45}Ca incorporation into micromass cultures at day 21 revealed no effect of the co-culture on the mineralisation potential of the cultures.

Altogether, the investigation of indirect cell-cell communication in the micromass culture system demonstrated significant effects on the osteogenic gene regulation in MSCs, but no such effects on MG63 cells. The obtained results could suggest both, suppression or stimulation of osteogenic differentiation of MSCs in co-culture with MG63. It has to be taken into account that the ALP activity assay was performed at day 14 and the analysis of osteogenic genes related to the early, mid-term and late differentiation stage at day 21. Since ALP activity and the expression of early (Runx2) and mid-term (ALP, COL1) was decreased, while OC mRNA expression increased in co-cultured MSCs at these time points, it could be hypothesised that the co-culture of MSCs with MG63 cells in micromass stimulates the osteogenic differentiation of MSCs. At the same time, the lack of any effect of co-culture on MG63 cells suggest that in micromass culture system, the more differentiated cell type stimulates the differentiation of more phenotypically primitive cell population. These results are especially interesting in relation to bone healing where coordinated communication between cells is highly important for the regeneration process.

A more detailed investigation focusing on the analysis at the molecular level at earlier time points, and histological analysis of protein expression would bring more clear insight and verification of the postulated beneficial effects of micromass co-culture on MSC differentiation. It would be interesting to analyse the one-way paracrine communication by culturing MSCs with medium conditioned by MG63 cells to assess whether the stimulation paracrine activity of osteoblasts is strictly related to the 3D or whether there is any feedback loop in MSCs-MG63. Additionally, the analysis of cell-cell communication in direct co-culture could be determined. Employing the MGreen63 cell line as an osteoblast cell model would allow for the separation of cells in co-culture and detailed analysis. Currently, more attention has been directed towards indirect cross-talk. From the reports focusing on analysis of the effects of the direct cell-cell communication, it is surprising that only a few looked at the interactions of osteoblasts with progenitor cells (Tsai et al., 2012;Csaki et al., 2009;Wang et al., 2007;Kim et al., 2003). In addition, these reports present conflicting results. It has been reported that in direct co-culture the differentiation of MSCs, marked by ALP activity and calcium deposition, depends on the proportion of cells in the co-culture. The ALP activity and mineralisation of nodules was found to be higher in co-cultures with increased proportion of osteoblast cells to 50% in co-cultures compared to controls (Tsai et al., 2012;Csaki et al., 2009). Concurrently, the calcium deposition was shown at lower level in co-cultures compared to single cell type cultures (Kim et al., 2003), which is opposed to the results presented here. Yet, it has to be kept in mind that all these studies as cell models included murine MSCs and osteoblasts or rabbit MSCs and rat osteoblast cells. This may explain the differences in the results, and raises questions regarding the relevance of these results in relation to human cells interactions (Tsai et al., 2012;Csaki et al., 2009;Kim et al., 2003).

The results regarding the cell crosstalk suggested that 1) the secretion of osteopermissive factors or/and 2) the sensitivity of cells to these factors can be modulated by *in vitro* culture environment. To verify the first hypothesis, we analysed whether the stimulation of the secretion profile of MSCs with IL1 β or SCF would exert a pronounced effect on osteogenic differentiation of unstimulated cells in monolayer culture (Chapter 5). The functional analysis

of the secretome from stimulated MSCs with IL1 β and SCF revealed no significant effect on unstimulated MSCs' proliferation or differentiation. Specifically, we reported similar ECM calcification in MSCs cultured with medium from stimulated or unstimulated cells. It is known that chronic supplementation of human MSCs cultures with IL1 β induces the osteogenic differentiation (Loebel et al., 2014b; Ferreira et al., 2012). Even shorter, 48 hours stimulation of rat MSC *in vitro* cultures with IL1 β , increased nodule formation and the calcium content within (Lin et al., 2010). However, there are no previous reports regarding the indirect effects of both, IL1 β and SCF on osteogenesis. Nevertheless, it was surprising that only small differences in the expression of osteogenic genes were reported only at day 7 suggesting the possible paracrine effects on MSCs at early, proliferative stage of cells. Nevertheless, recently it was reported that much shorter treatment of cells induces long term response of MSCs. Recently, it has been shown that only 15 minutes stimulation of MSCs with BMP2 induces the stimulation of osteogenic differentiation over the nonstimulated cells (Overman et al., 2013a; Overman et al., 2013b). Even though, these results become from directly stimulated cells, it was very interesting that in this study the effect of stimulation was reported only when cells were cultured on a calcium phosphate scaffold, while in monolayer there was no significant effect of BMP2 stimulation on differentiation (Overman et al., 2013a). The osteogenic differentiation and response to the stimulation is regulated in a different manner in monolayer and in 3D culture. As presented in the co-culture of MSCs and MG63 (chapter 4) the regulation of MSC osteogenic differentiation was stimulated in a 3D culture (micromass), but it was inhibited in monolayer. It seems that in monolayer cells became unresponsive to the action of certain factors. Hence, the application of the proper *in vitro* culture model is critical for the analysis of the effects of bioactive molecules in relation to the directing of cell differentiation.

In summary, based on our results from monolayer and micromass co-culture, and the aforementioned report by Overmann and co-workers (Overman et al., 2013a; Overman et al., 2013b), it appears that the sensitivity of progenitor cells to paracrine factors is modulated by *in vitro* culture environment.

7.3. *In vitro* culture environment and osteogenic differentiation

The evaluation of the *in vitro* cell environment focused on the analysis and comparison of osteoblast phenotype development of MSCs in micromass or type I collagen-hydroxyapatite gel, to the differentiation of cells in monolayer (chapter 6). Micromass was chosen for these investigations since the positive influence of co-culture with MG63 on MSCs osteogenic differentiation in micromass was observed (chapter 4). The motivation to develop a type I collagen-hydroxyapatite gel as second 3D culture model was based on the physiological relevance of both components of this model.

Conventionally, in the monolayer culture system the osteogenic differentiation of cells progress through 3 phases, proliferation, matrix synthesis, and mineralisation (Lian and Stein, 1992). Each stage can be characterised by the expression of specific genes and proteins (Owen et al., 1990;Lian and Stein, 1992). In our study, the analysis of early (Sox9, Runx2), mid-term (ALP, COL1) and late (OC, E11) osteogenic markers was analysed at protein and/or gene expression level.

Our results demonstrated that in monolayer MSC culture, in the presence of osteogenic supplements, osteogenic differentiation is induced, as demonstrated by the increase of Runx2 gene expression and Runx2/Sox9 ratio. Based on the ALP protein data, the maturation of ECM could be expected after day 14 of monolayer culture. This is not unusual with primary human MSCs. The analysed expression of OC and E11 gene demonstrated no changes in mRNA expression by day 14 in both DM and GM conditions. These results support the conclusion that the differentiation of human MSCs into a mature osteoblastic phenotype in monolayer occurs at a later time point than that included in this study, which is in line with previous reports (Lian and Stein, 1992;Guillot et al., 2008).

In micromass, the induction and progression of MSCs differentiation was more strongly induced compared to monolayer. The ALP protein activity, relative to the DNA amount, was the highest for micromass maintained in differentiation medium compared to the other groups. Although, the OC gene expression was similar in micromass as in monolayer, the expression of other late osteogenic

marker, E11, was strongly up-regulated in micromass cultures. E11 expression is considered as reflecting an advanced stage of osteogenic differentiation and formation of cell processes associated with osteoblast-osteocyte transformation (Zhang et al., 2006; Franz-Odenaal et al., 2006). Based on these results, we could speculate that the potential of high density micromass culture of MSCs to promote enhanced osteogenic differentiation compared to monolayer within the 14 day time frame.

In fact, high density cell culture models have attracted a lot of attention within the last few years as potential culture models for recapitulating events occurring during *in vivo* endochondral ossification. The formation of chondro-osseous structures within pellet culture of MSCs or human femur foetal-derived cells was demonstrated (Muraglia et al., 2003; Scotti et al., 2010; Tortelli et al., 2010; El-Serafi et al., 2011). Interestingly, the morphological structure of pellets is highly dependent on cell type, density and culture media. Human femur foetal-derived cells in pellet cultures maintained in osteogenic medium only were able to form the osseous shell around the cartilage-like pellet core, while in the case of MSCs from bone marrow pellet culture, the stimulation of both, chondrogenic followed by osteogenic differentiation, is required to obtain similar results (El-Serafi et al., 2011; Muraglia et al., 2003). The development of an even more mature phenotype is facilitated in a high density pellet culture system as demonstrated previously in our group (Jahn et al., 2010). In a pellet culture system of primary human osteoblast cells, where proliferation of cells is restricted to the population at the outer part of a pellet, a rapid differentiation of towards osteocyte-like phenotype was achieved (Jahn et al., 2010). Here, we demonstrated temporal changes in osteogenic differentiation of MSCs at the gene expression level, and faster stimulation of osteogenic differentiation of MSCs in micromass compared to monolayer culture. The results are in agreement with the aforementioned studies which supports the potential of this simple culture model for *in vitro* research of endochondral bone formation. Nevertheless, it would be of interest to perform more detailed analysis of the influence of micromass culture on osteogenic differentiation of MSCs on both gene expression and protein level over the long term, to establish a defined serum-free culture medium formulation.

This would provide a culture model in which the differentiation would be strictly directed by cells without any influence of the factors present in serum.

Based on the fact that type I collagen is the main protein of bone and its accumulation is fundamental for osteoblast differentiation (Lynch et al., 1995), the third culture model included in this chapter for the analysis of directing MSCs osteogenic differentiation was type I collagen-hydroxyapatite gel. Type I collagen gel influences the osteogenic differentiation interacting with $\alpha_2\beta_1$ integrin on cell surface which activates mitogen-activated protein kinase (MAPK) signalling pathway, leading to phosphorylation of Runx2 and osteocalcin expression promoter (Wenstrup et al., 1996;Xiao et al., 1998;Uchihashi et al., 2012). The approach of utilising type I collagen gel for osteoblast cell culture has been addressed (Lynch et al., 1995;Buxton et al., 2008). However, instead of maintaining cells on pre-coated surface as previously described, attention was directed to establish a type I collagen gel culture system with the approach of formulating in this thesis a culture system with an even distribution of cells within the gel, while not compromising cell viability.

Since the previous reports indicated a negative influence of the collagen cross-linking agents on cell viability (Brinkman et al., 2003;Wollensak et al., 2004), we focused on the formulation of gel without the cross-linking of collagen fibres. Hydroxyapatite was added as it possesses osteoconductive properties and in addition improves the mechanical stability of the gel. The results from preliminary experiments showed retained stability of the gel and cell viability up to 37 days. Further analysis indicated that the type I collagen-hydroxyapatite culture system supported MSC differentiation towards osteoblasts, which was marked by the high levels of Runx2/Sox9 ratio, COL1, ALP, OC and E11 gene expression. In addition, ALP activity was demonstrated by immunolabelling in type I collagen-hydroxyapatite cultured cells in both differentiation and control medium. The immunostaining of OC did not reveal clear correlation with gene expression results. Instead, comparable detection intensity was reported in MSCs maintained in both types of medium. These results are not surprising, taking into the account the regulatory processes occurring after mRNA is transcribed, including post-

transcriptional, translational and protein degradation regulation, which control steady-state protein abundances (Vogel and Marcotte, 2012). It seems that the OC protein expressions undergo specific regulatory processes and further parallel/simultaneous analysis of OC mRNA and protein expression over time would reveal the significance of this discrepancy.

Similarly to our results, the positive stimulation of OC gene expression and ALP activity was demonstrated for rat osteoblast cultures on type I collagen tissue polystyrene surface (Lynch et al., 1995). Further investigations revealed the promotion of mineral deposition of osteogenic cells in culture system based on type I collagen gel (Pedraza et al., 2010;Thibault et al., 2010). In our study, we did not analyse the mineralisation process directly. However, based on presented results, including the expression of E11 gene, we could speculate that the differentiation of MSCs towards the osteocytic phenotype is promoted in type I collagen-hydroxyapatite gel. Uchihashi and co-workers demonstrated the potential of type I collagen culture of osteoblasts to support differentiation of osteoblast cells into osteocyte phenotype (Uchihashi et al., 2012). In more detail, the expression of sclerostin (SOST), phosphate-regulating neutral endopeptidase X-linked (PHEX), dentin matrix acidic phosphoprotein 1 (DMP1), which are associated with the osteocytic phenotype, was reported after 21 days of culture (Uchihashi et al., 2012). We believe that type I collagen-hydroxyapatite gel could serve as model for the investigation of full osteocytic differentiation process of MSCs. However, further evaluation is needed, including the analysis the expression of osteocyte-specific markers, to make strong conclusions regarding the potential of osteocyte phenotype development in the type I collagen-hydroxyapatite gel. With the positive results, type I collagen-hydroxyapatite gel could serve, for instance, as a model for the research of indirect effects of stimulation with different cytokines.

7.4. Enhancing the secretion profile of MSCs

It has been recognised that in addition to their direct support of tissue regeneration through lineage specific differentiation, stem cells secrete bioactive factors acting in auto- and paracrine manner and regulating the immune response (Hsiao et al.,

2012;Tsiridis et al., 2007;Zhukareva et al., 2010). This recent identification regarding the potential of paracrine MSCs signalling within the damaged tissue contributed to naming MSCs as an “injury drugstore” (Caplan and Correa, 2011).

Bone TE, combined with stem cell therapy, emerged as an alternative to the gold standard autologous bone graft for bone reconstruction. Currently, the focus is directed towards a one-step procedure as it overcomes the disadvantages of two-step procedures, including the requirement for two surgical procedures, increased risk of contamination and extensive *in vitro* cell expansion (Coelho et al., 2012). The intra-operative enrichment and application of autologous bone marrow aspiration concentrate for the treatment of diseases of the musculoskeletal system has been evaluated as a safe and effective procedure (Hendrich et al., 2009). Yet, the limited amount of the osteoprogenitor cells is critical for the successful outcome (Hernigou et al., 2008). Together with the decreasing number of osteoprogenitor cells with age (Caplan, 1994;Maijenburg et al., 2011), concern arises regarding the engraftment yield and further performance of cells, including the production of bioactive molecules and paracrine activity of cells.

In chapter 5 of this thesis, the modulation of paracrine activity of MSCs was performed by preconditioning of cells. Its principle is to prepare cells by mimicking the hostile microenvironment, in which the cells will be engrafted, by pre-exposure to growth factors, cytokines or chemical agents. It is surprising that the application of pre-conditioned stem cells has been widely explored in relation to soft tissues and to a lesser extent in relation to bone (reviewed by (Baraniak and McDevitt, 2010;Haque et al., 2013;Hsiao et al., 2013)). This motivated us to investigate the influence of pre-conditioning of cells with cytokines normally present at the site of bone injury, including Stem Cell Factor (SCF), interleukin 1 β (IL1 β), stromal cell-derived factor 1 (SDF1) and granulocyte colony-stimulating factor (GCSF). Having in mind a one-step clinical concept for bone regeneration, we limited the stimulation time to 2 hours, which is clinically applicable. To our knowledge, this is the first study undertaking this aim in relation to bone tissue.

By stimulating MSCs with different cytokines for 2 hours, we reported sustained effects of the treatment after 48 and 72 hours on gene and protein expression level of various cytokines. At first, the influence of the pre-conditioning with cytokines was evaluated at the gene expression level for four different factors, IL1 β , GCSF, SCF and SDF1. The obtained results confirmed our hypothesis that the short-term stimulation of MSCs *in vitro* has a long term effect on the regulation of the gene expression profile of the cells.

Following these results, we were interested whether the pre-conditioning has more functional effects, i.e. is the regulation of cytokine genes coupled with the regulation of protein expression? To answer this question, the following experiments focused on the closer examination of gene and protein expression profile of MSCs stimulated with IL1 β or SCF. The analysis of the obtained results, of the regulated cytokine genes and proteins, revealed that 2 hours stimulation has a strong influence on both, cytokine gene and protein expression. The secretome analysis demonstrated that forty eight hours after the stimulation 20 cytokine proteins of 174 were regulated in a similar manner in MSCs from 5 donors in response to IL1 β and 12 in response to SCF treatment. The functional analysis of the protein data indicated that these cytokines induce the secretion mainly different classes of cytokines (chapter 5, tab.5.2). Specifically, IL1 β induced the secretion of proteins acting during cell mobilisation, proinflammatory response, angiogenic and osteogenic differentiation, while SCF regulated mitogenic, chondrogenic and ECM regulation proteins.

In addition, we reported interesting associations of Wnt signalling pathway components with the expression of genes and proteins regulating osteoclastogenesis. Based on these results we speculated that short term stimulation with IL1 β and SCF could have an indirect inhibitory effect on osteoclastogenesis. Currently, IL1 β is considered as a potent inducer of osteoclasts differentiation, nucleation and survival (Nakamura and Jimi, 2006;Konig et al., 1988), which in chronic inflammatory conditions, such as rheumatoid arthritis, leads to bone resorption (Abramson and Amin, 2002;Teitelbaum, 2006). On the other hand, IL1 β is inadequate to induce osteoclast differentiation from precursors (Kim et al, 2009). Our study indicated the possible mechanisms of osteoclastogenesis inhibition

as a secondary effect of MSCs stimulation with IL1 β (through down-regulation of RANKL and up-regulation of TNFRSF11 genes in stimulated cells) which could have an effect on the promotion of osteoclast differentiation. Conversely, the secretion of RANTES and GM-CSF, factors stimulating osteoclasts differentiation, after IL1 β treatment was previously demonstrated (Zhukareva et al., 2010). However, the secretion of these proteins was reported after 24 hours treatment (Zhukareva et al., 2010). These results together with the proteins secretion data show a strong influence of IL1 β on stimulation of early events occurring during bone regeneration and the potential in its support. Hence, it emerges as an attractive factor for aiding the regeneration of bone in complicated injuries or severe conditions where the concerns regarding a successful outcome of the treatment are high.

Similar results regarding the regulation mechanism of osteoclastic differentiation as for IL1 β were reported for SCF treatment. In addition, other secondary mechanisms potentially involved in the regulation of osteoclastogenesis were modulated by SCF, including the up-regulation of IL18 stimulating the production of granulocyte macrophage colony-stimulating factor (GM-CSF), known as osteoclasts inhibitor, by T-cells (Harwood, 1998; Gracie, 2003). Stem cell factor (SCF) plays important role during development in haematopoiesis, melanogenesis and spermatogenesis, as well as during the regeneration of damaged tissues. It has been suggested that SCF strongly stimulates survival, mobilization and differentiation of hematopoietic stem cells. Indeed, upon activation SCF induces mobilization, recruitment and neovascularization activity of endothelial progenitor cells (EPCs) (Kim et al., 2011). *In vivo* studies demonstrated that intravenous administration of SCF promoted heart regeneration after myocardial infarction and recovered haematopoiesis after irradiation. SCF activates cells through binding to tyrosine kinase proto-oncogene receptor, c-kit, which is expressed on primitive and mature progenitor cells within bone marrow, megakaryocytes and platelets (McNiece and Briddell, 1995). Very recently, SCF has been described as fast acting chemokine due to its immediate effect on ERK and AKT phosphorylation observed after only 3-5 min stimulation of dental pulp cells (Pan et al., 2013). SCF-containing collagen sponges implanted subcutaneously in mice contained more cells, capillaries and had increased remodelling comparing to constructs without SCF (Pan et al.,

2013). The results presented in this thesis show, for the first time, that SCF activity is not limited to the direct stimulation of chemotaxis and differentiation of hematopoietic cells, but could exert a powerful effects during bone repair. With the 2 hours stimulation of MSCs, the processes of endochondral bone regeneration, including chondrogenesis, ECM regulation and osteoclastogenesis, can be regulated by SCF in indirect way. Further *in vitro* experiments with stimulation of freshly isolated MSCs in suspension are essential for the closer insight of the stimulation effects in clinical application setting of stem cell therapy. Following this, *in vivo* analysis is essential to evaluate the functional effects of preconditioned cells at the injury site. It has to be considered that the potential of implanted cells may change in response to the microenvironment.

The results we reported here were obtained from MSCs isolated from bone marrow of different donors. The effect of donor-variability was clearly seen in the magnitude of response to the treatment. Similarly to recent report by Zhukareva and co-workers, we demonstrated that similar patterns of expression can be reported for cells from responsive donors (Zhukareva et al., 2010). In addition to the donor variability, the variation of secretion profile from MSCs is associated with the site of isolation. Comparing the basic level of secreted proteins significant differences were demonstrated between MSCs derived from adipose tissue, bone marrow, dermal tissues (dermal sheath cells and dermal papilla cells) and umbilical cord blood regarding the angiogenic paracrine activity of MSCs (Hsiao, 2010; Jin, 2013). The superiority of cells derived from adipose tissue over the other sources has been demonstrated (Hsiao, 2010), which also suggest the possible differential response of MSCs from different isolation origin to stimulation with cytokines.

7.5. Influence of the culture model and dexamethasone on osteocalcin expression

It cannot remain unnoticed that in our experimental settings of co-cultures and 3D cultures osteocalcin gene expression was up-regulated in control conditions, i.e. in medium without any osteogenic supplements. Specifically, regarding co-

culture experiments (chapter 4), at day 14 the OC gene expression was higher in MG63 co-cultured with MSCs in monolayer and in MSCs co-cultured with MG63 in micromass. Similarly, primary human bone derived cells stimulated the expression of Runx2, COL1, ALP, OC, BSP and mineralisation of human embryonic stem cells (CHA-hES3) in the absence of any exogenous factors (Ahn et al., 2006). A more detailed analysis of gene expression over time would reveal whether this could be observed for earlier osteoblastic markers, such as Runx2, COL1 and ALP. In co-culture with conditioned medium of MSCs, OC mRNA was at higher level at day 7 and 14 in cells from cultures without any exogenous differentiation factors supplementation (chapter 5). Although, it is likely that these effects are related to the indirect co-culture, it is also possible that the regulation of OC gene expression is associated with the presence of osteogenic supplements. In fact, when MSCs were cultured alone in monolayer and 3D cultures (chapter 6), the expression of OC gene expression was strongly up-regulated in cells cultured in type I collagen-hydroxyapatite gel in growth medium. Based, on our results we could speculate that the regulation of OC gene expression in MSCs is stimulated by both, paracrine factors secreted by other cells and by the interaction of cells with type I collagen gel which is inhibited by the presence of osteogenic supplements. The most probably this is caused by dexamethasone.

Dexamethasone is a synthetic member of the glucocorticoid class of steroid drugs which imitates the action of many glucocorticoids located in the body, including cortisol, estradiol, testosterone, vitamin D₃, thyroxine and retinoic acid (Kamran et al., 2011). Since it was demonstrated that dexamethasone up-regulation of ALP gene and protein expression and therefore, promotes the osteogenic differentiation of cells in *in vitro* culture (Wong et al., 1990), it has been included as the constituent of osteogenic differentiation medium. In fact, dexamethasone acts at multiple stages of the differentiation process to stimulate osteoblastic maturation *in vitro* (Porter, 2003). With time it became evident that the effect of dexamethasone on osteogenic differentiation of bone cells depends on the cell origin, donor age, glucocorticoid concentration and the duration of administration (Dietrich et al., 1979; Wong et al., 1990; Sutherland et al., 1995; Fernandes et al., 1997; Coelho and Fernandes, 2000; Porter et al., 2003; Jorgensen et al., 2004). In relation to rat bone marrow

stromal derived cells, dexamethasone is a necessity for *in vitro* bone nodule formation and mineralisation (Maniatopoulos et al., 1988). Similarly, it was concluded that the optimal *in vitro* osteogenic differentiation of human cells can be achieved upon stimulation of cell cultures with supplementation, including dexamethasone (Jaiswal et al., 1997). Importantly, a strong relation of dexamethasone treatment of osteoblastic cells on decreased proliferation and type I collagen synthesis and increased ALP activity and mineralization have been demonstrated (Wong et al., 1990; Kim et al., 1999; Jorgensen et al., 2004; Cheng et al., 1994). At the same time of stimulation of mineralization, a negative influence of dexamethasone has been widely reported. Specifically, dexamethasone is a powerful inhibitor of OC mRNA expression which was demonstrated by the sustained down-regulation of OC gene over 28 day culture period after the stimulation of human bone marrow stromal cells for only 24 hours (Cheng et al., 1996). Moreover, in human osteoblastic cells the vitamin D₃-induced osteocalcin expression is strongly inhibited upon the exposure of cells to dexamethasone (Wong et al., 1990; Jaiswal et al., 1997; Jorgensen et al., 2004).

All of the presented evidences regarding the action of dexamethasone on the regulation of osteogenic differentiation are based on the results from single cell type culture of osteoblast lineage cells in monolayer. In fact, in some cases the expression of osteocalcin was absent without the stimulation with vitamin D₃ of monolayer osteoblast cell cultures (Jaiswal et al., 1997; Jorgensen et al., 2004). Interestingly, the accelerated expression of osteocalcin was reported in 3D cultures compared to monolayer or in 3D co-cultures of progenitor cells co-cultured with osteoblasts in monolayer (Lynch et al., 1995; Ahn et al., 2006; Uchihashi et al., 2012). The results of OC gene expression in different culture settings and conditions collected in this thesis are in the agreement with these studies. In addition they indicate only little influence of dexamethasone supplementation in single cell type monolayer culture of cells on OC gene expression. Hence, we speculate that osteocalcin could be successfully induced upon 3D cell-ECM or paracrine interaction of cells in 3D *in vitro* culture. In support of the second part of this statement, it should be noted that the inhibition of IL1 β -induced paracrine mediators

in human MSCs, osteoblasts and retinal microvascular pericytes by dexamethasone was demonstrated (Chaudhary and Avioli, 1994; Nehme and Edelman, 2008).

7.6. Summary

The results presented in this thesis demonstrated that significant differences exist between *in vitro* osteoblast lineage cells and culture models. The use of cell lines as an osteoblast cell model should be carefully considered and limited to appropriate and specific research questions due to the phenotypic variances compared to primary human osteoblast cells. In addition, the type cell culture model is critical for investigating the osteogenic differentiation and cell-cell communication *in vitro*. An active signalling pathway between MSCs and osteoblasts exist which is altered in monolayer and 3D (micromass) culture model. While the paracrine activity of cells can be modulated by cytokines in monolayer, the secondary effects of cytokine treatment do not exert any profound response on cells in monolayer culture. A 3D *in vitro* culture model emerges as being more physiologically relevant for the analysis of cell-cell communication and osteoblastic differentiation. The progression in osteogenesis depends on the applied 3D culture model. While in both, micromass and type I collagen-hydroxyapatite gel, the differentiation is enhanced compared to monolayer, the regulation of this process is triggered different manner. Further investigations are advised to elucidate in more details to what extent the osteogenic differentiation can be recapitulated in these 3D *in vitro* models. Ultimately, our data provide substantial evidence that the osteoblastic differentiation of cells *in vitro* is differentially modulated in 2D and 3D culture models. With the proper application of *in vitro* model a more *in vivo*-related osteogenic differentiation and its regulation can be achieved and investigated. This is fundamental for the development of new cell-therapeutic strategies and regenerative medicine.

REFERENCES

Aarden EM, Wassenaar AM, Alblas MJ, Nijweide PJ (1996) Immunocytochemical demonstration of extracellular matrix proteins in isolated osteocytes. *Histochem Cell Biol* **106**: 495-501.

Abe Y, Aida Y, Abe T, Hirofuji T, Anan H, Maeda K (2000) Development of mineralized nodules in fetal rat mandibular osteogenic precursor cells: requirement for dexamethasone but not for beta-glycerophosphate. *Calcif Tissue Int* **66**: 66-69.

Abramson SB, Amin A (2002) Blocking the effects of IL-1 in rheumatoid arthritis protects bone and cartilage. *Rheumatology (Oxford)* **41**: 972-980.

Ahmadbeigi N, Shafiee A, Seyedjafari E, Gheisari Y, Vassei M, Amanpour S, Amini S, Bagherizadeh I, Soleimani M (2011) Early spontaneous immortalization and loss of plasticity of rabbit bone marrow mesenchymal stem cells. *Cell Prolif* **44**: 67-74.

Ahn SE, Kim S, Park KH, Moon SH, Lee HJ, Kim GJ, Lee YJ, Park KH, Cha KY, Chung HM (2006) Primary bone-derived cells induce osteogenic differentiation without exogenous factors in human embryonic stem cells. *Biochem Biophys Res Commun* **340**: 403-408.

Anderson HC (2003) Matrix vesicles and calcification. *Curr Rheumatol Rep* **5**: 222-226.

Arnett TR (1990) Update on bone cell biology. *Eur J Orthod* **12**: 81-90.

Arnsdorf EJ, Tummala P, Jacobs CR (2009) Non-canonical Wnt signaling and N-cadherin related beta-catenin signaling play a role in mechanically induced osteogenic cell fate. *PLoS One* **4**: e5388.

Aronow MA, Gerstenfeld LC, Owen TA, Tassinari MS, Stein GS, Lian JB (1990) Factors that promote progressive development of the osteoblast phenotype in cultured fetal rat calvaria cells. *J Cell Physiol* **143**: 213-221.

Artaza JN, Bhasin S, Magee TR, Reisz-Porszasz S, Shen R, Groome NP, Meerasahib MF, Gonzalez-Cadavid NF (2005) Myostatin inhibits myogenesis and promotes adipogenesis in C3H 10T(1/2) mesenchymal multipotent cells. *Endocrinology* **146**: 3547-3557.

Aubin JE (1998) Advances in the osteoblast lineage. *Biochem Cell Biol* **76**: 899-910.

- Aubin JE, Triffitt JT (2002) Mesenchymal stem cells and osteoblast differentiation. In: Principles in bone biology (Bilezikian, J. P., Rodan, G. A., and Raisz, L. G., eds), 2nd edn. Academic Press, 59-81.
- Auf'mkolk B, Hauschka PV, Schwartz ER (1985) Characterization of human bone cells in culture. *Calcif Tissue Int* **37**: 228-235.
- Auf'mkolk B, Schwartz ER (1985) Biochemical characterizations of human osteoblasts in culture. *Prog Clin Biol Res* **187**: 201-214.
- Baraniak PR, McDevitt TC (2010) Stem cell paracrine actions and tissue regeneration. *Regen Med* **5**: 121-143.
- Bard DR, Dickens MJ, Smith AU, Zarek JM (1972) Isolation of living cells from mature mammalian bone. *Nature* **236**: 314-315.
- Battmann A, Battmann A, Jundt G, Schulz A (1997) Endosteal human bone cells (EBC) show age-related activity in vitro. *Exp Clin Endocrinol Diabetes* **105**: 98-102.
- Bellows CG, Aubin JE, Heersche JN (1987) Physiological concentrations of glucocorticoids stimulate formation of bone nodules from isolated rat calvaria cells in vitro. *Endocrinology* **121**: 1985-1992.
- Bellows CG, Aubin JE, Heersche JN, Antosz ME (1986) Mineralized bone nodules formed in vitro from enzymatically released rat calvaria cell populations. *Calcif Tissue Int* **38**: 143-154.
- Bellows CG, Heersche JN, Aubin JE (1992) Inorganic phosphate added exogenously or released from beta-glycerophosphate initiates mineralization of osteoid nodules in vitro. *Bone Miner* **17**: 15-29.
- Bellows CG, Wang YH, Heersche JN, Aubin JE (1994) 1,25-dihydroxyvitamin D3 stimulates adipocyte differentiation in cultures of fetal rat calvaria cells: comparison with the effects of dexamethasone. *Endocrinology* **134**: 2221-2229.
- Bergot C, Wu Y, Jolivet E, Zhou LQ, Laredo JD, Bousson V (2009) The degree and distribution of cortical bone mineralization in the human femoral shaft change with age and sex in a microradiographic study. *Bone* **45**: 435-442.
- Bilbe G, Roberts E, Birch M, Evans DB (1996) PCR phenotyping of cytokines, growth factors and their receptors and bone matrix proteins in human osteoblast-like cell lines. *Bone* **19**: 437-445.
- Billiau A, Edy VG, Heremans H, Van DJ, Desmyter J, Georgiades JA, De SP (1977) Human interferon: mass production in a newly established cell line, MG-63. *Antimicrob Agents Chemother* **12**: 11-15.

- Bilousova G, Jun dH, King KB, De LS, Chick WS, Torchia EC, Chow KS, Klemm DJ, Roop DR, Majka SM (2011) Osteoblasts derived from induced pluripotent stem cells form calcified structures in scaffolds both in vitro and in vivo. *Stem Cells* **29**: 206-216.
- Bitar M, Brown RA, Salih V, Kidane AG, Knowles JC, Nazhat SN (2008) Effect of cell density on osteoblastic differentiation and matrix degradation of biomimetic dense collagen scaffolds. *Biomacromolecules* **9**: 129-135.
- Boland GM, Perkins G, Hall DJ, Tuan RS (2004) Wnt 3a promotes proliferation and suppresses osteogenic differentiation of adult human mesenchymal stem cells. *J Cell Biochem* **93**: 1210-1230.
- Bolander ME (1992) Regulation of fracture repair by growth factors. *Proc Soc Exp Biol Med* **200**: 165-170.
- Bonewald LF (2010) The Amazing Osteocyte. *J Bone Miner Res.*
- Bonewald LF, Harris SE, Rosser J, Dallas MR, Dallas SL, Camacho NP, Boyan B, Boskey A (2003) von Kossa staining alone is not sufficient to confirm that mineralization in vitro represents bone formation. *Calcif Tissue Int* **72**: 537-547.
- Bonjour JP, Theintz G, Buchs B, Slosman D, Rizzoli R (1991) Critical years and stages of puberty for spinal and femoral bone mass accumulation during adolescence. *J Clin Endocrinol Metab* **73**: 555-563.
- Boskey AL (2008) Cell culture systems for studies of bone and tooth mineralization. **108**: 4716-4733.
- Bostrom MP, Lane JM, Berberian WS, Missri AA, Tomin E, Weiland A, Doty SB, Glaser D, Rosen VM (1995) Immunolocalization and expression of bone morphogenetic proteins 2 and 4 in fracture healing. *J Orthop Res* **13**: 357-367.
- Boyce BF, Aufdemorte TB, Garrett IR, Yates AJ, Mundy GR (1989) Effects of interleukin-1 on bone turnover in normal mice. *Endocrinology* **125**: 1142-1150.
- Boyle WJ, Simonet WS, Lacey DL (2003) Osteoclast differentiation and activation. *Nature* **423**: 337-342.
- Brinkman WT, Nagapudi K, Thomas BS, Chaikof EL (2003) Photo-cross-linking of type I collagen gels in the presence of smooth muscle cells: mechanical properties, cell viability, and function. *Biomacromolecules* **4**: 890-895.
- Buttery LD, Bourne S, Xynos JD, Wood H, Hughes FJ, Hughes SP, Episkopou V, Polak JM (2001) Differentiation of osteoblasts and in vitro bone formation from murine embryonic stem cells. *Tissue Eng* **7**: 89-99.

- Buxton PG, Bitar M, Gellynck K, Parkar M, Brown RA, Young AM, Knowles JC, Nazhat SN (2008) Dense collagen matrix accelerates osteogenic differentiation and rescues the apoptotic response to MMP inhibition. *Bone* **43**: 377-385.
- Cao XY, Yin MZ, Zhang LN, Li SP, Cao Y (2006) Establishment of a new model for culturing rabbit osteoblasts in vitro. *Biomed Mater* **1**: L16-L19.
- Caplan AI (1994) The mesengenic process. *Clin Plast Surg* **21**: 429-435.
- Caplan AI, Correa D (2011) The MSC: an injury drugstore. *Cell Stem Cell* **9**: 11-15.
- Carano RA, Filvaroff EH (2003) Angiogenesis and bone repair. *Drug Discov Today* **8**: 980-989.
- Chaudhary LR, Avioli LV (1994) Dexamethasone regulates IL-1 beta and TNF-alpha-induced interleukin-8 production in human bone marrow stromal and osteoblast-like cells. *Calcif Tissue Int* **55**: 16-20.
- Chen L, Tredget EE, Wu PY, Wu Y (2008) Paracrine factors of mesenchymal stem cells recruit macrophages and endothelial lineage cells and enhance wound healing. *PLoS One* **3**: e1886.
- Chen TL, Fry D (1999) Hormonal regulation of the osteoblastic phenotype expression in neonatal murine calvarial cells. *Calcif Tissue Int* **64**: 304-309.
- Cheng SL, Yang JW, Rifas L, Zhang SF, Avioli LV (1994) Differentiation of human bone marrow osteogenic stromal cells in vitro: induction of the osteoblast phenotype by dexamethasone. *Endocrinology* **134**: 277-286.
- Cheng SL, Zhang SF, Avioli LV (1996) Expression of bone matrix proteins during dexamethasone-induced mineralization of human bone marrow stromal cells. *J Cell Biochem* **61**: 182-193.
- Chomczynski P, Sacchi N (1987) Single-step method of RNA isolation by acid guanidinium thiocyanate-phenol-chloroform extraction. *Anal Biochem* **162**: 156-159.
- Chu ML, de WW, Bernard M, Ding JF, Morabito M, Myers J, Williams C, Ramirez F (1984) Human pro alpha 1(I) collagen gene structure reveals evolutionary conservation of a pattern of introns and exons. *Nature* **310**: 337-340.
- Civitelli R (2008) Cell-cell communication in the osteoblast/osteocyte lineage. *Arch Biochem Biophys* **473**: 188-192.
- Clarke MS, Sundaresan A, Vanderburg CR, Banigan MG, Pellis NR (2013) A three-dimensional tissue culture model of bone formation utilizing rotational co-culture of human adult osteoblasts and osteoclasts. *Acta Biomater* **9**: 7908-7916.

- Clover J, Dodds RA, Gowen M (1992) Integrin subunit expression by human osteoblasts and osteoclasts in situ and in culture. *J Cell Sci* **103** (Pt 1): 267-271.
- Clover J, Gowen M (1994) Are MG-63 and HOS TE85 human osteosarcoma cell lines representative models of the osteoblastic phenotype? *Bone* **15**: 585-591.
- Coelho MB, Cabral JM, Karp JM (2012) Intraoperative stem cell therapy. *Annu Rev Biomed Eng* **14**: 325-349.
- Coelho MJ, Fernandes MH (2000) Human bone cell cultures in biocompatibility testing. Part II: effect of ascorbic acid, beta-glycerophosphate and dexamethasone on osteoblastic differentiation. *Biomaterials* **21**: 1095-1102.
- Collignon H, Davicco MJ, Barlet JP (1997) Isolation of cells from ovine fetal long bone and characterization of their osteoblastic activities during in vitro mineralization. *Arch Physiol Biochem* **105**: 158-166.
- Collin EC, Grad S, Zeugolis DI, Vinatier CS, Clouet JR, Guicheux JJ, Weiss P, Alini M, Pandit AS (2011) An injectable vehicle for nucleus pulposus cell-based therapy. *Biomaterials* **32**: 2862-2870.
- Csaki C, Matis U, Mobasher A, Shakibaei M (2009) Co-culture of canine mesenchymal stem cells with primary bone-derived osteoblasts promotes osteogenic differentiation. *Histochem Cell Biol* **131**: 251-266.
- Currey J (2008) Collagen and the mechanical properties of bone and calcified cartilage. In: *Collagen - structure and mechanics* (Fratzl, P., ed), 1 edn. Springer, 397-420.
- Czekanska EM (2011) Assessment of cell proliferation with resazurin-based fluorescent dye. *Methods Mol Biol* **740**: 27-32.
- Czekanska EM, Stoddart MJ, Ralphs JR, Richards RG, Hayes JS (2013) A phenotypic comparison of osteoblast cell lines versus human primary osteoblasts for biomaterials testing. *J Biomed Mater Res A*.
- Czekanska EM, Stoddart MJ, Richards RG, Hayes JS (2012) In search of an osteoblast cell model for in vitro research. *Eur Cell Mater* **24**: 1-17.
- Dahl KN, Kahn SM, Wilson KL, Discher DE (2004) The nuclear envelope lamina network has elasticity and a compressibility limit suggestive of a molecular shock absorber. *J Cell Sci* **117**: 4779-4786.
- Dalby MJ, Biggs MJ, Gadegaard N, Kalna G, Wilkinson CD, Curtis AS (2007) Nanotopographical stimulation of mechanotransduction and changes in interphase centromere positioning. *J Cell Biochem* **100**: 326-338.

- Dalby MJ, Riehle MO, Sutherland DS, Agheli H, Curtis AS (2005) Morphological and microarray analysis of human fibroblasts cultured on nanocolumns produced by colloidal lithography. *Eur Cell Mater* **9**: 1-8.
- Dallas SL, Bonewald LF (2010) Dynamics of the transition from osteoblast to osteocyte. *Ann N Y Acad Sci* **1192**: 437-443.
- Davis JW, Ross PD, Wasnich RD (1994) Evidence for both generalized and regional low bone mass among elderly women. *J Bone Miner Res* **9**: 305-309.
- de Wet W, Bernard M, Benson-Chanda V, Chu ML, Dickson L, Weil D, Ramirez F (1987) Organization of the human pro-alpha 2(I) collagen gene. *J Biol Chem* **262**: 16032-16036.
- Declercq H, Van d, V, De Maeyer E, Verbeeck R, Schacht E, De Ridder L, Cornelissen M (2004) Isolation, proliferation and differentiation of osteoblastic cells to study cell/biomaterial interactions: comparison of different isolation techniques and source. *Biomaterials* **25**: 757-768.
- Degasne I, Basle MF, Demais V, Hure G, Lesourd M, Grolleau B, Mercier L, Chappard D (1999) Effects of roughness, fibronectin and vitronectin on attachment, spreading, and proliferation of human osteoblast-like cells (Saos-2) on titanium surfaces. *Calcif Tissue Int* **64**: 499-507.
- Di Silvio R, Gurav N (2001) Osteoblasts. In: *Human Cell Culture* (Koller, M. R., Pallson, B. O., and Masters, J. R. W., eds). Kluwer Academic Publishers, 221-241.
- Dietrich JW, Canalis EM, Maina DM, Raisz LG (1979) Effects of glucocorticoids on fetal rat bone collagen synthesis in vitro. *Endocrinology* **104**: 715-721.
- Dobnig H, Turner RT (1995) Evidence that intermittent treatment with parathyroid hormone increases bone formation in adult rats by activation of bone lining cells. *Endocrinology* **136**: 3632-3638.
- Dowthwaite GP, Bishop JC, Redman SN, Khan IM, Rooney P, Evans DJ, Haughton L, Bayram Z, Boyer S, Thomson B, Wolfe MS, Archer CW (2004) The surface of articular cartilage contains a progenitor cell population. *J Cell Sci* **117**: 889-897.
- Drago D, Cossetti C, Iraci N, Gaude E, Musco G, Bachi A, Pluchino S (2013) The stem cell secretome and its role in brain repair. *Biochimie*.
- Ducy P (2000) Cbfa1: a molecular switch in osteoblast biology. *Dev Dyn* **219**: 461-471.
- Ducy P, Zhang R, Geoffroy V, Ridall AL, Karsenty G (1997) Osf2/Cbfa1: a transcriptional activator of osteoblast differentiation. *Cell* **89**: 747-754.

- Duttenhoefer F, Lara de FR, Meury T, Loibl M, Benneker LM, Richards RG, Alini M, Verrier S (2013) 3D scaffolds co-seeded with human endothelial progenitor and mesenchymal stem cells: evidence of prevascularisation within 7 days. *Eur Cell Mater* **26**: 49-64.
- Eames BF, Sharpe PT, Helms JA (2004) Hierarchy revealed in the specification of three skeletal fates by Sox9 and Runx2. *Dev Biol* **274**: 188-200.
- Ecarot-Charrier B, Glorieux FH, van der Rest M, Pereira G (1983) Osteoblasts isolated from mouse calvaria initiate matrix mineralization in culture. *J Cell Biol* **96**: 639-643.
- Efron JE, Frankel HL, Lazarou SA, Wasserkrug HL, Barbul A (1990) Wound healing and T-lymphocytes. *J Surg Res* **48**: 460-463.
- Einhorn TA (1998) The cell and molecular biology of fracture healing. *Clin Orthop Relat Res* **S7-21**.
- El-Serafi AT, Wilson DI, Roach HI, Oreffo RO (2011) Developmental plasticity of human foetal femur-derived cells in pellet culture: self assembly of an osteoid shell around a cartilaginous core. *Eur Cell Mater* **21**: 558-567.
- Evans CE, Galasko CS, Ward C (1990) Effect of donor age on the growth in vitro of cells obtained from human trabecular bone. *J Orthop Res* **8**: 234-237.
- Fedarko NS, Vetter UK, Weinstein S, Robey PG (1992) Age-related changes in hyaluronan, proteoglycan, collagen, and osteonectin synthesis by human bone cells. *J Cell Physiol* **151**: 215-227.
- Fernandes JC, Martel-Pelletier J, Pelletier JP (2002) The role of cytokines in osteoarthritis pathophysiology. *Biorheology* **39**: 237-246.
- Fernandes MH, Costa MA, Carvalho GS (1997) Mineralization in serially passaged human alveolar bone cells. *J Mater Sci Mater Med* **8**: 61-65.
- Fernandes RJ, Harkey MA, Weis M, Askew JW, Eyre DR (2007) The post-translational phenotype of collagen synthesized by SAOS-2 osteosarcoma cells. *Bone* **40**: 1343-1351.
- Ferreira E, Porter RM, Wehling N, O'Sullivan RP, Boskey A, Estok DM, Harris MB, Vragas MS, Evans CH, Wells JW (2012) Inflammatory cytokines induce a unique mineralising phenotype in human stromal cells. Unpublished.
- Franceschi RT, Iyer BS (1992) Relationship between collagen synthesis and expression of the osteoblast phenotype in MC3T3-E1 cells. *J Bone Miner Res* **7**: 235-246.

- Franceschi RT, James WM, Zerlauth G (1985) 1 alpha, 25-dihydroxyvitamin D3 specific regulation of growth, morphology, and fibronectin in a human osteosarcoma cell line. *J Cell Physiol* **123**: 401-409.
- Franceschi RT, Romano PR, Park KY (1988) Regulation of type I collagen synthesis by 1,25-dihydroxyvitamin D3 in human osteosarcoma cells. *J Biol Chem* **263**: 18938-18945.
- Franz-Odendaal TA, Hall BK, Witten PE (2006) Buried alive: how osteoblasts become osteocytes. *Dev Dyn* **235**: 176-190.
- Fraser JD, Price PA (1988) Lung, heart, and kidney express high levels of mRNA for the vitamin K-dependent matrix Gla protein. Implications for the possible functions of matrix Gla protein and for the tissue distribution of the gamma-carboxylase. *J Biol Chem* **263**: 11033-11036.
- Fuchs S, Jiang X, Schmidt H, Dohle E, Ghanaati S, Orth C, Hofmann A, Motta A, Migliaresi C, Kirkpatrick CJ (2009) Dynamic processes involved in the pre-vascularization of silk fibroin constructs for bone regeneration using outgrowth endothelial cells. *Biomaterials* **30**: 1329-1338.
- Gallagher JA (2003) Human Osteoblast Culture. In: *Bone Research Protocols* (Helfrich M.H., Ralston S. H., ed). Humana Press Inc, New Jersey, 3-18.
- Gay CV, Gilman VR, Sugiyama T (2000) Perspectives on osteoblast and osteoclast function. *Poult Sci* **79**: 1005-1008.
- Gelse K, Poschl E, Aigner T (2003) Collagens--structure, function, and biosynthesis. *Adv Drug Deliv Rev* **55**: 1531-1546.
- Gerber I, ap Gwynn I (2002) Differentiation of rat osteoblast-like cells in monolayer and micromass cultures. *Eur Cell Mater* **3**: 19-30.
- Gerstenfeld LC, Thiede M, Seibert K, Mielke C, Phippard D, Svagr B, Cullinane D, Einhorn TA (2003) Differential inhibition of fracture healing by non-selective and cyclooxygenase-2 selective non-steroidal anti-inflammatory drugs. *J Orthop Res* **21**: 670-675.
- Giannoudis PV, Einhorn TA, Marsh D (2007) Fracture healing: the diamond concept. *Injury* **38 Suppl 4**: S3-S6.
- Gnecchi M, He H, Noiseux N, Liang OD, Zhang L, Morello F, Mu H, Melo LG, Pratt RE, Ingwall JS, Dzau VJ (2006) Evidence supporting paracrine hypothesis for Akt-modified mesenchymal stem cell-mediated cardiac protection and functional improvement. *FASEB J* **20**: 661-669.

- Gotoh Y, Hiraiwa K, Nagayama M (1990) In vitro mineralization of osteoblastic cells derived from human bone. *Bone Miner* **8**: 239-250.
- Gracie JA, Robertson SE, McInnes IB (2003) Interleukin-18. *J Leukoc Biol* **73**: 213-224.
- Gray H (1973) Osteology. In: *Gray's Anatomy* (Warwick, R. and Williams, P. L., eds), 35 edn. Longman Group Ltd., Edinburgh, 200-387.
- Grellier M, Bordenave L, Amedee J (2009) Cell-to-cell communication between osteogenic and endothelial lineages: implications for tissue engineering. *Trends Biotechnol* **27**: 562-571.
- Griffon DJ (2007) Fracture healing. In: *AO principles of fracture management in the dog and cat* (Johnsson, A. L, Houlton, J. E. F., and Vannini, R., eds). AO Publishing, Davos, 72-97.
- Grigoriadis AE, Petkovich PM, Ber R, Aubin JE, Heersche JN (1985) Subclone heterogeneity in a clonally-derived osteoblast-like cell line. *Bone* **6**: 249-256.
- Guillot PV, De BC, Dell'Accio F, Kurata H, Polak J, Fisk NM (2008) Comparative osteogenic transcription profiling of various fetal and adult mesenchymal stem cell sources. *Differentiation* **76**: 946-957.
- Hall TJ, Chambers TJ (1989) Optimal bone resorption by isolated rat osteoclasts requires chloride/bicarbonate exchange. *Calcif Tissue Int* **45**: 378-380.
- Hammoudi TM, Rivet CA, Kemp ML, Lu H, Temenoff JS (2012) Three-dimensional in vitro tri-culture platform to investigate effects of crosstalk between mesenchymal stem cells, osteoblasts, and adipocytes. *Tissue Eng Part A* **18**: 1686-1697.
- Hamrick MW, Shi X, Zhang W, Pennington C, Thakore H, Haque M, Kang B, Isales CM, Fulzele S, Wenger KH (2007) Loss of myostatin (GDF8) function increases osteogenic differentiation of bone marrow-derived mesenchymal stem cells but the osteogenic effect is ablated with unloading. *Bone* **40**: 1544-1553.
- Hansen JC, Lim JY, Xu LC, Siedlecki CA, Mauger DT, Donahue HJ (2007) Effect of surface nanoscale topography on elastic modulus of individual osteoblastic cells as determined by atomic force microscopy. *J Biomech* **40**: 2865-2871.
- Haque N, Rahman MT, Abu Kasim NH, Alabsi AM (2013) Hypoxic culture conditions as a solution for mesenchymal stem cell based regenerative therapy. *ScientificWorldJournal* **2013**: 632972.
- Hara M, Yuasa S, Shimoji K, Onizuka T, Hayashiji N, Ohno Y, Arai T, Hattori F, Kaneda R, Kimura K, Makino S, Sano M, Fukuda K (2011) G-CSF influences mouse

skeletal muscle development and regeneration by stimulating myoblast proliferation. *J Exp Med* **208**: 715-727.

Harris H (1990) The human alkaline phosphatases: what we know and what we don't know. *Clin Chim Acta* **186**: 133-150.

Harris SA, Enger RJ, Riggs BL, Spelsberg TC (1995) Development and characterization of a conditionally immortalized human fetal osteoblastic cell line. *J Bone Miner Res* **10**: 178-186.

Hauschka PV, Lian JB, Cole DE, Gundberg CM (1989) Osteocalcin and matrix Gla protein: vitamin K-dependent proteins in bone. *Physiol Rev* **69**: 990-1047.

Hausser HJ, Brenner RE (2005) Phenotypic instability of Saos-2 cells in long-term culture. *Biochem Biophys Res Commun* **333**: 216-222.

Hayes JS, Khan IM, Archer CW, Richards RG (2010) The role of surface microtopography in the modulation of osteoblast differentiation. *Eur Cell Mater* **20**: 98-108.

Haynesworth SE, Goshima J, Goldberg VM, Caplan AI (1992) Characterization of cells with osteogenic potential from human marrow. *Bone* **13**: 81-88.

Hendrich C, Franz E, Waertel G, Krebs R, Jager M (2009) Safety of autologous bone marrow aspiration concentrate transplantation: initial experiences in 101 patients. *Orthop Rev (Pavia)* **1**: e32.

Heremans H, Billiau A, Cassiman JJ, Mulier JC, de Somer P (1978) In vitro cultivation of human tumor tissues. II. Morphological and virological characterization of three cell lines. *Oncology* **35**: 246-252.

Hernigou P, Daltro G, Filippini P, Mukasa MM, Manicom O (2008) Percutaneous implantation of autologous bone marrow osteoprogenitor cells as treatment of bone avascular necrosis related to sickle cell disease. *Open Orthop J* **2**: 62-65.

Hoch AI, Binder BY, Genetos DC, Leach JK (2012) Differentiation-dependent secretion of proangiogenic factors by mesenchymal stem cells. *PLoS One* **7**: e35579.

Hofmann A, Ritz U, Verrier S, Eglin D, Alini M, Fuchs S, Kirkpatrick CJ, Rommens PM (2008) The effect of human osteoblasts on proliferation and neo-vessel formation of human umbilical vein endothelial cells in a long-term 3D co-culture on polyurethane scaffolds. *Biomaterials* **29**: 4217-4226.

Holtrop ME (1990) Light and electron microscopic structure of bone-forming cells. In: *The osteoblast and osteocyte* (Hall, B. K, ed), 1 edn. The Telford Press, 1-40.

- Hong D, Chen HX, Yu HQ, Liang Y, Wang C, Lian QQ, Deng HT, Ge RS (2010) Morphological and proteomic analysis of early stage of osteoblast differentiation in osteoblastic progenitor cells. *Exp Cell Res* **316**: 2291-2300.
- Horwood NJ, Udagawa N, Elliott J, Grail D, Okamura H, Kurimoto M, Dunn AR, Martin T, Gillespie MT (1998) Interleukin 18 inhibits osteoclast formation via T cell production of granulocyte macrophage colony-stimulating factor. *J Clin Invest* **101**: 595-603.
- Hoshi K, Amizuka N, Oda K, Ikehara Y, Ozawa H (1997) Immunolocalization of tissue non-specific alkaline phosphatase in mice. *Histochem Cell Biol* **107**: 183-191.
- Hoshiba T, Yamada T, Lu H, Kawazoe N, Chen G (2011) Maintenance of cartilaginous gene expression on extracellular matrix derived from serially passaged chondrocytes during in vitro chondrocyte expansion. *J Biomed Mater Res A*.
- Hsiao ST, Asgari A, Lokmic Z, Sinclair R, Disting GJ, Lim SY, Dilley RJ (2012) Comparative analysis of paracrine factor expression in human adult mesenchymal stem cells derived from bone marrow, adipose, and dermal tissue. *Stem Cells Dev* **21**: 2189-2203.
- Hsiao ST, Lokmic Z, Peshavariya H, Abberton KM, Disting GJ, Lim SY, Dilley RJ (2013) Hypoxic conditioning enhances the angiogenic paracrine activity of human adipose-derived stem cells. *Stem Cells Dev* **22**: 1614-1623.
- Hughes FJ, Aubin JE (1998) Culture of cells of the osteoblast lineage. In: *Methods in bone biology* (Arnett, T. and Henderson, B., eds), 1 edn. Chapman & Hall, London, 1-49.
- Hulmes DJS (2008) Collagen diversity, synthesis and assembly. In: *Collagen - structure and mechanics* (Fratzl, P., ed). Springer Science+Business Media, LLC, New York, USA, 15-80.
- Hunter GK, Goldberg HA (1993) Nucleation of hydroxyapatite by bone sialoprotein. *Proc Natl Acad Sci U S A* **90**: 8562-8565.
- Hunter GK, Hauschka PV, Poole AR, Rosenberg LC, Goldberg HA (1996) Nucleation and inhibition of hydroxyapatite formation by mineralized tissue proteins. *Biochem J* **317 (Pt 1)**: 59-64.
- Hwang HJ, Chang W, Song BW, Song H, Cha MJ, Kim IK, Lim S, Choi EJ, Ham O, Lee SY, Shim J, Joung B, Pak HN, Kim SS, Choi BR, Jang Y, Lee MH, Hwang KC (2012) Antiarrhythmic potential of mesenchymal stem cell is modulated by hypoxic environment. *J Am Coll Cardiol* **60**: 1698-1706.

- Ibaraki K, Termine JD, Whitson SW, Young MF (1992) Bone matrix mRNA expression in differentiating fetal bovine osteoblasts. *J Bone Miner Res* **7**: 743-754.
- Ilmer M, Karow M, Geissler C, Jochum M, Neth P (2009) Human osteoblast-derived factors induce early osteogenic markers in human mesenchymal stem cells. *Tissue Eng Part A* **15**: 2397-2409.
- Ito KPSM (2007) Biology and biomechanics in bone healing. In: *AO principles of fracture management* (Ruedi, T. P. Buckley R. E. Moran C. G., ed), 2 edn. Stuttgart, NY, 8-31.
- Jaehn K. (2010) Ex vivo and in vitro culture models of human osteoblast-like cells and the effects of TGF-beta3 and serum-free culture. In. Cardiff University.
- Jahn K, Richards RG, Archer CW, Stoddart MJ (2010) Pellet culture model for human primary osteoblasts. *Eur Cell Mater* **20**: 149-161.
- Jaiswal N, Haynesworth SE, Caplan AI, Bruder SP (1997) Osteogenic differentiation of purified, culture-expanded human mesenchymal stem cells in vitro. *J Cell Biochem* **64**: 295-312.
- Johansen JS, Williamson MK, Rice JS, Price PA (1992) Identification of proteins secreted by human osteoblastic cells in culture. *J Bone Miner Res* **7**: 501-512.
- Jonsson KB, Frost A, Larsson R, Ljunghall S, Ljunggren O (1997) A new fluorometric assay for determination of osteoblastic proliferation: effects of glucocorticoids and insulin-like growth factor-I. *Calcif Tissue Int* **60**: 30-36.
- Jonsson KB, Frost A, Nilsson O, Ljunghall S, Ljunggren O (1999) Three isolation techniques for primary culture of human osteoblast-like cells: a comparison. *Acta Orthop Scand* **70**: 365-373.
- Jorgensen NR, Henriksen Z, Sorensen OH, Civitelli R (2004) Dexamethasone, BMP-2, and 1,25-dihydroxyvitamin D enhance a more differentiated osteoblast phenotype: validation of an in vitro model for human bone marrow-derived primary osteoblasts. *Steroids* **69**: 219-226.
- Jukkola A, Risteli L, Melkko J, Risteli J (1993) Procollagen synthesis and extracellular matrix deposition in MG-63 osteosarcoma cells. *J Bone Miner Res* **8**: 651-657.
- Kadler KE, Holmes DF, Trotter JA, Chapman JA (1996) Collagen fibril formation. *Biochem J* **316** (Pt 1): 1-11.

- Kaigler D, Krebsbach PH, West ER, Horger K, Huang YC, Mooney DJ (2005) Endothelial cell modulation of bone marrow stromal cell osteogenic potential. *FASEB J* **19**: 665-667.
- Kale S, Biermann S, Edwards C, Tarnowski C, Morris M, Long MW (2000) Three-dimensional cellular development is essential for ex vivo formation of human bone. *Nat Biotechnol* **18**: 954-958.
- Kamran K, Rashid I, Zuki AB, Tengku AI (2011) Mesenchymal stem cells, osteogenic lineage and bone tissue engineering: a review. *Journal of Animal and Veterinary Advances* **10**: 2317-2330.
- Kapoor M, Martel-Pelletier J, Lajeunesse D, Pelletier JP, Fahmi H (2011) Role of proinflammatory cytokines in the pathophysiology of osteoarthritis. *Nat Rev Rheumatol* **7**: 33-42.
- Kartsogiannis V, Ng KW (2004) Cell lines and primary cell cultures in the study of bone cell biology. *Mol Cell Endocrinol* **228**: 79-102.
- Kasperk C, Wergedal J, Strong D, Farley J, Wangerin K, Gropp H, Ziegler R, Baylink DJ (1995) Human bone cell phenotypes differ depending on their skeletal site of origin. *J Clin Endocrinol Metab* **80**: 2511-2517.
- Katzburg S, Lieberherr M, Ornoy A, Klein BY, Hendel D, Somjen D (1999) Isolation and hormonal responsiveness of primary cultures of human bone-derived cells: gender and age differences. *Bone* **25**: 667-673.
- Kellum E, Starr H, Arounleut P, Immel D, Fulzele S, Wenger K, Hamrick MW (2009) Myostatin (GDF-8) deficiency increases fracture callus size, Sox-5 expression, and callus bone volume. *Bone* **44**: 17-23.
- Kessler SB, Hallfeldt KK, Perren SM, Schweiberer L (1986) The effects of reaming and intramedullary nailing on fracture healing. *Clin Orthop Relat Res* 18-25.
- Kim CH, Cheng SL, Kim GS (1999) Effects of dexamethasone on proliferation, activity, and cytokine secretion of normal human bone marrow stromal cells: possible mechanisms of glucocorticoid-induced bone loss. *J Endocrinol* **162**: 371-379.
- Kim H, Lee JH, Suh H (2003) Interaction of mesenchymal stem cells and osteoblasts for in vitro osteogenesis. *Yonsei Med J* **44**: 187-197.
- Kim JH, Liu X, Wang J, Chen X, Zhang H, Kim SH, Cui J, Li R, Zhang W, Kong Y, Zhang J, Shui W, Lamplot J, Rogers MR, Zhao C, Wang N, Rajan P, Tomal J, Statz J, Wu N, Luu HH, Haydon RC, He TC (2013) Wnt signaling in bone formation and its therapeutic potential for bone diseases. *Ther Adv Musculoskelet Dis* **5**: 13-31.

- Kim KL, Meng Y, Kim JY, Baek EJ, Suh W (2011) Direct and differential effects of stem cell factor on the neovascularization activity of endothelial progenitor cells. *Cardiovasc Res* **92**: 132-140.
- Kirkham GR, Cartmell SH (2007) Genes and proteins involved in the regulation of osteogenesis. In: *Topics in tissue engineering* (Ashammaki, N., Reis, R., and Chiellini, E., eds). 1-22.
- Kitaori T, Ito H, Schwarz EM, Tsutsumi R, Yoshitomi H, Oishi S, Nakano M, Fujii N, Nagasawa T, Nakamura T (2009) Stromal cell-derived factor 1/CXCR4 signaling is critical for the recruitment of mesenchymal stem cells to the fracture site during skeletal repair in a mouse model. *Arthritis Rheum* **60**: 813-823.
- Knighton DR, Fiegel VD (1989) The macrophages: effector cell wound repair. *Prog Clin Biol Res* **299**: 217-226.
- Kolar P, Gaber T, Perka C, Duda GN, Buttgerit F (2011) Human early fracture hematoma is characterized by inflammation and hypoxia. *Clin Orthop Relat Res* **469**: 3118-3126.
- Komori T (2010) Regulation of bone development and extracellular matrix protein genes by RUNX2. *Cell Tissue Res* **339**: 189-195.
- Komori T, Yagi H, Nomura S, Yamaguchi A, Sasaki K, Deguchi K, Shimizu Y, Bronson RT, Gao YH, Inada M, Sato M, Okamoto R, Kitamura Y, Yoshiki S, Kishimoto T (1997) Targeted disruption of *Cbfa1* results in a complete lack of bone formation owing to maturational arrest of osteoblasts. *Cell* **89**: 755-764.
- Konig A, Muhlbauer RC, Fleisch H (1988) Tumor necrosis factor alpha and interleukin-1 stimulate bone resorption in vivo as measured by urinary [3H]tetracycline excretion from prelabeled mice. *J Bone Miner Res* **3**: 621-627.
- Kumarasuriyar A, Murali S, Nurcombe V, Cool SM (2009) Glycosaminoglycan composition changes with MG-63 osteosarcoma osteogenesis in vitro and induces human mesenchymal stem cell aggregation. *J Cell Physiol* **218**: 501-511.
- Lajeunesse D, Frondoza C, Schoffield B, Sacktor B (1990) Osteocalcin secretion by the human osteosarcoma cell line MG-63. *J Bone Miner Res* **5**: 915-922.
- Lane TF, Sage EH (1994) The biology of SPARC, a protein that modulates cell-matrix interactions. *FASEB J* **8**: 163-173.
- Lee YM, Fujikado N, Manaka H, Yasuda H, Iwakura Y (2010) IL-1 plays an important role in the bone metabolism under physiological conditions. *Int Immunol* **22**: 805-816.

- Leibovich SJ, Ross R (1975) The role of the macrophage in wound repair. A study with hydrocortisone and antimacrophage serum. *Am J Pathol* **78**: 71-100.
- Leis HJ, Hulla W, Gruber R, Huber E, Zach D, Gleispach H, Windischhofer W (1997) Phenotypic heterogeneity of osteoblast-like MC3T3-E1 cells: changes of bradykinin-induced prostaglandin E2 production during osteoblast maturation. *J Bone Miner Res* **12**: 541-551.
- Li F, Niyibizi Ch (2012) Differentiating multipotent mesenchymal stromal cells generate factors that exert paracrine activities on exogenous MSCs: Implications for paracrine activities in bone regeneration. In.
- Lian JB, Shalhoub V, Aslam F, Frenkel B, Green J, Hamrah M, Stein GS, Stein JL (1997) Species-specific glucocorticoid and 1,25-dihydroxyvitamin D responsiveness in mouse MC3T3-E1 osteoblasts: dexamethasone inhibits osteoblast differentiation and vitamin D down-regulates osteocalcin gene expression. *Endocrinology* **138**: 2117-2127.
- Lian JB, Stein GS (1992) Concepts of osteoblast growth and differentiation: basis for modulation of bone cell development and tissue formation. *Crit Rev Oral Biol Med* **3**: 269-305.
- Lian JB, Stein GS (1995) Development of the osteoblast phenotype: molecular mechanisms mediating osteoblast growth and differentiation. *Iowa Orthop J* **15**: 118-140.
- Liao H, Andersson AS, Sutherland D, Petronis S, Kasemo B, Thomsen P (2003) Response of rat osteoblast-like cells to microstructured model surfaces in vitro. *Biomaterials* **24**: 649-654.
- Lin FH, Chang JB, McGuire MH, Yee JA, Brigman BE (2010) Biphasic effects of interleukin-1beta on osteoblast differentiation in vitro. *J Orthop Res* **28**: 958-964.
- Lincks J, Boyan BD, Blanchard CR, Lohmann CH, Liu Y, Cochran DL, Dean DD, Schwartz Z (1998) Response of MG63 osteoblast-like cells to titanium and titanium alloy is dependent on surface roughness and composition. *Biomaterials* **19**: 2219-2232.
- Ling L, Nurcombe V, Cool SM (2009) Wnt signaling controls the fate of mesenchymal stem cells. *Gene* **433**: 1-7.
- Loebel C, Czekanska EM, Bruderer M, Salzmann G, Alini M, Stoddart MJ (2014a) Osteogenic potential of human MSCs is predicted by Runx2/Sox9 ratio. Submitted to *Tissue Engineering*.

- Loebel C, Czekanska EM, Staudacher J, Salzmann G, Richards RG, Alini M, Stoddart MJ (2014b) The osteogenic potential of human bone-derived mesenchymal stem cells can be enhanced by interleukin 1-beta. Submitted to Tissue Engineering and Regenerative Medicine.
- Lou N, Wang Y, Sun D, Zhao J, Wang Y, Gao Z (2010) Isolation of stem-like cells from human MG-63 osteosarcoma cells using limiting dilution in combination with vincristine selection. *Indian J Biochem Biophys* **47**: 340-347.
- Lynch MP, Stein JL, Stein GS, Lian JB (1995) The influence of type I collagen on the development and maintenance of the osteoblast phenotype in primary and passaged rat calvarial osteoblasts: modification of expression of genes supporting cell growth, adhesion, and extracellular matrix mineralization. *Exp Cell Res* **216**: 35-45.
- Maeda K, Kobayashi Y, Udagawa N, Uehara S, Ishihara A, Mizoguchi T, Kikuchi Y, Takada I, Kato S, Kani S, Nishita M, Marumo K, Martin TJ, Minami Y, Takahashi N (2012) Wnt5a-Ror2 signaling between osteoblast-lineage cells and osteoclast precursors enhances osteoclastogenesis. *Nat Med* **18**: 405-412.
- Maeda K, Takahashi N, Kobayashi Y (2013) Roles of Wnt signals in bone resorption during physiological and pathological states. *J Mol Med (Berl)* **91**: 15-23.
- Maekawa K, Yoshida Y, Mine A, van MB, Suzuki K, Kuboki T (2008) Effect of polyphosphoric acid pre-treatment of titanium on attachment, proliferation, and differentiation of osteoblast-like cells (MC3T3-E1). *Clin Oral Implants Res* **19**: 320-325.
- Maes C, Kobayashi T, Kronenberg HM (2007) A novel transgenic mouse model to study the osteoblast lineage in vivo. *Ann N Y Acad Sci* **1116**: 149-164.
- Maijenburg MW, van der Schoot CE, Voermans C (2011) Mesenchymal stromal cell migration, possibilities to improve cellular therapy. *Stem Cells Dev*.
- Manduca P, Palermo C, Caruso C, Brizzolara A, Sanguineti C, Filanti C, Zicca A (1997) Rat tibial osteoblasts III: propagation in vitro is accompanied by enhancement of osteoblast phenotype. *Bone* **21**: 31-39.
- Maniopoulos C, Sodek J, Melcher AH (1988) Bone formation in vitro by stromal cells obtained from bone marrow of young adult rats. *Cell Tissue Res* **254**: 317-330.
- Manolagas SC (2000) Birth and death of bone cells: basic regulatory mechanisms and implications for the pathogenesis and treatment of osteoporosis. *Endocr Rev* **21**: 115-137.
- Marsell R, Einhorn TA (2011) The biology of fracture healing. *Injury* **42**: 551-555.

- Martin D, Galisteo R, Gutkind JS (2009) CXCL8/IL8 stimulates vascular endothelial growth factor (VEGF) expression and the autocrine activation of VEGFR2 in endothelial cells by activating NFkappaB through the CBM (Carma3/Bcl10/Malt1) complex. *J Biol Chem* **284**: 6038-6042.
- Martinez ME, Del Campo MT, Medina S, Sanchez M, Sanchez-Cabezudo MJ, Esbrit P, Martinez P, Moreno I, Rodrigo A, Garces MV, Munuera L (1999) Influence of skeletal site of origin and donor age on osteoblastic cell growth and differentiation. *Calcif Tissue Int* **64**: 280-286.
- Maruyama Z, Yoshida CA, Furuichi T, Amizuka N, Ito M, Fukuyama R, Miyazaki T, Kitaura H, Nakamura K, Fujita T, Kanatani N, Moriishi T, Yamana K, Liu W, Kawaguchi H, Nakamura K, Komori T (2007) Runx2 determines bone maturity and turnover rate in postnatal bone development and is involved in bone loss in estrogen deficiency. *Dev Dyn* **236**: 1876-1890.
- Maxson S, Burg KJ (2008) Conditioned media cause increases in select osteogenic and adipogenic differentiation markers in mesenchymal stem cell cultures. *J Tissue Eng Regen Med* **2**: 147-154.
- McAllister RM, Gardner MB, Greene AE, Bradt C, Nichols WW, Landing BH (1971) Cultivation in vitro of cells derived from a human osteosarcoma. *Cancer* **27**: 397-402.
- McKee MD, Nanci A (1996) Osteopontin: an interfacial extracellular matrix protein in mineralized tissues. *Connect Tissue Res* **35**: 197-205.
- McKibbin B (1978) The biology of fracture healing in long bones. *J Bone Joint Surg Br* **60-B**: 150-162.
- McNiece IK, Briddell RA (1995) Stem cell factor. *J Leukoc Biol* **58**: 14-22.
- Mirza R, DiPietro LA, Koh TJ (2009) Selective and specific macrophage ablation is detrimental to wound healing in mice. *Am J Pathol* **175**: 2454-2462.
- Molnar J, Fong KS, He QP, Hayashi K, Kim Y, Fong SF, Fogelgren B, Szauter KM, Mink M, Csiszar K (2003) Structural and functional diversity of lysyl oxidase and the LOX-like proteins. *Biochim Biophys Acta* **1647**: 220-224.
- Montjovent MO, Burri N, Mark S, Federici E, Scaletta C, Zambelli PY, Hohlfeld P, Leyvraz PF, Applegate LL, Pioletti DP (2004) Fetal bone cells for tissue engineering. *Bone* **35**: 1323-1333.
- Morike M, Schulz M, Brenner RE, Bushart GB, Teller WM, Vetter U (1993) In vitro expression of osteoblastic markers in cells isolated from normal fetal and postnatal

- human bone and from bone of patients with osteogenesis imperfecta. *J Cell Physiol* **157**: 439-444.
- Morike M, Schulz M, Nerlich A, Koschnik M, Teller WM, Vetter U, Brenner RE (1995) Expression of osteoblastic markers in cultured human bone and fracture callus cells. *J Mol Med* **73**: 571-575.
- Moss DW (1997) Physicochemical and pathophysiological factors in the release of membrane-bound alkaline phosphatase from cells. *Clin Chim Acta* **257**: 133-140.
- Mountziaris PM, Spicer PP, Kasper FK, Mikos AG (2011) Harnessing and modulating inflammation in strategies for bone regeneration. *Tissue Eng Part B Rev* **17**: 393-402.
- Muller WE, Wang X, Diehl-Seifert B, Kropf K, Schlossmacher U, Lieberwirth I, Glasser G, Wiens M, Schroder HC (2011) Inorganic polymeric phosphate/polyphosphate as an inducer of alkaline phosphatase and a modulator of intracellular Ca²⁺ level in osteoblasts (SaOS-2 cells) in vitro. *Acta Biomater* **7**: 2661-2671.
- Mumme M, Scotti C, Papadimitropoulos A, Todorov A, Hoffmann W, Bocelli-Tyndall C, Jakob M, Wendt D, Martin I, Barbero A (2012) Interleukin-1beta modulates endochondral ossification by human adult bone marrow stromal cells. *Eur Cell Mater* **24**: 224-236.
- Muraglia A, Corsi A, Riminucci M, Mastrogiacomo M, Cancedda R, Bianco P, Quarto R (2003) Formation of a chondro-osseous rudiment in micromass cultures of human bone-marrow stromal cells. *J Cell Sci* **116**: 2949-2955.
- Murray E, Provvedini D, Curran D, Catherwood B, Sussman H, Manolagas S (1987) Characterization of a human osteoblastic osteosarcoma cell line (SAOS-2) with high bone alkaline phosphatase activity. *J Bone Miner Res* **2**: 231-238.
- Nakamura I, Jimi E (2006) Regulation of osteoclast differentiation and function by interleukin-1. *Vitam Horm* **74**: 357-370.
- Nakayama Y, Kato N, Nakajima Y, Shimizu E, Ogata Y (2004) Effect of TNF-alpha on human osteosarcoma cell line Saos2--TNF-alpha regulation of bone sialoprotein gene expression in Saos2 osteoblast-like cells. *Cell Biol Int* **28**: 653-660.
- Nehme A, Edelman J (2008) Dexamethasone inhibits high glucose-, TNF-alpha-, and IL-1beta-induced secretion of inflammatory and angiogenic mediators from retinal microvascular pericytes. *Invest Ophthalmol Vis Sci* **49**: 2030-2038.

- Newman E, Turner AS, Wark JD (1995) The potential of sheep for the study of osteopenia: current status and comparison with other animal models. *Bone* **16**: 277S-284S.
- Neyt JG, Buckwalter JA, Carroll NC (1998) Use of animal models in musculoskeletal research. *Iowa Orthop J* **18**: 118-123.
- Oh S, Daraio C, Chen LH, Pisanic TR, Finones RR, Jin S (2006) Significantly accelerated osteoblast cell growth on aligned TiO₂ nanotubes. *J Biomed Mater Res A* **78**: 97-103.
- Olivares-Navarrete R, Hyzy SL, Chaudhri RA, Zhao G, Boyan BD, Schwartz Z (2010) Sex dependent regulation of osteoblast response to implant surface properties by systemic hormones. *Biol Sex Differ* **1**: 4.
- Orgel JP, San Antonio JD, Antipova O (2011) Molecular and structural mapping of collagen fibril interactions. *Connect Tissue Res* **52**: 2-17.
- Orimo H (2010) The mechanism of mineralization and the role of alkaline phosphatase in health and disease. *J Nippon Med Sch* **77**: 4-12.
- Orriss AI, Taylor SEB, Arnett TA (2012) Rat osteoblast cultures. In: *Bone research protocols* (Helflich, M. P. and Ralston, S. H., eds). Humana Press, London, 31-41.
- Osugi M, Katagiri W, Yoshimi R, Inukai T, Hibi H, Ueda M (2012) Conditioned media from mesenchymal stem cells enhanced bone regeneration in rat calvarial bone defects. *Tissue Eng Part A* **18**: 1479-1489.
- Overman JR, Farre-Guasch E, Helder MN, ten Bruggenkate CM, Schulten EA, Klein-Nulend J (2013a) Short (15 minutes) bone morphogenetic protein-2 treatment stimulates osteogenic differentiation of human adipose stem cells seeded on calcium phosphate scaffolds in vitro. *Tissue Eng Part A* **19**: 571-581.
- Overman JR, Helder MN, ten Bruggenkate CM, Schulten EA, Klein-Nulend J, Bakker AD (2013b) Growth factor gene expression profiles of bone morphogenetic protein-2-treated human adipose stem cells seeded on calcium phosphate scaffolds in vitro. *Biochimie* **95**: 2304-2313.
- Owen TA, Aronow M, Shalhoub V, Barone LM, Wilming L, Tassinari MS, Kennedy MB, Pockwinse S, Lian JB, Stein GS (1990) Progressive development of the rat osteoblast phenotype in vitro: reciprocal relationships in expression of genes associated with osteoblast proliferation and differentiation during formation of the bone extracellular matrix. *J Cell Physiol* **143**: 420-430.
- Palumbo C (1986) A three-dimensional ultrastructural study of osteoid-osteocytes in the tibia of chick embryos. *Cell Tissue Res* **246**: 125-131.

- Pan S, Dangaria S, Gopinathan G, Yan X, Lu X, Kolokythas A, Niu Y, Luan X (2013) SCF Promotes Dental Pulp Progenitor Migration, Neovascularization, and Collagen Remodeling - Potential Applications as a Homing Factor in Dental Pulp Regeneration. *Stem Cell Rev*.
- Parfitt MA (1990) Bone-forming cells in clinical conditions. In: *Osteoblast and osteocyte* (Hall B.K., ed). The Telford Press, Caldwell, 351-430.
- Park JE, Barbul A (2004) Understanding the role of immune regulation in wound healing. *Am J Surg* **187**: 11S-16S.
- Parr BA, Shea MJ, Vassileva G, McMahon AP (1993) Mouse Wnt genes exhibit discrete domains of expression in the early embryonic CNS and limb buds. *Development* **119**: 247-261.
- Pautke C, Schieker M, Tischer T, Kolk A, Neth P, Mutschler W, Milz S (2004) Characterization of osteosarcoma cell lines MG-63, Saos-2 and U-2 OS in comparison to human osteoblasts. *Anticancer Res* **24**: 3743-3748.
- Pearce AI, Richards RG, Milz S, Schneider E, Pearce SG (2007) Animal models for implant biomaterial research in bone: a review. *Eur Cell Mater* **13**: 1-10.
- Pedraza CE, Marelli B, Chicatun F, McKee MD, Nazhat SN (2010) An in vitro assessment of a cell-containing collagenous extracellular matrix-like scaffold for bone tissue engineering. *Tissue Eng Part A* **16**: 781-793.
- Peroglio M, Grad S, Mortisen D, Sprecher CM, Illien-Junger S, Alini M, Eglin D (2011) Injectable thermoreversible hyaluronan-based hydrogels for nucleus pulposus cell encapsulation. *Eur Spine J*.
- Perren SM (1979) Physical and biological aspects of fracture healing with special reference to internal fixation. *Clin Orthop Relat Res* 175-196.
- Peter B, Zambelli PY, Guicheux J, Pioletti DP (2005) The effect of bisphosphonates and titanium particles on osteoblasts: an in vitro study. *J Bone Joint Surg Br* **87**: 1157-1163.
- Peterson WJ, Tachiki KH, Yamaguchi DT (2004) Serial passage of MC3T3-E1 cells down-regulates proliferation during osteogenesis in vitro. *Cell Prolif* **37**: 325-336.
- Pierschbacher MD, Dedhar S, Ruoslahti E, Argraves S, Suzuki S (1988) An adhesion variant of the MG-63 osteosarcoma cell line displays an osteoblast-like phenotype. *Ciba Found Symp* **136**: 131-141.

- Pittenger MF, Mackay AM, Beck SC, Jaiswal RK, Douglas R, Mosca JD, Moorman MA, Simonetti DW, Craig S, Marshak DR (1999) Multilineage potential of adult human mesenchymal stem cells. *Science* **284**: 143-147.
- Ponten J, Saksela E (1967) Two established in vitro cell lines from human mesenchymal tumours. *Int J Cancer* **2**: 434-447.
- Porter RM, Huckle WR, Goldstein AS (2003) Effect of dexamethasone withdrawal on osteoblastic differentiation of bone marrow stromal cells. *J Cell Biochem* **90**: 13-22.
- Poser JW, Price PA (1979) A method for decarboxylation of gamma-carboxyglutamic acid in proteins. Properties of the decarboxylated gamma-carboxyglutamic acid protein from calf bone. *J Biol Chem* **254**: 431-436.
- Price PA, Lothringer JW, Baukol SA, Reddi AH (1981) Developmental appearance of the vitamin K-dependent protein of bone during calcification. Analysis of mineralizing tissues in human, calf, and rat. *J Biol Chem* **256**: 3781-3784.
- Probst A, Spiegel HU (1997) Cellular mechanisms of bone repair. *J Invest Surg* **10**: 77-86.
- Quarles LD, Yohay DA, Lever LW, Caton R, Wenstrup RJ (1992) Distinct proliferative and differentiated stages of murine MC3T3-E1 cells in culture: an in vitro model of osteoblast development. *J Bone Miner Res* **7**: 683-692.
- Rahn BA (2002) Bone healing: histologic and physiologic concepts. In: *Bone in Clinical Orthopaedics* (Fackelman, G. E., ed). Thieme, Stuttgart, NY, 287-326.
- Rao LG, Sutherland MK, Reddy GS, Siu-Caldera ML, Uskokovic MR, Murray TM (1996) Effects of 1alpha,25-dihydroxy-16ene, 23yne-vitamin D3 on osteoblastic function in human osteosarcoma SaOS-2 cells: differentiation-stage dependence and modulation by 17-beta estradiol. *Bone* **19**: 621-627.
- Read AP, Strachan T (1999) Cancer Genetics. In: *Human molecular genetics* 2, 2 edn. Wiley-Liss, New York.
- Richards RG (2008) The relevance of implant surfaces in hand fracture fixation. In: *Osteosynthesis in the Hand: Current Concepts*. (Herren D.B., Nagy L., and Campbell D.A., eds). Karger, Basel, 20-30.
- Roach HI (1994) Why does bone matrix contain non-collagenous proteins? The possible roles of osteocalcin, osteonectin, osteopontin and bone sialoprotein in bone mineralisation and resorption. *Cell Biol Int* **18**: 617-628.

- Robey PG (2002) Bone matrix proteoglycans and glycoproteins. In: Principles of bone biology (Bilezikian J.P., Raisz L. G. Rodan G. A, ed), 2 edn. Academic Press, London, 225-238.
- Rodan SB, Imai Y, Thiede MA, Wesolowski G, Thompson D, Bar-Shavit Z, Shull S, Mann K, Rodan GA (1987) Characterization of a human osteosarcoma cell line (Saos-2) with osteoblastic properties. *Cancer Res* **47**: 4961-4966.
- Romberg RW, Werness PG, Riggs BL, Mann KG (1986) Inhibition of hydroxyapatite crystal growth by bone-specific and other calcium-binding proteins. *Biochemistry* **25**: 1176-1180.
- Rosset J, de Crombrughe B (2002) Type I collagen - structure, synthesis and regulation. In: Principles of bone biology (Bilezikian J.P., Raisz L. G. Rodan G. A, ed), 2 edn. Academic Press, San Diego, 189-210.
- Ryoo HM, Hoffmann HM, Beumer T, Frenkel B, Towler DA, Stein GS, Stein JL, van Wijnen AJ, Lian JB (1997) Stage-specific expression of Dlx-5 during osteoblast differentiation: involvement in regulation of osteocalcin gene expression. *Mol Endocrinol* **11**: 1681-1694.
- Sakai D, Nakai T, Mochida J, Alini M, Grad S (2009) Differential phenotype of intervertebral disc cells: microarray and immunohistochemical analysis of canine nucleus pulposus and annulus fibrosus. *Spine (Phila Pa 1976)* **34**: 1448-1456.
- Saldana L, Bensiamar F, Bore A, Vilaboia N (2011) In search of representative models of human bone-forming cells for cytocompatibility studies. *Acta Biomater* **7**: 4210-4221.
- Saleh FA, Whyte M, Genever PG (2011) Effects of endothelial cells on human mesenchymal stem cell activity in a three-dimensional in vitro model. *Eur Cell Mater* **22**: 242-257.
- Salo J, Lehenkari P, Mulari M, Metsikko K, Vaananen HK (1997) Removal of osteoclast bone resorption products by transcytosis. *Science* **276**: 270-273.
- Scheven BA, Marshall D, Aspden RM (2002) In vitro behaviour of human osteoblasts on dentin and bone. *Cell Biol Int* **26**: 337-346.
- Schinke T, Karsenty G (2002) Transcriptional Control of Osteoblast Differentiation and Function. In: Principles of Bone Biology (Bilezikian J.P., Raisz L. G. Rodan G. A, ed), 2 edn. Academic Press, London, 83-92.
- Schlosser S, Dennler C, Schweizer R, Eberli D, Stein JV, Enzmann V, Giovanoli P, Erni D, Plock JA (2012) Paracrine effects of mesenchymal stem cells enhance vascular regeneration in ischemic murine skin. *Microvasc Res* **83**: 267-275.

- Schwetz V, Pieber T, Obermayer-Pietsch B (2012) The endocrine role of the skeleton: background and clinical evidence. *Eur J Endocrinol* **166**: 959-967.
- Scotti C, Tonnarelli B, Papadimitropoulos A, Scherberich A, Schaeren S, Schauerte A, Lopez-Rios J, Zeller R, Barbero A, Martin I (2010) Recapitulation of endochondral bone formation using human adult mesenchymal stem cells as a paradigm for developmental engineering. *Proc Natl Acad Sci U S A* **107**: 7251-7256.
- Semenza GL (1998) Hypoxia-inducible factor 1: master regulator of O₂ homeostasis. *Curr Opin Genet Dev* **8**: 588-594.
- Seto SP, Casas ME, Temenoff JS (2012) Differentiation of mesenchymal stem cells in heparin-containing hydrogels via coculture with osteoblasts. *Cell Tissue Res* **347**: 589-601.
- Sfeir Ch, Ho L, Doll BA, Azari K, Hollinger JO (2005) Fracture Repair. In: *Bone Regeneration and Repair: Biology and Clinical Applications* (Lieberman, J. R. and Friedlaender, G. E., eds). Humana Press Inc., Totowa, NJ, 21-44.
- Shapiro F (1988) Cortical bone repair. The relationship of the lacunar-canalicular system and intercellular gap junctions to the repair process. *J Bone Joint Surg Am* **70**: 1067-1081.
- Shapiro F (2008) Bone development and its relation to fracture repair. The role of mesenchymal osteoblasts and surface osteoblasts. *Eur Cell Mater* **15**: 53-76.
- Shaw KY, Tang JS, Chao CF (1989) Functional evaluation of cultured rabbit osteoblast-like cells. *Proc Natl Sci Counc Repub China B* **13**: 192-200.
- Shigeno Y, Ashton BA (1995) Human bone-cell proliferation in vitro decreases with human donor age. *J Bone Joint Surg Br* **77**: 139-142.
- Siddiqi MH, Siddiqi MZ, Ahn S, Kang S, Kim YJ, Veerappan K, Yang DU, Yang DC (2014) Stimulative Effect of Ginsenosides Rg5:Rk1 on Murine Osteoblastic MC3T3-E1 Cells. *Phytother Res*.
- Siggelkow H, Rebenstorff K, Kurre W, Niedhart C, Engel I, Schulz H, Atkinson MJ, Hufner M (1999) Development of the osteoblast phenotype in primary human osteoblasts in culture: comparison with rat calvarial cells in osteoblast differentiation. *J Cell Biochem* **75**: 22-35.
- Simon AM, Manigrasso MB, O'Connor JP (2002) Cyclo-oxygenase 2 function is essential for bone fracture healing. *J Bone Miner Res* **17**: 963-976.
- Sinha RK, Tuan RS (1996) Regulation of human osteoblast integrin expression by orthopedic implant materials. *Bone* **18**: 451-457.

- Sodek J, Ganss B, McKee MD (2000) Osteopontin. *Crit Rev Oral Biol Med* **11**: 279-303.
- Sonomoto K, Yamaoka K, Oshita K, Fukuyo S, Zhang X, Nakano K, Okada Y, Tanaka Y (2012) Interleukin-1beta induces differentiation of human mesenchymal stem cells into osteoblasts via the Wnt-5a/receptor tyrosine kinase-like orphan receptor 2 pathway. *Arthritis Rheum* **64**: 3355-3363.
- Stahl A, Wenger A, Weber H, Stark GB, Augustin HG, Finkenzeller G (2004) Bi-directional cell contact-dependent regulation of gene expression between endothelial cells and osteoblasts in a three-dimensional spheroidal coculture model. *Biochem Biophys Res Commun* **322**: 684-692.
- Stains JP, Civitelli R (2005) Cell-cell interactions in regulating osteogenesis and osteoblast function. *Birth Defects Res C Embryo Today* **75**: 72-80.
- Stein GS, Lian JB (1993) Molecular mechanisms mediating proliferation/differentiation interrelationships during progressive development of the osteoblast phenotype. *Endocr Rev* **14**: 424-442.
- Stringa E, Filanti C, Giunciuglio D, Albin A, Manduca P (1995) Osteoblastic cells from rat long bone. I. Characterization of their differentiation in culture. *Bone* **16**: 663-670.
- Sudo H, Kodama HA, Amagai Y, Yamamoto S, Kasai S (1983) In vitro differentiation and calcification in a new clonal osteogenic cell line derived from newborn mouse calvaria. *J Cell Biol* **96**: 191-198.
- Sutherland MS, Rao LG, Muzaffar SA, Wylie JN, Wong MM, McBroom RJ, Murray TM (1995) Age-dependent expression of osteoblastic phenotypic markers in normal human osteoblasts cultured long-term in the presence of dexamethasone. *Osteoporos Int* **5**: 335-343.
- Taguchi K, Ogawa R, Migita M, Hanawa H, Ito H, Orimo H (2005) The role of bone marrow-derived cells in bone fracture repair in a green fluorescent protein chimeric mouse model. *Biochem Biophys Res Commun* **331**: 31-36.
- Tang FP, Wu XH, Yu XL, Yang SH, Xu WH, Li J (2009) Effects of granulocyte colony-stimulating factor and stem cell factor, alone and in combination, on the biological behaviours of bone marrow mesenchymal stem cells. *Journal of biomedical science and engineering* **2**: 200-207.
- Tashiro K, Inamura M, Kawabata K, Sakurai F, Yamanishi K, Hayakawa T, Mizuguchi H (2009) Efficient adipocyte and osteoblast differentiation from mouse induced pluripotent stem cells by adenoviral transduction. *Stem Cells* **27**: 1802-1811.

- Tasso R, Fais F, Reverberi D, Tortelli F, Cancedda R (2010) The recruitment of two consecutive and different waves of host stem/progenitor cells during the development of tissue-engineered bone in a murine model. *Biomaterials* **31**: 2121-2129.
- Teitelbaum SL (2006) Osteoclasts; culprits in inflammatory osteolysis. *Arthritis Res Ther* **8**: 201.
- Termine JD, Kleinman HK, Whitson SW, Conn KM, McGarvey ML, Martin GR (1981) Osteonectin, a bone-specific protein linking mineral to collagen. *Cell* **26**: 99-105.
- Thibault RA, Scott BL, Mikos AG, Kasper FK (2010) Osteogenic differentiation of mesenchymal stem cells on pregenerated extracellular matrix scaffolds in the absence of osteogenic cell culture supplements. *Tissue Eng Part A* **16**: 431-440.
- Thomas GP, Bourne A, Eisman JA, Gardiner EM (2000) Species-divergent regulation of human and mouse osteocalcin genes by calciotropic hormones. *Exp Cell Res* **258**: 395-402.
- Thompson DD, Simmons HA, Pirie CM, Ke HZ (1995) FDA Guidelines and animal models for osteoporosis. *Bone* **17**: 125S-133S.
- Toricelli P, Fini M, Giavaresi G, Borsari V, Carpi A, Nicolini A, Giardino R (2003) Comparative interspecies investigation on osteoblast cultures: data on cell viability and synthetic activity. *Biomed Pharmacother* **57**: 57-62.
- Tortelli F, Tasso R, Loiacono F, Cancedda R (2010) The development of tissue-engineered bone of different origin through endochondral and intramembranous ossification following the implantation of mesenchymal stem cells and osteoblasts in a murine model. *Biomaterials* **31**: 242-249.
- Tsai MT, Lin DJ, Huang S, Lin HT, Chang WH (2012) Osteogenic differentiation is synergistically influenced by osteoinductive treatment and direct cell-cell contact between murine osteoblasts and mesenchymal stem cells. *Int Orthop* **36**: 199-205.
- Tsiridis E, Upadhyay N, Giannoudis P (2007) Molecular aspects of fracture healing: which are the important molecules? *Injury* **38 Suppl 1**: S11-S25.
- Uchihashi K, Aoki S, Matsunobu A, Toda S (2012) Osteoblast migration into type I collagen gel and differentiation to osteocyte-like cells within a self-produced mineralized matrix: A novel system for analyzing differentiation from osteoblast to osteocyte. *Bone*.
- Udagawa N, Takahashi N, Jimi E, Matsuzaki K, Tsurukai T, Itoh K, Nakagawa N, Yasuda H, Goto M, Tsuda E, Higashio K, Gillespie MT, Martin TJ, Suda T (1999)

Osteoblasts/stromal cells stimulate osteoclast activation through expression of osteoclast differentiation factor/RANKL but not macrophage colony-stimulating factor: receptor activator of NF-kappa B ligand. *Bone* **25**: 517-523.

Ueno A, Kitase Y, Moriyama K, Inoue H (2001) MC3T3-E1-conditioned medium-induced mineralization by clonal rat dental pulp cells. *Matrix Biol* **20**: 347-355.

Unger RE, Sartoris A, Peters K, Motta A, Migliaresi C, Kunkel M, Bulnheim U, Rychly J, Kirkpatrick CJ (2007) Tissue-like self-assembly in cocultures of endothelial cells and osteoblasts and the formation of microcapillary-like structures on three-dimensional porous biomaterials. *Biomaterials* **28**: 3965-3976.

Vaananen HK, Zhao H, Mulari M, Halleen JM (2000) The cell biology of osteoclast function. *J Cell Sci* **113** (Pt 3): 377-381.

Vaananen K, Zhao H (2002) Osteoclast function - biology and mechanisms. In: Principles of bone biology (Bilezikian J.P., Raisz L. G. Rodan G. A, ed), 2 edn. Academic Press, London, 127-168.

Veis A, Dorvee JR (2013) Biomineralization mechanisms: a new paradigm for crystal nucleation in organic matrices. *Calcif Tissue Int* **93**: 307-315.

Viereck V, Siggelkow H, Tauber S, Raddatz D, Schutze N, Hufner M (2002) Differential regulation of Cbfa1/Runx2 and osteocalcin gene expression by vitamin-D3, dexamethasone, and local growth factors in primary human osteoblasts. *J Cell Biochem* **86**: 348-356.

Voegelé TJ, Voegelé-Kadletz M, Esposito V, Macfelda K, Oberndorfer U, Vecsei V, Schabus R (2000) The effect of different isolation techniques on human osteoblast-like cell growth. *Anticancer Res* **20**: 3575-3581.

Vogel E, Marcotte EM (2012) Insights into the regulation of protein abundance from proteomic and transcriptomic analyses. In: 13 edn. 227-232.

Wahl DA, Czernuszka JT (2006) Collagen-hydroxyapatite composites for hard tissue repair. *Eur Cell Mater* **11**: 43-56.

Wang D, Christensen K, Chawla K, Xiao G, Krebsbach PH, Franceschi RT (1999) Isolation and characterization of MC3T3-E1 preosteoblast subclones with distinct in vitro and in vivo differentiation/mineralization potential. *J Bone Miner Res* **14**: 893-903.

Wang Y, Volloch V, Pindrus MA, Blasioli DJ, Chenand J, Kaplan DL (2007) Murine osteoblasts regulate mesenchymal stem cells via WNT and catherin pathways: mechanism depends on cell-cell contact mode. *Journal of tissue engineering and regenerative medicine* **1**: 39-50.

- Washington JT, Schneiderman E, Spears R, Fernandez CR, He J, Opperman LA (2011) Biocompatibility and osteogenic potential of new generation endodontic materials established by using primary osteoblasts. *J Endod* **37**: 1166-1170.
- Wenstrup RJ, Witte DP, Florer JB (1996) Abnormal differentiation in MC3T3-E1 preosteoblasts expressing a dominant-negative type I collagen mutation. *Connect Tissue Res* **35**: 249-257.
- Whitson SW, Harrison W, Dunlap MK, Bowers DE, Jr., Fisher LW, Robey PG, Termine JD (1984) Fetal bovine bone cells synthesize bone-specific matrix proteins. *J Cell Biol* **99**: 607-614.
- Whitson SW, Whitson MA, Bowers DE, Jr., Falk MC (1992) Factors influencing synthesis and mineralization of bone matrix from fetal bovine bone cells grown in vitro. *J Bone Miner Res* **7**: 727-741.
- Whyte MP (2002) Hypophosphatasia. In: *Principles in Bone Biology* (Bilezikian J.P., Raisz L. G. Rodan G. A, ed), 2 edn. Academic Press, 1229-1248.
- Wirth C, Grosgeat B, Lagneau C, Jaffrezic-Renault N, Ponsonnet L (2008) Biomaterial surface properties modulate in vitro rat calvaria osteoblasts response: Roughness and or chemistry? *Materials Science and Engineering: C* **28**: 990-1001.
- Wollensak G, Spoerl E, Wilsch M, Seiler T (2004) Keratocyte apoptosis after corneal collagen cross-linking using riboflavin/UVA treatment. *Cornea* **23**: 43-49.
- Wong MM, Rao LG, Ly H, Hamilton L, Tong J, Sturtridge W, McBroom R, Aubin JE, Murray TM (1990) Long-term effects of physiologic concentrations of dexamethasone on human bone-derived cells. *J Bone Miner Res* **5**: 803-813.
- Wozney JM (2002) Overview of bone morphogenetic proteins. *Spine (Phila Pa 1976)* **27**: S2-S8.
- Xiao G, Wang D, Benson MD, Karsenty G, Franceschi RT (1998) Role of the alpha2-integrin in osteoblast-specific gene expression and activation of the Osf2 transcription factor. *J Biol Chem* **273**: 32988-32994.
- Yamamoto N, Furuya K, Hanada K (2002) Progressive development of the osteoblast phenotype during differentiation of osteoprogenitor cells derived from fetal rat calvaria: model for in vitro bone formation. *Biol Pharm Bull* **25**: 509-515.
- Yang L, Tao T, Wang X, Du N, Chen W, Tao S, Wang Z, Wu L (2003) Effects of dexamethasone on proliferation, differentiation and apoptosis of adult human osteoblasts in vitro. *Chin Med J (Engl)* **116**: 1357-1360.

- Yee JA (1983) Properties of osteoblast-like cells isolated from the cortical endosteal bone surface of adult rabbits. *Calcif Tissue Int* **35**: 571-577.
- Yohay DA, Zhang J, Thraillkill KM, Arthur JM, Quarles LD (1994) Role of serum in the developmental expression of alkaline phosphatase in MC3T3-E1 osteoblasts. *J Cell Physiol* **158**: 467-475.
- Yu YY, Lieu S, Lu C, Miclau T, Marcucio RS, Colnot C (2010) Immunolocalization of BMPs, BMP antagonists, receptors, and effectors during fracture repair. *Bone* **46**: 841-851.
- Zhang H, Lewis CG, Aronow MS, Gronowicz GA (2004) The effects of patient age on human osteoblasts' response to Ti-6Al-4V implants in vitro. *J Orthop Res* **22**: 30-38.
- Zhang K, Barragan-Adjemian C, Ye L, Kotha S, Dallas M, Lu Y, Zhao S, Harris M, Harris SE, Feng JQ, Bonewald LF (2006) E11/gp38 selective expression in osteocytes: regulation by mechanical strain and role in dendrite elongation. *Mol Cell Biol* **26**: 4539-4552.
- Zhang Y, Schedle A, Matejka M, Rausch-Fan X, Andrukhov O (2010) The proliferation and differentiation of osteoblasts in co-culture with human umbilical vein endothelial cells: An improved analysis using fluorescence-activated cell sorting. *Cell Mol Biol Lett* **15**: 517-529.
- Zhou B, Han ZC, Poon MC, Pu W (2007) Mesenchymal stem/stromal cells (MSC) transfected with stromal derived factor 1 (SDF-1) for therapeutic neovascularization: enhancement of cell recruitment and entrapment. *Med Hypotheses* **68**: 1268-1271.
- Zhou G, Zheng Q, Engin F, Munivez E, Chen Y, Sebald E, Krakow D, Lee B (2006) Dominance of SOX9 function over RUNX2 during skeletogenesis. *Proc Natl Acad Sci U S A* **103**: 19004-19009.
- Zhukareva V, Obrocka M, Houle JD, Fischer I, Neuhuber B (2010) Secretion profile of human bone marrow stromal cells: donor variability and response to inflammatory stimuli. *Cytokine* **50**: 317-321.
- Zinger O, Zhao G, Schwartz Z, Simpson J, Wieland M, Landolt D, Boyan B (2005) Differential regulation of osteoblasts by substrate microstructural features. *Biomaterials* **26**: 1837-1847.

APPENDIX 1: CELL TITER-BLUE[®] PROTOCOL

OPTIMISATION

For the optimisation of incubation time cells were seeded at various densities per well in 24-well plates. After 4 hours medium was aspirated and cells were incubated for certain time with medium containing a 10% solution of Cell Titer-Blue[®]. Two no cell control wells were included for every time point. After incubation a 150µl aliquot of each sample and media with dye alone, were transferred to a 96-well plate in duplicate and fluorescence values of samples were measured (excitation/emission: 560/590 nm) using a Multilabel Counter Wallac 1420 (Perkin Elmer). The results were calculated by averaging fluorescent values of the samples and subtracting average value of samples without cells. Subsequently, the obtained values were plotted and R² value was calculated for each cell type (Tab.A1.). From this experiment, the 2 hours incubation time was chosen for assessing the cell growth kinetics in primary human osteoblast cells and 4 hours for other cell types used in this study.

HOb		MC3T3E1		MG63		SaOs2	
Incubation time	R ²	Incubation time	R ²	Incubation time	R ²	Incubation time	R ²
2 hours	0.995	2 hours	0.989	2 hours	1	4 hours	0.995
2.5 hours	0.998	3 hours	0.999	3 hours	0.997	5 hours	0.99
4 hours	0.992	4 hours	0.998	4 hours	0.996	-	-

Table A1. Incubation time and R-squared value for primary human osteoblasts (HOb), MC3T3E1, MG63 and SaOs2 cells with Cell Titer-Blue[®].

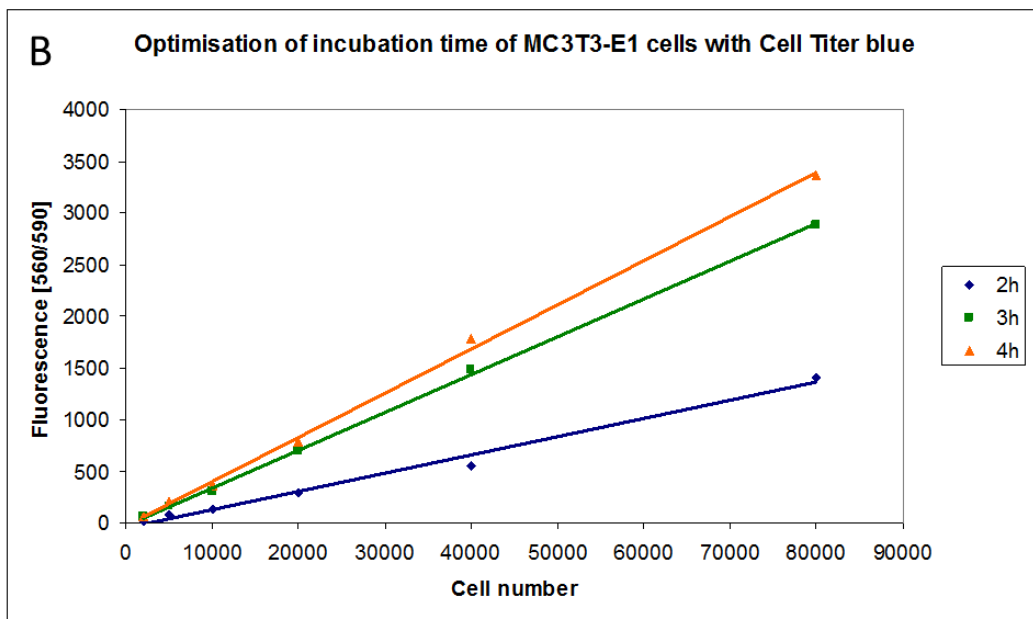
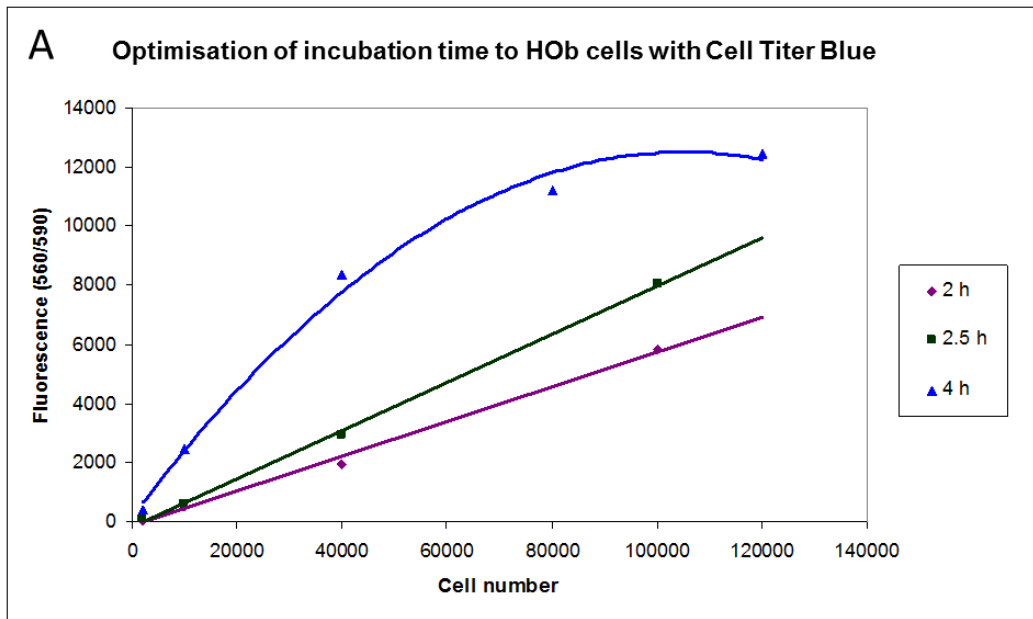


Figure A3.A-B. Diagrams show the fluorescence intensity of Cell Titer-Blue[®] against HOb (A) and MC3T3E1 (B) cell number after different time of incubation.

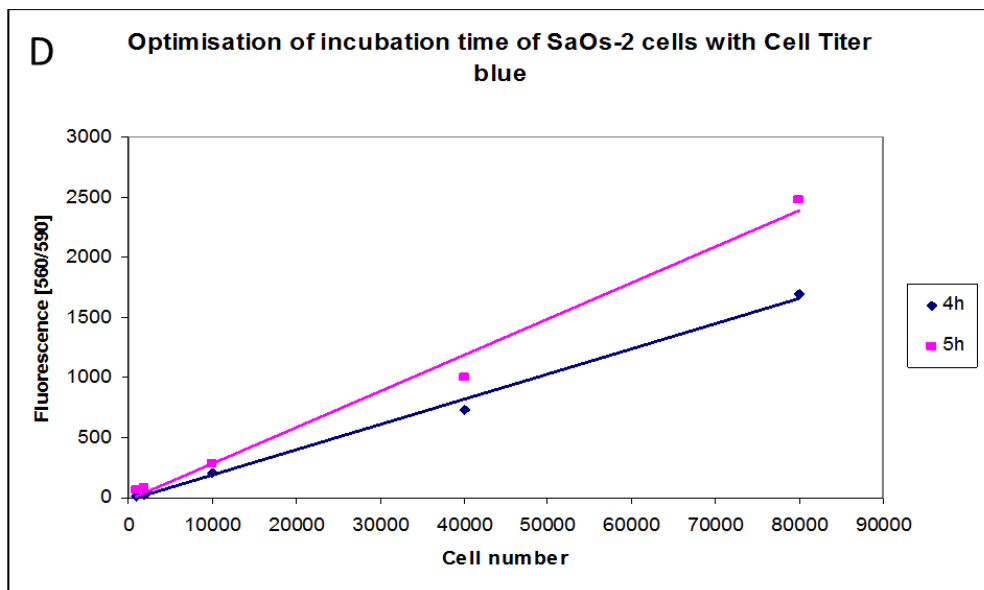
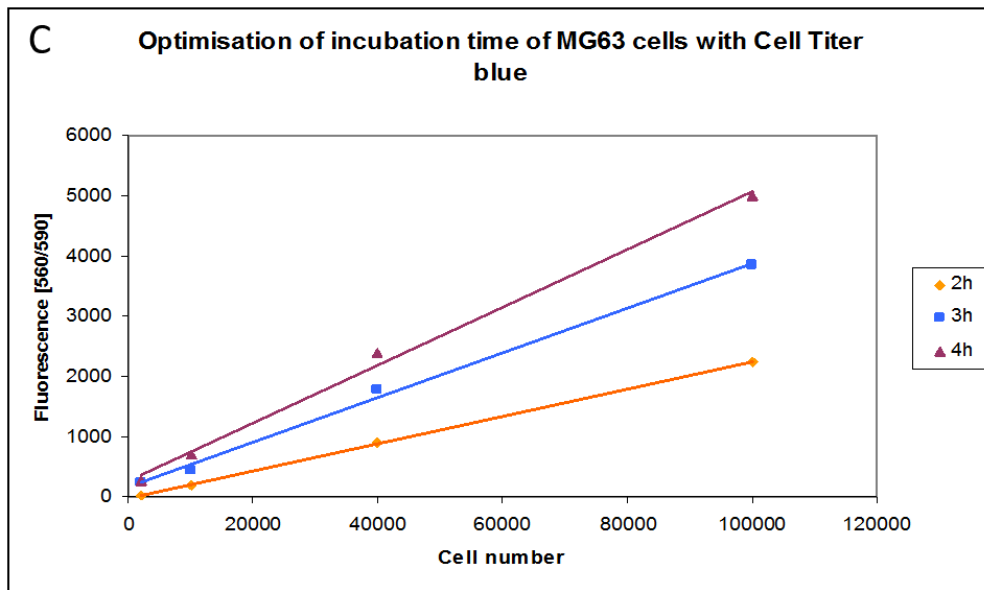
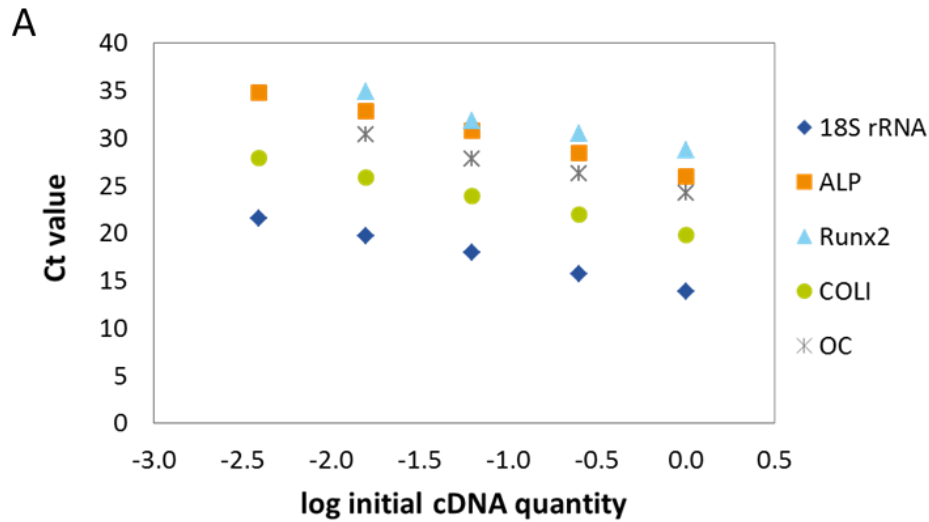


Figure A3.C-D. Diagrams show the fluorescence intensity of Cell Titer-Blue[®] against HOb (A) and MC3T3E1 (B) cell number after different time of incubation.

APPENDIX 2: PRIMER EFFICIENCY OPTIMISATION

Real time PCR is a sensitive method to detect the expression of mRNA in the cells. For the accuracy of the method it is critical to optimise the reaction conditions including the primer efficiency. The amplification efficiency of both, the target and reference gene, should be close to 100% and not different than $\pm 10\%$. For the optimisation of the amplification efficiency of human and murine genes a diluted template from a positive control of osteoblast cells cultured in differentiation medium was used. The efficiency was calculated from the linear regression curve of concentrations against the logarithm of dilution (Fig.A1.A,B&Fig.A2.A,B). Additionally, to ensure the specificity of the primers a melting curve was generated after the reactions to analyse the dissociation-characteristics of double-stranded DNA during heating (Fig.A1.C&Fig.A2.C). This step is important for evaluation of the assay specificity. At the temperature about 80°C the whole amplified product is expected to dissociate. If primer dimers were amplified an additional peak is observed at lower temperature (about 70°C).



B

	Gene				
	18S rRNA	ALP	Runx2	Collagen I	OC
Slope	-3.2202	-3.5194	-3.3062	-3.3246	-3.3116
R-squared	0.9983	0.9984	0.9974	0.9997	0.9923
Efficiency [%]	104.4	92.4	100.7	99.9	100.4

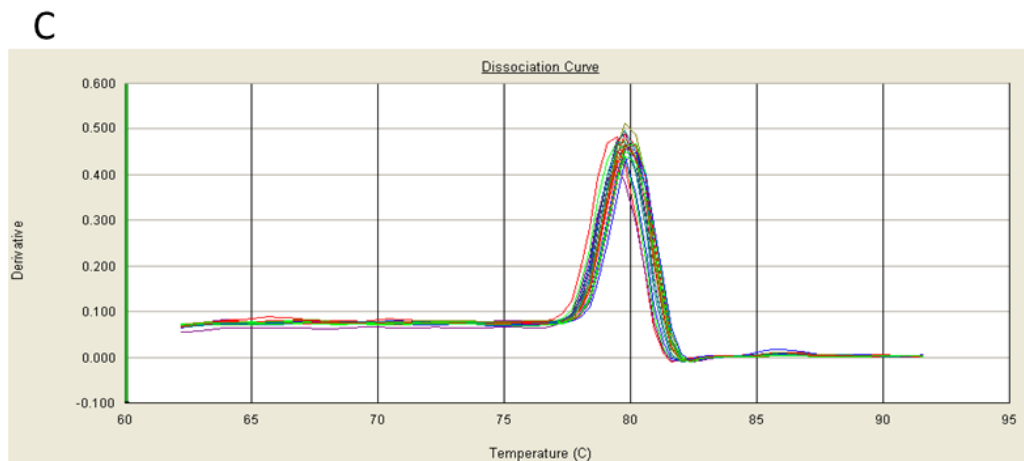
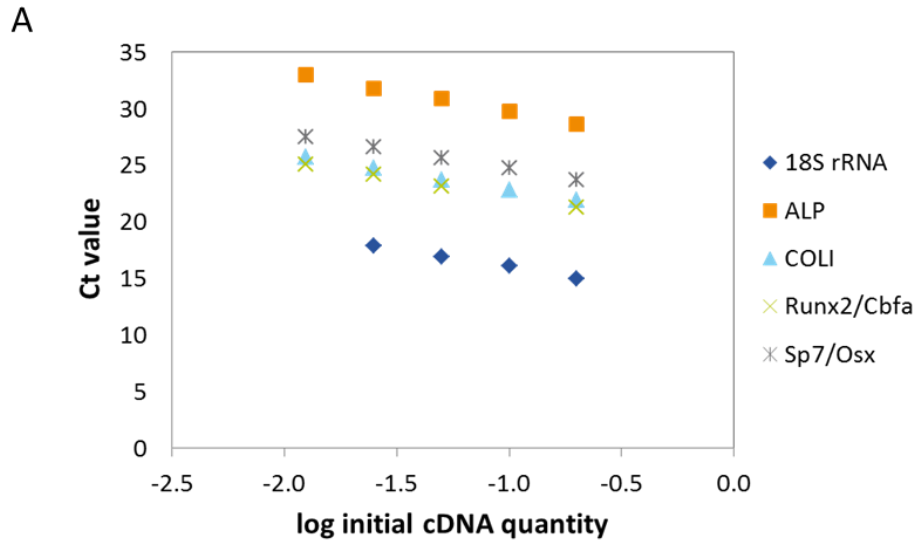


Figure A1. Human primers efficiency optimisation. A: Diagram shows the Ct values for 18S rRNA, Alkaline phosphatase (ALP), core-binding factor subunit alpha-1 (Cbfa1)/Runx2-related transcription factor 2 (Runx2), type I collagen (COLI) and osteocalcin (OC) against the logarithm of the cDNA amount used for the reactions, B: The efficiency calculated for each primers set from the linear regression curve, C: Melting curve results obtained after the real-time PCR results.



B

	Gene				
	18S rRNA	ALP	collagen I	Runx2/Cbfa	Sp7/Osx
slope	-3.18	-3.55	-3.14	-3.2	-3.14
R ²	0.9965	0.9984	0.999	1	0.9994
Efficiency [%]	106.4	91.3	108.3	105.3	108.2

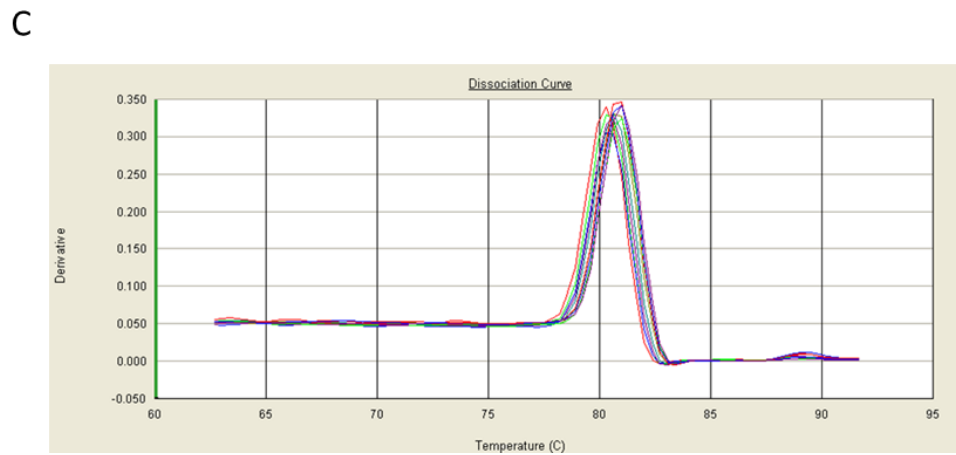


Figure A2. Murine primers efficiency optimisation. A: Diagram shows the Ct values for 18S rRNA, Alkaline phosphatase (ALP), Runt-related transcription factor 2 (Runx2), type I collagen (COLI) and osteocalcin (OC) against the logarithm of the cDNA amount used for the reactions, B: The efficiency calculated for each primers set from the linear regression curve, C: Melting curve results obtained after the real-time PCR results.

APPENDIX 3: RAYBIO[®] PROTEIN ARRAY MAP

The analysis of proteomic profile of cytokines secreted by cells was performed using RayBio[®] Human Cytokine Antibody Array G-series 2000. Antibodies for 174 cytokines are divided within 3 glass slides: RayBio[®] Human Cytokine Antibody Array G6, G7 and G8 (Fig.A4.A-C). After binding of the proteins results were obtained by scanning the glass slides using GenePix 4000B Microarray Scanner (Axon Instruments; Molecular Devices, CA, US).

A

	A	B	C	D	E	F	G	H	I	J	K	L	M	N
1	POS1	POS2	POS3	NEG	NEG	ANG	BDNF	BLC	BMP-4	BMP-6	Ckβ 8-1	CNTF	EGF	CCL11
2	POS1	POS2	POS3	NEG	NEG	ANG	BDNF	BLC	BMP-4	BMP-6	Ckβ 8-1	CNTF	EGF	CCL11
3	CCL24	CCL26	FGF6	FGF7	Flt-3L	CX3CL1	GCP-2	GDNF	CSF2	I-309	IFN-γ	IGFBP1	IGFBP2	IGFBP4
4	CCL24	CCL26	FGF6	FGF7	Flt-3L	CX3CL1	GCP-2	GDNF	CSF2	I-309	IFN-γ	IGFBP1	IGFBP2	IGFBP4
5	IGF-I	IL-10	IL-13	IL-15	IL-16	IL-1α	IL-1β	IL-1ra	IL-2	IL-3	IL-4	IL-5	IL-6	IL-7
6	IGF-I	IL-10	IL-13	IL-15	IL-16	IL-1α	IL-1β	IL-1ra	IL-2	IL-3	IL-4	IL-5	IL-6	IL-7
7	Leptin	LIGHT	MCP1	MCP2	MCP3	MCP4	M-CSF	MDC	MIG	MIP-1δ	MIP-3α	NAP-2	NT-3	PARC
8	Leptin	LIGHT	MCP1	MCP2	MCP3	MCP4	M-CSF	MDC	MIG	MIP-1δ	MIP-3α	NAP-2	NT-3	PARC
9	PDGF-BB	RANTES	SCF	SDF-1	TARC	TGF-β1	TGF-β3	TNF-α	TNF-β	NEG	NEG	NEG	NEG	NEG
10	PDGF-BB	RANTES	SCF	SDF-1	TARC	TGF-β1	TGF-β3	TNF-α	TNF-β	NEG	NEG	NEG	NEG	NEG

B

	A	B	C	D	E	F	G	H	I	J	K	L	M	N
1	POS1	POS2	POS3	NEG	NEG	Acip30	AgRP	ANGPT2	AREG	Axl	bFGF	β-NGF	BTC	CCL28
2	POS1	POS2	POS3	NEG	NEG	Acip30	AgRP	ANGPT2	AREG	Axl	bFGF	β-NGF	BTC	CCL28
3	CTACK	Dtk	EGFR	ENA-78	Fas	FGF4	FGF9	CSF3	GITRL	GITR	GRO	GRO-α	HCC-4	HGF
4	CTACK	Dtk	EGFR	ENA-78	Fas	FGF4	FGF9	CSF3	GITRL	GITR	GRO	GRO-α	HCC-4	HGF
5	ICAM1	ICAM3	IGFBP3	IGFBP6	sIGF-1R	IL1R4	IL-1 R1	IL-11	IL-12 p40	IL-12 p70	IL-17	IL-2 Rα	sIL-6R	IL-8
6	ICAM1	ICAM3	IGFBP3	IGFBP6	sIGF-1R	IL1R4	IL-1 R1	IL-11	IL-12 p40	IL-12 p70	IL-17	IL-2 Rα	sIL-6R	IL-8
7	HTAC	XCL1	MIF	MIP-1α	MIP-1β	MIP-3β	MSP-α	NT-4	OPG	OSM	PLGF	sgp130	sTNFR2	sTNFR1
8	HTAC	XCL1	MIF	MIP-1α	MIP-1β	MIP-3β	MSP-α	NT-4	OPG	OSM	PLGF	sgp130	sTNFR2	sTNFR1
9	TECK	TIMP1	TIMP2	THPO	TRAIL R3	TRAIL R4	uPAR	VEGFA	VEGF-D	NEG	NEG	NEG	NEG	NEG
10	TECK	TIMP1	TIMP2	THPO	TRAIL R3	TRAIL R4	uPAR	VEGFA	VEGF-D	NEG	NEG	NEG	NEG	NEG

Figure A4.A-B. RayBio[®] Human Cytokine Antibody G-Series map. A: Array G6, B: G7.

C

	A	B	C	D	E	F	G	H	I	J	K	L	M	N
1	POS1	POS2	POS3	NEG	NEG	ActivinA	ALCAM	B7-1 (CD80)	BMP-5	BMP-7	CTF1	CD14	CXCL16	DR6
2	POS1	POS2	POS3	NEG	NEG	ActivinA	ALCAM	B7-1 (CD80)	BMP-5	BMP-7	CTF1	CD14	CXCL16	DR6
3	Endoglin	ErbB3	SELE	FASLG	ICAM2	IGF-II	IL-1 R2	IL-10 R β	IL-13 R α 2	IL-18 B P α	IL-18 R β	MMP3	IL-2 R β	IL-2 R γ
4	Endoglin	ErbB3	SELE	FASLG	ICAM2	IGF-II	IL-1 R2	IL-10 R β	IL-13 R α 2	IL-18 B P α	IL-18 R β	MMP3	IL-2 R β	IL-2 R γ
5	IL-21 R	IL-5 R α	IL-9	IP-10	LAP	Leptin R	LIF	SELL	CSF1R	MMP1	MMP13	MMP9	MPIF1	NGFR
6	IL-21 R	IL-5 R α	IL-9	IP-10	LAP	Leptin R	LIF	SELL	CSF1R	MMP1	MMP13	MMP9	MPIF1	NGFR
7	PDGF-AA	PDGF-AB	PDGF R α	PDGF R β	PECAM1	Proctatin	SCFR	SDF-1 β	Siglec-5	TGF- α	TGF- β 2	Tie-1	Tie-2	TIMP4
8	PDGF-AA	PDGF-AB	PDGF R α	PDGF R β	PECAM1	Proctatin	SCFR	SDF-1 β	Siglec-5	TGF- α	TGF- β 2	Tie-1	Tie-2	TIMP4
9	CDH5	VEGF R2	VEGF R3	NEG	NEG	NEG	NEG	NEG	NEG	NEG	NEG	NEG	NEG	NEG
10	CDH5	VEGF R2	VEGF R3	NEG	NEG	NEG	NEG	NEG	NEG	NEG	NEG	NEG	NEG	NEG

Figure A4.C. RayBio[®] Human Cytokine Antibody G-Series map. C: Array G8.

APPENDIX 4: PROTEIN RESULTS

Cytokine protein levels secreted by unstimulated MSCs analysed using RayBio Cytokine Array G-Series. Cells in monolayer were cultured for 48 hours in serum-free medium. After that time, medium was collected, centrifuged and stored at -20°C until analysis. The analysis was performed using GenePix 4000B Microarray Scanner (Axon Instruments; Molecular Devices, CA, US). Protein presence was determined by the fluorescence signal intensity: *n.d.* (= not detected) - for the signal intensity up to 10; *low* – signal intensity of 10-1000; *medium* – signal intensity of 1001-10000; *high* – signal intensity above 10000 (Fig.A5.A-D).

Protein	donor 5	donor 6	doonor 7	donor 8	donor 9
Angiogenin	medium	high	high	high	high
BDNF	low	low	low	low	low
BLC	low	low	low	low	n.d.
BMP-4	low	n.d.	n.d.	n.d.	n.d.
BMP-6	n.d.	n.d.	n.d.	n.d.	low
CK beta 8-1	low	low	low	low	n.d.
CNTF	low	low	low	low	low
EGF	n.d.	n.d.	n.d.	n.d.	low
Eotaxin	low	n.d.	n.d.	low	n.d.
Eotaxin-2	n.d.	n.d.	n.d.	n.d.	n.d.
Eotaxin-3	low	low	low	low	low
FGF-6	low	low	low	low	low
FGF-7	low	low	low	low	low
Flt-3 Ligand	low	low	low	low	low
Fractalkine	low	n.d.	n.d.	n.d.	n.d.
GCP-2	low	low	n.d.	low	n.d.
GDNF	low	low	low	low	n.d.
GM-CSF	low	low	low	low	low
I-309	low	n.d.	n.d.	low	n.d.
IFN-gamma	low	low	low	low	low
IGFBP-1	low	low	low	low	n.d.
IGFBP-2	low	low	low	low	low
IGFBP-4	low	low	low	low	n.d.
IGF-I	n.d.	n.d.	n.d.	n.d.	n.d.
IL-10	low	low	low	low	low
IL-13	low	low	low	low	low
IL-15	low	low	low	low	low

Figure A5. Protein level secreted by unstimulated MSCs (control) determined by the fluorescence signal intensity: *n.d.* (= not detected) - for the signal intensity up to 10; *low* – signal intensity of 10-1000; *medium* – signal intensity of 1001-10000; *high* – signal intensity above 10000.

Protein	donor 5	donor 6	donor 7	donor 8	donor 9
IL-16	n.d.	n.d.	n.d.	n.d.	n.d.
IL-1alpha	low	low	low	low	low
IL-1beta	low	low	low	low	low
IL-1ra	low	low	low	low	low
IL-2	low	low	low	low	low
IL-3	low	low	low	low	low
IL-4	n.d.	n.d.	n.d.	n.d.	n.d.
IL-5	low	low	low	low	low
IL-6	high	medium	medium	high	high
IL-7	low	low	low	low	low
Leptin	low	low	low	low	low
LIGHT	low	n.d.	n.d.	low	n.d.
MCP-1	high	high	high	high	high
MCP-2	low	low	low	low	low
MCP-3	low	low	low	low	low
MCP-4	low	low	low	low	low
M-CSF	low	low	low	low	low
MDC	low	n.d.	n.d.	n.d.	n.d.
MIG	low	low	low	low	low
MIP-1-delta	n.d.	n.d.	n.d.	n.d.	n.d.
MIP-3-alpha	low	n.d.	n.d.	n.d.	n.d.
NAP-2	low	low	low	low	n.d.
NT-3	low	low	low	low	n.d.
PARC	low	low	low	low	low
PDGF-BB	low	low	low	low	low
RANTES	low	low	low	low	low
SCF	low	low	low	low	low
SDF-1	low	low	low	low	low
TARC	low	low	low	low	n.d.
TGF-beta 1	low	low	low	low	low
TGF-beta 3	n.d.	n.d.	n.d.	n.d.	n.d.
TNF-alpha	low	low	low	low	low
TNF-beta	low	low	low	low	low
Acyr30	low	low	low	low	low
AgRP	low	low	low	low	low
Angiopoietin-2	medium	low	low	low	low
Amphiregulin	n.d.	low	low	low	low
Axl	n.d.	low	low	low	low
bFGF	n.d.	low	low	low	low
b-NGF	n.d.	low	low	low	low
BTC	low	low	low	low	low
CCL-28	low	low	low	low	low
CTACK	low	low	low	low	low
Dtk	n.d.	low	low	low	low
EGF-R	low	low	low	low	low
ENA-78	n.d.	low	low	low	low
Fas/TNFRSF6	low	low	low	low	low
FGF-4	n.d.	low	low	low	low
FGF-9	n.d.	low	low	low	low

Figure A5. Protein level secreted by unstimulated MSCs (control) determined by the fluorescence signal intensity: *n.d.* (= not detected) - for the signal intensity up to 10; *low* – signal intensity of 10-1000; *medium* – signal intensity of 1001-10000; *high* – signal intensity above 10000.

Protein	donor 5	donor 6	donor 7	donor 8	donor 9
GCSF	low	low	low	low	low
GITR-Ligand	low	low	low	low	low
GITR	n.d.	low	low	low	low
GRO	medium	medium	medium	medium	medium
GRO-alpha	low	low	low	low	low
HCC-4	low	low	low	low	low
HGF	medium	medium	n.d.	medium	high
ICAM-1	n.d.	low	low	low	low
ICAM-3	n.d.	low	n.d.	low	low
IGFBP-3	n.d.	low	low	low	low
IGFBP-6	low	low	medium	medium	medium
IGF-I SR	medium	low	low	low	low
IL-1 R4/ST2	low	low	low	low	low
IL-1 RI	low	low	low	low	low
IL-11	low	low	low	low	low
IL-12 p40	n.d.	low	low	low	low
IL-12 p70	n.d.	low	low	low	low
IL-17	low	low	low	low	low
IL-2 Rapha	low	low	low	low	low
IL-6 R	n.d.	low	low	low	low
IL-8	low	low	low	low	low
I-TAC	low	n.d.	low	low	low
Lymphotactin	n.d.	low	low	low	low
MIF	medium	low	medium	low	low
MIP-1alpha	n.d.	n.d.	low	low	low
MIP-1beta	n.d.	low	low	low	low
MIP-3beta	n.d.	low	low	low	low
MSP-alpha	low	n.d.	low	low	low
NT-4	low	low	low	low	low
Osteoprotegerin	high	high	high	high	high
Oncostatin M	low	low	low	low	low
PIGF	low	low	low	low	low
sgp130	low	low	low	low	low
sTNF RII	n.d.	low	low	n.d.	low
sTNF-RI	low	low	medium	medium	medium
TECK	n.d.	low	low	low	low
TIMP-1	medium	medium	medium	medium	medium
TIMP-2	high	high	high	high	high
Thrombopoietin	low	low	low	low	low
TRAIL R3	n.d.	low	low	low	low
TRAIL R4	low	low	low	low	low
uPAR	low	medium	low	low	low
VEGF	low	low	low	low	low
VEGF-D	n.d.	low	low	low	low
Activin A	low	low	low	low	low
ALCAM	low	low	low	n.d.	low
B7-1(CD80)	n.d.	low	low	n.d.	low
BMP-5	low	low	low	low	low
BMP-7	low	low	low	low	low

Figure A5. Protein level secreted by unstimulated MSCs (control) determined by the fluorescence signal intensity: *n.d.* (= not detected) - for the signal intensity up to 10; *low* – signal intensity of 10-1000; *medium* – signal intensity of 1001-10000; *high* – signal intensity above 10000.

Protein	donor 5	donor 6	donor 7	donor 8	donor 9
Cardiotrophin-1	low	low	low	low	low
CD14	low	n.d.	low	n.d.	low
CXCL- 16	low	low	low	low	low
DR6 (TNFRSF21)	low	low	low	low	low
Endoglin	low	low	low	low	low
ErbB3	low	low	low	low	low
E-Selectin	low	low	low	low	low
Fas Ligand	low	low	low	low	low
ICAM-2	low	low	low	low	low
IGF-II	medium	medium	medium	medium	medium
IL-1 R II	low	low	low	low	low
IL-10 Rbeta	low	low	low	low	low
IL-13 Ralpha2	low	low	low	low	low
IL-18 BPalpa	low	low	low	low	low
IL-18 Rbeta	low	low	low	low	low
IL-2 Ralpha	low	low	low	low	low
IL-2 Rbeta	low	low	low	low	low
IL-2 Rgamma	low	low	low	low	low
IL-21R	low	low	low	low	low
IL-5 Ralpha	low	low	low	low	low
IL-9	low	low	low	low	low
IP-10	low	low	low	low	low
LAP	medium	medium	medium	medium	medium
Leptin R	low	low	low	low	low
LIF	low	low	low	low	low
L-Selectin	low	low	low	low	low
M-CSF R	low	low	low	low	low
MMP-1	low	low	low	low	low
MMP-13	low	low	low	n.d.	low
MMP-9	n.d.	low	low	n.d.	low
MPIF-1	low	low	low	low	low
NGF R	low	low	low	low	low
PDGF AA	low	low	low	low	low
PDGF-AB	low	low	low	low	low
PDGF Ralpha	low	low	low	low	low
PDGF Rbeta	low	low	low	low	low
PECAM-1	n.d.	n.d.	n.d.	n.d.	low
Prolactin	low	low	low	low	low
SCF R	low	low	low	low	low
SDF-1beta	low	low	low	low	low
Siglec-5	low	low	low	low	low
TGF-alpha	n.d.	n.d.	n.d.	n.d.	low
TGF beta2	low	low	low	low	low
Tie-1	low	low	low	low	low
Tie-2	low	low	low	low	low
TIMP-4	low	n.d.	low	n.d.	low
VE-Cadherin	low	low	low	low	low
VEGF R2	low	low	low	low	low
VEGF R3	low	low	low	low	low

Figure A5. Protein level secreted by unstimulated MSCs (control) determined by the fluorescence signal intensity: *n.d.* (= not detected) - for the signal intensity up to 10; *low* – signal intensity of 10-1000; *medium* – signal intensity of 1001-10000; *high* – signal intensity above 10000.

APPENDIX 5: GENE EXPRESSION RESULTS

Human bone marrow mesenchymal stem cells (MSCs) were cultured in monolayer (ML), micromass (MM) or in type I collagen-hydroxyapatite gel (CHAP). The gene expression of Sox9, Runx2, COL1, ALP, OC and E11 was analysed at day 2, 7 and 14. During culturing time cells were maintained in growth medium (GM) or differentiation medium (DM).

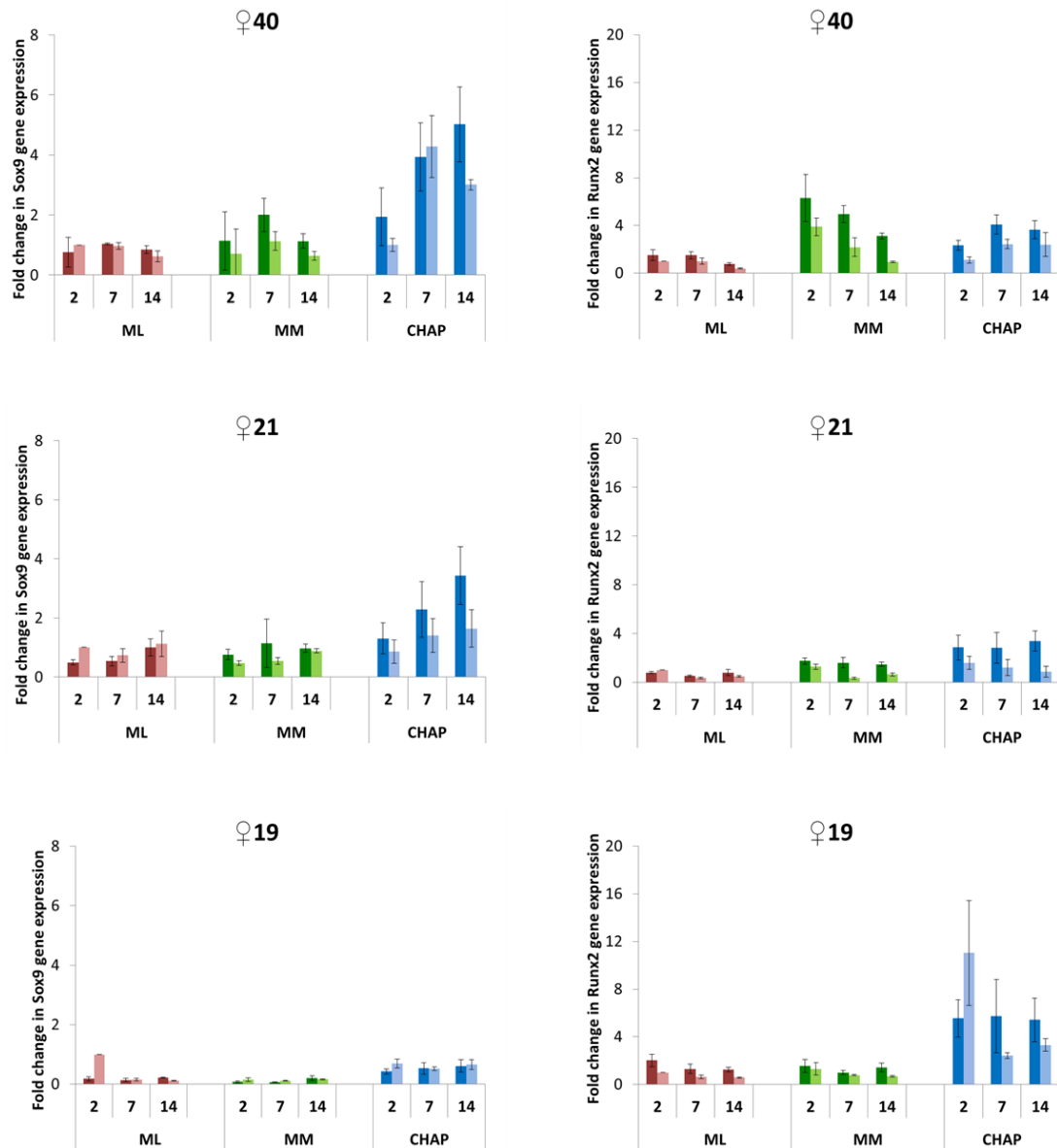


Figure A6. Diagrams show the mean of relative gene expression of Sox9 and Runt-related transcription factor 2 (Runx2) with the standard deviation of the mean in cells from 3 different donors (3 females at age 40, 21 and 19).

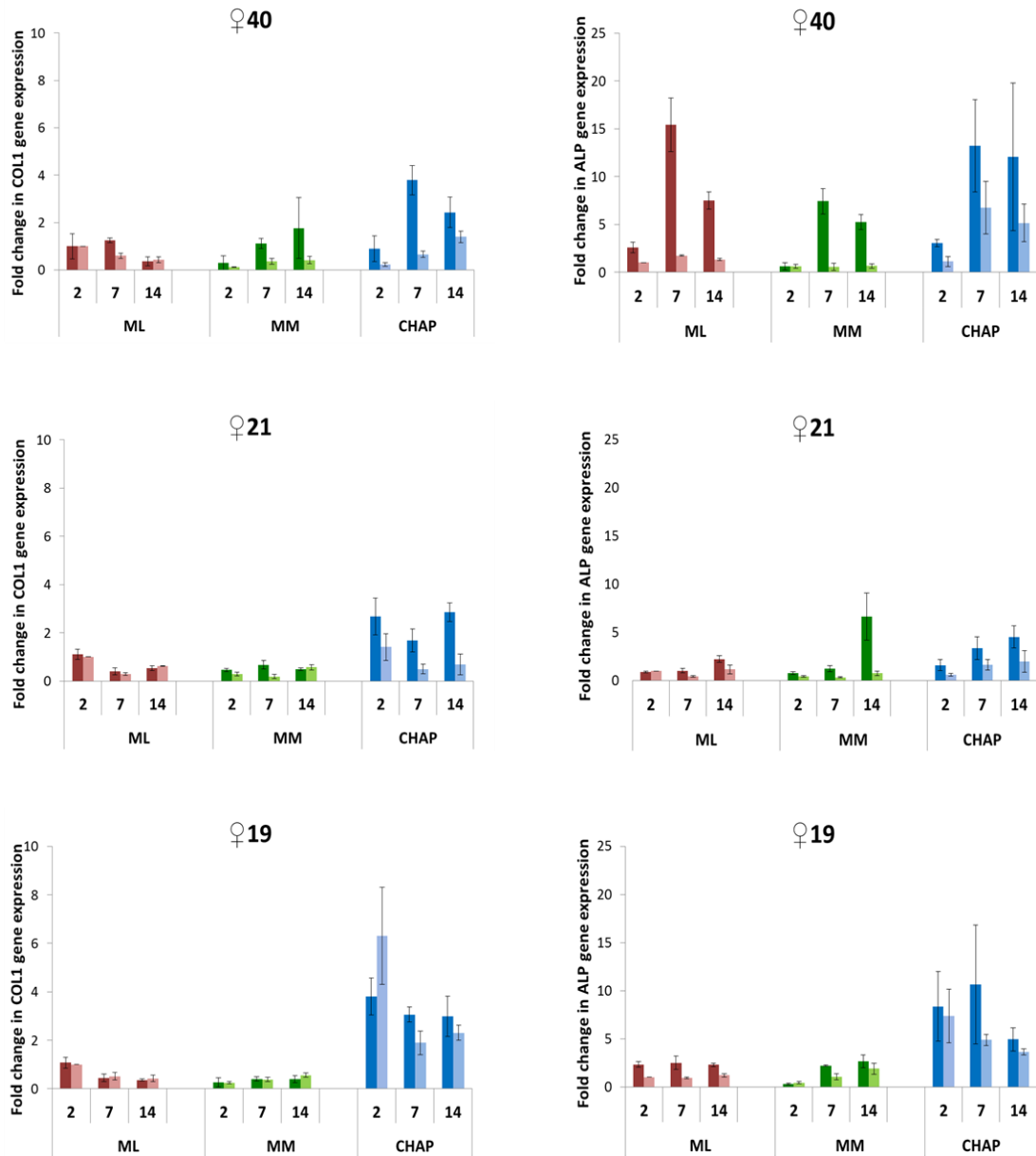


Figure A7. Diagrams show the mean of relative gene expression of type I collagen (COL1) and alkaline phosphatase activity (ALP) with the standard deviation of the mean in cells from 3 different donors.

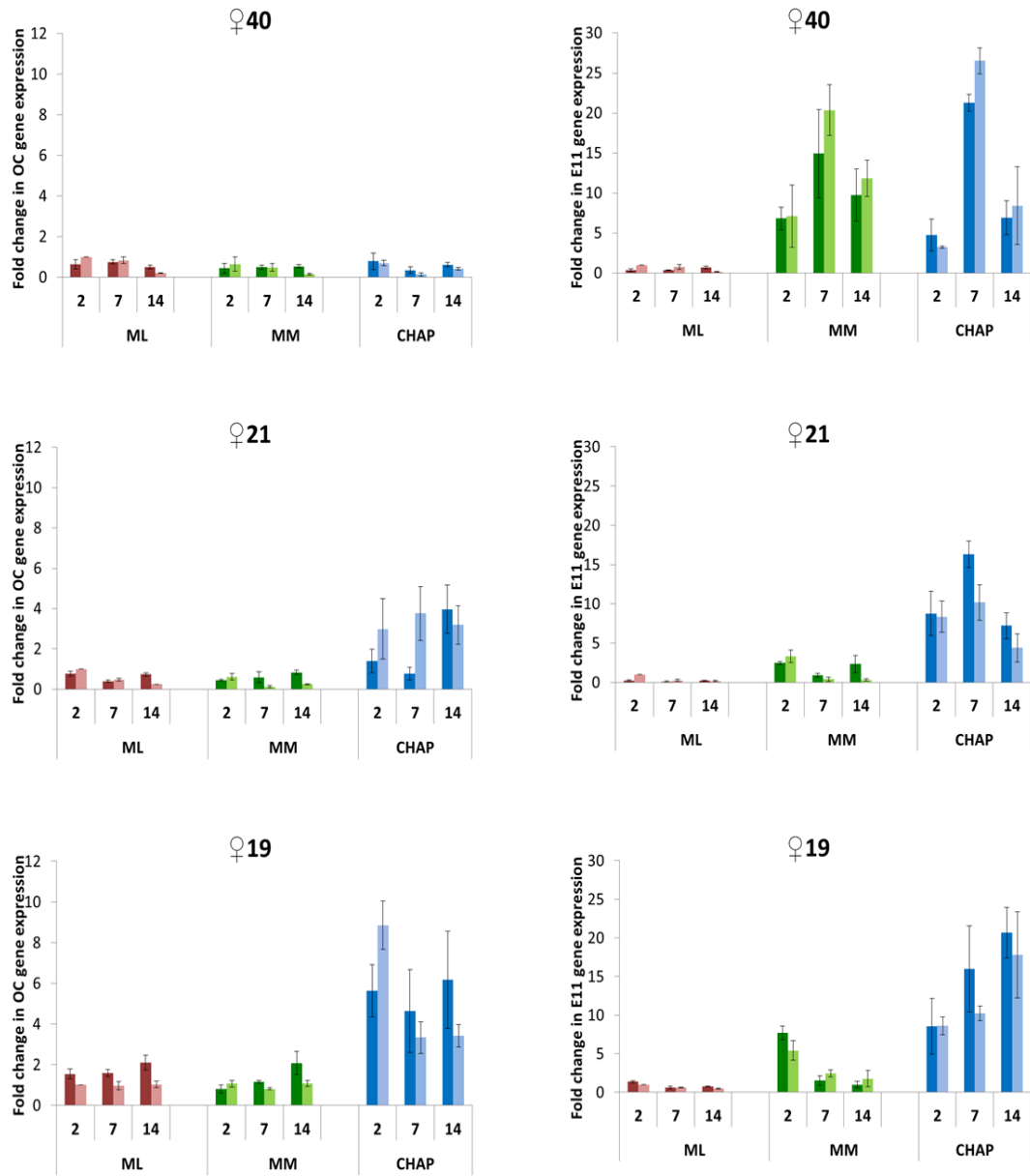


Figure A8. Diagrams show the mean of relative gene expression of osteocalcin (OC) and E11 with the standard deviation of the mean in cells from 3 different donors.